



Durham E-Theses

Synthesis, reactivity and mechanistic studies on Oxo, Imido and Alkylidene complexes of the early transition metals

Mitchell, Jonathan Paul

How to cite:

Mitchell, Jonathan Paul (1992) *Synthesis, reactivity and mechanistic studies on Oxo, Imido and Alkylidene complexes of the early transition metals*, Durham theses, Durham University. Available at Durham E-Theses Online: <http://etheses.dur.ac.uk/5788/>

Use policy

The full-text may be used and/or reproduced, and given to third parties in any format or medium, without prior permission or charge, for personal research or study, educational, or not-for-profit purposes provided that:

- a full bibliographic reference is made to the original source
- a [link](#) is made to the metadata record in Durham E-Theses
- the full-text is not changed in any way

The full-text must not be sold in any format or medium without the formal permission of the copyright holders.

Please consult the [full Durham E-Theses policy](#) for further details.

The copyright of this thesis rests with the author.
No quotation from it should be published without
his prior written consent and information derived
from it should be acknowledged.

**Synthesis, Reactivity and Mechanistic Studies on
Oxo, Imido and Alkylidene Complexes of
The Early Transition Metals.**

by

Jonathan Paul Mitchell, B.Sc. G.R.S.C.

University of Durham

**A thesis submitted in part fulfillment of the requirements for the degree of
Doctor of Philosophy at the University of Durham.**

January 1992



- 9 JUL 1992

Statement of Copyright

The Copyright of this thesis rests with the author. No quotation from it should be published without his prior written consent and information derived from it should be acknowledged.

Declaration

The work described in this thesis was carried out in the Department of Chemistry at the University of Durham between October 1988 and September 1991. All the work is my own, unless stated to the contrary, and it has not been submitted previously for a degree at this or any other University.

For my Family and Friends.

Acknowledgements

There are a number of people I would like to thank for their assistance and encouragement over the last three years.

Primarily, I must express my sincere thanks to Vernon Gibson for being a good friend, mentor and role-model throughout my period of study at Durham. His constant support and forgiving nature has made it a great pleasure to work within his research group.

I am grateful to all past and present members of the "*cutting edge*" (CG 101/19): Terry, Alan, Dave, Pete, Andy, Oli, Phil, Matt, Tina, Ulrich, Jens and Kayumars for providing an outstanding atmosphere in which to work and filling the traps when I forgot.

To all my close friends, particularly Jane, Martin and Ed (the Reeves and Mortimer of the Chemistry Department), Gary (Gapes), Mike (Pudsey), Paul, the sad "115 Boys", Alex and Nigel (the other members of the infamous "Matt Jolly Experience") and Sarah, Michelle and Jane from over the road at the New Inn go my heartfelt thanks.

I am particularly indebted to Dr W. Clegg and Mr D.C.R. Hockless (University of Newcastle-upon-Tyne) for solving the crystal structure herein, and to Professors Dick Schrock and Jim Feast and Dr. Ezat Khosravi for many stimulating discussions over the past three years. I would also like to thank Dick Schrock, Gui Bazan and John Bercaw for their hospitality during my visits to M.I.T. and Caltech. Furthermore, without the help of the technical staff here at Durham (particularly Ray, Gordon, Alan and Julia) none of this work would have been possible.

I would also like to thank the remaining members of 98 Hallgarth Street : Gail, Karen and Julie for putting up with loud music at all hours and my attempts to play the guitar .

Finally, the award of an S.E.R.C. studentship and a Messel Scholarship from the Society of Chemical Industry are gratefully acknowledged, and I would like to thank all my family for moral support.

Abstract

Synthesis, Reactivity and Mechanistic Studies on Oxo, Imido and Alkylidene Complexes of the Early Transition Metals.

This thesis describes studies directed towards the synthesis and reactivity of transition metal species containing multiply bonded oxo, imido and alkylidene ligands, with particular emphasis on the use of alkylidene complexes of the type $\text{Mo}(\text{NAr})(\text{CHCMe}_2\text{R})(\text{O-t-Bu})_2$ ($\text{R} = \text{Me, Ph}$) as initiators in living ring opening metathesis polymerization (ROMP).

Chapter 1 highlights areas of transition metal chemistry of relevance to the general theme of this thesis, including recent advances in the ROMP of functionalized norbornene and norbornadiene monomers.

Chapter 2 shows how a "Wittig like" capping reaction may be used to introduce a wide range of potentially useful functional groups onto the end of polymer chains generated via living ROMP. Amongst the functional groups introduced in this manner are Cl, Me, OMe, CHO, CN, NMe_2 , NO_2 , NH_2 , CF_3 and CO_2Me . Unusual 2-oxametallacycle intermediates have been observed in solution for benzaldehyde derivatives possessing electron withdrawing substituents.

Chapter 3 develops the use of styrene and several of its derivatives as chain transfer agents in living ROMP. The use of substituted styrenes allows for functionalization of the start of the polymer chain.

Chapter 4 investigates the "heteroatom exchange" reactivity of a variety of four coordinate molybdenum complexes. The exchange of multiply bonded oxo, imido and alkylidene units between such species, and to and from external substrates, has been investigated, and such studies have helped to identify bimolecular decomposition pathways responsible for the high molecular weight impurity sometimes observed in polymer samples prepared by living ROMP.

Chapter 5 describes the synthesis and characterization of several niobium and tantalum half-sandwich imido complexes of the type $\text{Cp}^*\text{M}(\text{NR})\text{Cl}_2$ ($\text{M} = \text{Nb, R} = \text{Me, 2,6-iPr}_2\text{C}_6\text{H}_3$; $\text{M} = \text{Ta, R} = \text{2,6-iPr}_2\text{C}_6\text{H}_3$). The "heteroatom exchange" reactivity of the imido unit in this environment has been investigated. The related half-sandwich alkylidene complex $\text{CpTa}(\text{CHCMe}_2\text{Ph})\text{Cl}_2$ has also been prepared and the exchange reactivity of the alkylidene ligand studied.

Chapter 6 gives experimental details for chapters 2-5.

Jonathan Paul Mitchell (January 1992)

Abbreviations

BTFMND	2,3-bis(trifluoromethyl)norbornadiene
Cp	Cyclopentadienyl (C ₅ H ₅)
Cp*	Pentamethylcyclopentadienyl (C ₅ Me ₅)
Cp'	Generalised (C ₅ R ₅) ligand
CT	Chain Transfer
DCMND	2,3-dicarbomethoxynorbornadiene
dme	Dimethoxyethane (MeOCH ₂ CH ₂ OMe)
eqm	Equilibrium
GPC	Gel Permeation Chromatography
mes	Mesityl
M _n	Number Average Molecular Weight
M _w	Weight Average Molecular Weight
NAr	2,6-diisopropylphenylimido
NMR	Nuclear Magnetic Resonance
IR	Infrared
LUMO	Lowest Unoccupied Molecular Orbital
NBE	Norbornene
PDI	Polydispersity Index
pyr	Pyridine
quin	Quinuclidene
ROMP	Ring Opening Metathesis Polymerization
SP	Square Pyramidal
TBP	Trigonal Bipyramidal
OTf	Trifluoromethansulphonate (OSO ₂ CF ₃)
THF	Tetrahydrofuran
TMS	Trimethylsilyl (Me ₃ Si)

<u>Contents</u>	Page
Chapter One - Transition Metal Oxo, Imido and Alkylidene Complexes. An Overview of their Occurrence, Structure and Applications.	1
1.1 Introduction	2
1.2 Occurrence.	3
1.3. Electronic Structure and Bonding.	5
1.3.1 Bonding Modes.	6
Oxo Complexes.	6
Imido Complexes.	7
Alkylidene Complexes.	9
Cis Multiply Bonded Ligands.	12
1.3.2 Ligand Field Description.	13
1.3.3 The " <i>Spectator Oxo Effect</i> ".	14
1.4 Spectroscopic Properties.	17
1.4.1 ¹ H NMR Spectroscopy.	17
Imido Complexes.	17
Alkylidene Complexes.	18
1.4.2 ¹³ C NMR Spectroscopy.	19
Imido Complexes	19
Alkylidene Complexes.	20
1.5 Olefin Metathesis and Living Ring Opening Metathesis Polymerization.	20
1.5.1 Introduction.	20
1.5.2 The Mechanism of the Olefin Metathesis Reaction.	21
1.5.3 Catalysts for the ROMP of Cyclic Monomers.	22
Classical Catalysts.	22
Well Defined Molybdenum and Tungsten "Schrock type" Catalysts.	23
1.5.4 Living ROMP using Well Defined Initiator Systems.	25

General Considerations.	25
The Mechanism of Living ROMP.	25
Stereochemistry.	29
1.5.5 Living ROMP of Functionalized Norbornene and Norbornadiene Derivatives.	30
1.5.6 Stable Intermediates in the Metathesis Process.	31
1.5.7 Stereoregular Polymerization of 2,3-bis(trifluoromethyl)norbornadiene.	34
1.5.8 Mono-adducts of Imido Alkylidene Complexes.	37
1.6 Heteroatom Exchange Reactions of Multiply Bonded Ligands.	38
1.6.1 Exchange Reactivity with External Organic Substrates.	39
Reaction with Carbonyl Compounds.	39
Reaction with Isocyanates.	39
Reaction with Other Heteroatom Exchange Reagents.	40
1.6.2 Heteroatom Exchange between Metal Centres.	41
1.7 Summary.	42
1.8 References.	42
 Chapter Two - Chain-end Functionalization of Living Polymers formed by Ring Opening Metathesis Polymerization.	 49
2.1 Introduction.	50
2.2 Reaction of Mo(NAr)(CH-t-Bu)(O-t-Bu) ₂ with Para-Substituted Benzaldehydes.	53
2.3 Reaction of Mo(NAr)(CH-t-Bu)(O-t-Bu) ₂ with other Substituted Aldehydes.	57
2.4 2-Oxametallacyclobutane Intermediates.	60
2.5 Solution Stability of 2-Oxametallacycles.	63
2.6 End-Capped Polymers via Reaction with Substituted Benzaldehydes.	65
2.7 Summary.	68
2.8 References.	69

Chapter Three - Styrene Based Chain Transfer Agents for Living Ring Opening Metathesis Polymerization.	71
3.1 Introduction.	72
3.2 Molybdenum Benzylidenes.	76
3.2.1 The Reaction of $\text{Mo}(\text{NAr})(\text{CH-t-Bu})(\text{O-t-Bu})_2$ with Substituted Styrenes.	76
3.2.2 The Reaction of Living Polynorbomene with Substituted Styrenes.	80
3.3 Chain Transfer Experiments.	81
3.3.1 The Norbornene/Styrene Chain Transfer System.	82
3.3.2 The Norbornene/Substituted Styrene Chain Transfer System.	84
3.3.3 The Functionalized Norbornadiene/Styrene Chain Transfer System.	85
3.4 Multiple Pulse Experiments.	86
3.5 Kinetic Study of Benzylidene Formation.	88
3.6 Summary.	91
3.7 References.	91
Chapter Four - Heteroatom Exchange Reactions of Four Coordinate Molybdenum Compounds.	93
4.1 Introduction.	94
4.2 Oxo/Imido Exchange.	95
4.2.1 Reaction of $\text{Mo}(\text{NAr})_2\text{Cl}_2(\text{dme})$ with Li-O-t-Bu. Preparation of $\text{Mo}(\text{NAr})_2(\text{O-t-Bu})_2$ (2).	96
4.2.2 Reaction of $\text{Mo}(\text{O})_2\text{Cl}_2$ with Li-O-t-Bu. Preparation of $\text{Mo}(\text{O})_2(\text{O-t-Bu})_2$ (3).	98
4.2.3 Kinetic Analysis of Oxo/Imido Exchange.	99
4.3 Attempted Preparation of $\text{Mo}(\text{O})_2(\text{OAr})_2$ Complexes.	104
4.4 Further Heteroatom Exchange Reactivity of $\text{Mo}(\text{NAr})_2(\text{O-t-Bu})_2$ (2).	104
4.4.1 Reaction of $\text{Mo}(\text{NAr})_2(\text{O-t-Bu})_2$ (2) with $\text{Mo}(\text{N-t-Bu})_2(\text{O-t-Bu})_2$ (7).	105
4.4.2 Reaction of $\text{Mo}(\text{NAr})_2(\text{O-t-Bu})_2$ (2) with t-BuNH ₂ .	106

4.4.3	Reaction of $\text{Mo}(\text{NAr})_2(\text{O}-t\text{-Bu})_2$ (2) with Benzaldehyde.	107
4.4.4	Reaction of $\text{Mo}(\text{NAr})_2(\text{O}-t\text{-Bu})_2$ (2) with Isocyanates.	108
	(a) NMR studies.	108
	(b) Reaction of $\text{Mo}(\text{NAr})_2(\text{O}-t\text{-Bu})_2$ (2) with excess PhNCO Preparation of $\text{Mo}(\text{N}(\text{Ar})\text{C}(\text{O})\text{N}(\text{Ph}))_2(\text{O}-t\text{-Bu})_2$ (14).	109
4.4.5	Reaction of $\text{Mo}(\text{NAr})_2(\text{O}-t\text{-Bu})_2$ (2) with Dioxygen.	112
4.4.6	Reaction of $\text{Mo}(\text{NAr})_2(\text{O}-t\text{-Bu})_2$ (2) with $\text{PhCH}=\text{N}-t\text{-Bu}$.	112
4.4.7	Factors Affecting Bonding in <i>Cis</i> Multiply Bonded Species.	113
4.4.8	Further Reactivity Studies on $\text{Mo}(\text{NAr})_2(\text{O}-t\text{-Bu})_2$ (2).	114
4.5	Alkoxide Exchange in Four Coordinate Molybdenum Alkylidene Complexes.	115
4.6	Relative Solution State Stabilities of Alkylidene Complexes.	117
	4.6.1 Thermal Stability.	117
	4.6.2 Stability towards Dioxygen.	119
4.7	Heteroatom Exchange in Four Coordinate Alkylidene Complexes.	120
	4.7.1 Thermal Stability of $\text{Mo}(\text{NAr})(\text{CH}-t\text{-Bu})(\text{O}-t\text{-Bu})_2$ (18).	120
	4.7.2 Reaction of $\text{Mo}(\text{NAr})(\text{CH}-t\text{-Bu})(\text{O}-t\text{-Bu})_2$ (18) with $\text{Mo}(\text{O})_2(\text{O}-t\text{-Bu})_2$ (3).	121
	4.7.3 Reaction of $\text{Mo}(\text{NAr})(\text{CH}-t\text{-Bu})(\text{O}-t\text{-Bu})_2$ (18) with $\text{Mo}(\text{N}-t\text{-Bu})_2(\text{O}-t\text{-Bu})_2$ (7).	122
	4.7.4 Reaction of $\text{W}(\text{NAr})(\text{CH}-t\text{-Bu})(\text{O}-t\text{-Bu})_2$ (21) with $\text{Mo}(\text{NAr})_2(\text{O}-t\text{-Bu})_2$ (2).	123
	4.7.5 Reaction of $\text{Mo}(\text{NAr})(\text{CHCMe}_2\text{Ph})(\text{OCMe}(\text{CF}_3)_2)_2$ (16) with $t\text{-BuNH}_2$.	123
	4.7.6 Reaction of $\text{Mo}(\text{NAr})(\text{CHR})(\text{OR}')_2$ with Dioxygen.	126
4.8	Bimolecular Termination in Living ROMP.	129
4.9	Summary.	131
4.10	References.	132

Chapter Five - Synthesis and Heteroatom Exchange Reactivity of Half-Sandwich Imido and Alkylidene Complexes of Niobium and Tantalum.	135
5.1 Introduction.	136
5.2 Reaction of $\text{Cp}^{\circ}\text{NbCl}_4$ with $(\text{TMS})_2\text{NMe}$. <i>Preparation of $\text{Cp}^{\circ}\text{Nb}(\text{NMe})\text{Cl}_2$ (1).</i>	136
5.3 Reaction of $\text{Cp}^{\circ}\text{NbCl}_4$ with ArNHTMS . <i>Preparation of $\text{Cp}^{\circ}\text{Nb}(\text{NAr})\text{Cl}_2$ (2).</i>	137
5.4.1 Reaction of $\text{Cp}^{\circ}\text{TaCl}_4$ with ArNHTMS . <i>Preparation of $\text{Cp}^{\circ}\text{Ta}(\text{NAr})\text{Cl}_2$ (3).</i>	138
5.4.2 The Molecular Structure of $\text{Cp}^{\circ}\text{Ta}(\text{NAr})\text{Cl}_2$ (3).	139
5.5 Imido Exchange Reactivity.	141
5.5.1 Reaction of $\text{Cp}^{\circ}\text{Nb}(\text{NMe})\text{Cl}_2$ (1) with $\text{CpNb}(\text{N-t-Bu})\text{Cl}_2$ (6).	141
5.5.2 Reaction of $\text{Cp}^{\circ}\text{Nb}(\text{NAr})\text{Cl}_2$ (2) with $\text{CpNb}(\text{N-t-Bu})\text{Cl}_2$ (6).	142
5.5.3 Reaction of $\text{Cp}^{\circ}\text{Nb}(\text{NAr})\text{Cl}_2$ (2) with $\text{CpNb}(\text{NMe})\text{Cl}_2$ (5).	143
5.5.4 Reaction of $\text{Cp}^{\circ}\text{Ta}(\text{NAr})\text{Cl}_2$ (3) with $\text{CpNb}(\text{NMe})\text{Cl}_2$ (5).	144
5.5.5 The Mechanism of Imido Exchange.	144
5.5.6 Reaction of $\text{Cp}^{\circ}\text{Ta}(\text{NAr})\text{Cl}_2$ (1) with $\text{Mo}(\text{NAr})(\text{CH-t-Bu})(\text{O-t-Bu})_2$ (12).	146
5.6 Preparation of $\text{CpTa}(\text{CHCMe}_2\text{Ph})\text{Cl}_2$ (15).	147
5.6.1 Reaction ZnCl_2 with $\text{PhMe}_2\text{CCH}_2\text{MgCl}$. <i>Preparation of $\text{Zn}(\text{CH}_2\text{CMe}_2\text{Ph})_2$ (17).</i>	147
5.6.2 Reaction of $\text{Zn}(\text{CH}_2\text{CMe}_2\text{Ph})_2$ (17) with TaCl_5 . <i>Preparation of $\text{Ta}(\text{CH}_2\text{CMe}_2\text{Ph})_2\text{Cl}_3$ (18).</i>	148
5.6.3 Reaction of $\text{Ta}(\text{CH}_2\text{CMe}_2\text{Ph})_2\text{Cl}_3$ (18) with TiCp . <i>Preparation of $\text{CpTa}(\text{CHCMe}_2\text{Ph})\text{Cl}_2$ (15).</i>	149
5.7 Investigation of the Alkylidene Exchange Reactivity of $\text{CpTa}(\text{CHCMe}_2\text{Ph})\text{Cl}_2$ (15).	151
5.7.1 Reaction of $\text{CpTa}(\text{CHCMe}_2\text{Ph})\text{Cl}_2$ (15) with $\text{Cp}^{\circ}\text{Ta}(\text{NAr})\text{Cl}_2$ (3).	151
5.7.2 Reaction of $\text{CpTa}(\text{CHCMe}_2\text{Ph})\text{Cl}_2$ (15) with $\text{Cp}^{\circ}\text{Nb}(\text{NAr})\text{Cl}_2$ (2).	152
5.7.3 Reaction of $\text{CpTa}(\text{CHCMe}_2\text{Ph})\text{Cl}_2$ (15) with $\text{Mo}(\text{N-t-Bu})_2\text{Cl}_2$ (21).	152

5.7.4 Reaction of CpTa(CHCMe ₂ Ph)Cl ₂ (15) with Mo(N- <i>t</i> -Bu) ₂ (O- <i>t</i> -Bu) ₂ (24).	153
5.8 Summary.	154
5.9 References.	155
 Chapter Six - Experimental Details.	 157
6.1 General.	158
6.1.1 Experimental Techniques.	158
6.1.2 Solvents and Reagents.	159
6.2 Experimental Details to Chapter Two.	161
6.2.1 Typical Capping Reaction of Mo(NAr)(CH- <i>t</i> -Bu)(O- <i>t</i> -Bu) ₂ with a Substituted Benzaldehyde.	161
6.2.2 ¹ H NMR observation of 2-Oxametallacycles.	161
(a) Mo(NAr)[CH(CMe ₃)CH(C ₆ H ₅)O](O- <i>t</i> -Bu) ₂ .	162
(b) Mo(NAr)[CH(CMe ₂ Ph)CH(C ₆ H ₅)O](O- <i>t</i> -Bu) ₂ .	162
(c) Mo(NAr)[CH(CMe ₃)CH(<i>p</i> -CNC ₆ H ₄)O](O- <i>t</i> -Bu) ₂ .	162
(d) Mo(NAr)[CH(CMe ₃)CH(<i>p</i> -NO ₂ C ₆ H ₄)O](O- <i>t</i> -Bu) ₂ .	162
(e) Mo(NAr)[CH(CMe ₃)CH(<i>p</i> -CHOC ₆ H ₄)O](O- <i>t</i> -Bu) ₂ .	163
(f) Mo(NAr)[CH(CMe ₃)CH(<i>p</i> -MeO ₂ CC ₆ H ₄)O](O- <i>t</i> -Bu) ₂ .	163
6.2.3 Typical Formation of polynorbornene capped with a <i>p</i> -substituted benzaldehyde.	163
6.3 Experimental Details to Chapter Three.	164
6.3.1 Typical Reaction of Mo(NAr)(CH- <i>t</i> -Bu)(O- <i>t</i> -Bu) ₂ with a substituted styrene derivative.	164
(a) Mo(NAr)(CHC ₆ H ₅)(O- <i>t</i> -Bu) ₂ .	164
(b) Mo(NAr)(CH- <i>p</i> -CH ₃ C ₆ H ₄)(O- <i>t</i> -Bu) ₂ .	165
(c) Mo(NAr)(CH- <i>p</i> -ClC ₆ H ₄)(O- <i>t</i> -Bu) ₂ .	165
(d) Mo(NAr)(CH- <i>p</i> -CH ₃ OC ₆ H ₄)(O- <i>t</i> -Bu) ₂ .	165
(e) Mo(NAr)(CH-3,5-(CF ₃) ₂ C ₆ H ₃)(O- <i>t</i> -Bu) ₂ .	166

6.3.2	Typical NMR Scale Chain Transfer Experiment Employing Norbornene.	166
6.3.3	Typical Preparative Scale Chain Transfer Experiment.	166
6.3.4	Typical Chain Transfer "Pulse" Experiment.	167
6.3.5	Reaction of $\text{Mo}(\text{NAr})(\text{CH-}t\text{-Bu})(\text{O-}t\text{-Bu})_2$ with Substituted Styrenes. <i>¹H NMR Determination of the Rate of Benzylidene Formation.</i>	168
6.4	Experimental Details to Chapter Four.	168
6.4.1	Reaction of $\text{Mo}(\text{NAr})_2\text{Cl}_2(\text{dme})$ with Li-O- <i>t</i> -Bu. <i>Preparation of $\text{Mo}(\text{NAr})_2(\text{O-}t\text{-Bu})_2$ (2).</i>	168
6.4.2	Reaction of $\text{Mo}(\text{O})_2\text{Cl}_2$ with Li-O- <i>t</i> -Bu. <i>Preparation of $\text{Mo}(\text{O})_2(\text{O-}t\text{-Bu})_2$ (3).</i>	169
6.4.3	Reaction of $\text{Mo}(\text{NAr})_2(\text{O-}t\text{-Bu})_2$ (2) with $\text{Mo}(\text{O})_2(\text{O-}t\text{-Bu})_2$ (3). <i>Determination of the Rate of Equilibration with $\text{Mo}(\text{NAr})(\text{O})(\text{O-}t\text{-Bu})_2$ (1).</i>	170
6.4.4	¹ H NMR Investigation of $\text{Mo}(\text{NAr})_2(\text{O-}t\text{-Bu})_2$ (2) Reactivity. Reagents Used.	171 171
6.4.5	Reaction of $\text{Mo}(\text{NAr})_2(\text{O-}t\text{-Bu})_2$ (2) with PhNCO. <i>Preparation of $\text{Mo}[\text{N}(\text{Ar})\text{C}(\text{O})\text{N}(\text{Ph})]_2(\text{O-}t\text{-Bu})_2$ (14).</i>	172
6.4.6	Alkoxide Exchange in Four Coordinate Alkylidene Complexes.	173
6.4.6a	Reaction of $\text{Mo}(\text{NAr})(\text{CHCMe}_2\text{Ph})(\text{O-}t\text{-Bu})_2$ (15) with $\text{Mo}(\text{NAr})(\text{CHCMe}_2\text{Ph})(\text{OCMe}(\text{CF}_3)_2)_2$ (16). <i>Preparation of $\text{Mo}(\text{NAr})(\text{CHCMe}_2\text{Ph})(\text{OCMe}(\text{CF}_3)_2)(\text{O-}t\text{-Bu})$ (17)</i>	173
6.4.6b	¹ H NMR Investigation of Alkoxide Exchange in Four Coordinate Alkylidene Complexes.	174
6.4.7	¹ H NMR Investigation of Alkylidene Exchange in Four Coordinate Alkylidene Complexes. Reagents Used.	174 175
	NMR Data for:	
	(a) <i>syn</i> $\text{Mo}(\text{NAr})(\text{CHCMe}_2\text{Ph})(\text{OCMe}(\text{CF}_3)_2)_2(t\text{-BuNH}_2)$ (24)	175
	(b) <i>anti</i> $\text{Mo}(\text{NAr})(\text{CHCMe}_2\text{Ph})(\text{OCMe}(\text{CF}_3)_2)_2(t\text{-BuNH}_2)$ (25)	175
6.5	Experimental Details to Chapter Five.	176
6.5.1	Reaction of Cp^*NbCl_4 with $(\text{TMS})_2\text{NMe}$. <i>Preparation of $\text{Cp}^*\text{Nb}(\text{NMe})\text{Cl}_2$ (1).</i>	176
6.5.2	Reaction of Cp^*NbCl_4 with ArNHTMS . <i>Preparation of $\text{Cp}^*\text{Nb}(\text{NAr})\text{Cl}_2$ (2).</i>	177

6.5.3	Reaction of Cp^*TaCl_4 with ArNHTMS . <i>Preparation of $\text{Cp}^*\text{Ta}(\text{NAr})\text{Cl}_2$ (3).</i>	178
6.5.4	^1H NMR Investigation of Imido Exchange.	179
6.5.5	Preparation of $\text{CpTa}(\text{CHCMe}_2\text{Ph})\text{Cl}_2$ (15).	180
6.5.5a	Reaction ZnCl_2 with $\text{PhMe}_2\text{CCH}_2\text{MgCl}$. <i>Preparation of $\text{Zn}(\text{CH}_2\text{CMe}_2\text{Ph})_2$ (17).</i>	180
6.5.5b	Reaction of $\text{Zn}(\text{CH}_2\text{CMe}_2\text{Ph})_2$ (17) with TaCl_5 . <i>Preparation of $\text{Ta}(\text{CH}_2\text{CMe}_2\text{Ph})_2\text{Cl}_3$ (18).</i>	180
6.5.5c	Reaction of $\text{Ta}(\text{CH}_2\text{CMe}_2\text{Ph})_2\text{Cl}_3$ (18) with TiCp . <i>Preparation of $\text{CpTa}(\text{CHCMe}_2\text{Ph})\text{Cl}_2$ (15).</i>	181
6.5.6	^1H NMR Investigation of the Alkylidene Exchange Reactivity of $\text{CpTa}(\text{CHCMe}_2\text{Ph})\text{Cl}_2$ (15).	182
	Reagents Used.	183
6.6	Further Experimental Details.	183
6.6.1	Preparation of $\text{Mo}(\text{NAr})(\text{CH-}t\text{-Bu})(\text{O-}t\text{-Bu})_2$.	183
6.6.1a	Preparation of $\text{Mo}(\text{NAr})_2\text{Cl}_2(\text{dme})$.	183
6.6.1b	Reaction of $\text{Mo}(\text{NAr})_2\text{Cl}_2(\text{dme})$ with $\text{Me}_3\text{CCH}_2\text{MgCl}$. <i>Preparation of $\text{Mo}(\text{NAr})_2(\text{CH}_2\text{CMe}_3)_2$.</i>	184
6.6.1c	Reaction of $\text{Mo}(\text{NAr})_2(\text{CH}_2\text{CMe}_3)_2$ with $\text{CF}_3\text{SO}_3\text{H}$. <i>Preparation of $\text{Mo}(\text{NAr})(\text{CH-}t\text{-Bu})(\text{OSO}_2\text{CF}_3)_2(\text{dme})$.</i>	184
6.6.1d	Reaction of $\text{Mo}(\text{NAr})(\text{CH-}t\text{-Bu})(\text{OSO}_2\text{CF}_3)_2(\text{dme})$ with $\text{Li-O-}t\text{-Bu}$. <i>Preparation of $\text{Mo}(\text{NAr})(\text{CH-}t\text{-Bu})(\text{O-}t\text{-Bu})_2$.</i>	185
6.6.2	Reaction of $\text{Mo}(\text{O})_2\text{Cl}_2$ with $\text{Li-O-}t\text{-Bu}$. <i>Preparation of $\text{Mo}(\text{O})_2\text{Cl}_2 \cdot \text{Li}$</i>	185
6.6.3	Reaction of $\text{Cp}^*\text{Ta}(\text{NAr})\text{Cl}_2$ with $\text{Li-O-}t\text{-Bu}$. <i>Preparation of $\text{Cp}^*\text{Ta}(\text{NAr})(\text{O-}t\text{-Bu})\text{Cl}$.</i>	186
6.6.4	Reaction of $\text{Cp}^*\text{Ta}(\text{N-}t\text{-Bu})\text{Cl}_2$ with $\text{Me}_3\text{CCH}_2\text{MgCl}$. <i>Preparation of $\text{Cp}^*\text{Ta}(\text{N-}t\text{-Bu})(\text{CH}_2\text{CMe}_3)\text{Cl}$.</i>	187
6.7	References.	188

Appendices.	189
Appendix 1:	190
Crystal Data for Cp [*] Ta(NAr)Cl ₂ .	190
Appendix 2:	191
First Year Induction Courses.	191
Research Colloquia and Lectures Organized by the Department of Chemistry During the Period 1988 - 1991.	191
Conferences and Symposia Attended.	202
Publications.	203
Appendix 3:	204
Synthesis and Characterization of Mo(O) ₂ Cl ₂ . Li	204
Synthesis and Characterization of Cp [*] Ta(NAr)(O-t-Bu)Cl.	205
Synthesis and Characterization of Cp [*] Ta(N-t-Bu)(CH ₂ CMe ₃)Cl.	206
References.	207

CHAPTER ONE

Transition Metal Oxo, Imido and Alkylidene Complexes. An Overview of their Occurrence, Structure and Applications.



1.1 Introduction.

This thesis is concerned primarily with the chemistry of mononuclear complexes in which a first row main group element - carbon, nitrogen, or oxygen - is multiply bonded to a transition metal of the group 5 or 6 triad.

This field of chemistry has expanded rapidly in recent years and it is now evident that it will remain an active area of industrial and academic research for many years to come. One of the principal factors governing the rapid growth of interest in this area is the vast range of important chemical processes in which complexes containing these multiply bonded ligands play a catalytic role, ranging from acting as homogeneous or heterogeneous catalysts to being involved in a wide number of enzymatic reactions.

However, as yet, we are only just beginning to understand the potential reactivity of such species. Therefore the aim of this thesis is to prepare a range of early transition metal complexes possessing oxo, imido and alkylidene moieties in different ligand environments, and to evaluate their reactivity. This includes the exchange of these ligands (either between two metal centres or to and from external substrates) and the use of such complexes as initiators in Ring Opening Metathesis Polymerization (ROMP). This thesis is therefore divided into two closely related, but distinct, areas.

Chapters 2 and 3 consider the use of metal alkylidene complexes for the preparation of well defined polymers via living ROMP. In particular, chapter 2 describes how important and potentially useful functional groups may be introduced to the end of these polymer chains via reaction of "living" oligomers with a variety of substituted aldehyde derivatives, whilst chapter 3 describes the use of styrene based derivatives to act as chain transfer agents in these living ROMP systems.

Chapters 4 and 5 describe "heteroatom exchange" reactions of oxo, imido and alkylidene complexes. Chapter 4 describes such reactions in four coordinate molybdenum complexes, whilst chapter 5 discusses imido and alkylidene exchange reactivity in a series of half sandwich compounds of the type $\text{Cp}'\text{M}(\text{NR})\text{Cl}_2$ ($\text{Cp}' = \text{C}_5\text{H}_5, \text{C}_5\text{Me}_5$; $\text{M} = \text{Nb}, \text{Ta}$; $\text{R} = \text{Me}, \text{t-Bu}, \text{NAr}$) and $\text{CpTa}(\text{CHCMe}_2\text{Ph})\text{Cl}_2$.

The remainder of this chapter is devoted to a review of metal oxo, imido, and alkylidene chemistry and is divided into three sections.

The first section (1.2 - 1.4) discusses general aspects of oxo, imido and alkylidene chemistry, including their occurrence, structure and bonding. The middle section (1.5) gives a general overview of the olefin metathesis reaction and the use of well defined transition metal alkylidene complexes as initiators in living ROMP. The final section (1.6) details the "heteroatom exchange" reactivity of transition metal multiply bonded units.

1.2 Occurrence.

Figure 1.1 summarises those *structurally characterized* complexes with metal oxo, imido and alkylidene ligands as a function of the position of the metal in the periodic table.

Whilst relatively few compounds are structurally characterized, this figure gives a realistic view of the overall distribution of these compounds, as a heavy emphasis is placed on structural studies in this area of chemistry.

As can clearly be seen, metals in groups 5, 6 and 7 tend to dominate with only a few examples from the late transition metals and the group 4 metals. The distribution is concentrated along the diagonal from vanadium to rhenium.

Figure 1.2 shows the distribution of complexes with these multiply bonded ligands as a function of d electron count.

As can be seen, all the titanium, niobium and tantalum structures are d^0 . Vanadium readily forms multiple bonds in both d^0 and d^1 configurations whilst chromium, molybdenum and tungsten form strong multiple bonds even even for the configuration d^2 .

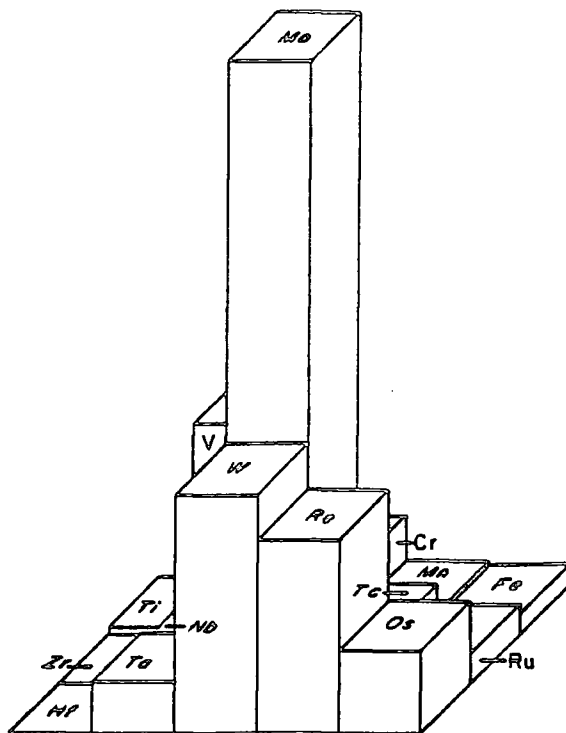


Figure 1.1 *Distribution of structurally characterized compounds with metal ligand multiple bonds in groups IVa-VIII as a function of position in the Periodic Table.*

G	G	G	G	G
IVa	Va	VIa	VIIa	VIII
Ti	V	Cr	Mn	Fe
d^0	$d^{0,1}$	$d^{0,1,2}$	$d^{0,1}$	d^4
Zr	Nb	Mo	Tc	Ru
	d^0	$d^{0,1,2}$	$d^{1,2}$	$d^{0,2,4}$
Hf	Ta	W	Re	Os
	d^0	$d^{0,1,2}$	$d^{0,1,2,4,5}$	$d^{0,2}$

Figure 1.2 *Distribution of structurally characterised compounds with metal ligand multiple bonds in groups IVa-VIII as a function of d electron count.*

Thus, on moving left to right across the periodic table, multiple bonding is found in higher d electron configurations. Electron counts exceeding five are not observed due to significant antibonding that occurs as the metal d-orbitals become filled. Complexes with greater than one multiply bonded ligand also show a similar trend. Vanadium forms di-oxo complexes only in the +5 oxidation state (d^0) whilst rhenium and osmium often form d^2 complexes with two multiply bonded ligands. Only two structures of d^1 complexes with greater than one multiply bonded ligand are known; MnO_4^{2-} and ReO_2R_2 ; instead, d^1 complexes prefer dimeric structures, having both terminal and bridging ligands, such as the common structures A and B shown in figure 1.3.

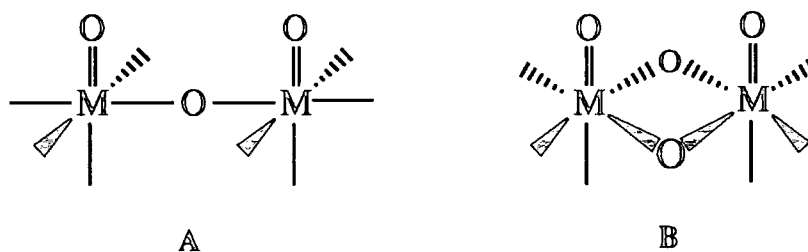


Figure 1.3 Common d^1 oxo structures.

The origin of this diagonal trend of multiple bonds is not fully understood, but is almost certainly related to energy and extension changes of metal d orbitals across the periodic table. The very early transition metals have higher energy diffuse d orbitals, and therefore form more ionic, less covalent bonds, whilst, for the late transition metals the d orbitals become too contracted for good π bonding and bridged structures are favoured.

1.3 Electronic Structure and Bonding.

This section serves to give a brief outline of the possible modes of coordination of transition metal oxo, imido and alkylidene complexes, and simple bonding descriptions of such species.

1.3.1 Bonding Modes.

Oxo Complexes.

Oxo complexes exhibit a wide range of bonding modes, as shown in Figure 1.4 below.

Only terminal oxo species (structures 1, 2 and 3) will be discussed.

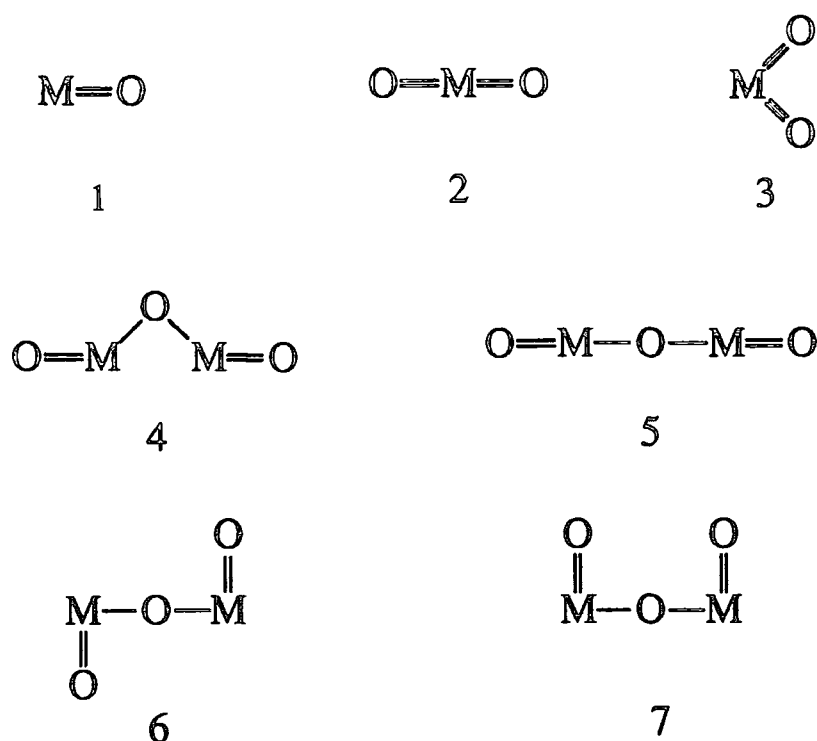
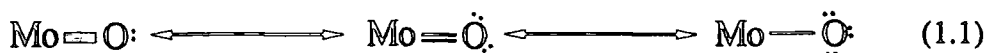


Figure 1.4 Some coordination modes of oxo ligands.

The description of oxo ligands as closed shell anions means that the p-orbitals are filled. Therefore a metal with empty d-orbitals (i.e. high oxidation state, low d electron count) is needed for productive π -bonding to this ligand. The vast majority of metal oxo compounds therefore have d^0 , d^1 or d^2 electronic configurations whilst only recently have a few d^4 and two d^5 complexes been prepared³⁻⁸.

Metal-oxo compounds appear to have bond orders ranging from three to one as shown in equation 1.1, with the high electronegativity of oxygen enabling it to tolerate

three lone pairs. Mono-oxo compounds usually contain metal-oxygen triple bonds, but for di-oxo complexes, the bond order is lower, as discussed later in this section.



Imido Complexes.

Five different bonding modes for the imido moiety have been established. These are shown in Figure 1.5, but again, only terminally bonded imido units (1 and 2) will be discussed.

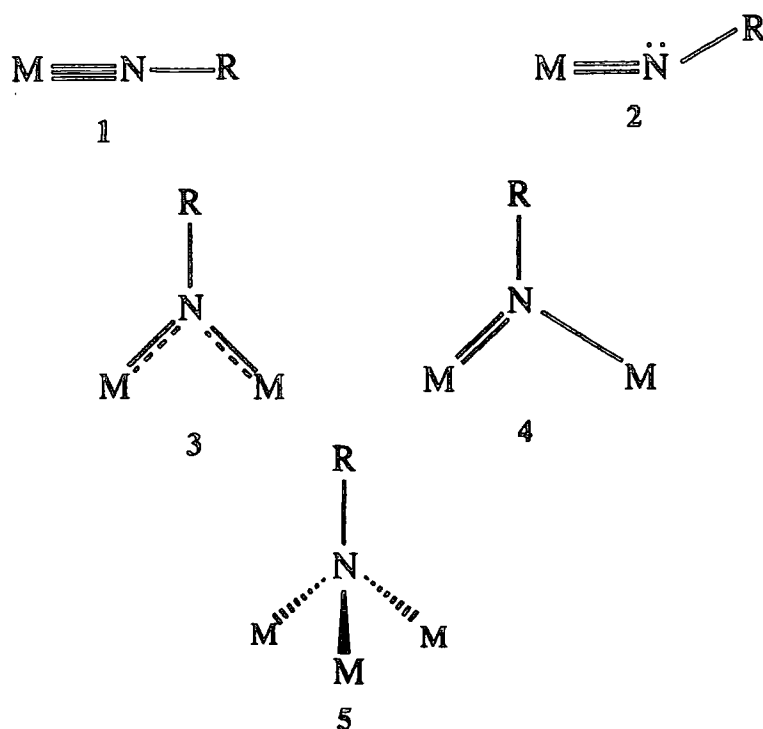


Figure 1.5 Bonding modes of imido ligands.

The most commonly observed arrangement is that shown in structure 1. A linear M-N-R arrangement implies that there is a metal nitrogen triple bond, formed by donation of the nitrogen lone pair of electrons to an empty metal d orbital. We therefore have a σ and two π bonds and the nitrogen is sp -hybridised. Bending of the terminal

imido unit (structure 2) implies the presence of a lone pair of electrons on the nitrogen and thus the bond order is reduced⁹.

Structure 2 is expected when the nitrogen lone pair cannot be donated to the metal, i.e. when a linear triply bonded ligand would cause the electron count to exceed 18 electrons (the effective atomic number rule)^{9,10}. In orbital terms, this occurs when the metal has filled d orbitals or when there is competition for this orbital with other π bonded ligands, thus allowing only one metal orbital of π symmetry to be available for bonding to nitrogen.

However, recently the validity of the assumption that linear or near-linear species donate the electron pair from the nitrogen to the metal has been questioned. Schrock and co-workers have prepared the terminal osmium imido species $\text{Os}(\text{N}-2,6\text{-iPr}_2\text{C}_6\text{H}_3)_3$. This "apparently 20 electron" trigonal planar species has Os-N-C bond angles of $178.0 (5)^\circ$ and 180° (by symmetry) and thus possesses linear imido units¹¹. Similarly, the related bis phosphine complex $\text{Os}(\text{N}-2,6\text{-iPr}_2\text{C}_6\text{H}_3)_2(\text{PMe}_2\text{Ph})_2$ has an Os-N-C bond angle of $177.9 (5)^\circ$ ¹¹. Schrock proposes that an electron pair in both these complexes is located in a nitrogen centered non-bonding orbital made up of the symmetric combination of two in-plane p-orbitals on the nitrogen atoms. The structure of the recently reported "20 electron" zirconium imido complex, $\text{Cp}_2\text{Zr}(\text{N}-t\text{-Bu})(\text{thf})$, with a Zr-N-C bond angle of $174.4 (3)^\circ$ also agrees with Schrock's observations¹².

There is only one example of a structurally characterized bent imido ligand, in the complex $\text{Mo}(\text{NPh})_2(\text{S}_2\text{CNET}_2)_2$ (Figure 1.6)¹³. This shows both a bent imido group (Mo-N-C bond angle of $139.9 (4)^\circ$) and a near linear imido group (Mo-N-C bond angle of $169.4 (4)^\circ$). This molecule is described as having one nitrogen triple bond (Mo-N = 1.754\AA) and one double bond (Mo-N = 1.789\AA), using the three d-orbitals of π symmetry on the molybdenum centre.

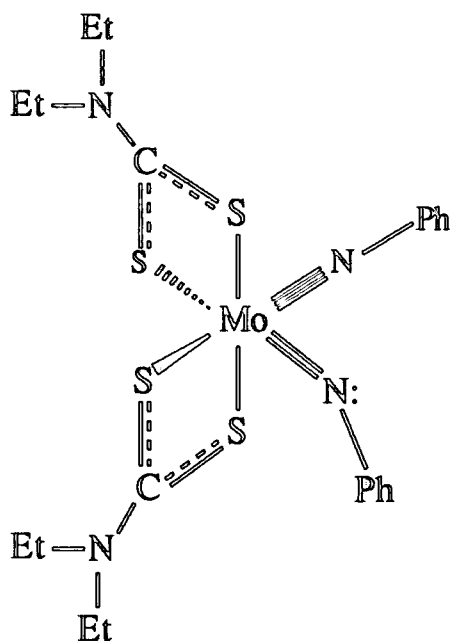


Figure 1.6 Molecular structure of $\text{Mo}(\text{NPh})_2(\text{S}_2\text{CNEt}_2)_2$.

Alkylidene Complexes.

The alkylidene ligand is different from the oxo and imido ligands discussed previously in that it is a single faced π donor and as such can only form one metal carbon π bond and therefore at most form a double bond .

Alkylidene ligands are best described as CR_2^{2-} only when they are bound to a high oxidation state metal centre and lack heteroatom substituents. These type of alkylidenes are the so called "Schrock type"; the first to be synthesised being $\text{Ta}(\text{CH-t-Bu})(\text{CH}_2\text{-t-Bu})_3$ prepared in 1973 during an attempted preparation of pentakisneopentyl tantalum (V)¹⁴. When treated as a neutral CR_2 ligand, in particular when the carbon atom bears a substituent with lone pairs (such as OR, SR, NR_2 etc), the ligand is classed as a "Fischer carbene".

At a simple level, the bonding in Fischer carbene and Schrock alkylidene ligands is similar, with Schrock alkylidenes tending to be more electron rich and therefore nucleophilic due to the diffuse, high energy orbitals of the early transition metal^{15,16}. This bonding has been the subject of several *ab initio* studies¹⁷⁻²⁴. These suggest that

the metal carbon interaction consists of a σ and a π bond and that this can be of two distinct types, as shown in Figure 1.7.

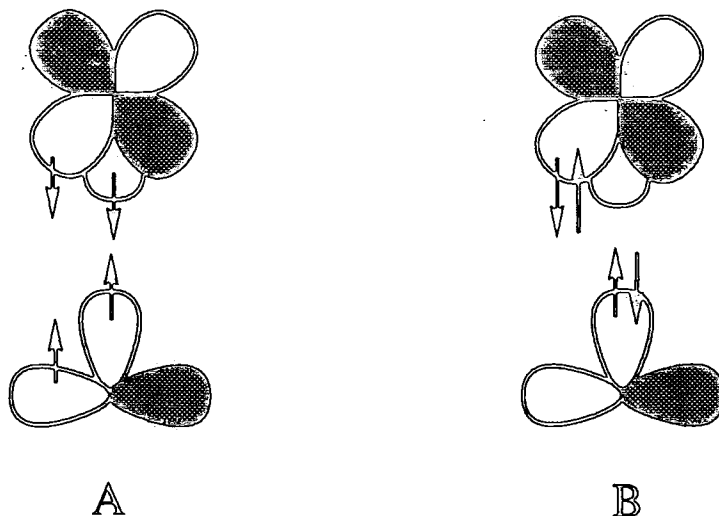


Figure 1.7 *Schematic picture of two types of metal-alkylidene bonding : ethylene like covalent bonding (A) and donor-acceptor bonding (B).*

Type (A) is a covalent bond resembling the carbon-carbon interaction in ethylene and depicts the interaction of a triplet alkyldiene fragment with a triplet metal centre. Type (B) involves a singlet carbene with donation of a lone pair from the carbon into an empty metal orbital, this being stabilized by backbonding from a filled metal orbital into a vacant carbene p-orbital. This resembles the Dewar-Chatt-Duncanson model for an olefin binding to a metal centre²⁵.

The carbene fragments in Fischer complexes have substituents with $p\pi$ lone pairs and have singlet ground states. These therefore resemble type (B) and are commonly low valent late transition metal complexes. However, alkyldienes with only hydrogen or alkyl substituents (CH_2 , CHR , CRR'), as found in Schrock alkyldienes, have triplet ground states and thus prefer the type of bonding depicted in (A). Complexes of this type are typically of the early transition metals in high oxidation states possessing few d electrons.

These bonding pictures explain the different reactivity of Schrock and Fischer complexes. Singlet carbene species (as in B) are electrophilic because they have an empty orbital on the carbon (albeit stabilized by metal backbonding). Triplet species (type A), on the other hand, have two covalent bonds and are nucleophilic at the carbon centre (as in ethylene).

Schrock type alkylidene complexes of the form $L_nM=CHR$ often show a large distortion about the alkylidene carbon, with large M-C-R angles, short M-H distances and low C-H stretching frequencies and coupling constants. At least two theoretical explanations have been offered to account for this distortion (figure 1.8).

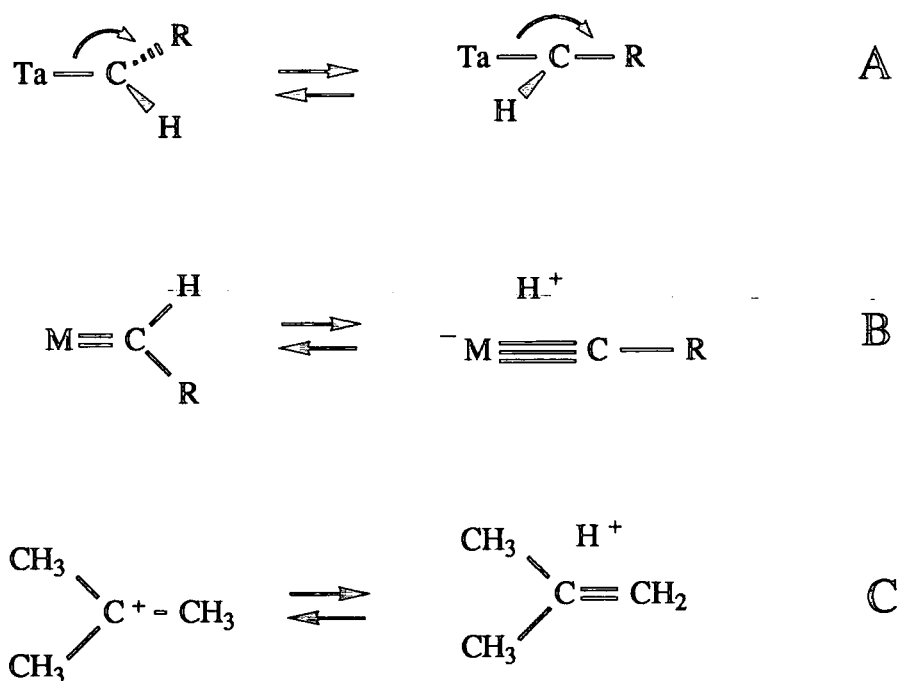


Figure 1.8

Hoffmann²⁶ has suggested that there is rotation of the alkylidene ligand (A in Figure 1.8), which allows overlap of the alkylidene σ orbital with an additional empty metal d-orbital. Metal-hydrogen overlap and thus weakening of the C-H bond occur as a secondary interaction, suggestive of an α -agostic bond.

Hehre²⁷, on the other hand, concludes that the distortion is due to hyperconjugation (B), by comparison with carbocations (C).

Cis Multiply Bonded Ligands.

In d^0 complexes containing cis multiply bonded oxo or imido ligands, the three d-orbitals available for π bonding to these atoms must be shared between the two ligands. This lack of available orbitals means that the formation of two triple bonds is not possible; one ligand can form at most a double bond, thus reducing the overall bond order^{28,29,30}.

If π bonding to other ligating atoms is ignored, there are three general structures which complexes of the type $M(O)_2$, $M(NR)_2$ and $M(O)(NR)$ can adopt. These are shown in Figure 1.9²⁸.

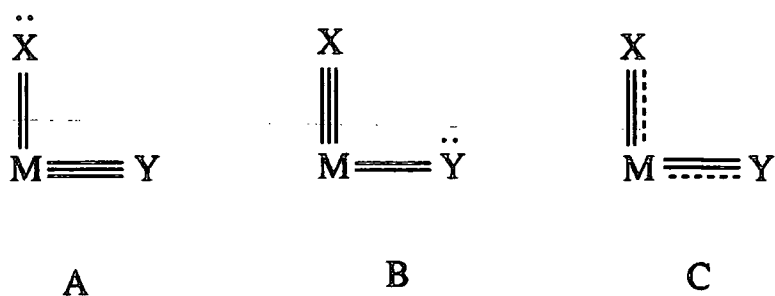


Figure 1.9 Possible bonding modes for $M(X)(Y)$

In structure A, the group designated by Y serves as a four electron donor whilst X is a two electron donor. In structure B, this ordering is reversed, with an additional lone pair of electrons being present on the ligands if X and Y are oxygen atoms. The electron density of either of these forms will be polarized toward the group which is linked to the metal by a double bond. Structure C can be considered as intermediate between structures A and B, and for this no polarization will be apparent.

The identical bond lengths in $Mo(O)_2(Pr_2dtc)_2$ ($Mo-O = 1.696(5) \text{ \AA}$)³¹ indicate that structure C ($X = Y = O$) most accurately describes the true structure of this

complex, whereas for $\text{Mo}(\text{O})_2(\text{acac})_2$ ³² ($\text{Mo}-\text{O} = 1.64 (2) \text{ \AA}, 1.72 (2) \text{ \AA}$) and $\text{Mo}(\text{O})_2\text{Br}_2(\text{bipy})$ ³³ ($\text{Mo}-\text{O} = 1.643 (17) \text{ \AA}, 1.826 (18) \text{ \AA}$), significantly different Mo-O bond lengths within each $\text{Mo}(\text{O})_2$ fragment indicate that the solid state structures of these are heavily weighted in favour of one of the equivalent polarized forms. One of the polarized forms is definitely favoured for $\text{Mo}(\text{NPh})_2(\text{Et}_2\text{dtc})_2$ ($X = Y = \text{NPh}$) as described earlier in this section¹³.

1.3.2 Ligand Field Description.

The vast majority of transition metal complexes containing multiply bonded ligands are six coordinate octahedral species. These are the easiest to analyze in molecular orbital terms because the σ and π orbitals are separate due to the high symmetry. Regardless of π interactions, all octahedral complexes have the same σ bonding framework. For a molecule assumed to have full octahedral symmetry, the five metal d-orbitals split into a degenerate e_g set ($d_x^2 - y^2, d_z^2$) of σ^* character and a nonbonding t_{2g} set (d_{xy}, d_{xz}, d_{yz}). Introduction of a single oxo, or triply bonded imido ligand lowers the symmetry to C_{4v} and splits the degeneracy of both the e_g and t_{2g} orbitals (Figure 1.10).

The e_g set is essentially unchanged since both orbitals remain σ^* ; the t_{2g} orbitals, however, are substantially split since two are now involved in π bonding (d_{xz} and d_{yz} if the metal-ligand bond is along the z-axis). Thus the ligand field portion of the molecular orbital diagram contains a non-bonding d_{xy} orbital, a π^* set and two σ^* levels. It should be noted that in this symmetry, the two π orbitals are degenerate and, unless the π^* orbitals are occupied, the multiple π bond must be regarded as a triple bond.

Compounds with more than one multiply bonded ligand adopt geometries that maximize π -bonding and minimize population of the π^* -antibonding orbitals. Therefore d^0 dioxo and bis-imido complexes prefer cis geometries so that all three d_π orbitals can be used in bonding. Compounds with both an alkylidene unit and an oxo or imido unit are all d^0 and have the 'CHR' and 'O' or 'NR' ligands aligned in the same plane so that

the alkylidene ligand π bonds with the one metal orbital not used in π -bonding to the other multiply bonded ligand.

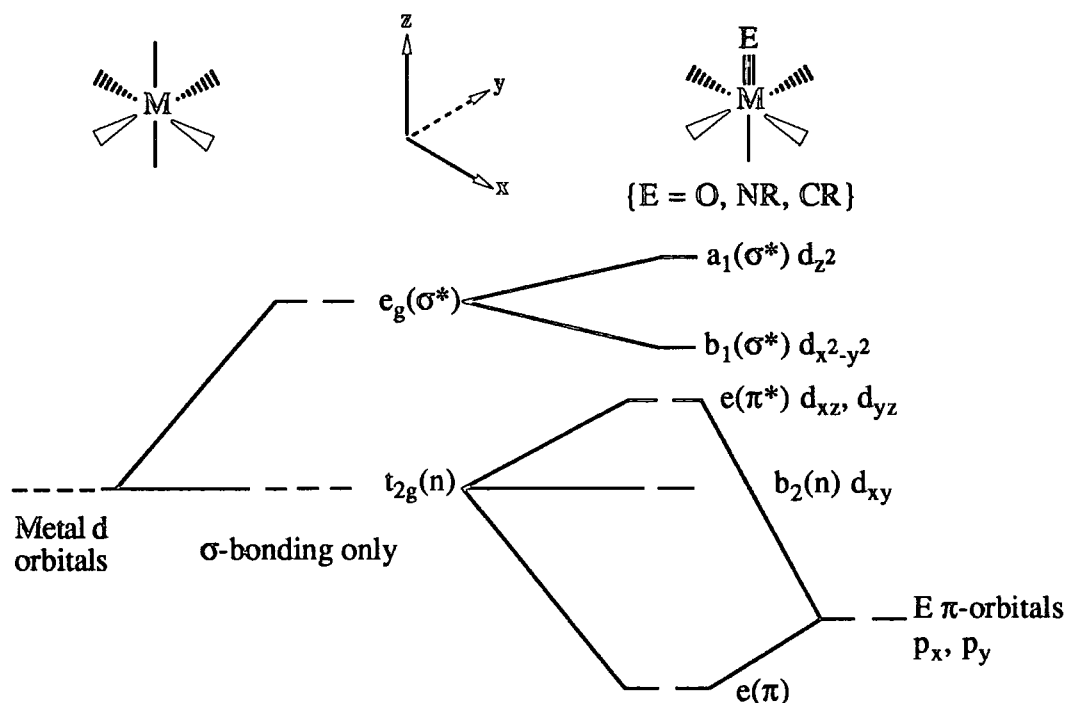


Figure 1.10 *Partial molecular orbital diagram for an octahedral complex with one oxo, linear imido or alkylidyne ligand*

1.3.3 The "Spectator Oxo Effect".

Goddard and Rappe have applied *ab initio* calculations to the study of a range of oxo and alkylidene complexes^{34,35,36}. The conclusions of these agree with the arguments above in that for complexes with one oxo group the M-O bond is a triple bond, whereas for di-oxo compounds the bond order is lowered. Moreover, these triple bonds were suggested to be composed of two covalent π bonds and a donor-acceptor σ bond formed by overlap of empty metal d-orbital with a lone pair on the oxygen atom pointing directly at the metal.

The most important conclusion of these calculations was that the increase in bond strength upon conversion of a metal oxygen double bond to a triple bond could provide a driving force for reactions occurring at a metal centre. Such an effect is known as the "*Spectator Oxo Effect*".

Thus, the reaction of $\text{Mo}(\text{O})_2\text{Cl}_2$ with an olefin is calculated to be 70 kcal mol^{-1} more favourable than the corresponding reaction with $\text{Mo}(\text{O})\text{Cl}_4$ (Figure 1.11)³⁴.

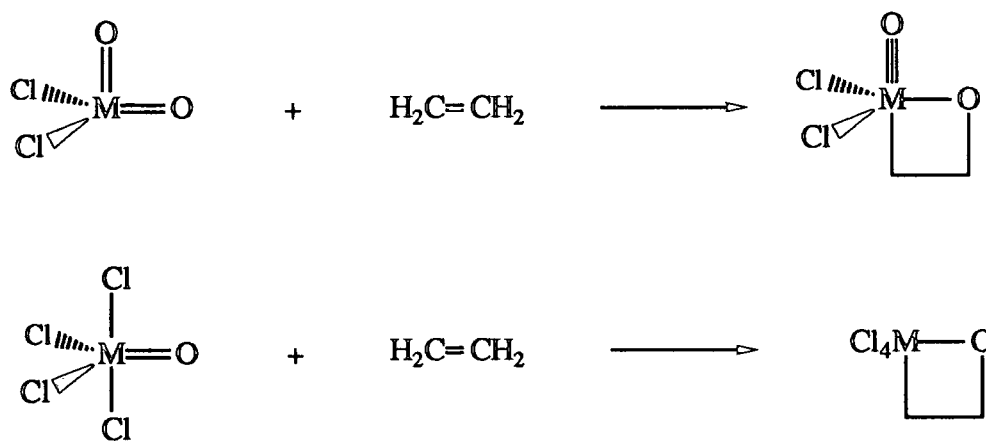


Figure 1.11 *Oxo Ligand Spectator Effect*

Similarly, for alkylidene complexes reacting with olefins, formation of a metallacycle is favoured in the presence of an oxo group. Figure 1.12 shows the proposed energetics for the reaction of ethylene with both $\text{Mo}(\text{CH}_2)\text{Cl}_4$ and $\text{Mo}(\text{O})(\text{CH}_2)\text{Cl}_2$. For the latter complex, the increased strength of the triply bonded oxo group on the metallacyclic intermediate versus the double bonded oxo of the alkylidene complex provides significant driving force for the reaction. Calculations for the model compound $\text{Mo}(\text{CH}_2)\text{Cl}_4$, with no spectator oxo, show this process to be endothermic by 15 kcal mol^{-1} (Figure 1.12)³⁴.

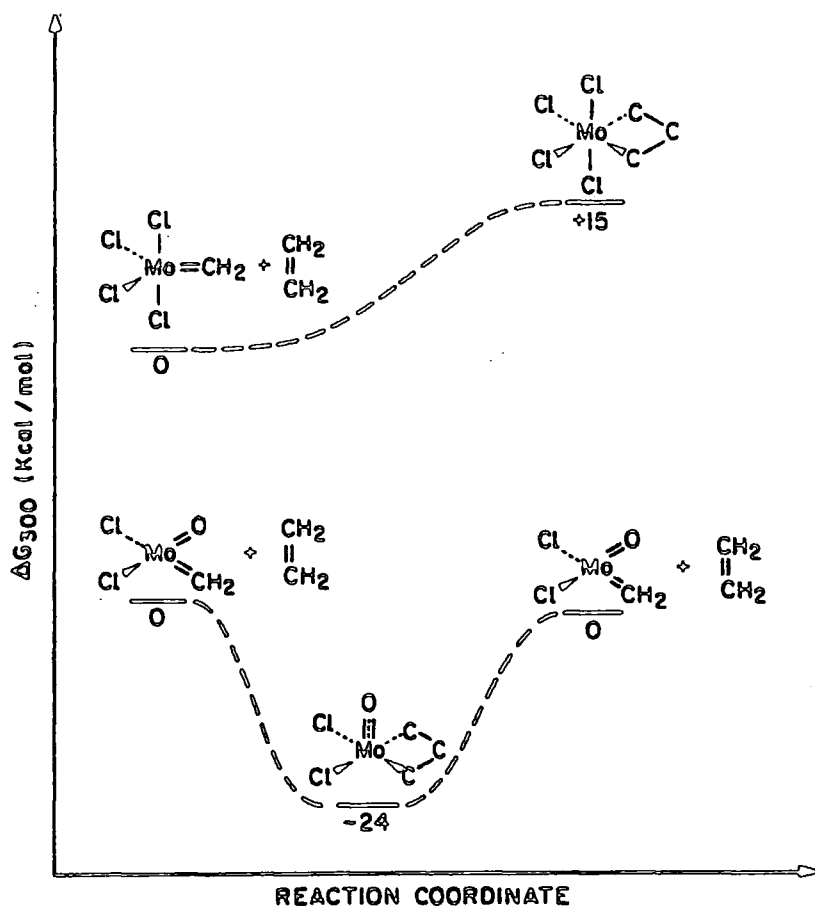


Figure 1.12 *Effect of a spectator oxo ligand in stabilizing the metallacyclobutane intermediate in the degenerate metathesis of ethylene.*

Similarly, multiply bonded imido groups can also have a spectator effect. The reaction shown in Figure 1.13 is approximately 16 kcal mol^{-1} more favourable than the corresponding reaction with $\text{Mo}(\text{X})\text{Cl}_4$ ²⁹.

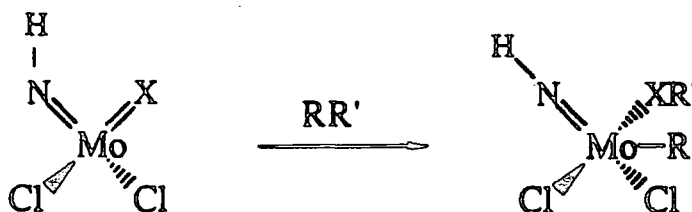
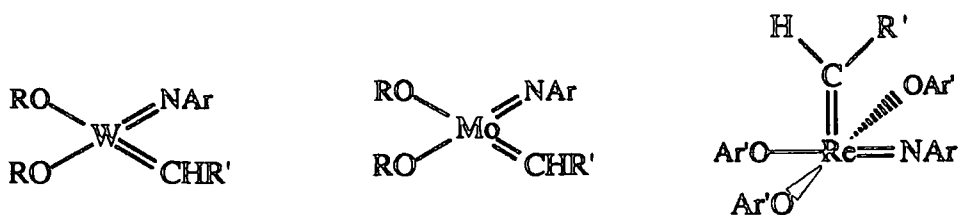


Figure 1.13 *Imido ligand spectator effect.*

In the original paper on this work³⁴, it was predicted that the smaller spectator effect of an imido ligand may prove advantageous in Lewis acid-free metathesis catalysts. This indeed turned out to be the case, and the latest well defined ROMP initiators developed by Schrock and co-workers³⁷⁻³⁹ possess an ancillary 2,6-diisopropylphenylimido unit cis to the alkylidene ligand (Figure 1.14).



$NAr = N-2,6-iPr_2C_6H_3$; $R = t-Bu, CMe_2CF_3, CMe(CF_3)_2$,
 $R' = t-Bu, CMe_2Ph$; $OAr' = OC_6F_5, O-2,6-Cl_2C_6H_3, OC_6Cl_5$.

Figure 1.14 Some well defined ROMP initiators containing spectator imido ligands.

1.4 Spectroscopic Properties.

1.4.1 ¹H NMR Spectroscopy.

Imido Complexes.

In d^0 alkyl imido complexes, the α protons are deshielded significantly, and occur 1 - 4 ppm downfield of the α resonance in trialkyl amines, which occur typically at 2.2 - 2.6 ppm⁴⁰. In d^2 imido complexes the situation is more complex with some of the α protons occurring upfield of the amine α proton. The origin of this effect is not known. The α proton resonances of some alkylimido species are shown in Table 1.1.

Complex	d electrons	δ (ppm)	Ref.
CpNb(NMe)Cl ₂	0	3.21	41
Cp [*] Nb(NMe)Cl ₂	0	3.25	42/43
CpNb(NMe)(O ^t Bu) ₂	0	3.43	43
CpNb(NMe)Cl ₂ (PMe ₃)	0	3.85	43
CpNb(NMe)(O-2,6-Me ₂ C ₆ H ₃) ₂	0	3.30	43
Cp [*] Ta(NMe)Me ₂	0	3.97	44
Ta(NEt)(NEt ₂) ₃	0	4.04	47
W(NMe)F ₅ ⁻	0	5.50	46
W(NEt)(O)Cl(NHEt)	0	7.3	49
Re(NMe)Cl ₃ (PEtPh ₂) ₃	2	0.2	50
Os(NMe)Me ₄	2	0.27	48
Cp [*] Re(NMe)Cl ₂	2	2.17	45

Table 1.1 *α -proton chemical shifts of some mononuclear alkylimido complexes.*

Alkylidene Complexes.

The position of the α -proton resonance in alkylidene complexes is sensitive to both electronic and structural factors. In typical alkylidenes this resonance occurs well downfield, normally being between 8 and 14 ppm⁵¹. However, in distorted alkylidene complexes, of the type observed in 14 electron systems, the α proton is significantly more shielded and occurs in the range -2 to 7 ppm. Table 1.2 shows selected NMR data for several alkylidene complexes.

Complex	δ ^1H	δ ^{13}C	J_{CH}	Ref.
$\text{Mo}(\text{NAr})(\text{CH}-t\text{-Bu})(\text{OTf})_2(\text{dme})$	14.29	331.9	121	37
$\text{Mo}(\text{NAr})(\text{CH}-t\text{-Bu})(\text{OCMe}(\text{CF}_3)_2)_2$	12.06	288.2	117	37
$\text{Mo}(\text{NAr})(\text{CH}-t\text{-Bu})(\text{OCMe}_2\text{CF}_3)_2$	11.61	276.8	118	37
$\text{Mo}(\text{NAr})(\text{CH}-t\text{-Bu})(\text{O}-t\text{-Bu})_2$	11.23	265.8	117	37
$\text{Mo}(\text{NAr})(\text{CH}-t\text{-Bu})(\text{O}-t\text{-Bu})(\text{OCMe}(\text{CF}_3)_2)$	11.71	274.0	—	57
$\text{Mo}(\text{NAr})(\text{CH}-t\text{-Bu})(\text{OCMe}(\text{CF}_3)_2)_2(\text{PMe}_3)$	11.90 ^a	293.2	110	56
$\text{Mo}(\text{NAr})(\text{CH}-t\text{-Bu})(\text{OCMe}(\text{CF}_3)_2)_2(\text{PMe}_3)$	13.25 ^b	313.9	138	56
$\text{Mo}(\text{NAr})(\text{CHFc})(\text{O}-t\text{-Bu})_2^c$	11.90	274	127	56
$\text{Cp}_2\text{Ta}(\text{CH}_2)\text{Me}$	10.22	228	132	52,53
$\text{CpTa}(\text{CH}-t\text{-Bu})\text{Cl}_2$	6.38	246	84	54
$\text{CpTa}(\text{CHCMe}_2\text{Ph})\text{Cl}_2$	6.88	244.4	82	42
$\text{W}(\text{CHPh})(\text{CO})(\text{PMe}_3)\text{Cl}_2$	-1.21	221.4	82	55

^a syn rotamer. ^b anti rotamer. ^c CHFc = CH(Ferrocene)

Table 1.2 NMR data for selected alkylidene complexes.

1.4.2 ^{13}C NMR Spectroscopy.

Imido Complexes.

^{13}C chemical shifts have been reported for a number of t-butyl imido complexes of d^0 transition metals^{43,44,58,59}. It has been shown that decreasing the electron density on the nitrogen atom causes an upfield shift in the β carbon resonance and a downfield shift in the α carbon resonance. Thus, the amount of electron density on the imido nitrogen can be probed by measuring the difference between the chemical shifts for the α and β carbon atoms ($\Delta\delta$). These values can also give an indication of the reactivity of imido complexes. Ashcroft et.al. state that imido ligands where $\Delta\delta$ is less than 50

react metathetically with benzaldehyde (equation 1.2) to afford the corresponding oxo complex whereas those with $\Delta\delta$ greater than 50 do not undergo this transformation⁶⁰. Indeed, it has recently been shown that for the bis t-butyl imido complex $\text{Mo}(\text{N-t-Bu})_2(\text{O-t-Bu})_2$ ($\delta C_\alpha = 67.9$ ppm, $\delta C_\beta = 32.4$ ppm, $\Delta\delta = 35.5$) this reaction does occur⁶¹. This type of reactivity is discussed in greater detail in chapter 4.



Alkylidene Complexes.

Typically, the α carbon resonance in "Schrock type" alkylidene complexes is observed in the 210 - 320 ppm region (see Table 1.2). The value of this shift does not correlate particularly well with structure, although one can see from Table 1.2 that for complexes of the type $\text{Mo}(\text{NAr})(\text{CH-t-Bu})(\text{OR})_2$, δC_α increases as R becomes more electron withdrawing. Schrock has noted that the J_{CH} coupling constant for the α carbon atom is usually small in "distorted" alkylidene ligands where the M-C-C angle differs greatly from the typical sp^2 value of 120° , suggestive of an α -agostic interaction⁵¹.

1.5 Olefin Metathesis and Living Ring Opening Metathesis Polymerization.

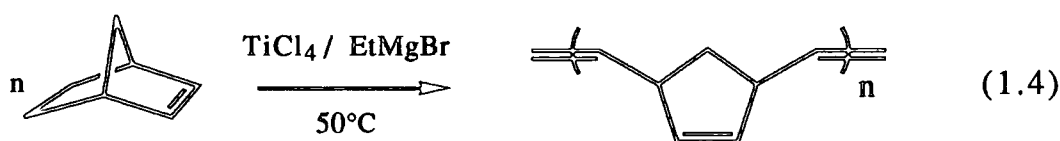
1.5.1 Introduction.

Olefin metathesis is a relatively new addition to the field of transition metal mediated reactions available to the synthetic organic chemist. A *metathesis* reaction is one in which two units which initially comprise a part of a larger entity are interchanged between pairs of such entities. In the case of "*olefin metathesis*" it is alkylidene units, pairs of which constitute an olefin, which are interchanged, as shown in equation 1.3.



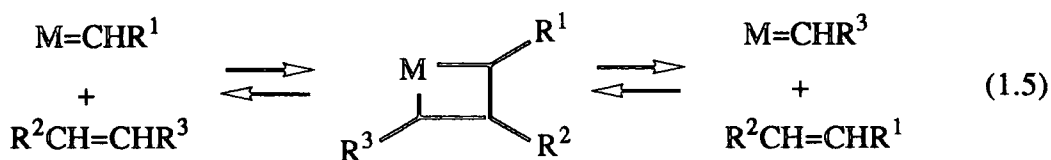
The term olefin metathesis was first used in the literature as recently as 1967 by Calderon (Goodyear)⁶². There have been a number of recent reviews which cover the metathesis reaction for acyclic olefins⁶³⁻⁶⁶.

A particular important application of olefin metathesis is the Ring Opening Metathesis Polymerization (ROMP) of cyclic olefins. The first example of this (albeit identified as such with hindsight) was the ROMP of bicyclo[2.2.1]hept-2-ene using a titanium catalyst (as shown in equation 1.4) in 1955 by work at DuPont⁶⁷.



1.5.2 The Mechanism of the Olefin Metathesis Reaction.

The first mechanisms proposed for olefin metathesis were based on pairwise processes involving metal-bound cyclobutanes or related structures⁶⁸⁻⁷¹. However, the currently accepted mechanism, proposed by Herisson and Chauvin in 1970, involves a reversible [2+2] cycloaddition of the olefin carbon-carbon double bond to a metal-carbon double bond (of the active initiator species) to yield a metallacyclobutane intermediate, as shown in equation 1.5⁷².



If the resulting metallacycle breaks up to yield a new olefin it is termed productive metathesis, whereas if the original olefin is obtained then degenerate metathesis is said

to have taken place. Proof for this Chauvin mechanism comes from labelling studies on cross metathesis reactions, which show that the products are incompatible with a pairwise mechanism⁷³⁻⁷⁵, and from the demonstration by Schrock, Osborn and Grubbs that discrete metal alkylidene and metallacyclobutane complexes can act as highly active ROMP initiators⁷⁶⁻⁷⁸.

The mechanism for the ROMP of cyclic olefins is similar to that for the metathesis of acyclics, and as this thesis is concerned with the former, the rest of this review section will concentrate on ROMP, with reference to the metathesis of acyclic olefins only when a direct comparison is to be made.

1.5.3 Catalysts for the ROMP of cyclic monomers.

There are a wide variety of both homogeneous and heterogeneous formulations which catalyze the ROMP reaction. The most commonly used catalysts are based on molybdenum, tungsten and rhenium and can be classified according to several types.

Classical Catalysts.

These catalysts were the first to be developed and typically involve two or more components (often a Lewis acid and an alkyltin co-catalyst). They can be divided into homogeneous and heterogeneous systems although the distinction between these is not always apparent. Heterogeneous formulations include $\text{Re}_2\text{O}_7/\text{Al}_2\text{O}_3$ ⁷⁹, $\text{MoO}_3/\text{CoO}/\text{Al}_2\text{O}_3$ ⁸⁰ and WO_3/SiO_2 ⁸¹. Homogeneous formulations include $\text{WCl}_6/\text{EtOH}/\text{EtAlCl}_2$ ⁸², $\text{W}(\text{O})\text{Cl}_4/\text{SnMe}_4$ ⁸³ and $\text{MeReO}_3/\text{AlCl}_3$ ⁸⁴. For a full review of classical initiator systems, the reader is referred to Ivin's book⁶⁵.

However, the activity of these systems depend upon a number of factors, such as chemical and thermal history and rate of mixing of catalyst, co-catalyst and monomer. It is also true that the metal-carbon double bonds generated to serve as active sites are formed in low yield and tend to decompose over the timescale of a typical

polymerization. Due to the high Lewis acidity of the metal centre, these classical catalysts tended also not to be tolerant of functional groups, limiting the number of monomers that could be polymerized. It is because of this lack of control over the polymerization process that the preparation of well characterized, highly active, Lewis acid free ROMP initiators became somewhat of a goal in this field⁸⁵. This has now culminated in Schrock's synthesis of tungsten, molybdenum and rhenium catalysts (see figure 1.14)^{37,38,39}. The activity of these complexes can be "tuned" accurately to the point where they become almost perfect ROMP catalysts for highly strained monomers. The ROMP chemistry of the molybdenum and tungsten catalysts forms the basis of the rest of this review.

Well defined Molybdenum and Tungsten "Schrock type" Catalysts.

These well defined catalysts with bulky alkoxide and spectator imido ligands have only recently become synthetically available^{37,38}. The tetrahedral coordination of these complexes allows relatively small substrates such as olefins to attack the metal to give five coordinate metallacyclobutane intermediates, whilst the bulky alkoxide and 2,6-diisopropylphenylimido units help prevent decomposition by ligand scrambling.

The development of these initiators stems from the formation in high yield of catalyst precursors of the type $M(NAr)(CHR)(OTf)_2(dme)$ ($M = Mo, W$; $R = t-Bu, CMe_2Ph$; $OTf = OSO_2CF_3$). Addition of two bulky alkoxides to this precursor results in loss of coordinated *dme* (for steric reasons) and formation of the four coordinate $M(NAr)(CHR)(OR')_2$ catalyst species. ($R' = t-Bu, CMe_2CF_3, CMe(CF_3)_2$). The X-Ray structure of $W(NAr)(CH-t-Bu)(O-t-Bu)_2$ is shown in Figure 1.15, this being typical of this range of catalysts.

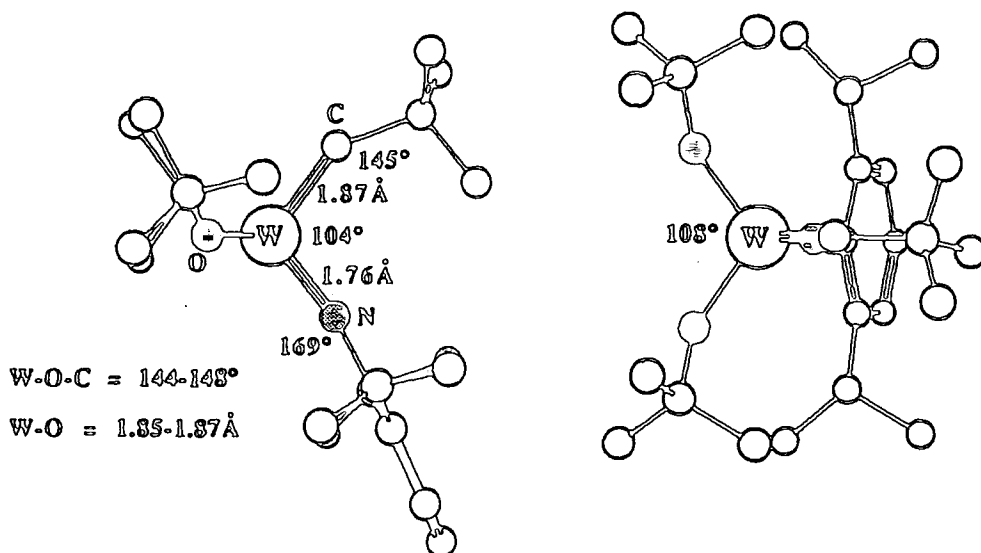


Figure 1.15 The structure of $W(NAr)(CH-t-Bu)(O-t-Bu)_2$.

It is a pseudo tetrahedral species with the alkylidene substituent pointing towards the imido nitrogen atom (syn rotamer). The linear triply bonded imido unit (W-N-C angle of 169°) forces the β -carbon atom of the alkylidene unit to lie in the same plane as the nitrogen, tungsten and α -carbon atoms. As well as the syn rotamer shown in the crystal structure, the anti rotamer, where the alkylidene substituent points away from the imido nitrogen atom, is also possible (figure 1.16).

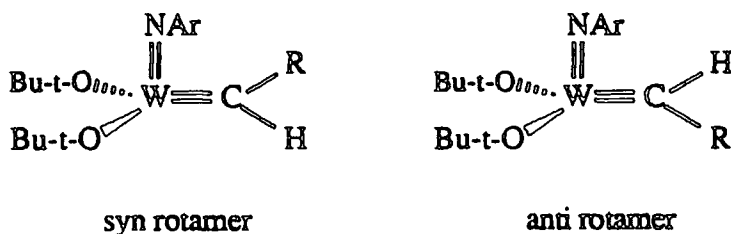


Figure 1.16 Rotameric forms of $W(NAr)(CHR)(O-t-Bu)_2$

There is evidence for syn and anti rotamers in several systems and these have been shown to interconvert readily on the NMR timescale by simple rotation about the metal-carbon double bond.

The acyclic olefin metathesis activity of these complexes is controlled by varying the nature of the alkoxide group. For example, $W(NAr)(CH-t-Bu)(OCMe(CF_3)_2)_2$ metathesizes 3700 equivalents of *cis*-pentene to equilibrium within five minutes at room temperature⁸⁶, whilst changing the alkoxide to one which is more electron donating reduces the catalytic activity dramatically, as is seen for $W(NAr)(CH-t-Bu)(O-t-Bu)_2$ which reaches only 30% of the equilibrium distribution of *cis*-pentene after six days at room temperature. This is because the interaction can be regarded as electrophilic attack on the olefin by the metal and the metal is significantly more electrophilic (and hence more reactive) with the electron withdrawing fluorinated alkoxides present. This "lack of reactivity" of the bis *t*-butoxide derivatives can be exploited in the polymerization of cyclic olefins, since both the molybdenum and tungsten complexes metathesize the strained double bond of norbornene to yield polymers, without reaction with the double bonds in the resulting polymer (backbiting) occurring. This gives the opportunity of preparing well defined polymers in a controlled living manner.

1.5.4 Living ROMP using Well Defined Initiator systems.

General Considerations.

For a truly living polymerization, each monomer unit must add irreversibly, chain transfer and chain termination must be slow on the time scale of the polymerization reaction itself, and the rate of initiation must be approximately equal to or greater than the rate of propagation⁸⁷⁻⁸⁹. Only then can polymers that have a narrow distribution of molecular weights (polydispersities approaching 1.00) be prepared.

The Mechanism of Living ROMP.

The overall mechanism for the ROMP of norbornene using the initiator $Mo(NAr)(CH-t-Bu)(O-t-Bu)_2$ is shown in figure 1.17.

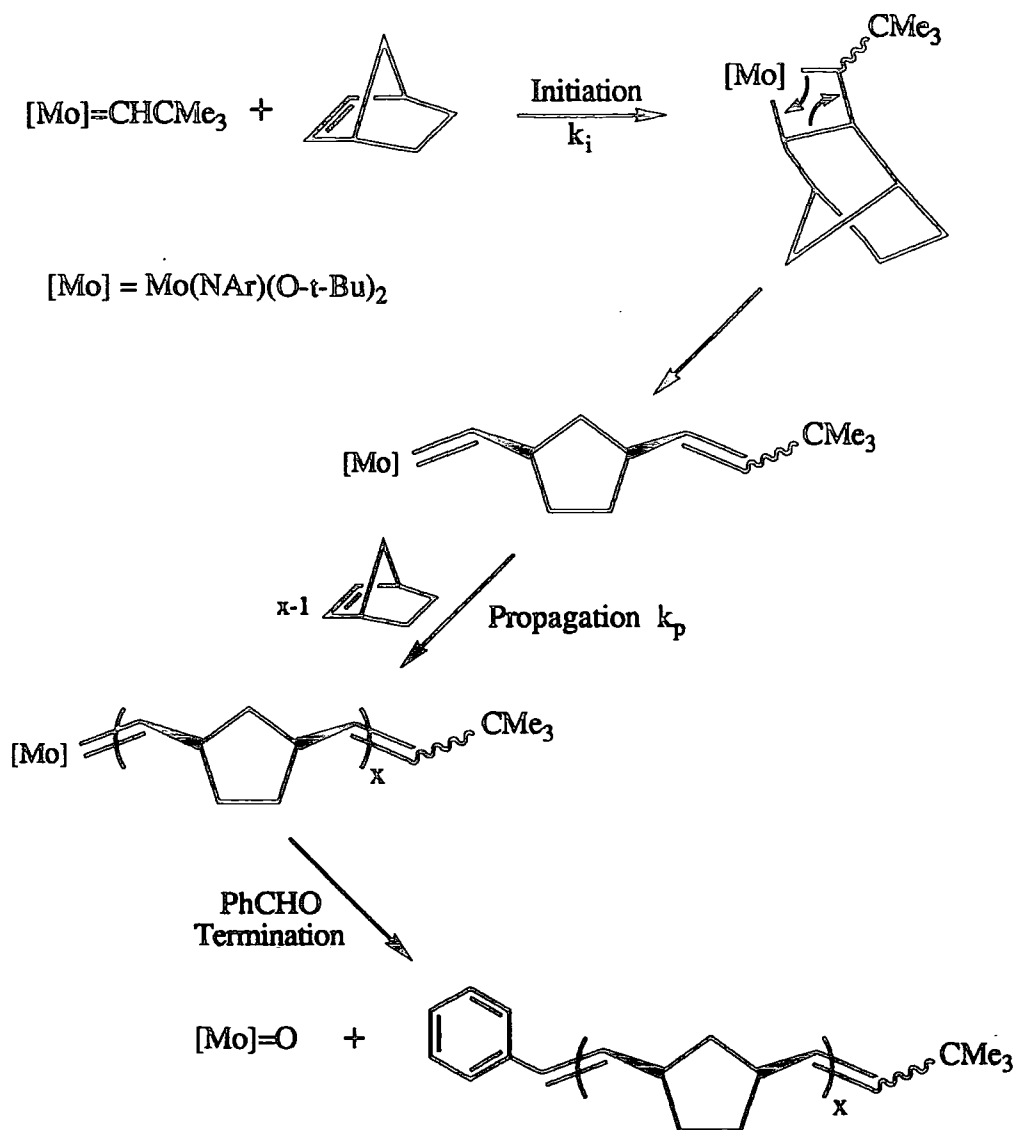


Figure 1.17 *The Mechanism of Living ROMP for Norbornene.*

The initiator reacts with an equivalent of the monomer to form a metallacyclobutane intermediate, which breaks up to yield a propagating alkylidene at a rate k_i . This then reacts with more monomer at a propagating rate k_p . The resulting polymer is living if there is no chain transfer, decomposition or backbiting during the timescale of the polymerization. More monomer can then be added and this will be consumed at a rate k_p . If a different monomer is added, the living polymer is now the initiator and this reacts with the new monomer at a rate k_i' to form a new propagating

species, which then reacts with more monomer at a new propagating rate k_p' . The polymer is finally cleaved from the metal centre (termination) in a "Wittig like" capping process by reaction with an aldehyde (typically pivaldehyde or benzaldehyde) to give $\text{Mo(O)(NAr)(O-t-Bu)}_2$.

By careful monitoring of the initial stages of the polymerization process by ^1H NMR spectroscopy, resonances due to the first, second and subsequent insertion products have been observed, as shown for the reaction of $\text{Mo(NAr)(CH-t-Bu)(O-t-Bu)}_2$ with 2,3-bis(trifluoromethyl)norbornadiene in figure 1.18 ⁵⁶.

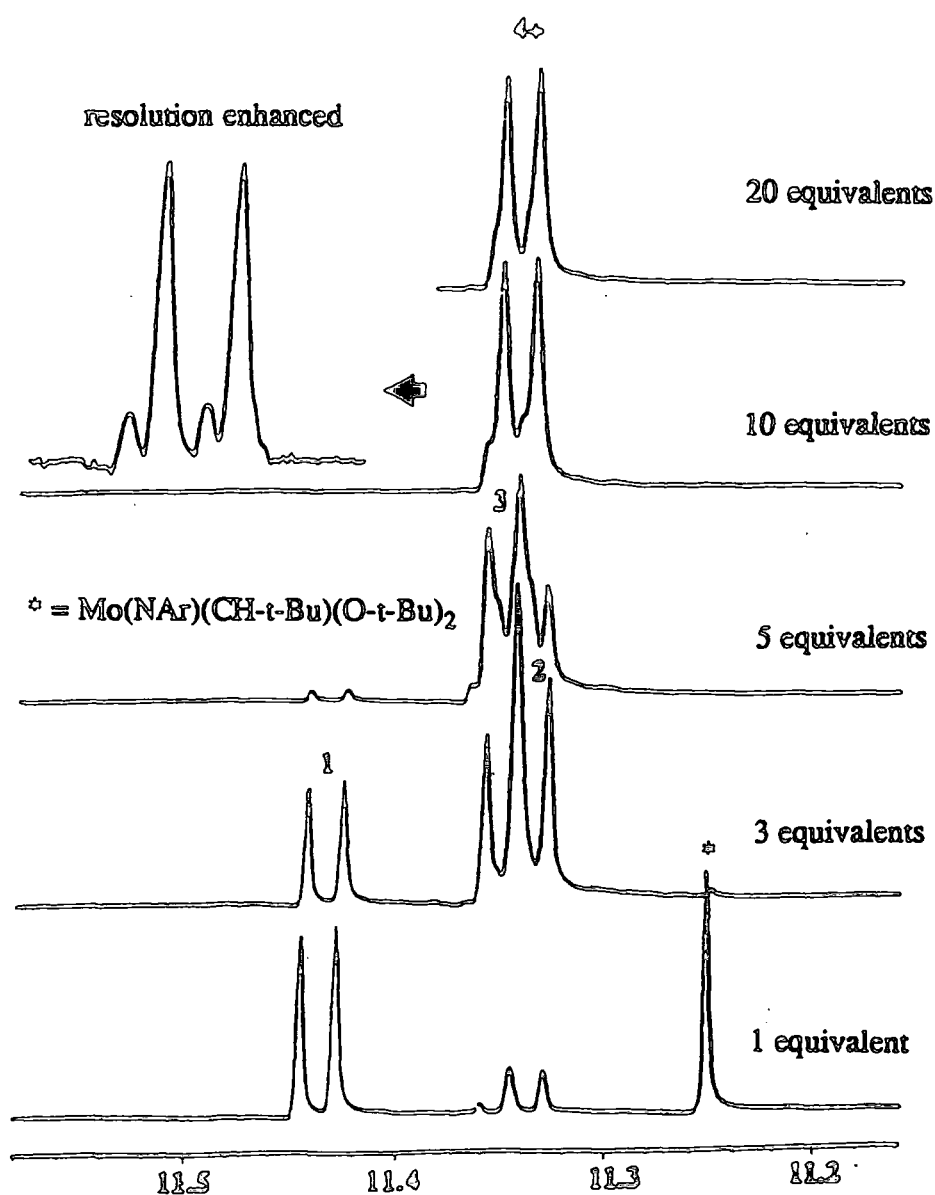


Figure 1.18 ^1H NMR spectra of $\text{Mo(NAr)(CH-t-Bu)(O-t-Bu)}_2$ and 1, 3, 5, 10 and 20 equivalents of BTFMND.

Values for the initiation and propagation rates for various monomers are shown in table 1.3⁵⁶.

monomer	r (k_p/k_i)	k_p ($M^{-1}s^{-1}$)	k_i ($M^{-1}s^{-1}$)
norbornene ^a	12.1 (5)		
Benzenorbornadiene ^a	7.0 (5)		
2,3-dicarbomethoxy norbornadiene ^a	3.0 (3)	2 (1)	0.7 (3)
2,3-bis(trifluoromethyl) norbornadiene ^b	0.72 (5)	0.057 (± 0.0007)	0.08 (1)

^a Significant errors arise from the fact that the reaction is fast and mixing is not instantaneous. ^b Measured by E. Khosravi.

Table 1.3 Rate constants for polymerizations at 22 °C.

For norbornene, benzenorbornadiene, and 2,3-dicarbomethoxynorbornadiene, k_p is greater than k_i because a complex containing the neopentylidene ligand is less reactive (due to steric congestion) than that containing the alkylidene ligand formed upon opening the carbon-carbon double bond in the monomer. For 2,3-bis(trifluoromethyl)norbornadiene, k_p/k_i is less than one i.e. the new propagating alkylidene is less reactive than the neopentylidene complex. This has been attributed to electronic deactivation of the propagating alkylidene as a nucleophile by the electron withdrawing trifluoromethyl groups⁵⁶.

Stereochemistry.

The stereochemistry of the repeat units within a polymer is of great interest as it determines many of its bulk properties. Stereochemistry in polymers of norbornene and its derivatives arises due to three features.

- (1) The carbon-carbon double bonds along the polymer backbone may have a *cis* or *trans* arrangement.
- (2) Since the two tertiary carbons in norbornene are chiral, the monomer can be opened to give a polymer in which the allylic carbons on pairs of adjacent rings (dyads) have either the same configuration (*racemic* dyads, $=(\text{R},\text{S})=(\text{S},\text{R})=(\text{R},\text{S})=$) which is syndiotactic, or have the opposite configuration (*meso* dyads, $=(\text{R},\text{S})=(\text{R},\text{S})=(\text{R},\text{S})=$) which is isotactic. Random configurations along the polymer chain lead to atactic polymer.
- (3) For unsymmetric monomers, head/head, head/tail or tail/tail sequences are also a possibility.

2,3-disubstituted norbornadienes have been convenient monomers to use for a study of polymer stereochemistry as head/tail effects are eliminated (due to symmetry) and only four primary structures are therefore possible. These are shown in figure 1.19.

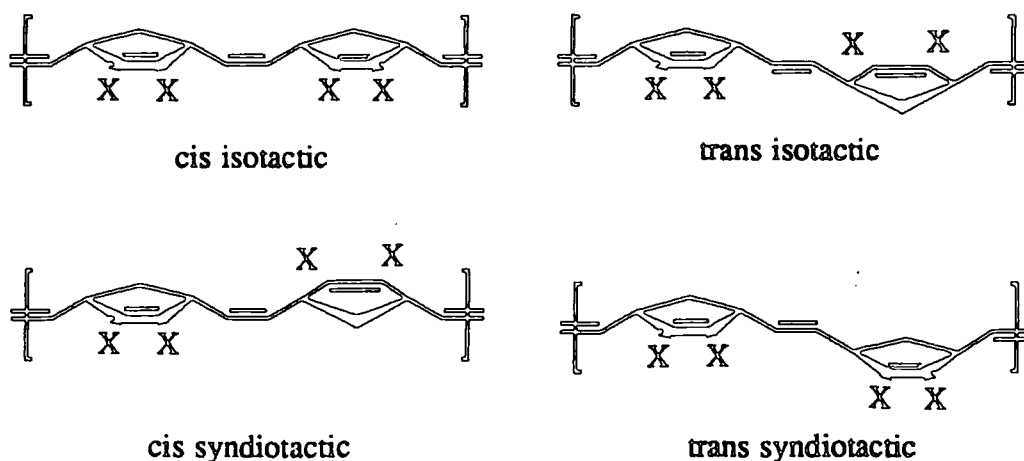


Figure 1.19 The four primary structures for poly-BTFMND.

1.5.5 Living ROMP of Functionalized Norbornene and Norbornadiene Derivatives.

Figure 1.20 shows some of the functionalized norbornene and norbornadiene monomers that can be polymerized successfully by $\text{Mo}(\text{NAr})(\text{CH-}t\text{-Bu})(\text{O-}t\text{-Bu})_2$ ^{90,91,92}. A polymerization is termed successful if monomer consumption is quantitative by ¹H NMR and the polymer is soluble, can be isolated and has a narrow polydispersity index (PDI).

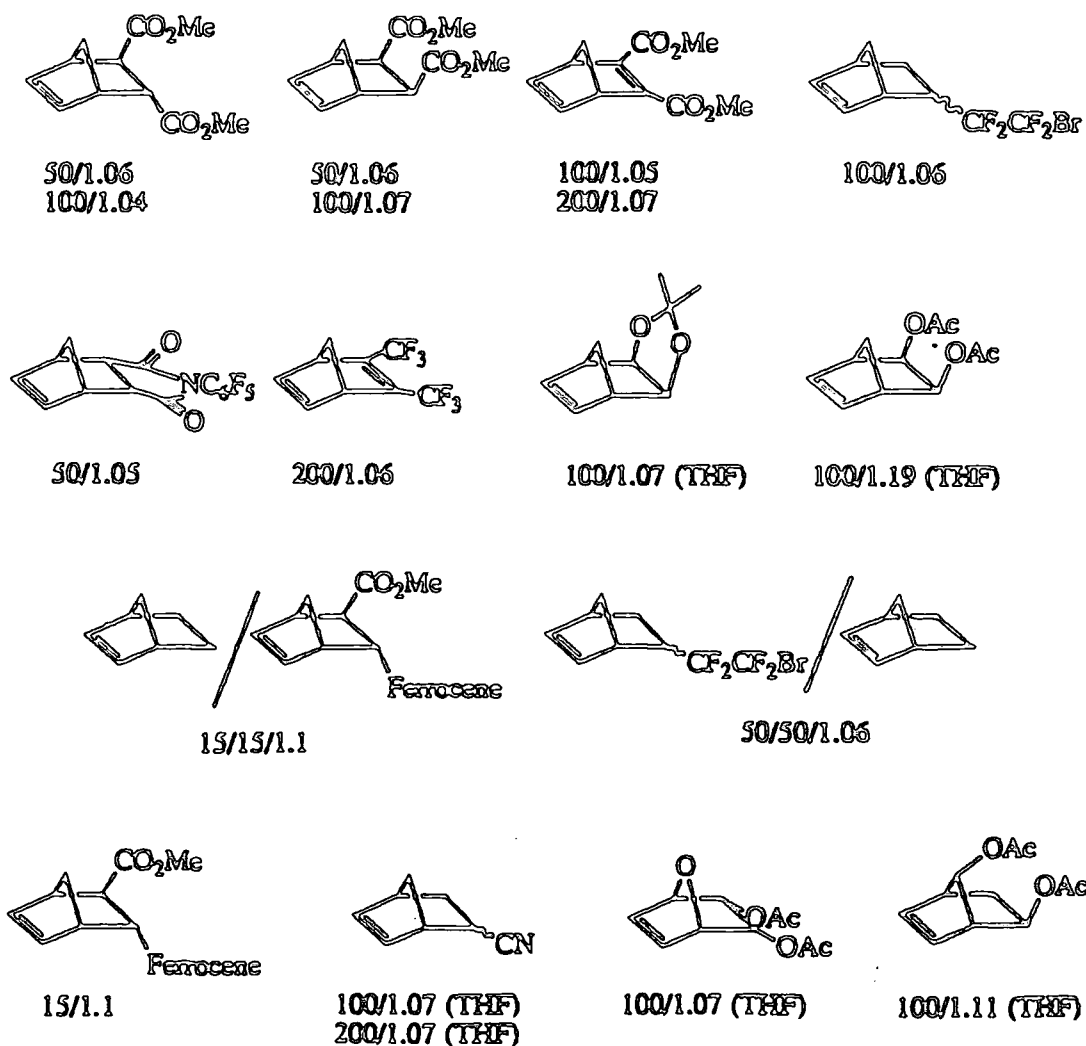


Figure 1.20 Some Norbornenes and Norbornadienes that can be polymerized by $\text{Mo}(\text{NAr})(\text{CH-}t\text{-Bu})(\text{O-}t\text{-Bu})_2$ (Equivalents/PDI).

The PDI data show that these polymers are essentially monodisperse (PDI's as low as 1.03 for up to 500 monomer equivalents) i.e. the distribution about the average chain length is as narrow as possible, indicative of a well behaved living polymerization process.

The tungsten analogue of this initiator does not successfully polymerize as wide a range of functionalized monomers as the molybdenum initiator³⁸. Reasons for this apparent failure include :- (1) the greater electrophilicity of tungsten vs. molybdenum, (2) tungsten may be more sensitive to low levels of impurity than molybdenum, and (3) the tungsten alkylidene may react more readily with a given functionality or active protons in the polymer chain than the molybdenum analogue does.

The solvent used has also been found to be an important factor in the ROMP of functionalized olefins. In particular the failure to polymerize 2-carbonitrilenorbornene in non-coordinating solvents such as toluene and its polymerization in THF is interesting⁹⁰. As yet this effect is not understood, but possible reasons may include (1) THF successfully competes with the functionality for the metal and therefore inhibits reaction between it and the metal and (2) A bulk solvent effect may keep the polar groups pointed away from the metal and into solution.

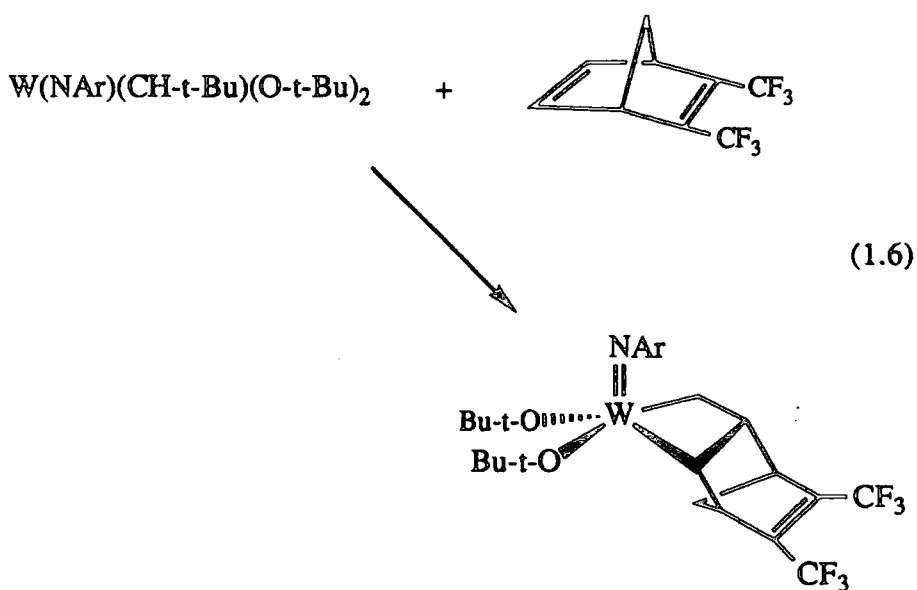
One of the most interesting monomers to be studied has proven to be 2,3-bis(trifluoromethyl)norbornadiene, due to the high stereoregularity of the resulting polymer. This is discussed in more detail in section 1.5.7.

1.5.6 Stable Intermediates in the Metathesis Process.

As shown in figure 1.17, the initiation step of the polymerization yields a metallacyclobutane which subsequently ring opens to give the first insertion product. Schrock has shown that these species are indeed intermediates in the reaction of $M(NAr)(CHR)(OR')_2$ with olefins and that in some cases they can be isolated and characterized^{37,38,76,86}.

Square pyramidal metallacycles form when the relatively electron donating *t*-butoxide ligands are present, and these appear to be more stable than the trigonal bipyramidal metallacycles that form when the alkoxides are more electron withdrawing ($R' = \text{OCMe}(\text{CF}_3)_2$). Both forms of the metallacycle are observed when R' is the intermediate alkoxide OCMe_2CF_3 . These different geometries are most clearly seen for the range of metallacycles $\text{W}(\text{NAr})(\text{CH}_2\text{CH}_2\text{CH}_2)(\text{OR}')_2$ formed by the reaction of $\text{W}(\text{NAr})(\text{CH-}t\text{-Bu})(\text{OR}')_2$ with excess ethylene⁹³. Two possible explanations have been offered for the various preferences for core geometries. With electron donating alkoxides, TBP metallacycles are disfavoured since the axial imido and alkoxide ligands must compete as π -donors for the same empty *d*-orbital on the metal. With electron withdrawing alkoxides, the electrophilicity of the metal centre is enhanced and therefore there is an increased tendency to form shorter metal-carbon bonds of higher order, as found in TBP species.

The reaction of $\text{W}(\text{NAr})(\text{CH-}t\text{-Bu})(\text{O-}t\text{-Bu})_2$ with 1 equivalent of 2,3-bis(trifluoromethyl)norbornadiene at -30°C yields an unstable but isolable SP metallacycle as shown in equation 1.6.

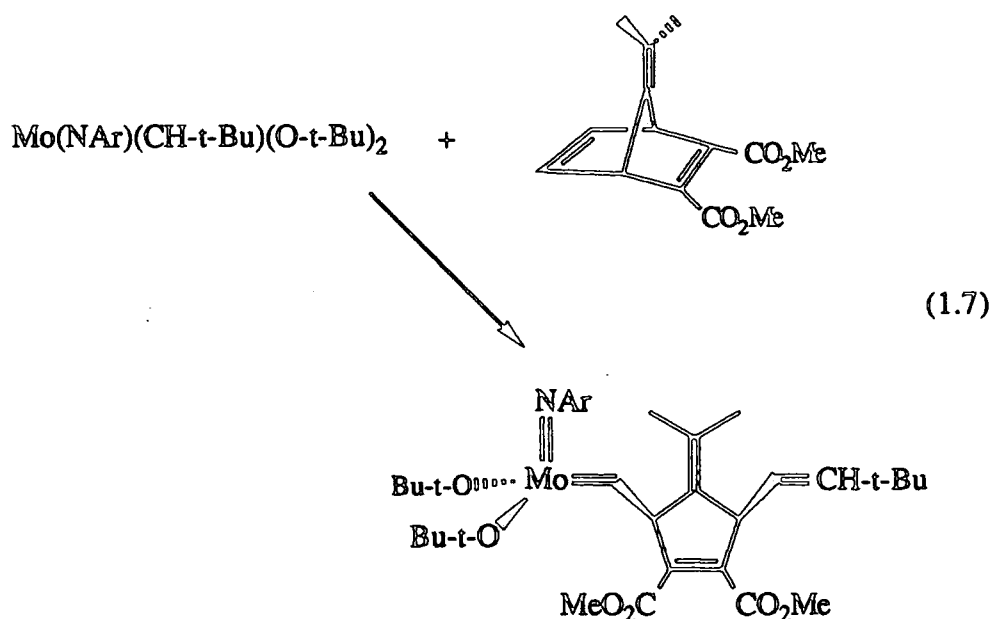


As can be seen, this is a SP metallacycle where the syn rotamer of the initiator has added to the more accessible *exo* face of the monomer, to give a *trans* tungstacycle. This has been shown to ring open to give both the syn and anti forms of the first insertion product. These are thermally unstable, providing some explanation as to why the tungsten catalyst does not smoothly polymerize this monomer (PDI's observed are typically 1.2 or greater, and decomposition of the tungsten catalyst is observed over the course of the polymerization).

Reversible metallacycle formation has also been observed in one case⁹⁰. Treatment of $\text{Mo}(\text{NAr})(\text{CH-t-Bu})(\text{O-t-Bu})_2$ with 5,6-dichloro-5,6-carbonatonorbornene gives an observable metallacycle which upon heating regenerates monomer, 50 % of the starting alkylidene and a living oligomer. The monomer then adds to the living oligomer. This is the first example of a metallacycle ring opening degenerately and will presumably be quite rare.

7-oxanorbornenes have also been shown to yield remarkably stable metallacycles⁵⁶. The reaction of $\text{Mo}(\text{NAr})(\text{CH-t-Bu})(\text{O-t-Bu})_2$ with (a) 7-oxa-2,3-bis(trifluoromethyl)norbornadiene, (b) 7-oxa-2,3-dicarbomethoxynorbornadiene and (c) 7-oxa-benzonorbornadiene yields SP metallacycles with relative stabilities (a) > (b) > (c). Indeed, the metallacycle formed with (a) is still 75 % present after 24 hours in solution at room temperature. The increased stability of these 7-oxa metallacycles has been attributed to induction differences between oxygen and carbon at the 7-position⁵⁶.

For molybdenum, there is one example of a structurally characterised first insertion product, formed from the reaction of $\text{Mo}(\text{NAr})(\text{CH-t-Bu})(\text{O-t-Bu})_2$ with 7-isopropylidene-2,3-dicarbomethoxynorbornadiene⁵⁶. This reaction is 350 times slower than that with 2,3-dicarbomethoxynorbornadiene, presumably due to the steric bulk of the monomer and only one equivalent reacts, even at 40°C, to give the isolable first insertion product shown in equation 1.7.



The new alkylidene is significantly larger than the original neopentylidene complex, and so no further propagation takes place ($k_p = 0$).

1.5.7 Stereoregular Polymerization of 2,3-bis(trifluoromethyl)norbornadiene.

Perhaps the most important finding of these recent studies is the fact that 2,3-bis(trifluoromethyl)norbornadiene can be polymerized to give a polymer of high stereoregularity when molybdenum initiators are used.

^{13}C NMR studies show that 2,3-bis(trifluoromethyl)norbornadiene is polymerized by $\text{Mo(NAr)(CH-t-Bu)(O-t-Bu)}_2$ to give a highly tactic polymer containing only one of the four possible types of olefinic carbon atoms shown in figure 1.19. This can be assigned to the all trans form in greater than 98%, with resonances for the cis form (< 2%) barely observable^{91,92}. Consistent with this tacticity has been the observation, by differential scanning calorimetry, of a well defined glass transition temperature at 97°C and a broad melting endotherm at approximately 200°C⁹². As yet it is not clear whether this polymer is trans-syndiotactic or trans-isotactic, but preliminary dielectric measurements have indicated a high dielectric constant,

suggesting the trans-syndiotactic structure (alignment of the polar CF_3 groups on one side of the polymer backbone)⁹⁴.

Formation of both trans-syndiotactic and trans-isotactic polymer can be rationalized with reference to figure 1.21⁹².

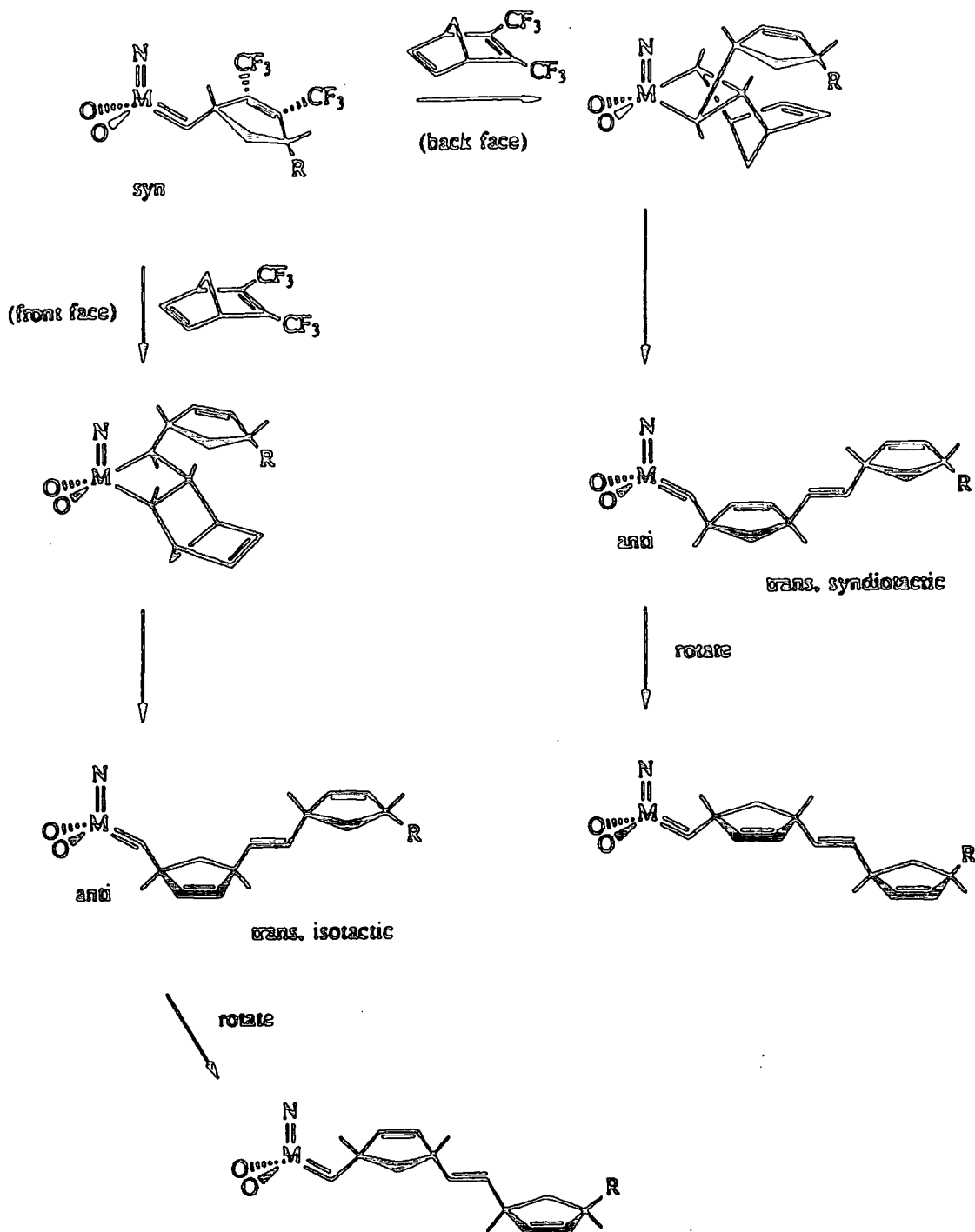


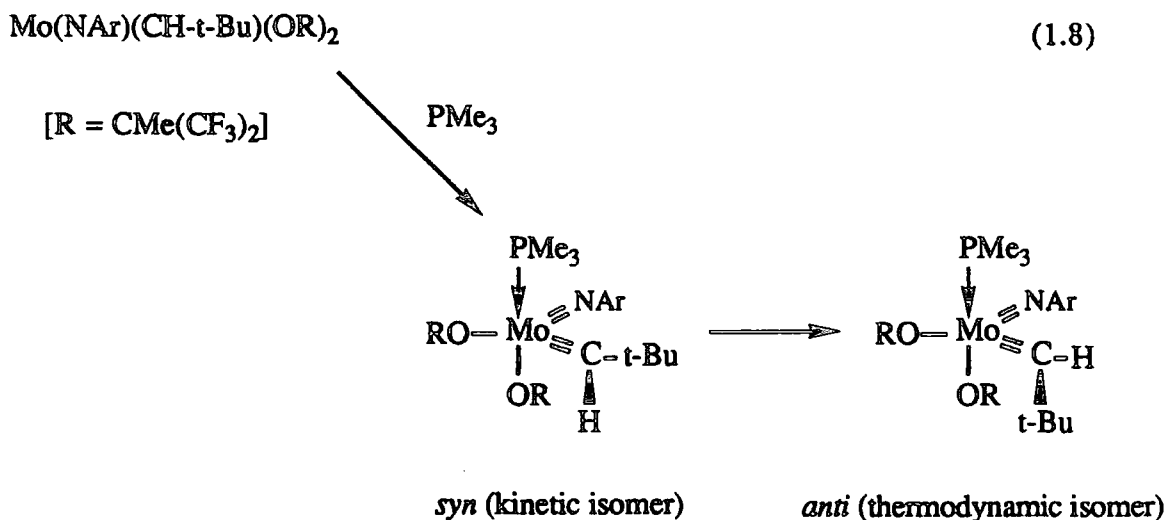
Figure 1.21 Stereoregular polymerization of BTFMND.

Only the syn isomer of the first insertion product is shown, with the cyclopentene ring alignment based on that observed in the crystal structure of the mono-insertion product obtained with 7-isopropylidene-2,3-dicarbomethoxynorbornadiene, as discussed in section 1.5.6. If the exo-face of the monomer approaches the front-face of the metal-carbon double bond, which is the sterically least hindered face, a trans metallacycle will be formed. If this then ring opens, before a rearrangement of the core "flips" the metallacycle relative to the imido nitrogen, the anti alkylidene shown is formed. This can then convert to the syn alkylidene form by simple rotation of the metal-carbon double bond, and the process continues to give a trans-isotactic structure. On the other hand, if the monomer approaches the back-face of the metal-carbon double bond (the sterically most hindered face) to give a trans-metallacycle, this ring opens to give an anti-alkylidene in which the chain is growing in a trans-syndiotactic way. This structure can then rotate to give the syn isomer and the process can again continue. An analogous scheme can be envisaged for addition to the anti rotamer, again leading to either trans-syndiotactic and trans-isotactic polymer. In this scenario it does not matter which rotamer reacts with the monomer, as long as (1) the monomer adds selectively to the same face of the metal-carbon double bond each time, (2) a trans-metallacycle is formed and (3) the rotamers interconvert during the timescale of the polymerization. It has also been proposed that the first metallacycle formed is a trigonal bipyramid formed by addition of the olefin to the C/N/O face of the tetrahedral catalyst^{92,95}. This contains a metallacyclobutane ring that spans both axial and equatorial sites which undergoes a series of rotations to give the observed SP (basal ring) and TBP (equatorial ring) intermediates from which the olefin is extruded.

Very recent results have also shown that simply by changing the activity of the initiator the stereospecificity of this polymerization can be totally reversed⁹⁶. Using the more active derivative $\text{Mo}(\text{NAr})(\text{CHCMe}_2\text{Ph})(\text{OCMe}(\text{CF}_3)_2)_2$, polymers which have greater than 98% cis double-bonds in the polymer backbone can be obtained, with no increase in the polydispersity index. Polymers with intermediate cis/trans ratios are obtained simply by using different mixtures of the two initiators.

1.5.8 Mono-adducts of Imido Alkylidene Complexes.

Schrock and co-workers have synthesized a series of trimethylphosphine and quinuclidene adducts of these four co-ordinate initiators^{56,97}. These can be considered as models for an initial (unobservable) olefin/alkylidene intermediate in the ROMP process. $\text{Mo}(\text{NAr})(\text{CH-t-Bu})(\text{OCMe}(\text{CF}_3)_2)_2$ has been shown to react with PMe_3 quantitatively to give a distorted TBP species ($\delta\text{H}_\alpha = 11.90$ ppm) in which the t-butyl group points toward the imido nitrogen atom (syn rotamer, kinetic isomer). This subsequently equilibrates in solution to the thermodynamic isomer which has an anti alkylidene configuration ($\delta\text{H}_\alpha = 13.25$ ppm), as shown in equation 1.8.



Changing the alkoxide has been shown to dramatically alter the stability of these adducts. Addition of excess PMe_3 to $\text{Mo}(\text{NAr})(\text{CH-t-Bu})(\text{O-t-Bu})_2$ at room temperature shows (by ^1H NMR spectroscopy) 55% of the base free initiator and 45% of the anti adduct ($\delta\text{H}_\alpha = 12.73$ ppm, $J_{\text{CH}} = 136$ Hz). It is only when the solution is cooled to -85°C that the base free initiator is no longer present and the syn rotamer of the adduct observed ($\delta\text{H}_\alpha = 11.80$ ppm, $J_{\text{CH}} = 110$ Hz). The difference in J_{CH} values has been attributed to the syn form being more sterically able to form a potential α -agostic

interaction with the metal than the anti form, where the C-H bond would be in competition with the strong donor imido ligand⁹⁷.

Quinuclidene adducts of the type $M(\text{NAr})(\text{CHR})(\text{OR}')_2(\text{quin})$ ($M = \text{Mo}, \text{W}$; $R = t\text{-Bu}, \text{CMe}_2\text{Ph}$; $R' = \text{CMe}_2\text{CF}_3, \text{CMe}(\text{CF}_3)_2$) have also been prepared⁹⁷. Again these have been shown to exist in two rotameric forms, with an initial adduct ($J_{\text{CH}} = 110 \text{ Hz}$) slowly converting to a second adduct ($J_{\text{CH}} = 135 \text{ Hz}$). Three isomers are observed for quinuclidene adducts of vinylalkylidene complexes; two syn rotamers (chiral and achiral) and one anti rotamer, with a crystal structure of the product from the reaction of $\text{W}(\text{NAr})(\text{CH-}t\text{-Bu})(\text{OCMe}(\text{CF}_3)_2)_2(\text{quin})$ with *trans* 1,3-pentadiene revealing an anti vinyl alkylidene arrangement⁹⁷.

These studies on base adducts suggest that :- (1) an olefin, which can be regarded as a σ base in these systems, most readily adds to the C/N/O face of the imido/alkylidene complex to yield an initial metallacyclobutane in which the ring spans axial and equatorial sites, and (2) due to the reactivity difference between a base and the two rotamers, the rate of rotamer interconversion may be more important than previously thought.

1.6 Heteroatom Exchange Reactions of Multiply Bonded Ligands.

This section serves to outline the type of reaction where an existing multiply bonded ligand is directly replaced by another upon treatment with an unsaturated reagent, which can either be an external substrate, such as an aldehyde or isocyanate, or be another multiply bonded metal bound ligand itself. The latter type of reactivity is comparatively rare with only a handful of previously reported examples.

1.6.1 Exchange Reactivity with External Organic Substrates.

Reaction with Carbonyl Compounds.

Reaction of a multiply bonded ligand with an aldehyde or ketone is a well documented method of preparing metal-oxo complexes. Alkylidene complexes react with organic carbonyl compounds to give an olefin and oxo species (see chapter two). An early example of this is the reaction of $\text{Ta}(\text{CH-t-Bu})(\text{CH}_2\text{CMe}_3)_3$ with acetone to give $[\text{Ta}(\text{O})(\text{CH}_2\text{CMe}_3)_3]_n$ and t-Bu-CH=CMe_2 ⁹⁸. With this tantalum reagent, several functionalized carbonyl compounds that do not react readily with Wittig reagents will undergo clean reaction. Related reactions of alkylidyne complexes that afford oxo-vinyl complexes have also been reported⁹⁹.

The reaction of organo-imido complexes with aldehydes has not proved as useful, although several cases have been reported¹⁰⁰⁻¹⁰². One successful example of this has been published by Nugent where treatment of $\text{Cr}(\text{N-t-Bu})_2(\text{OSiMe}_3)_2$ with one equivalent of benzaldehyde cleanly gives the oxo-imido complex $\text{Cr}(\text{N-t-Bu})(\text{O})(\text{OSiMe}_3)_2$, which has not proven possible to prepare by other routes¹⁰³.

Reaction with Isocyanates.

The use of phenyl isocyanate for conversion of a metal oxo species to an imido species with loss of carbon dioxide is well documented, as shown in equation 1.9.



This was first used to convert the rhenium oxo complex $\text{Re}(\text{O})\text{Cl}_3(\text{PEt}_2\text{Ph})_2$ to $\text{Re}(\text{NPh})\text{Cl}_3(\text{PEt}_2\text{Ph})_2$ ¹⁰⁴, and has subsequently developed into an important synthetic route¹⁰⁵⁻¹⁰⁹.

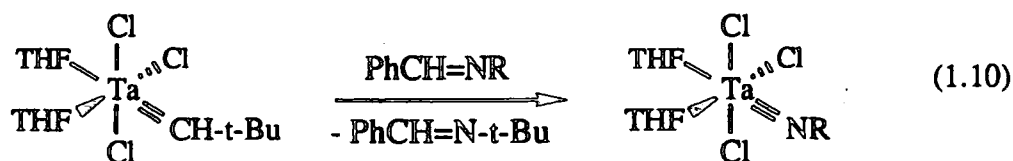
The exchange of imido ligands by reaction with isocyanates has also been recently reported¹¹⁰. The dimolybdenum tetra-imido complex $[(MeC_5H_4)Mo(NPh)(\mu-NPh)]_2$ reacts with excess *p*-tolyl isocyanate to give both the mono and bis terminal *p*-tolyl imido species. Prolonged heating does not, however, lead to substitution of the bridging phenylimido ligands.

In the case of $Cp_2Mo(O)$, reaction with phenyl isocyanate has been shown to give the structurally characterized cyclometallacarbamate species $Cp_2Mo[OC(O)N(Ph)]$ ¹¹¹, showing this reaction to proceed via the expected [2+2] Wittig like intermediate. Unusual reactivity has been observed for the complexes $Mo(O)_2(mesityl)_2$ and $Mo(N-t-Bu)_2(mesityl)_2$ ¹¹². Reaction with phenyl isocyanate does not yield the expected $Mo(NPh)_2(mesityl)_2$, but instead gives phenyl mesityl amide ($PhNHCO(mes)$) as the sole identified product.

Reaction with other Heteroatom Exchange Reagents.

Phosphinimines ($R_3P=NR'$) have also found some use as heteroatom exchange reagents. They were first used to synthesise $Re(NPh)Cl_3L_3$ ¹¹³, and have since been used for the synthesis of $Mo(NPh)(dtc)_2$ ¹¹⁴ and the di- and tri-imido analogues of OsO_4 ¹¹⁵.

Schrock has shown that benzyldiene alkylamines can be used in the formation of imido ligands from alkylidenes, as shown in equation 1.10¹⁰¹. An analogous reaction using $PhCH=NN=CHPh$ has been shown to give $\mu-N_2$ derivatives^{58,116}.

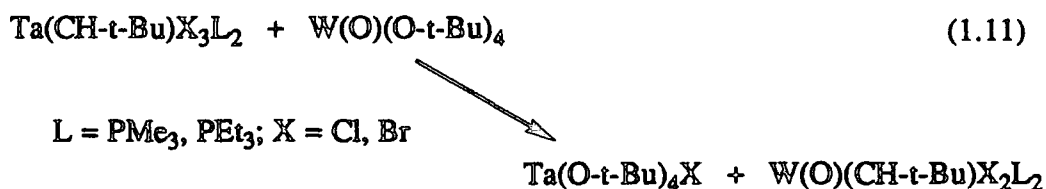


Paetzold has shown that alkylidene ligands can be transferred to iminoboranes to yield neopentylideneborane species¹¹⁷.

The reaction of $\text{CpTa}(\text{CH-}t\text{-Bu})\text{Cl}_2$ with $\text{Me}_3\text{Si}(\text{N-}t\text{-Bu})\text{N}=\text{B}=\text{N-}t\text{-Bu}$ affords $\text{CpTa}(\text{N-}t\text{-Bu})\text{Cl}_2$ and $\text{Me}_3\text{Si}(\text{N-}t\text{-Bu})\text{N}=\text{B}=\text{CH-}t\text{-Bu}$ via an isolable four centered Ta-C-B-N intermediate metallacycle. Carbene exchange has also been reported by Fischer where the reaction of $(\text{CO})_5\text{W}=\text{CHPh}$ with $\text{PhN}=\text{C}=\text{CPh}_2$ affords the exchange products $(\text{CO})_5\text{W}=\text{C}=\text{CPh}_2$ and $\text{PhN}=\text{CHPh}$ ¹¹⁸.

1.6.2 Heteroatom Exchange between Metal Centres.

This type of reaction has been exploited only briefly in the past. Schrock has shown (equation 1.11) that an alkylidene ligand may be transferred from tantalum to tungsten, with a redistribution of the remaining ligands¹¹⁹.



Oxo/alkylidene exchange has also been demonstrated between molybdenum and tungsten. The reaction of $\text{Mo}(\text{O})(\text{NAr})(\text{O-}t\text{-Bu})_2$ with $\text{W}(\text{NAr})(\text{CH-}t\text{-Bu})(\text{O-}t\text{-Bu})_2$ yields $\text{Mo}(\text{NAr})(\text{CH-}t\text{-Bu})(\text{O-}t\text{-Bu})_2$ and $\text{W}(\text{O})(\text{NAr})(\text{O-}t\text{-Bu})_2$ quantitatively⁹⁵.

More recently oxo/imido exchange at osmium has been reported. The reaction of $\text{Mo}(\text{NAr})_2(\text{O-}t\text{-Bu})_2$ with OsO_4 gives the di-oxo bis-imido complex $\text{Os}(\text{NAr})_2(\text{O})_2$ (and presumably $\text{Mo}(\text{O})_2(\text{O-}t\text{-Bu})_2$)¹²⁰.

This relatively new type of reactivity is developed further in chapters four and five of this thesis.

1.7 Summary.

This chapter has attempted to highlight a part of the vast range of chemistry associated with transition metal oxo, imido and alkylidene complexes. We have seen that these multiply bonded ligands help to stabilize early transition metal complexes in their highest oxidation states and that the formation of strong multiple bonds can form the driving force for many important catalytic processes. The remaining chapters of this thesis further explore the chemistry of these multiply bonded units with a view to gaining a better understanding of these important transformations.

1.8 References.

1. G.J. Palenik, *Inorg. Chem.* 1967, 6, 507.
2. P. Stravopoulos, P.G. Edwards, T. Behling, G. Wilkinson, M. Montevalli, M.B. Hursthouse, *J. Chem. Soc. Dalton Trans.* 1987, 169.
3. J.M. Mayer, T.H. Tulip, J.C. Calabrese, E. Valencia, *J. Am. Chem. Soc.* 1987, 109, 157.
4. J.M. Mayer, D.L. Thorn, T.H. Tulip, *J. Am. Chem. Soc.* 1985, 107, 7454.
5. L. Roeker, T.J. Meyer, *J. Am. Chem. Soc.* 1986, 108, 4066.
6. M.E. Marmion, K.J. Takeuchi, *J. Am. Chem. Soc.* 1986, 108, 510.
7. D.W. Pipes, T.J. Meyer, *Inorg. Chem.* 1986, 25, 3256.
8. E. Valencia, B.D. Santarsiero, S.J. Geib, A.L. Rheingold, J.M. Mayer, *J. Am. Chem. Soc.* 1987, 109, 6896.
9. W.A. Nugent, B.L. Haymore, *Coord. Chem. Rev.* 1980, 31, 123.
10. W.A. Nugent, J.M. Mayer, *"Metal Ligand Multiple Bonds"*, Wiley, New York, 1988.
11. J.T. Anhaus, T.P. Kee, M.H. Schofield, R.R. Schrock, *J. Am. Chem. Soc.* 1990, 112, 1642.

12. P.J. Walsh, F.J. Hollander, R.G. Bergman, *J. Am. Chem. Soc.* 1988, 110, 8729.
13. B.L. Haymore, E.A. Maata, R.A.D. Wentworth, *J. Am. Chem. Soc.* 1979, 101, 2063.
14. R.R. Schrock, *J. Am. Chem. Soc.* 1974, 96, 6796.
15. D. Seyferth, ed. *"Transition Metal Carbene Complexes"*, Verlag Chemie, Weinheim, 1983.
16. R. Hoffmann, G.D. Zeiss, G.W. VanDine, *J. Am. Chem. Soc.* 1968, 90, 1485.
17. H. Nakatsuji, J. Ushio, S. Han, T. Yonezawa, *J. Am. Chem. Soc.* 1983, 105, 426.
18. J. Ushio, H. Nakatsuji, T. Yonewaza, *J. Am. Chem. Soc.* 1984, 106, 5892.
19. E.A. Carter, W.A. Goddard III, *J. Am. Chem. Soc.* 1986, 108, 2180 and 4746.
20. M. Sodupe, J.M. Lluche, A. Oliva, J. Bertran, *Organometallics*, 1989, 8, 1837.
21. T.E. Taylor, M.B. Hall, *J. Am. Chem. Soc.* 1984, 106, 1576.
22. A.K. Rappe, W.A. Goddard III, *J. Am. Chem. Soc.* 1977, 99, 3966.
23. D. Spangler, J.J. Wendoloski, M. Dupuis, M.M.L. Chen, H.F. Schaefer III, *J. Am. Chem. Soc.* 1981, 103, 3985.
24. T.R. Cunclari, M.S. Gordon, *J. Am. Chem. Soc.* 1991, 113, 5231.
25. J.R. Collmann, L.S. Hegedus, J.R. Norton, R.G. Finke, *"Principles and Applications of Organometallic Chemistry"*, University Science Press, Mill Valley, CA, 1987.
26. R.J. Goddard, R. Hoffmann, E.D. Jemmes, *J. Am. Chem. Soc.* 1980, 102, 7667.
27. M.M. Francl, W.J. Pietro, R.F. Hout Jr., W.J. Hehre, *Organometallics*, 1983, 2, 281.
28. E.A. Maatta, R.A.D. Wentworth. *Inorg. Chem.* 1979, 18, 2409.

29. J.A. Allison, W.A. Goddard III, A.C.S. Symposium Series "Solid State Chemistry in Catalysis", 1985, 25, 279.
30. D.M.P Mingos, *J. Organomet. Chem.* 1979, 179, C29.
31. L. Ricard, J. Estienne, P. Karagravanidis, P. Toledano, J. Fiscger, A. Metscler, R. Weiss, *J. Coord Chem.* 1974, 3, 277.
32. B. Kamenar, M. Penavic, C. Prout, *Cryst. Struct. Comm.* 1973, 2, 41.
33. R.H. Fenn, *J. Chem. Soc. A*, 1969, 1764.
34. A.K. Rappe, W.A. Goddard III, *J. Am. Chem. Soc.* 1982, 104, 448.
35. A.K. Rappe, W.A. Goddard III, *J. Am. Chem. Soc.* 1982, 104, 3287.
36. A.K. Rappe, *Inorg. Chem.* 1984, 23, 995.
37. R.R. Schrock, J.S. Murdzek, G.C. Bazan, J. Robbins, M. DiMare, M.B. O'Regan, *J. Am. Chem. Soc.* 1990, 112, 3875.
38. R.R. Schrock, R.T. Depue, J. Feldman, K.B. Yap, D.C. Yang, W.M. Davis, L.Y. Park, M. DiMare, M.H. Schofield, J.T. Anhaus, E. Walborsky, E. Evitt, C. Kruger, P. Betz, *Organometallics*, 1990, 9, 2262.
39. M.H. Schofield, R.R. Schrock, L.Y. Park, *Organometallics*, 1991, 10, 1844.
40. R.M. Silverstein, C.G. Bassler, T.C. Morill, "Spectrometric Identification of Organic Compounds", 4th Ed, Wiley, New York, 1981.
41. V.C. Gibson, D.N. Williams, W. Clegg, D.C.R. Hockless, *Polyhedron*, 1989, 8, 1819.
42. This Thesis, Chapter 5.
43. D.N. Williams, J.P. Mitchell, A.D. Poole, U. Siemeling, W. Clegg, D.C.R. Hockless, P.A. O'Neil, V.C. Gibson, *J. Chem. Soc. Dalton Trans.* in press.
44. J.M. Mayer, C.J. Curtis, J.E. Bercaw, *J. Am. Chem. Soc.* 1983, 105, 2651.
45. W.A. Herrmann, G. Weichselbaumer, R.A. Paciello, R.A. Fischer, E. Herdtweck, J. Okuda, D.W. Marz, *Organometallics*, 1990, 9, 489.
46. O.R. Chambers, M.E. Harman, D.S. Rycroft, D.W.A. Sharp, J.M. Winfield, *J. Chem. Res.* 1977, 1849.
47. D.C. Bradley, M.H. Gitlitz, *J. Chem. Soc. A*. 1969, 980.

48. P.A.B. Shapley, Z.Y. Own, J.C. Huffman, *Organometallics*, 1986, 5, 1269.
49. A.A. Kuznetsova, Yu. G. Podzolkov, Yu. A. Busalev, *Russ. J. Inorg. Chem.* 1969, 14, 393.
50. J. Chatt, J.R. Dilworth, G.J. Leigh, *J. Chem. Soc. A.* 1970, 2239.
51. R.R. Schrock, *Acc. Chem. Res.* 1979, 12, 98.
52. L.J. Guggenberger, R.R. Schrock, *J. Am. Chem. Soc.* 1975, 97, 6578.
53. M.R. Churchill, J.R. Missert, W.J. Youngs, *Inorg. Chem.* 1981, 20, 3388.
54. C.D. Wood, S.J. McLain, R.R. Schrock, *J. Am. Chem. Soc.* 1979, 101, 3210.
55. A. Mayr, M.F. Asaro, M.A. Kjelsberg, S.L. Lee, D. Van Erigon, *Organometallics*, 1987, 6, 432.
56. G.C. Bazan, Ph.D. Thesis, Massachusetts Institute of Technology, 1990.
57. This Thesis, Chapter Four.
58. S.M. Rocklage, R.R. Schrock, *J. Am. Chem. Soc.* 1982, 104, 3077.
59. W.A. Nugent, R.J. McKinney, R.V. Kasowski, F.A. Van Gartledge, *Inorg. Chem. Acta.* 1982, 65, L91.
60. B.R. Ashcroft, G.R. Clark, A.J. Nielson, C.E.F. Rickard, *Polyhedron*, 1986, 5, 2081.
61. V.C. Gibson, M. Jolly, unpublished results.
62. N. Calderon, *Chem. Eng. News.* 1967, 45, 51.
63. R.R. Schrock, in "*Reactions of Coordinated Ligands*", P.R. Braterman Ed., Plenum, New York, 1986.
64. R.H. Grubbs, in "*Comprehensive Organometallic Chemistry*", G. Wilkinson, F.G.A. Stone, E.W. Abi Eds. Pergamon, Vol 8, 1982.
65. K.J. Ivin, "*Olefin Metathesis*", Academic Press, London, 1983.
66. V. Draughton, A.T. Babalan, M. Dimonic, "*Olefin Metathesis and Ring Opening Polymerization of cyclo olefins*", 2nd edition, Wiley Interscience, 1985.
67. A.W. Anderson, N.G. Merckling, *U.S. Pat 2721 189* 1955, *Chem. Abstr.* 1955, 50, 3008.
68. C.P.C. Bradshaw, E.J. Howman, L. Turner, *J. Catal.* 1967, 7, 269.

69. F.D. Mango, J. Schachtschneider, *J. Am. Chem. Soc.* 1971, 93, 1123.
70. G.S. Lewandos, R. Pettit, *J. Am. Chem. Soc.* 1971, 93, 7078.
71. R.H. Grubbs, T.K. Brunck, *J. Am. Chem. Soc.* 1972, 94, 2538.
72. J.L. Herisson, Y. Chauvin, *Makromol. Chem.* 1970, 141, 161.
73. T.J. Katz, R. Rothchild, *J. Am. Chem. Soc.* 1976, 98, 2519.
74. R.H. Grubbs, D.D. Carr, C. Hoppin, P.L. Burk, *J. Am. Chem. Soc.* 1976, 98, 3478.
75. T.J. Katz, J. McGinnis, *J. Am. Chem. Soc.* 1977, 99, 1903.
76. R.R. Schrock, *Acc. Chem. Res.* 1990, 23, 158.
77. J. Kress, J.A. Osborn, R.M.E. Green, K.J. Ivin, J.J. Rooney, *J. Am. Chem. Soc.* 1987, 109, 899.
78. R.H. Grubbs, L.R. Gilliom, *J. Am. Chem. Soc.* 1986, 108, 733.
79. J.C. Mol, J.A. Moulijn, C. Boelhouwer, *J. Chem. Soc. Chem. Comm.* 1968, 663.
80. R.H. Grubbs, S. Swetnick, *J. Mol. Catal.* 1980, 8, 25.
81. F. Pennella, *J. Catal.* 1981, 69, 206.
82. N. Calderon, E.A. Ofstead, J.P. Ward, W.A. Judy, K.W. Scott, *J. Am. Chem. Soc.* 1968, 90, 4133.
83. J.L. Herisson, Y. Chauvin, N.H. Phung, G. Lefebvre, *C.R. Acad. Sci. Ser. C.* 1969, 269, 661.
84. W.A. Herrmann, J.G. Kuchler, J.K. Felixberger, E. Herdtweck, W. Wagner, *Angew. Chem. Int. Ed. Engl.* 1988, 27, 394.
85. R.R. Schrock, *J. Organomet. Chem.* 1986, 300, 249.
86. R.R. Schrock, R. DePue, J. Feldman, C.J. Schaverien, J.C. Dewan, A.H. Liu, *J. Am. Chem. Soc.* 1988, 110, 1423.
87. L Gold, *J. Chem. Phys.* 1958, 28, 91.
88. G. Odian, "*Principles of Polymerization*", Wiley, New York, 1981.
89. A.H.E. Muller, "*Comprehensive Polymer Science*", Pergamon, New York, Volume 3, Chapter 26, 1989.

90. G.C. Bazan, R.R. Schrock, H.N. Cho, V.C. Gibson, *Macromolecules*, 1991, 24, 4495.
91. G.C. Bazan, R.R. Schrock, E. Khosravi, W.J. Feast, V.C. Gibson, *Polymer Comm.* 1989, 30, 258.
92. G.C. Bazan, R.R. Schrock, E. Khosravi, W.J. Feast, V.C. Gibson, M.B. O'Regan, J.K. Thomas, W.M. Davis, *J. Am. Chem. Soc.* 1990, 112, 8378.
93. J. Feldman, W.M. Davis, J.K. Thomas, R.R. Schrock, *Organometallics*, 1990, 9, 2535.
94. H. V. St. A. Hubbard, E.L.V. Lewis, University of Leeds, Work in Progress.
95. G.C. Bazan, R.R. Schrock, M.B. O'Regan, *Organometallics*, 1991, 10, 1062.
96. V.C. Gibson, E.L. Marshall, Unpublished Results.
97. R.R. Schrock, W.E. Crowe, G.C. Bazan, M. DiMare, M.B. O'Regan, M.H. Schofield, *Organometallics*, 1991, 10, 1832.
98. R.R. Schrock, *J. Am. Chem. Soc.* 1976, 98, 5399.
99. J.H. Freudenberger, R.R. Schrock, *Organometallics*, 1986, 5, 398.
100. W.A. Nugent, R.L. Harlow, *J. Chem. Soc. Chem. Comm.* 1978, 579.
101. S.M. Rocklage, R.R. Schrock, *J. Am. Chem. Soc.* 1980, 102, 7808.
102. F.A. Cotton, W.T. Hall, *J. Am. Chem. Soc.* 1979, 101, 5094.
103. W.A. Nugent, *Inorg. Chem.* 1983, 22, 965.
104. I.S. Kolomnikov, Yu. D. Koreshkov, T.S. Lobeeva, M.E. Volpin, *J. Chem. Soc. Chem. Comm.* 1970, 1432.
105. S.F. Pederson, R.R. Schrock, *J. Am. Chem. Soc.* 1982, 104, 7483.
106. A.J. Nielson, *Inorg. Synth.* 1986, 24, 194.
107. E.A. Maatta, *Inorg. Chem.* 1984, 23, 2560.
108. M.L.H. Green, G. Hogarth, P.C. Konidaris, P. Mountford, *J. Organomet. Chem.* 1990, 394, C9.
109. M.R. Cook, W.A. Herrmann, P. Kiprof, J. Takacs, *J. Chem. Soc. Dalton Trans.* 1991, 797.
110. G. Hogarth, P.C. Konidaris, *J. Organomet. Chem.* 1990, 399, 149.

111. P. Jernakoff, G.L. Geoffrey, A.L. Rheingold, S.J. Geib, *J. Chem. Soc. Chem. Comm.* 1987, 1610.
112. R. Lai, S. Mabile, A. Croux, S. LeBot, *Polyhedron*, 1991, 10, 463.
113. J. Chatt, J.R. Dilworth, *J. Chem. Soc. Chem. Comm.* 1972, 549.
114. E.A. Maatta, B.L. Haymore, R.A.D. Wentworth, *Inorg. Chem.* 1980, 19, 1055.
115. A.O. Chong, K. Oshima, K.B. Sharpless, *J. Am. Chem. Soc.* 1977, 99, 3420.
116. H.W. Turner, J.D. Fellmann, S.M. Rocklage, R.R. Schrock, M.R. Churchill, H.J. Wasserman, *J. Am. Chem. Soc.* 1980, 102, 7809.
117. I. Manners, P. Paetzold, *J. Chem. Soc. Chem. Comm.* 1988, 183,
118. H. Fischer, A. Schlageter, W. Bidell, A. Fruh, *Organometallics*, 1991, 10, 389.
119. R.R. Schrock, S. Rocklage, G. Rupprecht, J. Fellmann, *J. Mol. Cat.* 1980, 8, 793.
120. J. Robbins, T.P. Kee, G.C. Bazan, R.R. Schrock, Abstract 259, *Inorganic Chemistry*, 4th Chemical Congress of North America, New York, 1991.

CHAPTER TWO

Chain-end Functionalization of Living Polymers formed by Ring Opening Metathesis Polymerization.

2.1 Introduction.

Since the discovery of the metathesis reaction, the vast majority of polymers prepared by ROMP have contained little functionality other than carbon-carbon multiple bonds. Although these materials are highly useful for structural purposes, other applications or properties require the incorporation of different functionalities, particularly oxygen and nitrogen containing units. Such functionalized polymers have a variety of uses including supports for solid phase synthesis, precursors to conductive materials and polymer bound catalysts^{1,2}.

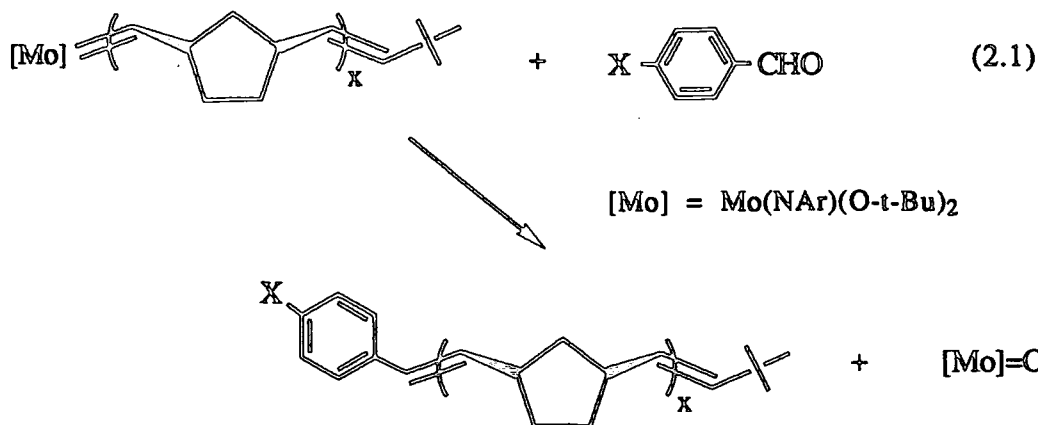
The preparation of such heteroatom containing materials using classical metathesis catalysts proved difficult in the past due to the sensitivity of these electrophilic metal complexes toward the heteroatom functionality^{3,4}. However, living ROMP catalysts have recently been prepared that are sufficiently "deactivated" to an extent that they do not react with the functionality, but still react with the strained carbon-carbon double bond of the monomer on the timescale of a polymerization.

It has been shown that complexes of the type $M(NAr)(CHCMe_2R)(O-t-Bu)_2$ ($M = Mo, W$; $R = Me, Ph$)^{5,6} will polymerize a wide range of norbornene and norbornadiene derivatives in a controlled living manner, leading to functionalized polymers with novel properties⁷⁻⁹. Such initiators offer a greater degree of control over the polymer microstructure than has traditionally been available in cationic and anionic systems.

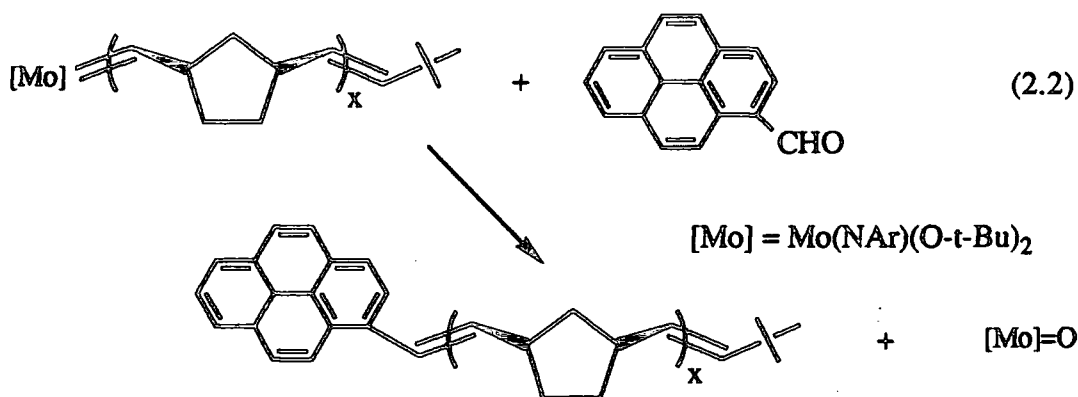
However, polymerization of such monomers only allows functionalization of the polymer backbone; to place functionalities on the polymer chain end requires a different strategy. This chapter therefore describes ways of introducing various potentially useful functionalities to the polymer chain end via means of a "Wittig like" capping reaction.

As described in chapter one, these catalysts are deactivated toward reaction with ordinary olefins, therefore the polymers are cleaved from the metal centre with an aldehyde (typically pivaldehyde or benzaldehyde) to form the metal oxo-imido species $M(NAr)(O)(O-t-Bu)_2$ and a t-butyl or phenyl end capped polymer respectively.

If substituted benzaldehydes are used, a wide variety of which are commercially available, functionalities may be introduced to the end of the polymer chain, as shown in equation 2.1.



This method of end group functionalization has previously been reported in only a limited number of cases. Schrock and Bazan have shown that the reaction of living oligomers with pyrenecarboxaldehyde can be used to introduce a pyrene group to the end of the polymer chain, as shown in equation 2.2¹⁰. Due to its strong affinity for carbon surfaces, this pyrene end group can be used to attach small polymer chains to such surfaces¹¹, a potentially useful application of which would be the modification of electrodes.



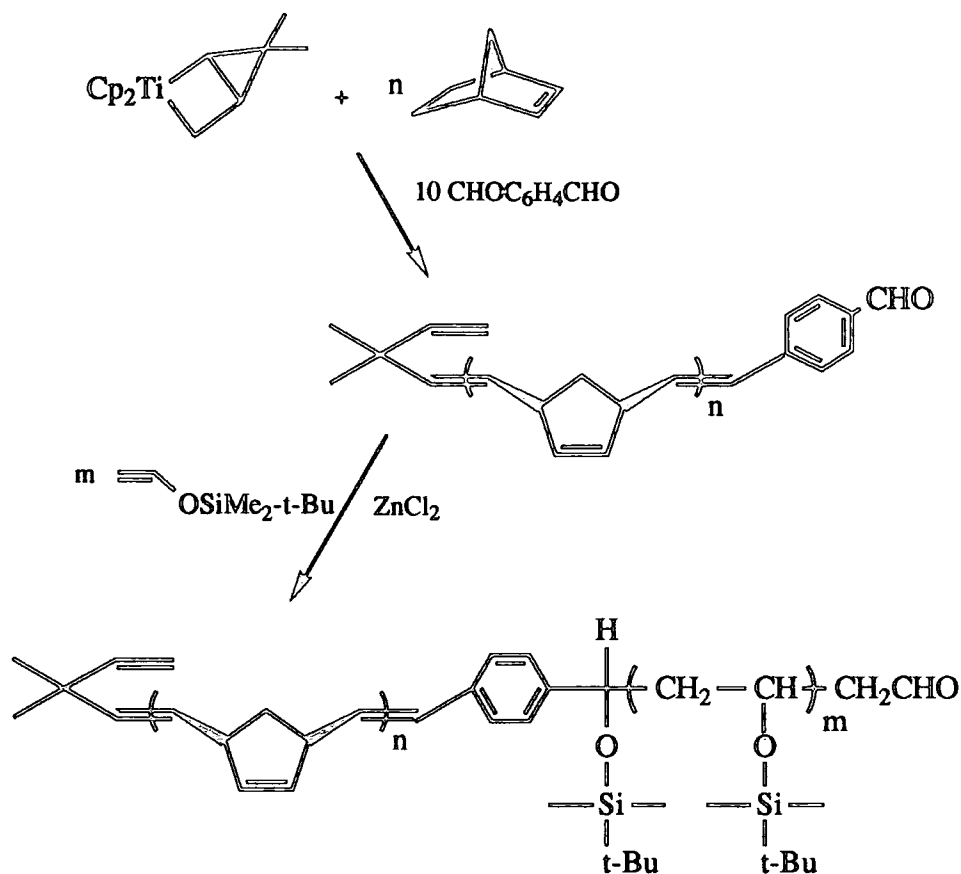
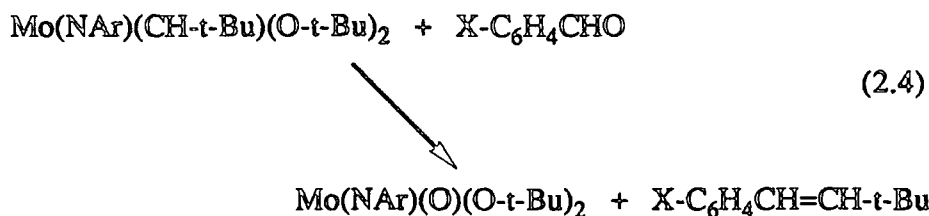


Figure 2.1 Formation of polynorbornene-block-poly(silyl-vinylether).

2.2 Reaction of $\text{Mo}(\text{NAr})(\text{CH-t-Bu})(\text{O-t-Bu})_2$ with Para-Substituted Benzaldehydes.

In experiments designed to test the tolerance of $\text{Mo}(\text{NAr})(\text{CH-t-Bu})(\text{O-t-Bu})_2$ (1) toward a variety of functionalities in this capping reaction, the initiator (1) was reacted with various *para*-substituted benzaldehyde derivatives (typically one to two equivalents) in C_6D_6 and the reaction monitored by ^1H NMR spectroscopy. The reaction is relatively fast and quantitative at room temperature for the functionalities listed in table 2.1, to yield $\text{Mo}(\text{NAr})(\text{O})(\text{O-t-Bu})_2$ (2) and $p\text{-X-C}_6\text{H}_4\text{CH=CH-t-Bu}$, as shown in equation 2.4. The metal oxo-imido species formed subsequently equilibrates with $\text{Mo}(\text{NAr})_2(\text{O-t-Bu})_2$ and $\text{Mo}(\text{O})_2(\text{O-t-Bu})_2$, an observation that is discussed further in chapter four.



The 250 MHz ^1H NMR spectrum of (2) in C_6D_6 (figure 2.2) reveals septet and doublet resonances at δ 4.33 and 1.35 due to the isopropyl methine and methyl protons respectively of the arylimido ligand. A singlet resonance at δ 1.26 is observed for the *t*-butoxide groups, and the expected triplet and doublet resonances of the three aromatic protons are observed at δ 6.97 and 7.07. This compound has also been prepared by Schrock and co-workers as a yellow oil, obtained from the reaction of Li-O-*t*-Bu with $\text{Mo(NAr)(O)Cl}_2(\text{pyr})$ in diethylether¹⁰. Repeated attempts to crystallize the compound failed, presumably due to its subsequent equilibration reactivity.

^1H NMR data for the *para*-substituted phenyl-*t*-butylethylene products of this reaction are listed in table 2.1.

The olefinic protons in the Wittig product represent an AB spin system and therefore differences in their NMR spectra can be attributed to changes in the relative values of the coupling constant (*J*) and the chemical shift difference of the two protons ($\delta\nu$). As $J / \delta\nu$ increases, the expected doublet of doublets move closer together and the outer two peaks are reduced in intensity. At very small $\delta\nu$ values (i.e as $J / \delta\nu \rightarrow \infty$) the two outer lines become vanishingly low in intensity and the two inner lines coalesce to give a singlet (as in the case of $\text{X} = \text{CN}$ and $\text{X} = \text{Cl}$)¹⁴.

$p\text{-XC}_6\text{H}_4\text{CH}=\text{CH}\text{-}t\text{-Bu}$	$\text{CH}=\text{CH}^a$	$^3J_{\text{HH}}$ (Hz)	$t\text{-Bu}$	X
X = H	6.37, 6.31	16.2	1.03	—
	6.23, 6.13	16.1		
X = CF ₃	6.13, 6.12	b	0.99	—
X = OMe	6.39, 6.32	16.2	1.07	3.31
	6.16, 6.09	16.2		
X = NMe ₂	6.49, 6.42	16.1	1.11	2.51
	6.23, 6.16	16.2		
X = CN	6.01	b	0.95	—
X = CO ₂ Me	6.29, 6.22	16.1	1.03	1.76
	6.12, 6.06	16.3		
X = CHO	6.17	b	0.98	9.71
	6.40, 6.34	16.3	1.06	
	6.20, 6.17	16.3		
X = NO ₂	6.05, 6.04	b	0.95	—
X = OH (2,6 di- <i>t</i> -Bu)	6.58, 6.50	16.1	1.12	4.93
	6.37, 6.29	16.1		
X = Cl ^c	6.22	b	1.09	—

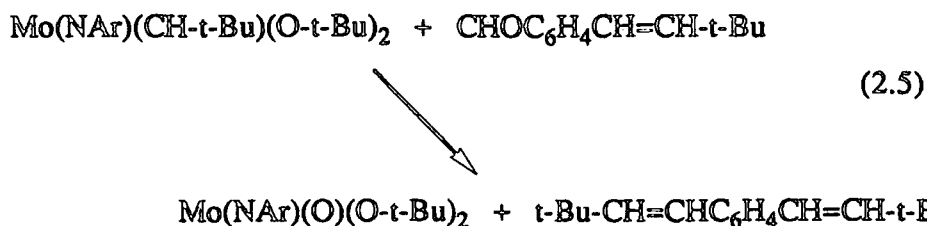
Table 2.1 Selected ¹H NMR data (C₆D₆) for *p*-XC₆H₄CH=CH-*t*-Bu

^a Observed (not calculated for an AB system) values quoted.

^b Outer resonances of AB splitting pattern not detectable.

^c Capping reaction performed in CDCl₃.

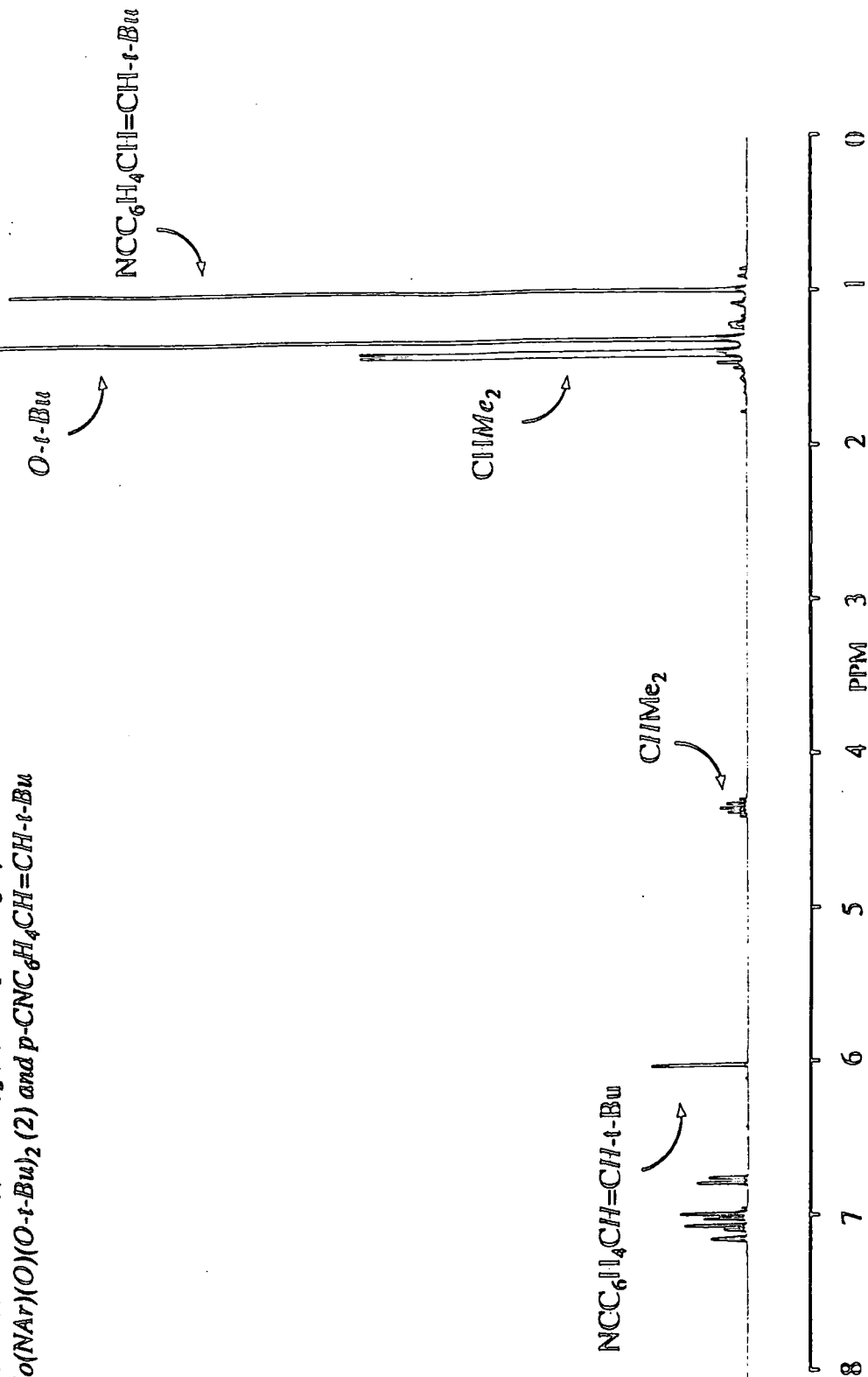
For X = CHO, in addition to the singlet resonance at 6.17 ppm, an additional doublet of doublets is observed (2%, ³J_{HH} = 16.3 Hz). This can be attributed to olefin formed by direct reaction of the Wittig product with initiator, as shown in equation 2.5.



In each case the observed $^3J_{\text{HH}}$ coupling constant of approximately 16 Hz indicate that the Wittig product is solely *trans*. In general *trans*-olefins are formed in reactions of benzaldehyde with neopentylidene initiators (2% *cis*-olefin is formed with $\text{W}(\text{NAr})(\text{CH-t-Bu})(\text{O-t-Bu})_2$) whilst *cis*-olefins are formed in reactions involving living alkylidenes. A representative ^1H NMR spectrum of the reaction between one equivalent of *p*-NCC₆H₄CHO and $\text{Mo}(\text{NAr})(\text{CH-t-Bu})(\text{O-t-Bu})_2$ in C₆D₆ is shown in figure 2.2.

From the range of *para*-substituted benzaldehydes evaluated in this manner, only *p*-HOC₆H₄CHO in C₆D₆ gave unidentifiable products. This is not altogether surprising as alternative reaction pathways are available to the initiator in the presence of the hydroxyl functionality. One such pathway is the exchange of alkoxide ligands at the molybdenum centre¹⁵. This has been shown to be rapid in C₆D₆, with the stability of the newly formed alkylidene complex dependent upon the steric bulk of the alkoxide ligands. For example, the reaction of $\text{Mo}(\text{NAr})(\text{CHCMe}_2\text{Ph})(\text{O-t-Bu})_2$ with 4.5 equivalents of dry ethanol in C₆D₆ yields three new alkylidene proton resonances at δ 12.02, 12.57 and 12.67, which can be attributed to rotameric forms of the mono and bis ethoxide derivatives of the initiator. These are only stable in solution (0.03M) for approximately 20 minutes before decomposition is observed¹⁵. In contrast, the reaction of (1) with the sterically more encumbered 2,6-di-isopropylphenol gives a mixture of the mono and bis aryloxy derivatives ($\delta_{\text{H}\alpha} = 11.57$ and 11.77 respectively) which are stable in solution for at least 24 hours. Schrock has independently prepared the 2,6-di-isopropylphenoxide derivative of the initiator as a fully characterized solid, via the reaction of $\text{Mo}(\text{NAr})(\text{CHCMe}_2\text{Ph})(\text{OTf})_2(\text{dme})$ with 2 equivalents of LiOAr, and found it to exist as two isomers (*syn* and *anti* rotamers) in solution⁵. Alkoxide exchange

Figure 2.2 250 MHz ^1H NMR spectrum (C_6D_6) of the reaction between $\text{Mo}(\text{NAr})(\text{CH}-t\text{-Bu})(\text{O}-t\text{-Bu})_2$ (1) and $p\text{-CNC}_6\text{H}_4\text{CHO}$ affording $\text{Mo}(\text{NAr})(\text{O})(\text{O}-t\text{-Bu})_2$ (2) and $p\text{-CNC}_6\text{H}_4\text{CH}=\text{CH}-t\text{-Bu}$



between four coordinate molybdenum alkylidene complexes is discussed further in chapter four.

The use of 3,5-di-*t*-butyl-4-hydroxybenzaldehyde, where the hydroxyl group is sterically protected, afforded $\text{Mo}(\text{NAr})(\text{O})(\text{O}-t\text{-Bu})_2$ and $\text{ArCH}=\text{CH}-t\text{-Bu}$ cleanly, showing that the hydroxyl functionality in this capping reagent is sufficiently sterically protected by the two bulky *t*-butyl groups to prevent reaction with the molybdenum centre during the timescale of the capping reaction. This is qualified by the fact that the reaction of (1) with 2 equivalents of 2,6-di-*t*-butylphenol in C_6D_6 proceeds very slowly (by ^1H NMR spectroscopy), with only 2 % of a new alkylidene resonance seen ($\delta \text{H}_\alpha = 11.89$ ppm) after 24 hours at room temperature¹⁵.

The use of "OH protected" trimethylsilyl derivatives may offer a way of circumventing the problem encountered with sterically unprotected hydroxyl functionalities.

2.3 Reaction of $\text{Mo}(\text{NAr})(\text{CH}-t\text{-Bu})(\text{O}-t\text{-Bu})_2$ with other Substituted Aldehydes.

Further investigations into the functional group tolerance of $\text{Mo}(\text{NAr})(\text{CH}-t\text{-Bu})(\text{O}-t\text{-Bu})_2$ toward various substituted aldehydes were also carried out on an NMR scale.

Reaction of (1) with 1.0 equivalents of *trans*-cinammaldehyde in C_6D_6 at room temperature afforded (2) and *trans* $\text{C}_6\text{H}_5\text{CH}=\text{CH}-\text{CH}-t\text{-Bu}$ cleanly. The reaction of (1) with 3.0 equivalents of 5-norbornenecarboxaldehyde in C_6D_6 at room temperature gave a mixture of the capped oxo-imido species (2) and polynorbornene, showing that the rate of reaction of the neopentylidene initiator with the aldehyde group competes with the rate of initiation of the polynorbornene chain. By varying the temperature at which this reaction is conducted, it may prove possible to favour the capping reaction over polymerization of the norbornene skeleton, thus allowing the formation of metathesis comb-polymers, as shown in figure 2.3.

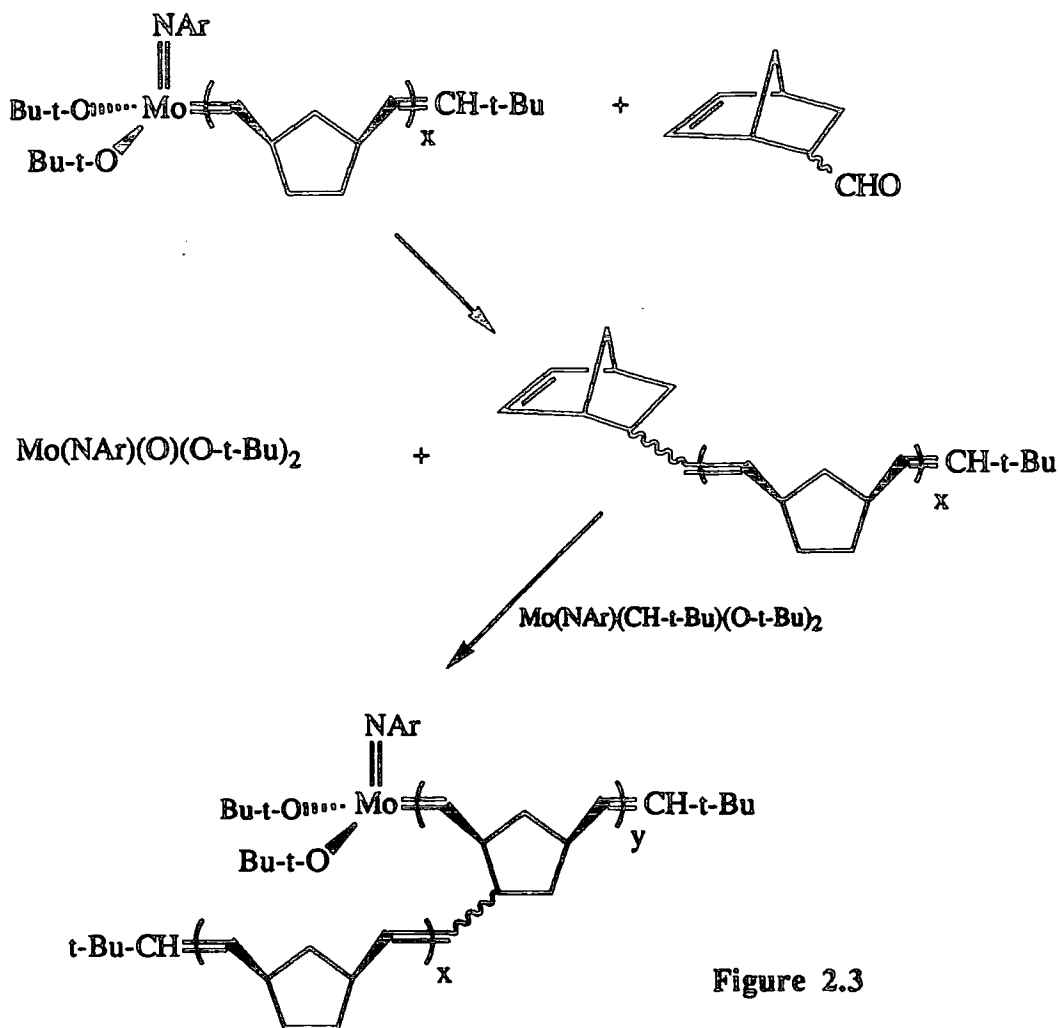
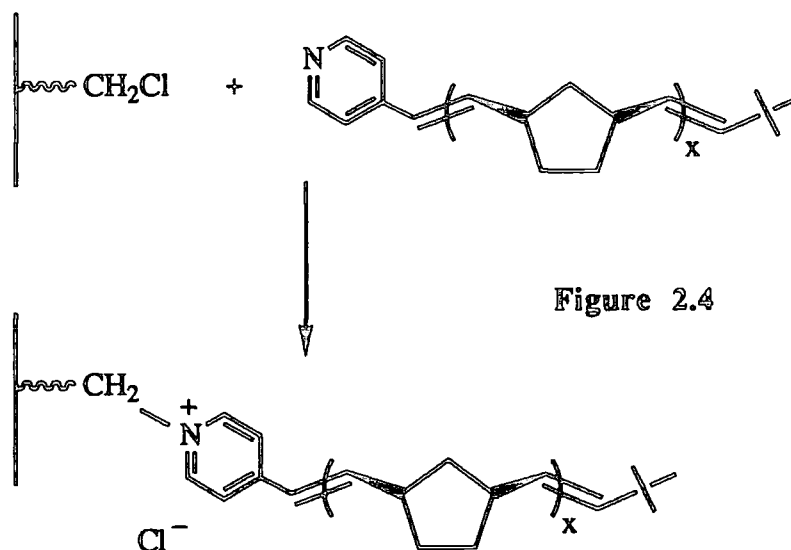


Figure 2.3

Reaction of (1) with 1.1 equivalents of pyridine-4-carboxaldehyde in C_6D_6 at room temperature cleanly affords the oxo imido species (2) and $\text{pyrCH}=\text{CH-t-Bu}$. Resonances for (2) in the 250 MHz ^1H NMR spectrum (C_6D_6) appear at δ 4.39 (septet) and 1.37 (doublet) for the methine and methyl protons respectively of the arylimido unit and at δ 1.29 (singlet) for the *t*-butoxide ligands. This slight shifting of resonances is suggestive of a weak adduct formation in solution via lone pair donation from the nitrogen atom of excess pyridine-4-carboxaldehyde present. Schrock has shown that $\text{Mo}(\text{NAr})(\text{O})\text{Cl}_2(\text{dme})$ can be prepared by the reaction of $\text{Mo}(\text{O})_2\text{Cl}_2(\text{thf})$ with ArNHTMS and that this readily converts to the related bis pyridine adduct $\text{Mo}(\text{NAr})(\text{O})\text{Cl}_2(\text{pyr})_2$ upon addition of 10 equivalents of pyridine. Upon reaction with 2 equivalents of Li-O-t-Bu , pyridine is lost from the coordination sphere to give

$\text{Mo}(\text{NAr})(\text{O})(\text{O}-t\text{-Bu})_2$ as a yellow oil¹⁰. Further evidence for nitrogen lone pair donation to form an adduct is provided by the reaction of (1) with 3.2 equivalents of benzaldehyde to give the oxo-imido species in the presence of excess (4.6 equivalents) pyridine. ^1H NMR resonances for the oxo-imido species appear at δ 4.38 (septet), 1.36 (doublet) and 1.28 (singlet), again slightly shifted from those for base free $\text{Mo}(\text{NAr})(\text{O})(\text{O}-t\text{-Bu})_2$.

Upon attachment to the end of a polymer chain, this pyridine end group could be used to anchor the polymer to a support, via a covalent bond formed between the nucleophilic pyridine end group and a suitable electrophilic group on the surface. This is depicted in figure 2.4.



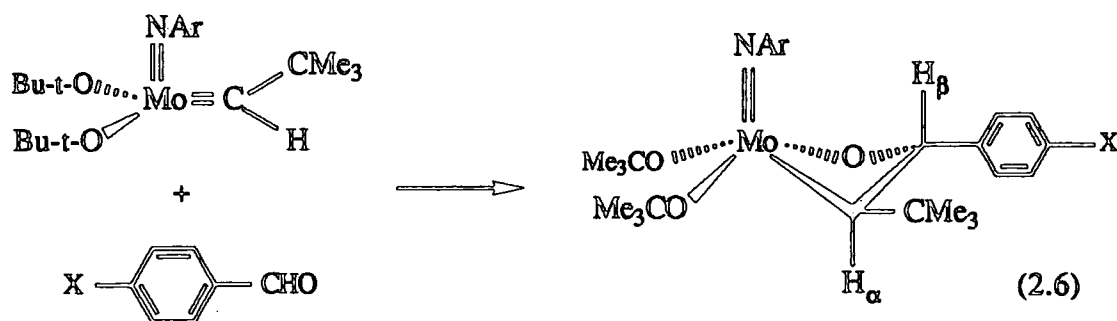
Changing the ancillary alkoxides on the molybdenum centre dramatically alters the rate of capping. The reaction of $\text{Mo}(\text{NAr})(\text{CHCMe}_2\text{Ph})(\text{OCMe}(\text{CF}_3)_2)_2$ with benzaldehyde is surprisingly much slower than for the *t*-butoxide analogue, taking approximately four hours at room temperature in C_6D_6 (0.04M) for complete conversion to the oxo-imido species. The 400 MHz ^1H NMR spectrum of $\text{Mo}(\text{NAr})(\text{O})(\text{OCMe}(\text{CF}_3)_2)_2$ (3) in C_6D_6 reveals a septet at δ 4.25 and a doublet at δ 1.27 for the methine and methyl protons respectively of the arylimido unit, and a singlet resonance at δ 1.46 for the methyl protons of the alkoxide ligands. The

increased stability of the bis hexafluoro-*t*-butoxide initiator can be attributed to electronic effects upon changing the alkoxide ligands, as changing from a neopentylidene to a neophylidene ligand does not drastically alter the rate of the capping reaction. For $\text{Mo}(\text{NAr})(\text{CHCMe}_2\text{Ph})(\text{OCMe}(\text{CF}_3)_2)_2$, the increased electron withdrawing ability of the fluorinated alkoxides enhances the electrophilicity of the metal centre and increases the metal ligand bond strengths, thus decreasing the rate of oxo/alkylidene exchange. The increased steric congestion around the metal centre provided by the bulky fluorine groups may also contribute to the observed slower rate of reaction.

$\text{Mo}(\text{NAr})(\text{CH-}t\text{-Bu})(\text{O-}t\text{-Bu})_2$ (1) did not react to any measurable extent (by ^1H NMR spectroscopy) with 0.5 equivalents of methyl formate in C_6D_6 at 50 °C for 3 days in a sealed NMR tube, with 1.1 equivalents of urea (9 days at room temperature in a sealed NMR tube), with 1.3 equivalents of tetramethylurea (14 days at room temperature in a sealed NMR tube), or with 2.0 equivalents of benzophenone in C_6D_6 (4 days at room temperature in a sealed NMR tube).

2.4 2-Oxametallacyclobutane Intermediates.

Inspection of the reaction of the neopentylidene initiator $\text{Mo}(\text{NAr})(\text{CH-}t\text{-Bu})(\text{O-}t\text{-Bu})_2$ (1) with 1 - 2 equivalents of $p\text{-XC}_6\text{H}_4\text{CHO}$ ($\text{X} = \text{H}, \text{CN}, \text{CHO}, \text{NO}_2, \text{CO}_2\text{Me}$) by ^1H NMR spectroscopy immediately after addition of the benzaldehyde derivative revealed in each case a single intermediate that formed rapidly and in high yield. This was observed to convert only relatively slowly to the oxo-imido species $\text{Mo}(\text{NAr})(\text{O})(\text{O-}t\text{-Bu})_2$ (2) and the olefinic product $p\text{-XC}_6\text{H}_4\text{CH}=\text{CH-}t\text{-Bu}$. These intermediates are proposed to be 2-oxametallacycle precursors to the products, and since (1) contains a *syn*-neopentylidene group (with the *t*-butyl group pointing toward the imido nitrogen atom), they are proposed to contain α -*t*-butyl and β - $\text{C}_6\text{H}_4\text{X}$ groups in the equatorial positions of a SP based metallacyclobutane ring, as shown in equation 2.6.

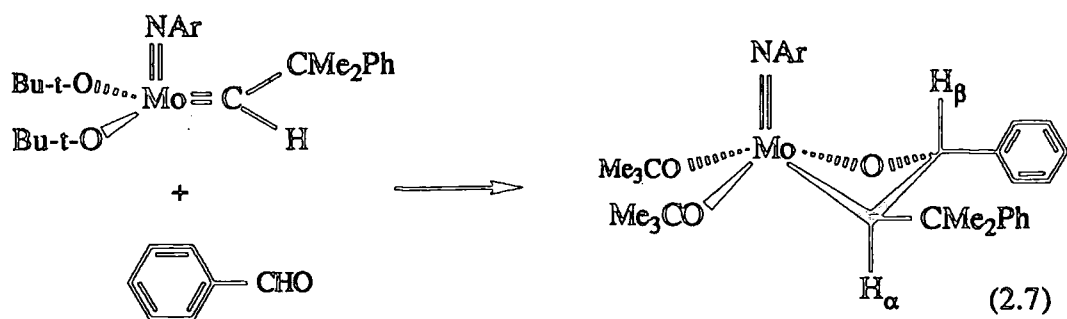


Related 2-oxametallacycles have been observed before¹⁶⁻²², and have been postulated as intermediates in transition metal catalyzed olefin epoxidation reactions²³⁻²⁵, and "Wittig like" reactions of carbonyl species with high oxidation state alkylidene complexes²⁶⁻²⁸. The reaction of $\text{Cp}^* \text{Ta}(\text{CH}_3)(\text{CH}_2)$ with aldehydes yields oxacyclobutane complexes²⁹, and the addition of ketenes to $\text{Cp}_2\text{Ti}(\text{CH}_2)$ yields β -alkylidene-titana-2-oxametallacyclobutane complexes³⁰. These complexes, however, tend not to be stable, with only a handful of X-ray structures being reported in the literature²⁸⁻³².

The 2-oxametallacycles are characterized by two distinct doublets for H_α and H_β , at δ 1.95 and 6.02 ($J_{\text{H}_\alpha\text{H}_\beta} = 7.1$ Hz) for $\text{X} = \text{CN}$, δ 2.08 and 6.16 ($J_{\text{H}_\alpha\text{H}_\beta} = 7.1$ Hz) for $\text{X} = \text{CHO}$, δ 1.96 and 6.07 ($J_{\text{H}_\alpha\text{H}_\beta} = 7.4$ Hz) for $\text{X} = \text{NO}_2$, δ 2.16 and 6.18 ($J_{\text{H}_\alpha\text{H}_\beta} = 7.6$ Hz) for $\text{X} = \text{CO}_2\text{Me}$ and δ 2.23 and 6.22 ($J_{\text{H}_\alpha\text{H}_\beta} = 7.6$ Hz) for $\text{X} = \text{H}$. These data are similar to those previously reported by Schrock for the analogous metallacycle formed upon the addition of pentafluorobenzaldehyde to (1)²⁸. The H_β resonances are shifted downfield compared with those in MC_3 metallacyclobutanes, formed by addition of an olefin to (1), presumably due to the presence of the electron withdrawing oxygen atom. An analogous metallacycle can also be observed for the addition of benzaldehyde to the neophylidene initiator $\text{Mo}(\text{NAr})(\text{CHCMe}_2\text{Ph})(\text{O}-t\text{-Bu})_2$ ($\delta \text{H}_\alpha = 2.72$, $\text{H}_\beta = 6.07$, $J_{\text{H}_\alpha\text{H}_\beta} = 6.8$ Hz), as shown in equation 2.7. Selected data for all these metallacycles are given in table 2.2.

For the reaction of (1) with $p\text{-Me}_2\text{NC}_6\text{H}_4\text{CHO}$, no 2-oxametallacycle intermediate could be observed; only slow conversion of (1) to (2) over a period of approximately 40 minutes at room temperature. This is consistent with the finding that

metallacyclobutanes are stabilized by electron withdrawing substituents on the ring, and is discussed in the following section^{28,33}.



metallacycle	R	H _β	H _α	CHMe ₂	OCMe ₃	CHMe ₂	CHCMe ₂ R
X = H	Me	6.22	2.23	4.21	1.54 1.45	1.32	1.14
X = H	Ph	6.07	2.72	4.20	1.48 1.43	not located	1.66 1.58
X = CN	Me	6.02	1.95	4.11	1.48 1.42	1.31 1.29	1.04
X = CHO ^a	Me	6.16	2.08	4.15	1.51 1.44	1.33 1.30	1.10
X = NO ₂	Me	6.07	1.96	4.11	1.49 1.44	1.31 1.29	1.06
X = CO ₂ Me ^b	Me	6.18	2.16	4.20	1.52 1.45	not located	1.12

Table 2.2 Selected ¹H NMR data (C₆D₆) for metallacycles of the type Mo(NAr)(CH(CMe₂R)CH(C₆H₄X)O)(O-t-Bu)₂.

^a CHO resonance of metallacycle at 9.68 ppm.

^b CO₂Me resonance of metallacycle at 1.73 ppm.

2.5 Solution Stability of 2-Oxametallacycles.

Analysis of the olefinic product ($p\text{-XC}_6\text{H}_4\text{CH=CHCMe}_2\text{R}$, R = Me, Ph) formed upon the decomposition of the various 2-oxametallacycles in C_6D_6 reveals it to be solely trans, as determined by coupling constants of approximately 16 Hz in the 250 MHz ^1H NMR spectrum (see table 2.1). No cis olefin could be detected, suggesting that a trans metallacycle decomposes only to give the trans olefin product. In the reaction of (1) with pentafluorobenzaldehyde²⁸, approximately 6% cis metallacycle has been observed, decomposing to give 6% cis olefin product (possessing a correspondingly lower $^3\text{J}_{\text{HH}}$ coupling constant of approximately 12 Hz). Again this suggests that a cis metallacycle decomposes to give only cis olefin product, with no significant amount of aldehyde being lost (degenerate metathesis) from the metallacycle of either isomer.

The overall mechanism for the capping reaction is shown in figure 2.5¹⁰. An initial aldehyde-metal interaction occurs (A), similar to that proposed for addition of an olefin to (1), possibly *initially* bonded via donation of a lone pair of electrons from the oxygen atom to the metal rather than donation from the C=O π system. This subsequently rearranges to form an as yet unobservable 2-oxametallacycle where the MOC_2 ring spans both axial and equatorial positions (B). For the olefin to be ejected from the metal centre, the metallacycle must adopt the correct geometry for olefin loss (D), by undergoing a Berry pseudorotation about the M=N bond. This rearrangement necessitates passing through the spectroscopically observed square pyramidal metallacycle (C).

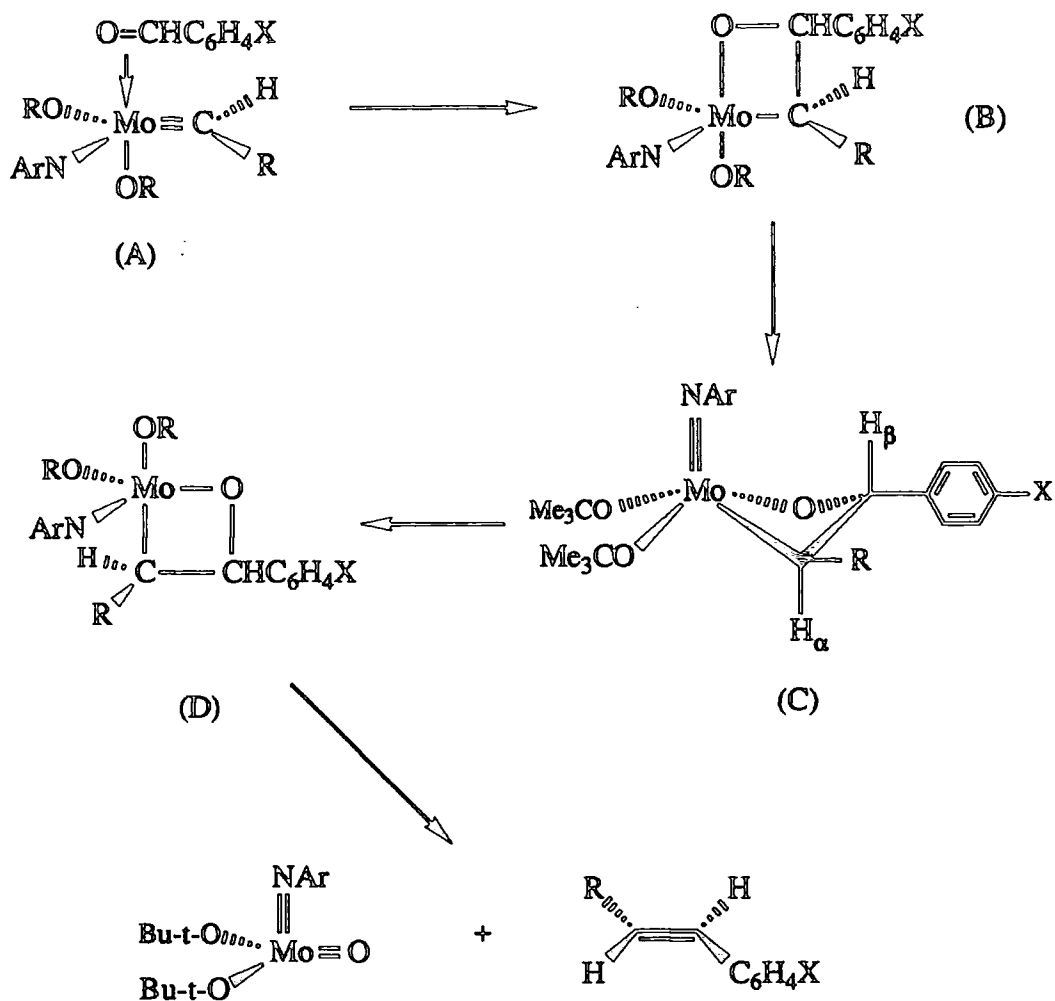


Figure 2.5

Although a detailed kinetic analysis of the rate of ring opening of the 2-oxametallacycles described here has not been undertaken, it can be noted qualitatively that for metallacycles derived from the neopentylidene initiator (i.e. possessing an α t-butyl group) each can be observed in solution in C₆D₆ (0.02M) for approximately 40 minutes at room temperature before conversion to the oxo-imido species (2) is complete. However, the metallacycle formed from the neophylidene initiator is still observable in C₆D₆ solution (0.02M) for over 50 minutes at room temperature. This increased stability of the 2-oxametallacycle upon changing from the neopentylidene to

neophylidene initiator is again consistent with recent results published by Schrock and co-workers^{10,28}, where the rate of decomposition of the α t-butyl containing metallacycle $\text{Mo}(\text{NAr})(\text{CH}(\text{CMe}_3)\text{CH}(\text{C}_6\text{F}_5)\text{O})(\text{O-t-Bu})_2$ ($6.7 \times 10^{-4} \text{ s}^{-1}$ at 35.1°C) was found to be approximately 25 times faster than the rate of decomposition of the corresponding neophyl analogue $\text{Mo}(\text{NAr})(\text{CH}(\text{CMe}_2\text{Ph})\text{CH}(\text{C}_6\text{F}_5)\text{O})(\text{O-t-Bu})_2$ ($0.25 \times 10^{-4} \text{ s}^{-1}$ at 35.0°C).

This stabilization of 2-oxametallacycles (and presumably C_3 analogues) by electron withdrawing groups and bulky C_α alkyl groups can be rationalized with reference to figure 2.5. Bulky groups hinder rotation of the ligands, especially in structure D of figure 2.5 where the bulky imido and alkyl groups are in close contact, thus slowing down formation of the metallacycle with the correct geometry for olefin loss. If the energetics of aldehyde binding to the metal centre is important, aldehydes with electron withdrawing groups will bind less strongly and hence also help to stabilize the metallacycle.

Also consistent with earlier findings is the observation that the metallacycle formed by the reaction of (1) with *p*-CNC₆H₄CHO appears to decompose more rapidly (within 30 minutes) in the presence of two equivalents of dimethoxyethane, suggesting that coordinating solvents *may* play an important role in metallacycle break up.

2.6 End-Capped Polymers via Reaction with Substituted Benzaldehydes.

For a successful capping reaction, the functionality must be introduced with negligible broadening of the molecular weight distribution of the resultant polymer.

Table 2.3 gives the results of gel permeation chromatographic analyses for a series of para-substituted phenyl end-capped polynorbornenes, formed by the reaction of $\text{Mo}(\text{NAr})(\text{CH-t-Bu})(\text{O-t-Bu})_2$ (1) with 100 equivalents of norbornene in toluene followed by capping with a *p*-substituted benzaldehyde. The resultant polymers were precipitated twice from methanol, dried *in vacuo*, and in each case isolated in greater

than 95% yield. A typical GPC trace for a 100-mer of norbornene capped with *p*-CNC₆H₄CHO is shown in figure 2.6.

Table 2.3 shows that, in most cases, the functionality may be introduced with negligible broadening of the molecular weight distribution. In the case of *p*-CHOC₆H₄CHO and *p*-NO₂C₆H₄CHO there is a slight increase in the PDI of the 100-mers up to 1.16, which for the dialdehyde is likely to arise due to some dimerization through the reaction of a living 100-mer with the CHO end-capped polymer, as depicted in equation 2.8. Such a dimerization was also seen (equation 2.5) for reaction of the dialdehyde directly with the initiator.

<i>p</i> -XC ₆ H ₄ CHO	M _n (Found) ^a	M _w (found) ^a	PDI (=M _w /M _n)
X = H	17620	18610	1.06
X = CF ₃	17710	19080	1.08
X = OMe	15850	16660	1.05
X = NMe ₂	16560	17770	1.07
X = CN	15090	15940	1.06
X = CO ₂ Me	16840	17790	1.06
X = CHO ^b	18410	21280	1.16
X = NO ₂ ^b	17800	20660	1.16
X = NH ₂ ^b	19120	21490	1.12
X = Cl ^b	17250	19180	1.11

Table 2.3 GPC data for living 100-mers of polynorbornene capped with various *para*-substituted benzaldehyde derivatives.

^a Relative to polystyrene standards in THF.

^b Shoulders to high molecular weight.

$M_n(\text{found}) = 15090$
 $M_w(\text{found}) = 15940$
 $PDI = 1.06$

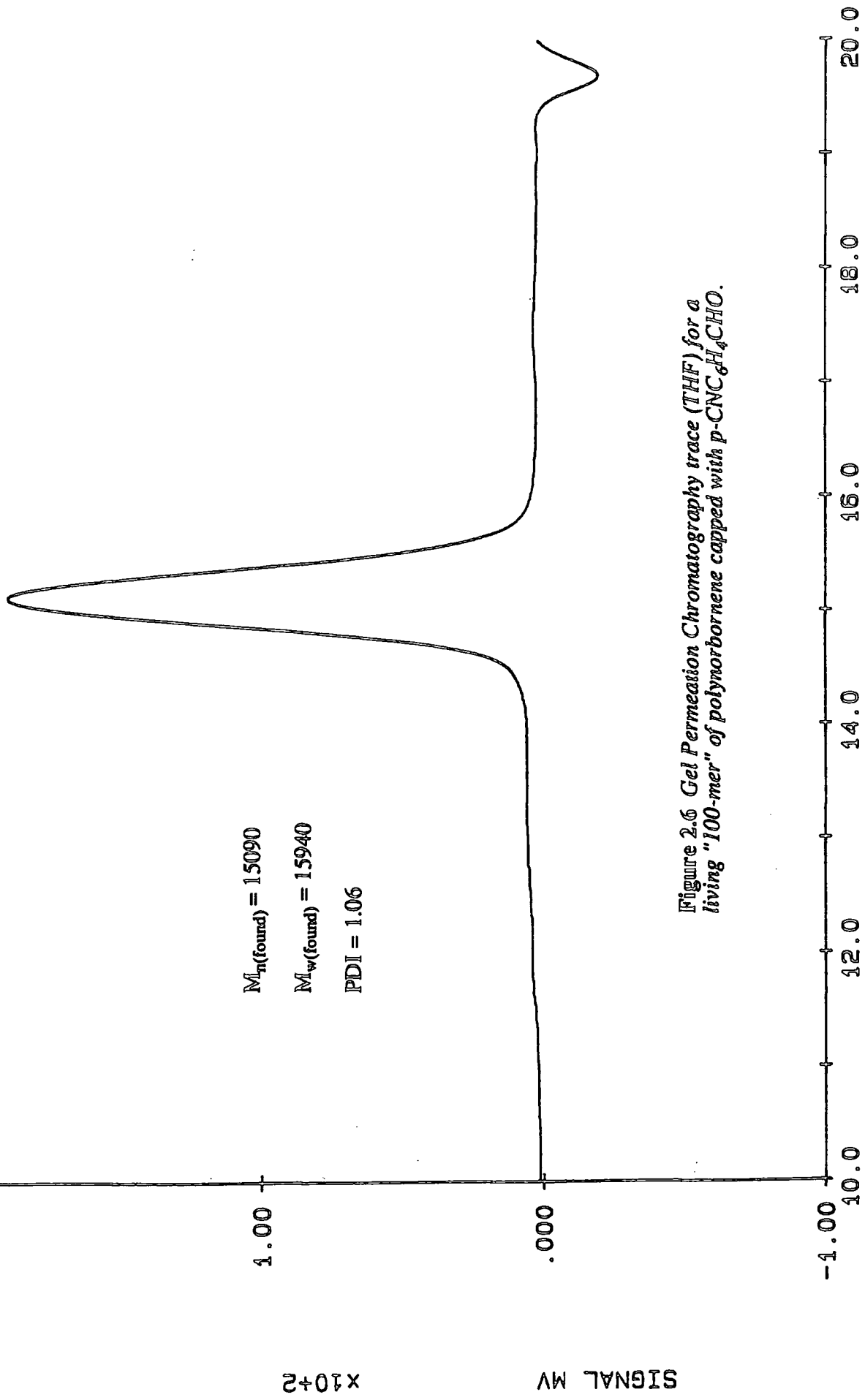
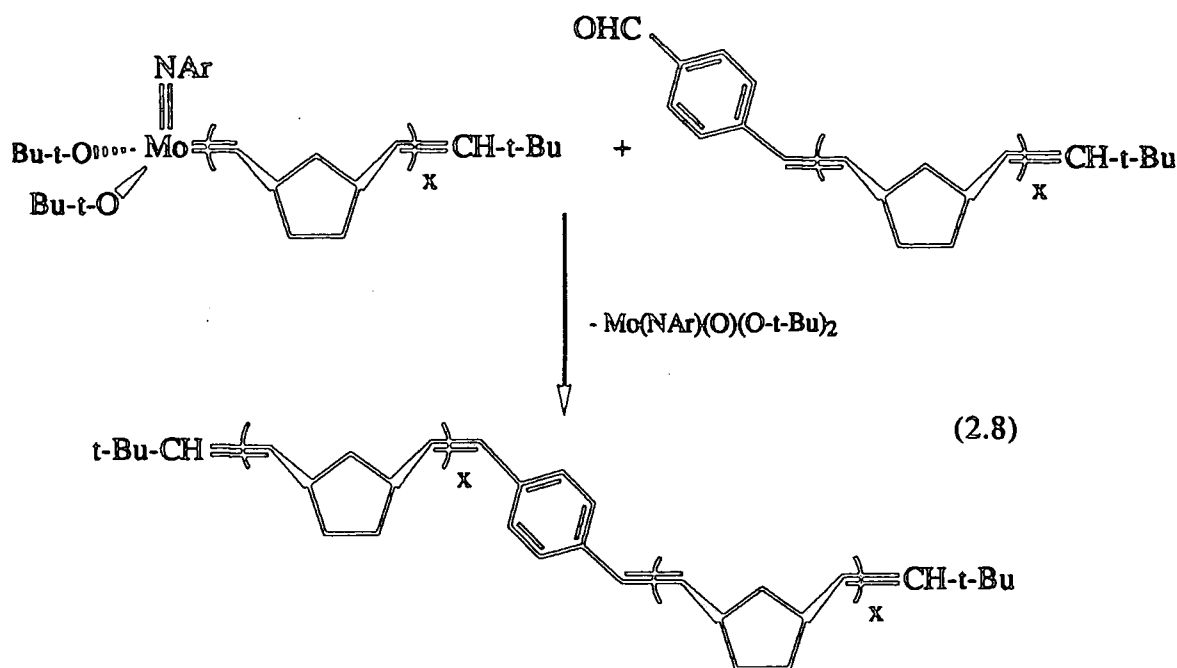


Figure 2.6 Gel Permeation Chromatography trace (THF) for a living "100-mer" of polynorbornene capped with $p\text{-CNC}_6\text{H}_4\text{CHO}$.

RET VOL



A larger excess of this capping reagent is therefore required to maintain the narrowest of distributions. The explanation of the broadening with $p\text{-NO}_2\text{C}_6\text{H}_4\text{CHO}$ is less clear. In order to test the stability of $\text{Mo}(\text{NAr})(\text{CH-t-Bu})(\text{O-t-Bu})_2$ (1) to the aromatic nitro group, (1) was treated with 0.5 and 1.0 equivalents of nitrobenzene respectively in C_6D_6 , and the reaction monitored by ^1H NMR spectroscopy. In each case, the initiator was found to react slowly to give the capped oxo-imido species (2), $t\text{-Bu-CH=CH-t-Bu}$ and other, as yet, unidentified species. The formation of $t\text{-Bu-CH=CH-t-Bu}$ can be rationalized by reaction of (2) formed initially with remaining initiator via exchange of oxo and alkylidene units, to give $\text{Mo}(\text{NAr})_2(\text{O-t-Bu})_2$ and $\text{Mo}(\text{O})(\text{CH-t-Bu})(\text{O-t-Bu})_2$, which subsequently decomposes by bimolecular coupling of the alkylidene units (as discussed further in chapter 4). Therefore, the nitro group may also facilitate cross-linking when in contact with living alkylidenes.

Where possible, the presence of the functional group on the polymer was confirmed using IR spectroscopy on a thin polymer film. Characteristic absorptions of the end groups within the isolated polymer are shown in table 2.4.

End Group	IR Data (cm ⁻¹)
X = CN	2235 (C-N stretch)
X = NO ₂	1522 (assym) 1345 (syymm N-O stretch)
X = CHO	1710 (C=O stretch)
X = CO ₂ Me	1774 (C=O stretch) 1195 (C-O-C stretch)
X = CF ₃	1329, 1169, 1130, 1070 (C-F stretch)
X = Cl	1069 (Ar-Cl stretch)
X = NH ₂	3410 (N-H stretch, broad)

Table 2.4 *Characteristic End-group Infrared Absorptions.*

2.7 Summary.

In this chapter it has been shown that a wide range of functionalities may be introduced to the end of the polymer chain, via means of a "Wittig like" capping reaction between the living polymer and a functionalized benzaldehyde derivative, with negligible broadening of the molecular weight distribution. Unusual 2-oxametallacycles can be observed in solution for several benzaldehyde derivatives possessing electron withdrawing substituents in the para position.

2.8 References.

1. P. Hodge, Sherington Eds. *"Polymer Supported Reactions in Organic Synthesis"*, Wiley, New York, 1980.
2. W.T. Ford Ed. *"Polymer Reagents and Catalysts"*, ACS Symposium Series No. 308, Washington, 1986.
3. K.J. Ivin, *"Olefin Metathesis"*, Academic Press, London, 1983.
4. R.H. Grubbs, W. Tumas, *Science*, 1989, 243, 907.
5. R.R. Schrock, J.S. Murdzek, G.C. Bazan, J. Robbins, M. DiMare, M.B. O'Regan, *J. Am. Chem. Soc.* 1990, 112, 3875.
6. R.R. Schrock, R.T. Depue, J. Feldman, K.B. Yap, D.C. Yang, W.M. Davis, L.Y. Park, M. DiMare, M.H. Schofield, J.A. Anhaus, E. Walborsky, E. Evitt, C. Kruger, P. Betz, *Organometallics*, 1990, 23, 158.
7. R.R. Schrock, *Acc. Chem. Res.* 1990, 23, 158.
8. G.C. Bazan, R.R. Schrock, H.N. Cho, V.C. Gibson, *Macromolecules*, 1991, 24, 4495.
9. G.C. Bazan, E. Khosravi, R.R. Schrock, W.J. Feast, V.C. Gibson, M.B. O'Regan, J.K. Thomas, W.M. Davis, *J. Am. Chem. Soc.* 1990, 112, 8378.
10. G.C. Bazan, Ph.D Thesis, Massachusetts Institute of Technology, 1990.
11. H. Jaegfelt, T. Kuwana, G. Johansson, *J. Am. Chem. Soc.* 1983, 105, 1805.
12. C.V. Pittman, *"Polymer Supported Catalysts"*, in *Comprehensive Organometallic Chemistry*, G. Wilkinson, F.G.A. Stone, E.W. Abel Eds. Vol 8, Pergamon, 1982.
13. W. Risse, R.H. Grubbs, *Macromolecules*, 1989, 22, 1558.
14. R.J. Abraham, *"The Analysis of High Resolution NMR Spectra"*, Elsevier, Amsterdam, 1971.
15. J.P. Mitchell, E.L. Marshall, V.C. Gibson, unpublished results.

16. J.F. Hartwig, R.G. Bergman, R.A. Anderson, *J. Am. Chem. Soc.* 1990, 112, 3234.
17. D.P. Klein, J.C. Hayes, R.G. Bergman, *J. Am. Chem. Soc.* 1988, 110, 3704.
18. R. Schlodder, J.A. Ibers, M. Lenarda, M. Graziani, *J. Am. Chem. Soc.* 1974, 96, 6893.
19. C.R. Bennett, D.C. Bradley, *J. Chem. Soc. Chem. Comm.* 1974, 29.
20. M. Lenarda, R. Ros, O. Traverso, W.D. Pitts, W.H. Bradley, M. Graziani, *Inorg. Chem.* 1977, 16, 3178.
21. S.J. Simpson, H.W. Turner, R.A. Anderson, *Inorg. Chem.* 1981, 20, 2991.
22. A. Miyashita, J. Ishida, H. Nohira, *Tetrahedron Lett.* 1986, 2127.
23. K.B. Sharpless, A.Y. Teranishi, J.E. Backvall, *J. Am. Chem. Soc.* 1977, 99, 3120.
24. J.P. Collman, J.L. Brauman, B. Meunier, T. Hayashi, T. Kodadek, S.A. Raybuck, *J. Am. Chem. Soc.* 1985, 107, 2000.
25. D.M. Walba, C.H. Depuy, J.J. Grabowski, V.M. Bierbaum, *Organometallics*, 1984, 3, 498.
26. S.L. Buchwald, R.H. Grubbs, *J. Am. Chem. Soc.* 1983, 105, 5490.
27. R.R. Schrock, *J. Am. Chem. Soc.* 1976, 98, 5399.
28. G.C. Bazan, R.R. Schrock, M.B. O'Regan, *Organometallics*, 1991, 10, 1062.
29. L.L. Whinnery Jr, L.M. Henling, J.E. Bercaw, *J. Am. Chem. Soc.* 1991, 113, 7575.
30. S.C. Ho, S. Hentges, R.H. Grubbs, *Organometallics*, 1988, 7, 780.
31. R.H. Grubbs, "Alkene and Alkyne Metathesis Reactions", in *Comprehensive Organometallic Chemistry*, G. Wilkinson, F.G.A. Stone, E.W. Abel Eds. Vol 8, Pergamon, 1982.
32. V. Draughton, A.T. Balaban, M. Dimonic, "Olefin Metathesis and Ring Opening Polymerization of Cyclo-Olefins", 2nd Edition, Wiley Interscience, 1985.
33. J. Feldman, W.M. Davis, J.K. Thomas, R.R. Schrock, *Organometallics*, 1990, 9, 2535.

CHAPTER THREE

Styrene Based Chain Transfer Agents for Living Ring Opening Metathesis Polymerization

3.1 Introduction.

Well defined catalysts of the type $M(NAr)(CHCMe_2R)(O-t-Bu)_2$ ($M = Mo^1, W^2$; $R = Me, Ph$) readily react with strained bicyclic olefins, but not with ordinary acyclic olefins, and therefore can be used to polymerize a range of norbornenes³ and 2,3 disubstituted norbornadienes⁴ by living ring opening metathesis polymerization. Living ROMP requires that a propagating alkylidene complex reacts only with the carbon-carbon double bond of the monomer, and not with those present in the growing polymer chain. The polymerization is usually quenched with an aldehyde, in order to remove the metal and cap the polymer in a "Wittig like" reaction (see chapter two⁵). However, if relatively low molecular weight polymers or oligomers are required, it is much more desirable to cleave the polymer from the metal centre and regenerate a new initiator that is active for further polymerizations, thereby making more efficient use of the initiator. This is usually accomplished using a chain transfer (CT) agent. However, no such reagents had been established for well-defined ROMP initiator systems.

The chain transfer reaction must be rapid and go to completion, with the new initiator generated being stable yet reactive. Effective chain transfer can be described as the physical termination of a polymer chain without destruction of the kinetic chain. That is, the new species formed in the chain transfer reaction, which terminates the growing polymer chain, is reactive enough to initiate a new polymer chain more or less within the same period of time required for the addition of a monomer molecule to a growing chain in the normal propagation step.

The nature of the well defined t-butoxide "Schrock type" initiators does not allow ordinary olefins to be used as chain transfer agents, a technique that has been employed in systems containing very reactive "classical" ROMP catalysts⁶⁻⁸. Therefore, an initial search for suitable chain transfer agents for these living ROMP systems focused on substituted cyclopentenes⁹. These were based on the principle that ring opening polymerization is disfavoured at 25°C for cyclohexene; indeed cyclohexene is known to be evolved from polymeric systems if it can form in a metathetical cyclization

reaction^{6,7}. By attaching an alkenyl side chain to a reactive cyclic olefin, such that a cyclohexene could form after the olefin is ring opened, it was hoped that a new alkylidene complex would be regenerated. Figure 3.1 depicts this strategy for a cyclopentene based derivative.

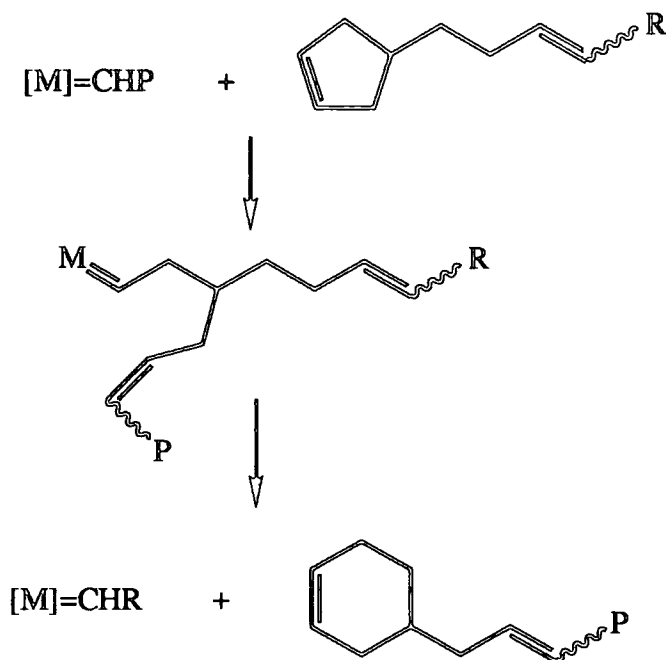
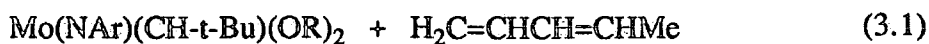


Figure 3.1 Chain transfer employing cyclopentene derivatives.

However, these CT agents were relatively unsuccessful because the cyclopentene double bond was not reactive enough, relative to a double bond in the polymer side chain, to make chain transfer fast and quantitative.

Schrock and co-workers therefore turned their attention to the use of 1,3-pentadienes as chain transfer agents. It had previously been shown¹⁰ that the reaction of $M(NAr)(CH-t-Bu)(OR)_2$ ($M = Mo, W$; $R = OMe_2CF_3, OMe(CF_3)_2$) with *cis*- or *trans*- 1,3 pentadiene, in the presence of the nitrogen base quinuclidine, generated vinyl alkylidene complexes and a number of these have since been isolated and characterized¹¹ (equation 3.1).



These species are also observable intermediates in the polymerization of acetylene¹² and 7,8-bis(trifluoromethyl)tricyclo[4.2.2.0^{2,5}]deca-3,7,9-triene¹³, which suggested that vinyl alkylidene complexes should be active as polymerization initiators themselves. Indeed, living polymers formed by the reaction of norbornene with $\text{M}(\text{NAr})(\text{CH-t-Bu})(\text{O-t-Bu})_2$ ($\text{M} = \text{Mo}, \text{W}$) were found to react with *cis*- or *trans*- 1,3-pentadiene to give methylene end-capped polymers and vinyl alkylidene complexes which could be used as initiators for subsequent polymerizations¹⁴. Although the tungsten complex decomposed over several hours in solution at room temperature in C_6D_6 , the molybdenum complex was stable for 24 hours at approximately 0.01M. The use of 1,3-pentadiene as a chain transfer agent is shown in figure 3.2.

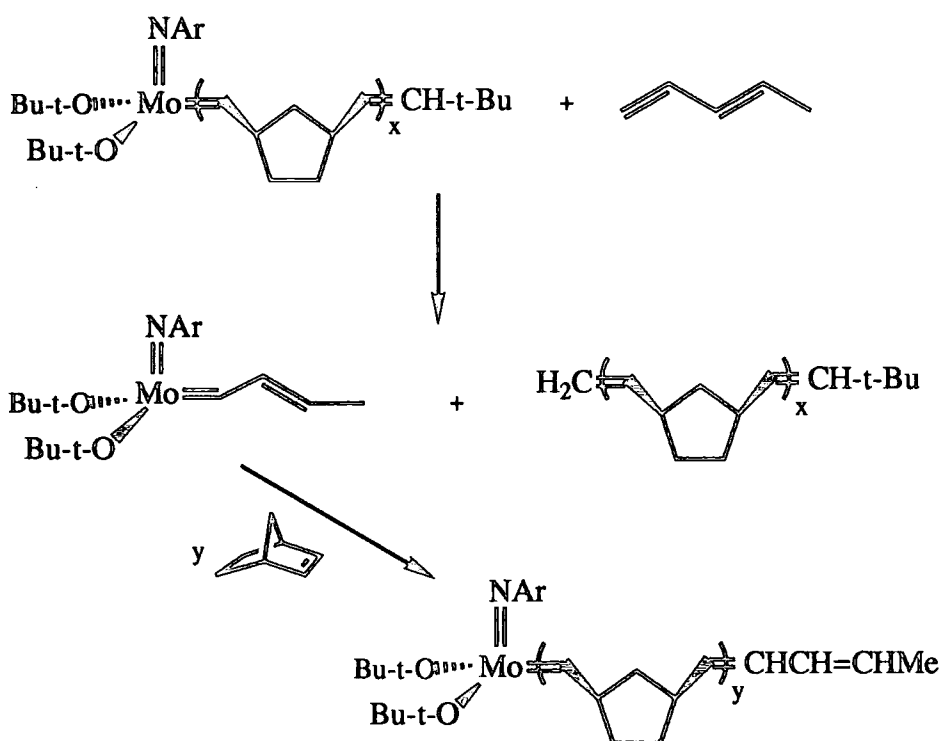


Figure 3.2 Chain transfer employing 1,3-pentadiene.

A particular focus of this work has been the introduction of functional groups onto each end of the polymer chain. Functionalized pentadienes are not readily available. However, a wide range of functionalized styrenes are commercially available and therefore at the same time as Schrock studied 1,3-pentadiene, a series of substituted styrenes were also considered as a chain transfer agents for living ROMP systems. These, if successful, should allow functionalization of the polymer chain head.

It is clear that a conjugated double bond is activated towards chain transfer, whereas non-conjugated olefins are unreactive in this role. The conjugation between the olefinic and aryl groups of styrenes suggested these too may be sufficiently reactive to act as chain transfer agents.

It was envisaged that the reaction of styrene with living polymers would occur in a similar manner to that shown in figure 3.2, generating a methylene end capped polymer and a new benzyldiene initiator $\text{Mo}(\text{NAr})(\text{CHPh})(\text{O-t-Bu})_2$.

The benzyldiene complex $\text{Mo}(\text{NAr})(\text{CHPh})(\text{OCMe}(\text{CF}_3)_2)_2$ has previously been observed *in situ*¹, (alkylidene proton resonance at 12.44 ppm in C_6D_6), formed by the reaction of 3 equivalents of styrene with $\text{Mo}(\text{NAr})(\text{CH-t-Bu})(\text{OCMe}(\text{CF}_3)_2)_2$, but was found to be unstable at room temperature in solution, decomposing over a period of approximately 3 days.

It was therefore hoped that by using the less reactive initiator possessing ancillary t-butoxide ligands, the benzyldiene complex would be sufficiently stable to enable styrene to act as a chain transfer agent, providing, of course, that these benzyldiene complexes behave as initiators for subsequent polymerizations.

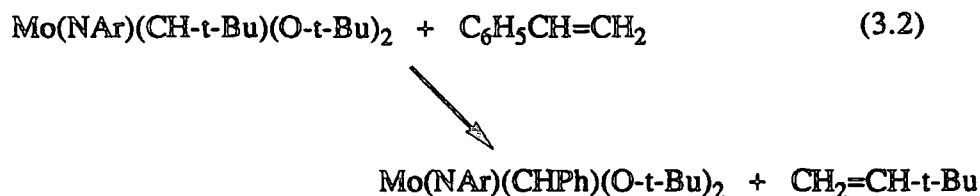
This chapter describes the use of styrene and several of its derivatives as chain transfer agents in these living ring opening metathesis polymerization systems.

3.2 Molybdenum Benzylidenes.

3.2.1 The Reaction of $\text{Mo}(\text{NAr})(\text{CH-t-Bu})(\text{O-t-Bu})_2$ with Substituted Styrenes.

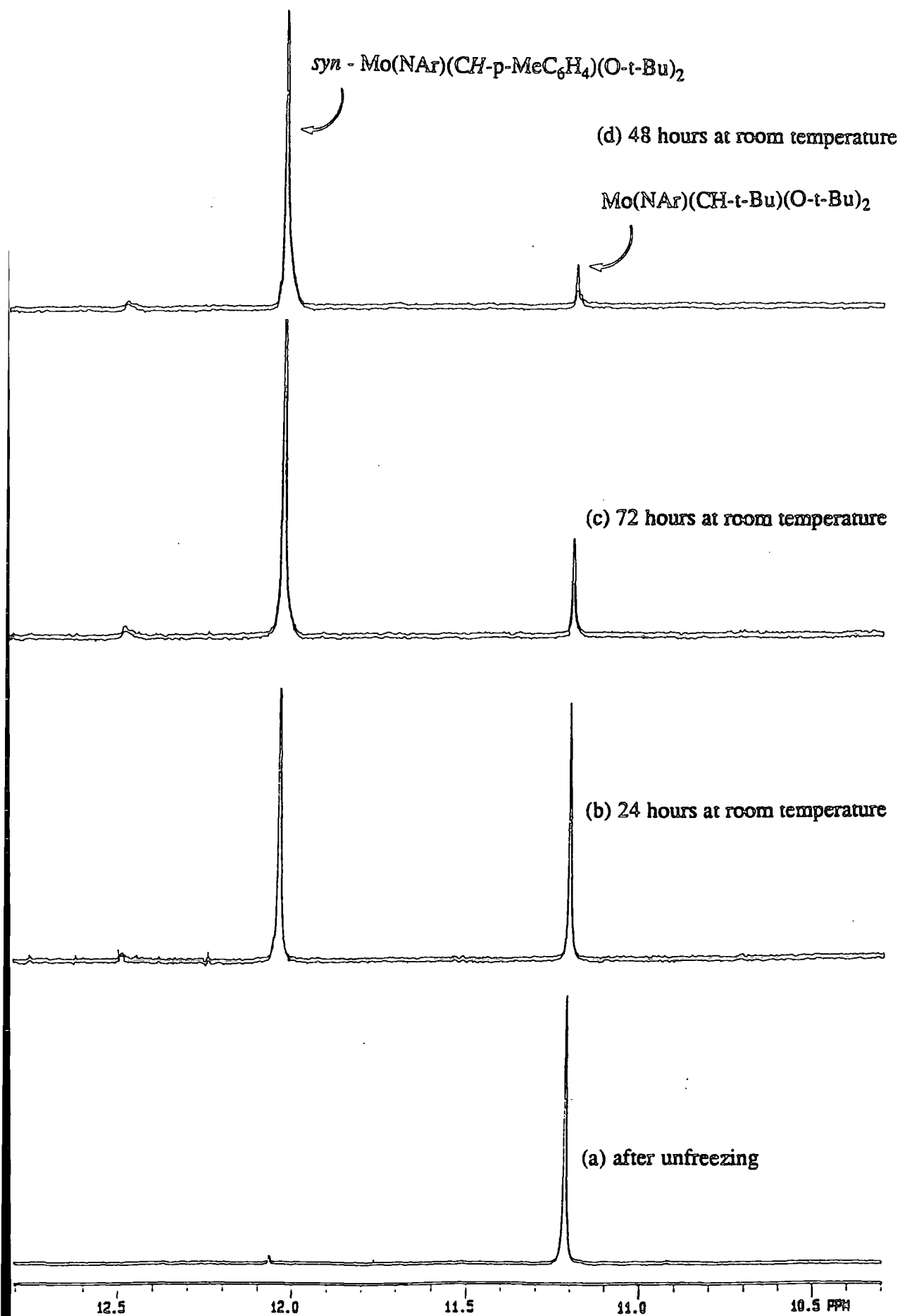
In experiments designed to test the formation and stability of various benzylidene derivatives, the initiator $\text{Mo}(\text{NAr})(\text{CH-t-Bu})(\text{O-t-Bu})_2$ (1) was reacted with a range of substituted styrenes (typically 5-10 equivalents) in C_6D_6 , and any subsequent reaction monitored by ^1H NMR spectroscopy.

For the bis *t*-butoxide derivative the reaction (equation 3.2) is relatively slow, typically taking four to five days at room temperature, but is quantitative in the presence of excess styrene.



In each case, the alkylidene resonance at 11.25 ppm for (1) decreases, and is replaced by a new resonance (typically to lower field) and resonances for the metathesis side-product neohexene. The rate of formation of the benzylidene complex can be increased by using a higher concentration of the styrene, or by heating the NMR sample (conversion being complete within 24 hours at 40°C). A representative series of ^1H NMR spectra monitoring the formation of $\text{Mo}(\text{NAr})(\text{CHp-MeC}_6\text{H}_4)(\text{O-t-Bu})_2$ is shown in figure 3.3. Table 3.1 shows the characteristic α proton ^1H NMR resonances for various benzylidene complexes generated in C_6D_6 .

Figure 3.3 Formation of $\text{Mo}(\text{NAr})(\text{CH-p-MeC}_6\text{H}_4)(\text{O-t-Bu})_2$



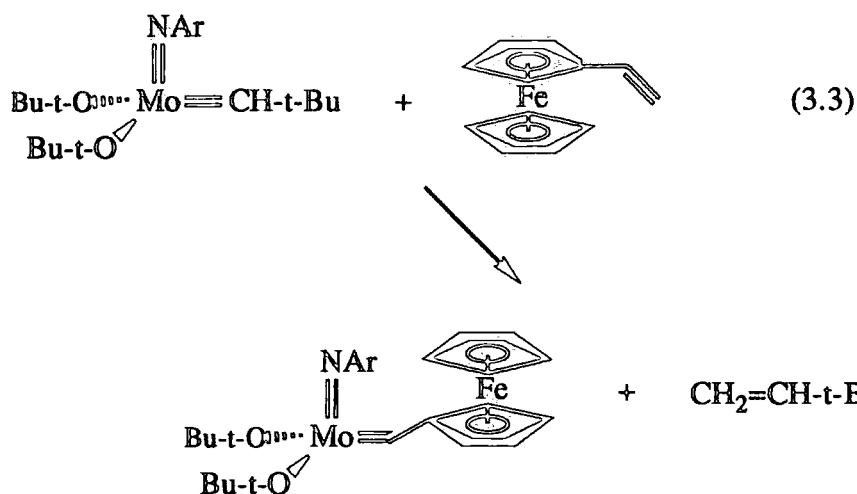
Benzylidene Complex (<i>CT Agent</i>)	δH_{α} (ppm)
Mo(NAr)(CHC ₁₀ H ₇)(O-t-Bu) ₂ (<i>vinyl anthracene</i>)	12.21 (syn) 12.64 (anti)
Mo(NAr)(CHC ₆ H ₅)(O-t-Bu) ₂ (<i>styrene</i>)	12.09
Mo(NAr)(CH- <i>p</i> -MeC ₆ H ₄)(O-t-Bu) ₂ (<i>p-methylstyrene</i>)	12.10 (syn) 12.55 (anti)
Mo(NAr)(CH- <i>p</i> -MeOC ₆ H ₄)(O-t-Bu) ₂ (<i>p-methoxystyrene</i>)	12.06 (syn) 12.52 (anti)
Mo(NAr)(CH- <i>p</i> -ClCH ₂ C ₆ H ₄)(O-t-Bu) ₂ (<i>p-chloromethylstyrene</i>)	12.04
Mo(NAr)(CH- <i>m</i> -ClCH ₂ C ₆ H ₄)(O-t-Bu) ₂ (<i>m-chloromethylstyrene</i>)	12.01
Mo(NAr)(CH- <i>p</i> -ClC ₆ H ₄)(O-t-Bu) ₂ (<i>p-chlorostyrene</i>)	11.88 (syn) 12.29 (anti)
Mo(NAr)(CH- <i>m</i> -NO ₂ C ₆ H ₄)(O-t-Bu) ₂ (<i>m-nitrostyrene</i>) ^a	11.84
Mo(NAr)(CH-3,5-(CF ₃) ₂ C ₆ H ₃)(O-t-Bu) ₂ (<i>3,5 bis(trifluoromethyl) styrene</i>)	11.81
Mo(NAr)(CH- <i>m</i> -NC ₅ H ₄)(O-t-Bu) ₂ (<i>m-vinylpyridene</i>)	11.44

Table 3.1 Selected NMR data for substituted benzylidene complexes.

^a Observed as described in section 3.2.2

It can be seen from the table that an increase in the electron withdrawing ability of substituents on the phenyl ring causes the alkylidene α proton resonance to shift to higher field. For several of the benzylidene complexes, a second alkylidene resonance due to a minor isomer can be observed. This can be attributed to the anti rotamer of the benzylidene complex, where the phenyl group of the benzylidene ligand points away from the imido nitrogen atom. ^{13}C NMR data has been obtained for three of the benzylidene complexes. The C_α resonance for $\text{Mo}(\text{NAr})(\text{CHC}_6\text{H}_5)(\text{O}-t\text{-Bu})_2$ occurs at 247.84 ppm as a doublet ($J_{\text{CH}} = 125.1$ Hz), whereas for $\text{Mo}(\text{NAr})(\text{CH}^p\text{-MeC}_6\text{H}_4)(\text{O}-t\text{-Bu})_2$ and $\text{Mo}(\text{NAr})(\text{CH}^p\text{-ClC}_6\text{H}_4)(\text{O}-t\text{-Bu})_2$ the C_α resonance appears as a doublet of triplets ($X = \text{Me}$, 247.94 ppm, $J_{\text{CH}} = 123.3$ Hz, $J_{\text{CH}} = 4.8$ Hz; $X = \text{Cl}$, 245.39 ppm, $J_{\text{CH}} = 125.1$ Hz, $J_{\text{CH}} = 4.8$ Hz). This further splitting can be attributed to coupling to the two ortho hydrogen atoms of the para-substituted phenyl ring. Why this should not be observed for the unsubstituted benzylidene complex is unclear.

These benzylidene complexes, with the exception of those described in more detail below, are stable in C_6D_6 solution (approximately 0.04M) for days. Schrock and Bazan have isolated a ferrocene methyldiene initiator in the solid state by the metathesis reaction of $\text{Mo}(\text{NAr})(\text{CH}-t\text{-Bu})(\text{O}-t\text{-Bu})_2$ with one equivalent of vinyl ferrocene (equation 3.3). The success of this reaction is attributed to vinyl ferrocene being more electron rich than styrene itself and the fact that the metathesis side product, neohexene, evaporates during the course of the reaction, forcing the equilibrium toward the side of the new initiator¹⁵.



For reaction of the initiator with a 75:25 mixture of para- and meta-chloromethylstyrene, both the para- and meta-isomers of the benzylidene adduct can be observed by 200 MHz ^1H NMR spectroscopy after 4 hours at room temperature in C_6D_6 (signals due to the benzylidene hydrogens are observed at 12.01 and 12.04 ppm respectively) in a corresponding 3:1 ratio. These, however, are not stable in solution and decompose at room temperature overnight (the para isomer being marginally more stable) to give unidentified products. Only one resonance is observed for the meta isomer, indicating that rotation about the $\text{C}_\alpha\text{-C}_{\text{ipso}}$ bond is rapid on the NMR timescale.

The initiator was found to react directly with 5.0 equivalents of *m*-nitrostyrene over a period of several hours to give the oxo-imido species $\text{Mo}(\text{NAr})(\text{O})(\text{O-t-Bu})_2$ and several unidentified olefinic by-products. This observation is consistent with the earlier finding (in chapter two of this thesis) that the initiator is not stable for any length of time in the presence of aromatic nitro groups.

$\text{Mo}(\text{NAr})(\text{CH-t-Bu})(\text{O-t-Bu})_2$ (1) was found not to react to any measurable extent with 5.2 equivalents of pentafluorostyrene in C_6D_6 at room temperature over a period of 7 days. This is presumably due to reduction of electron density in the carbon-carbon double bond by the electron withdrawing fluorine atoms, thus rendering this styrene much less reactive.

3.2.2 The Reaction of Living Polynorbornene with Substituted Styrenes.

After evaluating the formation of benzylidene complexes by direct reaction of the initiator with a styrene derivative, tests were carried out on an NMR scale to confirm that living polymers would react with styrene derivatives to generate benzylidene complexes and methylene end-capped polymers.

These involved the polymerization of 25 equivalents of norbornene, using standard solutions of initiator (0.1M) and norbornene (1.0M) in C_6D_6 , followed by the addition of 10 equivalents of chain transfer agent. The resulting solution was frozen and any subsequent reaction monitored by 1H NMR spectroscopy.

For the chain transfer agents listed in table 3.1, reaction to form the benzylidene complex and a methylene end-capped polymer was rapid (typically less than 30 minutes at room temperature) and quantitative by 1H NMR. The doublet resonance at 11.54 ppm (characteristic of the α -proton in living polynorbornene) decreases in intensity and is replaced by the alkylidene resonance of the new initiator (see table 3.1). This is accompanied by a darkening of the solution from orange to red as the benzylidene complex forms, providing a convenient way of following the chain transfer process. The reaction of living polynorbornene with *p*-methoxystyrene is shown in figure 3.4.

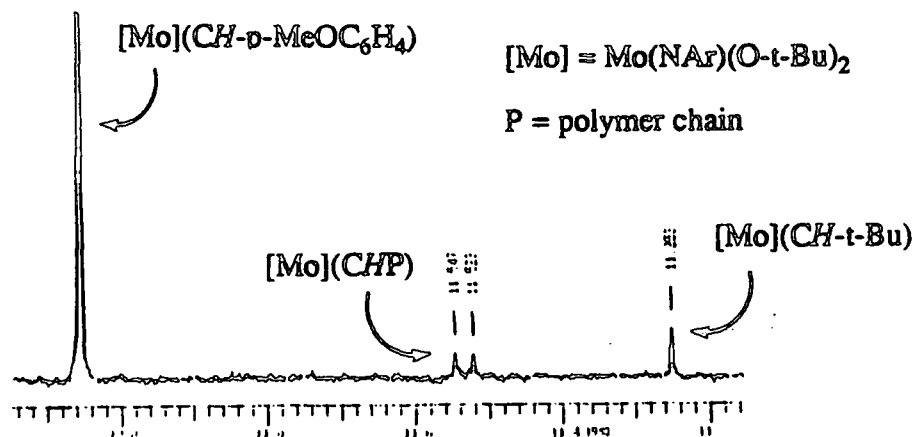


Figure 3.4 Reaction of living polynorbornene with *p*-methoxystyrene.

^a The alkylidene proton resonance of the initiator is still observed due to the high value of k_p/k_i for norbornene.

Reaction of living polynorbornene with *m*-nitrostyrene generates an initial benzylidene complex observable directly after unfreezing ($\delta H_{\alpha} = 11.84$), but again this subsequently converts to the oxo-imido complex by exchange of an oxygen atom with the aromatic nitro group.

Neither allylbenzene nor 1-pentene were successful as chain transfer agents¹⁰. Since the living polynorbornene is stable in their presence, it is presumed that these olefins are not sufficiently reactive towards the living alkylidene for chain transfer to occur.

Cis-stilbene also failed as a chain transfer agent in reactions with living polynorbornene. Since stilbene possesses a relatively activated carbon-carbon double bond similar to styrene itself, this must be attributed to the second phenyl ring providing too great a steric hindrance for reaction to occur.

3.3 Chain transfer experiments

After evaluating these styrene based chain transfer agents on an NMR scale, the reactions were "scaled up", to confirm that well behaved chain transfer (i.e. resulting polymers having low polydispersities) would occur on a larger preparative scale.

Experiments were devised where $\text{Mo}(\text{NAr})(\text{CH-t-Bu})(\text{O-t-Bu})_2$ (1) in toluene was treated with 100 equivalents of monomer, followed by the chain transfer agent and subsequently by a further 200 equivalents of monomer, before cleaving the polymer from the metal centre using pivaldehyde.

If chain transfer is well behaved, two polymeric products should be obtained with GPC characteristics for a 100-mer and a 200-mer, with no 300-mer being formed. This has been shown to be resolvable from the 200-mer peak and thus will be observed if produced. This type of experiment is summarised in Figure 3.5.

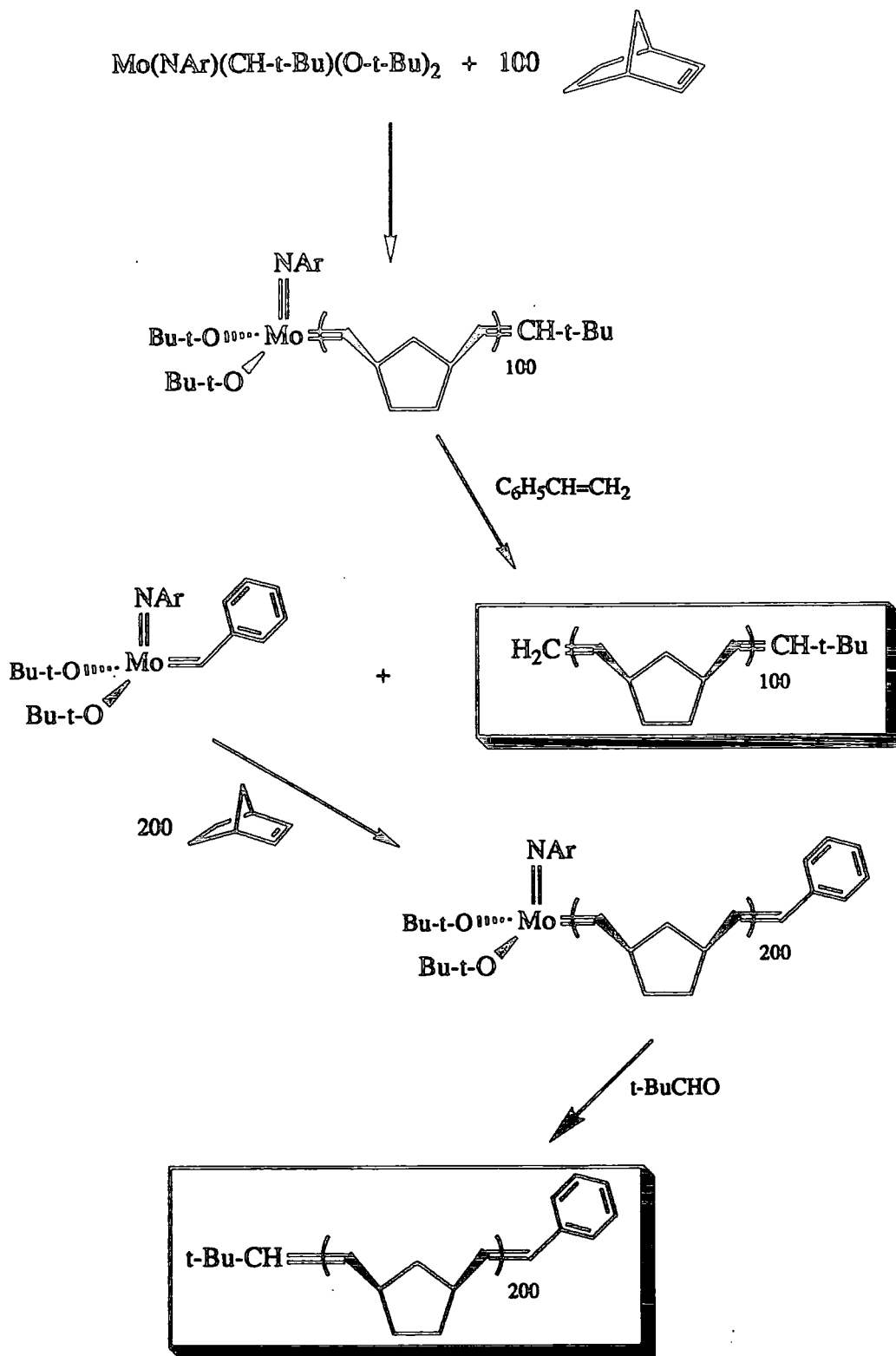


Figure 3.5 Chain Transfer employing Styrene.

3.3.1 The Norbornene / Styrene Chain Transfer System.

Norbornene and styrene were initially chosen for these experiments as they possess no functionalities and are thus best suited for use in establishing whether chain transfer will occur on a preparative scale in a well-defined manner.

When $\text{Mo}(\text{NAr})(\text{CH-t-Bu})(\text{O-t-Bu})_2$ (1) was treated with 100 equivalents of norbornene, followed (after 8 minutes vigorous stirring to allow polymerization to be completed) by 5 equivalents of styrene, the initial yellow solution became red within 30 minutes, a colour attributable to the benzyldiene complex $\text{Mo}(\text{NAr})(\text{CHPh})(\text{O-t-Bu})_2$. Further treatment of this red solution with an additional 200 equivalents of norbornene caused the colour to immediately bleach back to yellow, characteristic of living polynorbornene being regenerated. Capping the reaction after a further 8 minutes vigorous stirring with pivaldehyde and subsequent precipitation from methanol yielded a polymer whose GPC characteristics (CH_2Cl_2) are shown in figure 3.6.

As can be seen, chain transfer has occurred, but not completely. In the refractometer trace peaks due to the 100-mer ($M_n = 19000$) and 200-mer ($M_n = 41860$) can be seen, as well as a 300-mer peak at $M_n = 60300$. A small amount of high molecular weight species is also observed at $M_n = 99680$. The polydispersity across the entire distribution is 1.32. In the UV trace two peaks are seen at $M_n = 41200$ (200-mer) and $M_n = 92140$ giving a PDI across the entire distribution of 1.16.

This apparent failure to fully complete chain transfer before the second addition of monomer can be attributed to the concentration of the chain transfer agent being too low, and hence the rate of chain transfer also being too low. Therefore, the reaction was repeated in exactly the same manner, but this time employing 20 equivalents of styrene as the chain transfer agent. After precipitation of the polymer from methanol and subsequent drying *in vacuo*, GPC analysis (CH_2Cl_2 , figure 3.7) revealed the presence of only two polymeric products, with molecular weight and UV properties consistent with $\text{H}_2\text{C}(\text{CHC}_5\text{H}_8\text{CH})_{100}\text{CH-t-Bu}$ (100-mer, $M_n = 19240$, PDI = 1.05) and $\text{t-Bu-CH}(\text{CHC}_5\text{H}_8\text{CH})_{200}\text{CHPh}$ (200-mer, $M_n = 41200$, PDI = 1.07). The PDI

Figure 3.6

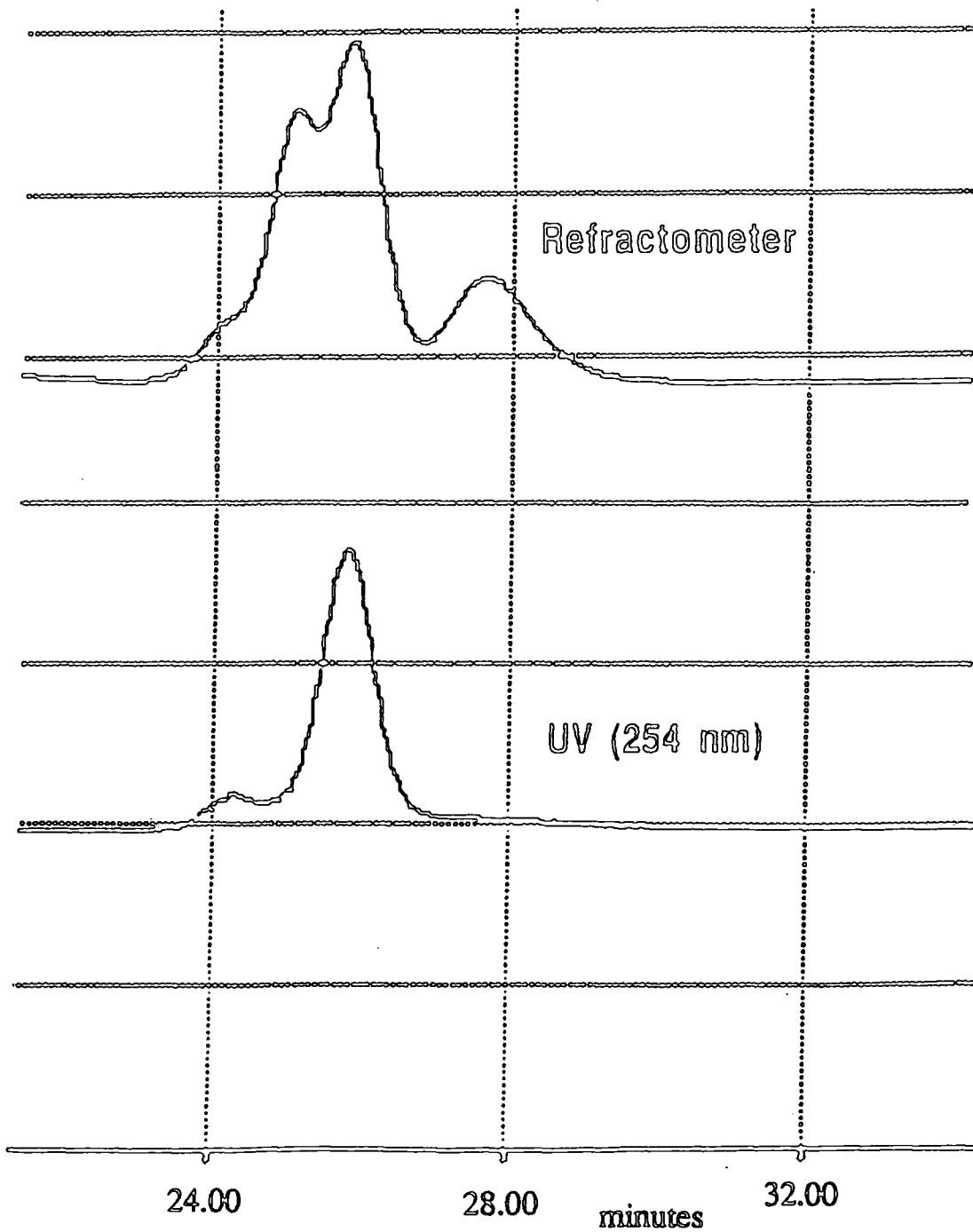
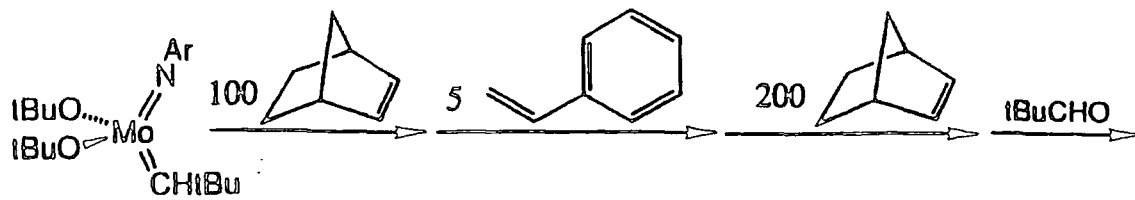
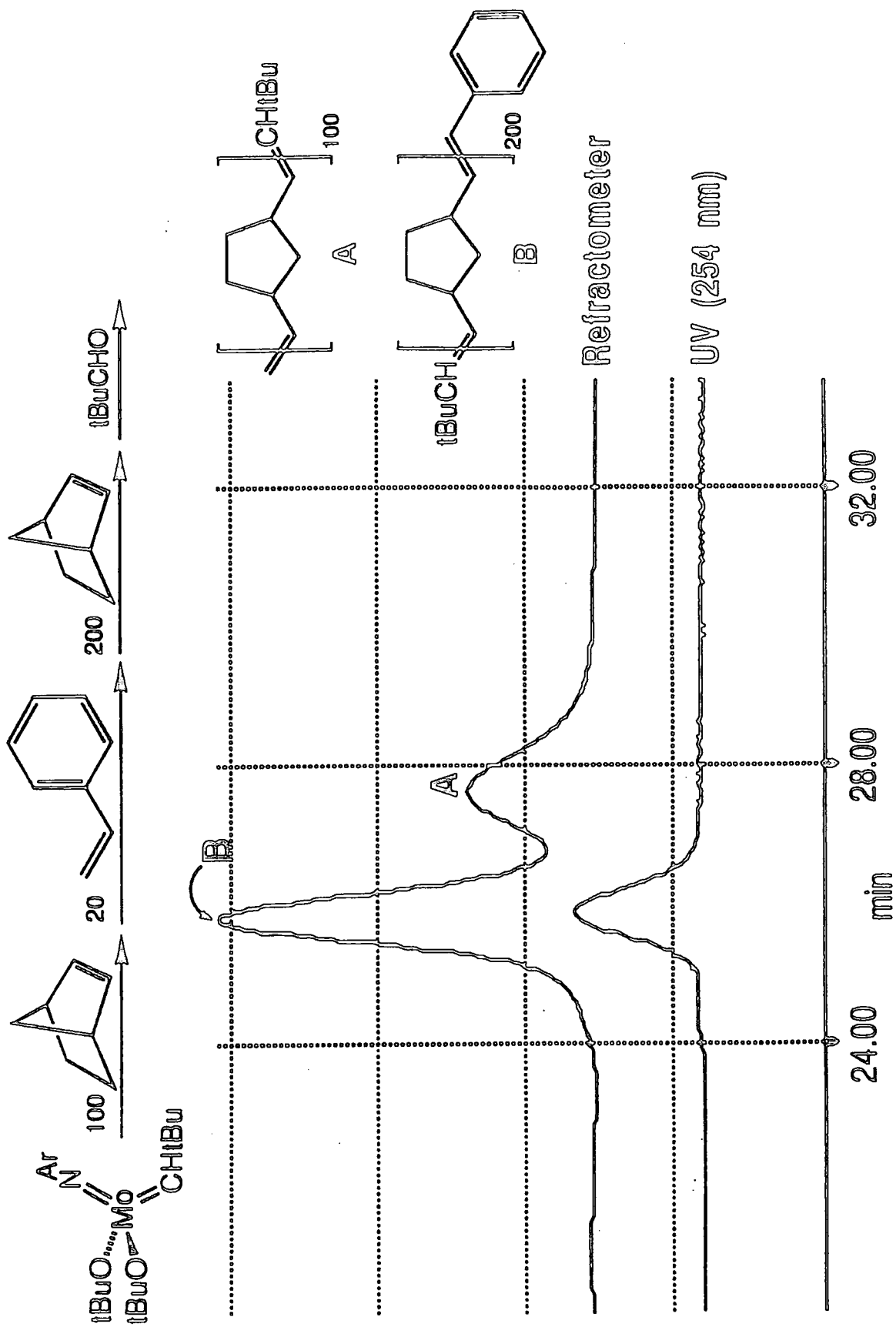


Figure 3.7

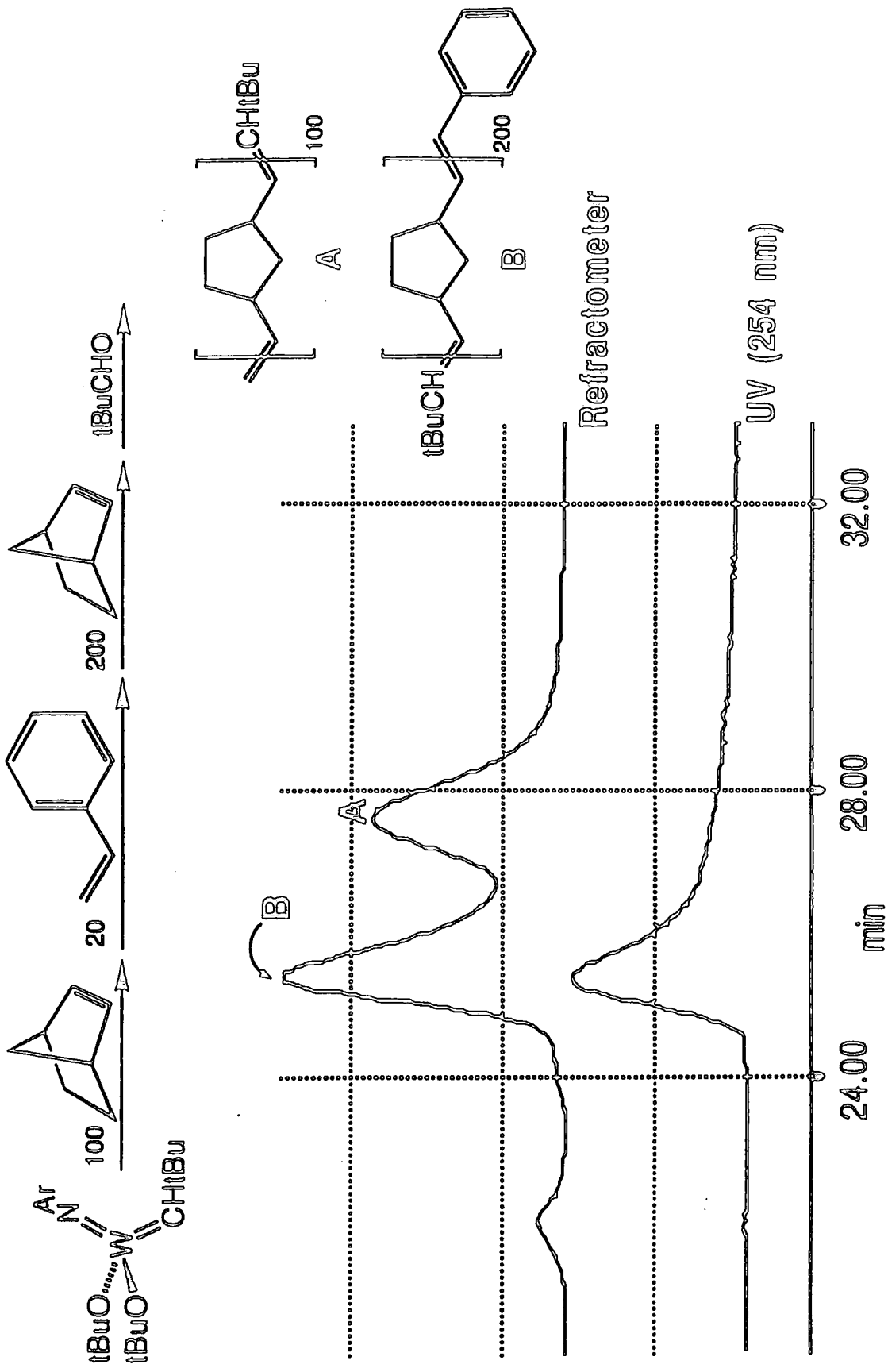


across the entire distribution is 1.24. The narrowness of the two peaks and the absence of a 300-mer peak indicate that chain transfer and subsequent initiation of the second polymer chain by the benzylidene initiator are both well behaved. Only one peak is observed in the UV trace as the only UV active component is the phenyl ring of the 200-mer, derived from the benzylidene initiator. Capping with pivaldehyde rather than benzaldehyde allows the phenyl group of the benzylidene initiator to be monitored.

Treatment of $\text{Mo}(\text{NAr})(\text{CH-t-Bu})(\text{O-t-Bu})_2$ firstly with 200 equivalents of norbornene then 100 equivalents of norbornene (employing 20 equivalents of styrene as the CT agent) again behaved in a well defined manner (100-mer $M_n = 21910$; 200-mer $M_n = 38720$, PDI across both peaks = 1.15). The UV active peak this time has a molecular weight of 22200 (PDI = 1.05), corresponding to the 100-mer derived from the benzylidene initiator.

An analogous "100/200" type reaction employing the tungsten initiator $\text{W}(\text{NAr})(\text{CH-t-Bu})(\text{O-t-Bu})_2$ was less successful. GPC analysis of the resulting polymeric products (CH_2Cl_2 , figure 3.8) showed two peaks at molecular weights $M_n = 19240$ and $M_n = 50010$ (PDI across both peaks = 1.34) and a small amount of very high molecular weight material ($M_n = 442800$). The UV trace shows a very broad peak at $M_n = 50850$ that tails off dramatically to low molecular weight (PDI = 5.49). This lack of control over chain transfer employing the tungsten initiator may be attributed to low stability of the *in situ* formed benzylidene complex, or possibly poor initiation of the second polymer chain by this species.

Figure 3.8



3.3.2 The Norbornene / Substituted Styrene Chain Transfer System.

As has been shown in section 3.2, a wide variety of substituted styrenes act as chain transfer agents on an NMR scale. The use of such species will allow functionalities to be introduced onto the alkylidene ligand of the initiator and thus onto the starting end of a polymer chain.

Two substituted styrenes that have been evaluated as CT agents on this preparative scale are *p*-MeC₆H₄CH=CH₂ and *p*-MeOC₆H₄CH=CH₂.

Treatment of Mo(NAr)(CH-*t*-Bu)(O-*t*-Bu)₂ (1) with 100/200 equivalents of norbornene using 20 equivalents of *p*-methylstyrene as chain transfer agent gave two polymeric materials whose GPC characteristics (THF) are consistent with a 100-mer ($M_n = 15760$) and a 200-mer ($M_n = 29783$), with a narrow PDI across both peaks of 1.20. The molecular weights are slightly different in THF than in CH₂Cl₂ due to differing conversion factors for the two solvents relative to polystyrene standards (approximately 1.6 and 2.0 respectively).

An analogous reaction employing 20 equivalents of *p*-methoxystyrene as the chain transfer agent again gave two peaks in the refractometer trace (CH₂Cl₂, 100-mer, $M_n = 20840$; 200-mer, $M_n = 40360$; PDI across both peaks = 1.17), and a single peak in the UV trace whose molecular weight corresponded to the 200-mer ($M_n = 36420$, PDI = 1.07).

These results show that chain transfer also occurs in a controlled manner using *p*-methylstyrene and *p*-methoxystyrene and that both the complexes Mo(NAr)(CH-*p*-MeC₆H₄)(O-*t*-Bu)₂ and Mo(NAr)(CH-*p*-MeOC₆H₄)(O-*t*-Bu)₂ act as well behaved initiators for the second polymerization.

3.3.3 The Functionalised Norbornadiene / Styrene Chain Transfer System.

As a complementary study to chain transfer employing norbornene, two functionalized monomers were tested to ascertain whether chain transfer occurred in a well defined manner in the presence of functional groups on the monomer.

Treatment of $\text{Mo}(\text{NAr})(\text{CH-t-Bu})(\text{O-t-Bu})_2$ with 100/200 equivalents of dicarbomethoxynorbornadiene, DCMND, (with 15 minutes stirring for polymerization to be assumed complete), using 20 equivalents of styrene as the chain transfer agent gives only two polymeric products in the refractometer trace (THF) of molecular weights $M_n = 20900$ and $M_n = 47490$, with a polydispersity index for the entire distribution of 1.28. For this monomer, chain transfer can be termed successful, although the resulting polydispersity is slightly higher across both peaks than for norbornene (c.f. 1.24). In a homopolymerization of 100 equivalents of the same batch of this monomer, the resulting polymer had a molecular weight of 23560 (THF), suggesting that the first polymeric product formed in the chain transfer reaction is marginally smaller than a "100-mer"; in fact the molecular weight corresponds to an "85-mer". This lowering of the molecular weight from that expected may be attributed to inadequate reaction time being left for polymerization to occur before the CT agent was added, as DCMND is known to polymerize at a slower rate than norbornene itself ($k_p = 2(1) \text{ M}^{-1} \text{ s}^{-1}$, $k_i = 0.7(3) \text{ M}^{-1} \text{ s}^{-1}$, $k_p/k_i = 3.0(3)$).

Consistent results for this monomer could only be obtained using freshly prepared and distilled batches of monomer. If old monomer was used, widely differing molecular weights were observed for the polymeric products obtained from chain transfer reactions, and bimodal traces (peaks observed at M_n and $2M_n$) were seen for simple homopolymerizations of 100 equivalents of the monomer. Reasons for this observation of double molecular weight polymer are addressed in chapter 4 (section 4.8).

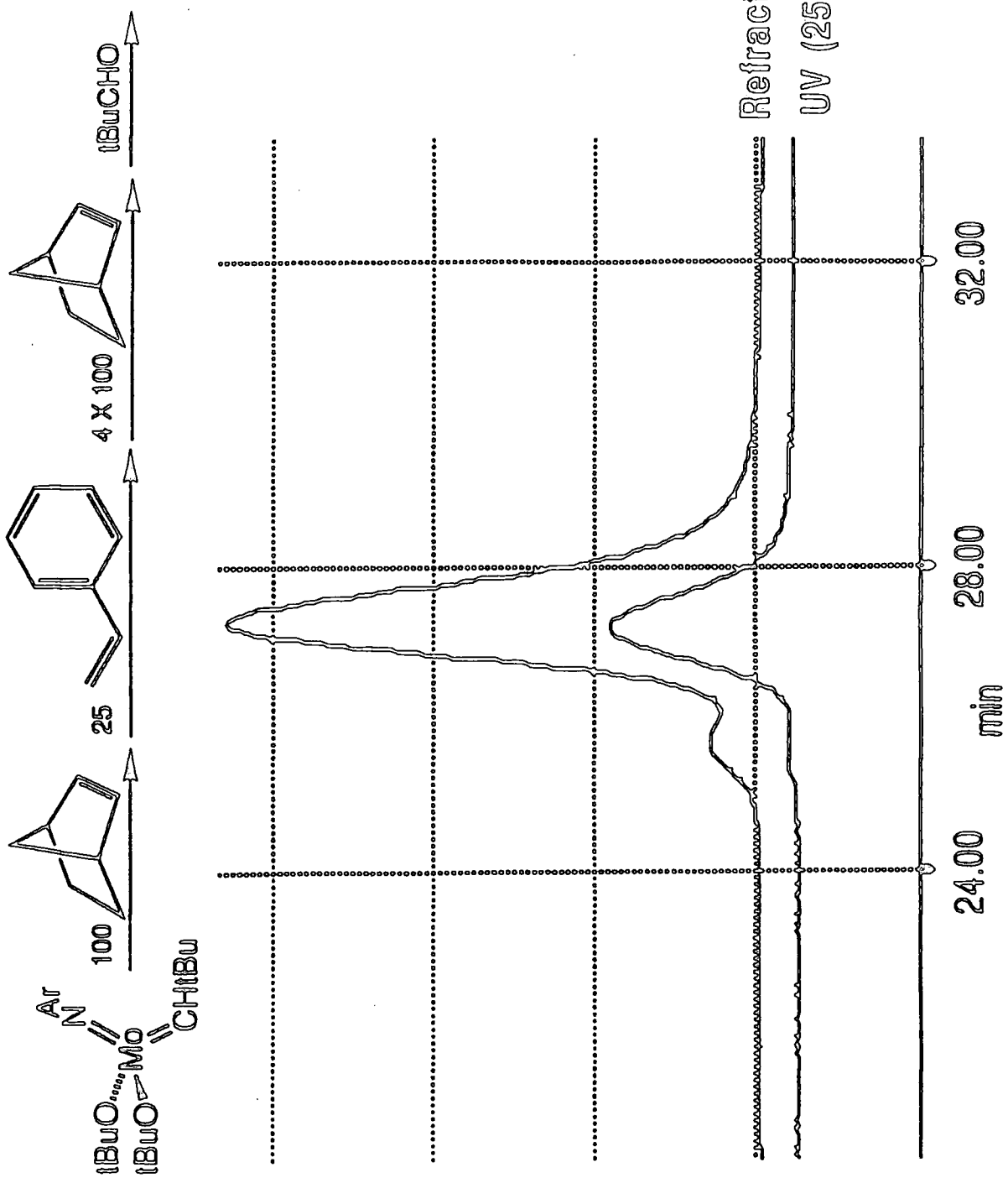
Chain transfer involving 2,3-bis(trifluoromethyl)norbornadiene (BTFMND) as the monomer in the presence of styrene gave a distribution of low molecular weight oligomers, a result that implies that styrene reacts with the living alkylidene at a rate roughly comparable to that of BTFMND, a relatively unreactive monomer compared to norbornene ($k_p = 0.057 \text{ M}^{-1} \text{ s}^{-1}$, $k_i = 0.08 \text{ M}^{-1} \text{ s}^{-1}$, $k_p/k_i = 0.72$) i.e. the rate of polymerization of this monomer is not fast enough relative to the rate of chain transfer for the two processes to occur independently.

3.4 Multiple Pulse Experiments.

The success of the initial "2-pulse" experiments involving polymerization of 100 and 200 equivalents of norbornene led us to investigate further the possibility of using these catalysts more efficiently in a continuous ("pulsed") mode, where subsequent aliquots of monomer are added to the catalyst solution in the presence of excess styrene, waiting for chain transfer to be complete before each subsequent pulse. Such pulsing experiments should allow polymodal blends to be prepared in one pot.

An initial experiment consisted of treating $\text{Mo}(\text{NAr})(\text{CH-t-Bu})(\text{O-t-Bu})_2$ with 100 equivalents of norbornene followed, after 8 minutes, by the addition of excess (25 equivalents) of styrene. The solution again changed from yellow to red over a period of 30 minutes as the benzylidene initiator formed, and changed back to yellow immediately after the second pulse of 100 equivalents of norbornene was added. A further 3 pulses (5 in all) of 100 equivalents of norbornene were subsequently added at 40 minute intervals, (10 minutes for polymerization to occur and 30 minutes for subsequent chain transfer to occur), with the expected yellow / red / yellow colour changes seen for each pulse. GPC analysis (CH_2Cl_2 , figure 3.9) of the resulting polymer revealed a unimodal polymer distribution in the refractometer trace ($M_n = 21910$, $\text{PDI} = 1.10$) and a single UV peak ($M_n = 22200$, $\text{PDI} = 1.05$) which both correspond to the weight average expected for a 100-mer. (The refractometer trace

Figure 3.9



shows a small amount (< 5%) of polymer with twice the expected molecular weight. The reason for this is discussed in chapter 4 of this thesis (section 4.8).

The narrowness of the molecular weight distribution and the absence of higher molecular weight polymeric species indicates that chain transfer has been successful for 5 pulses of 100 equivalents of norbornene.

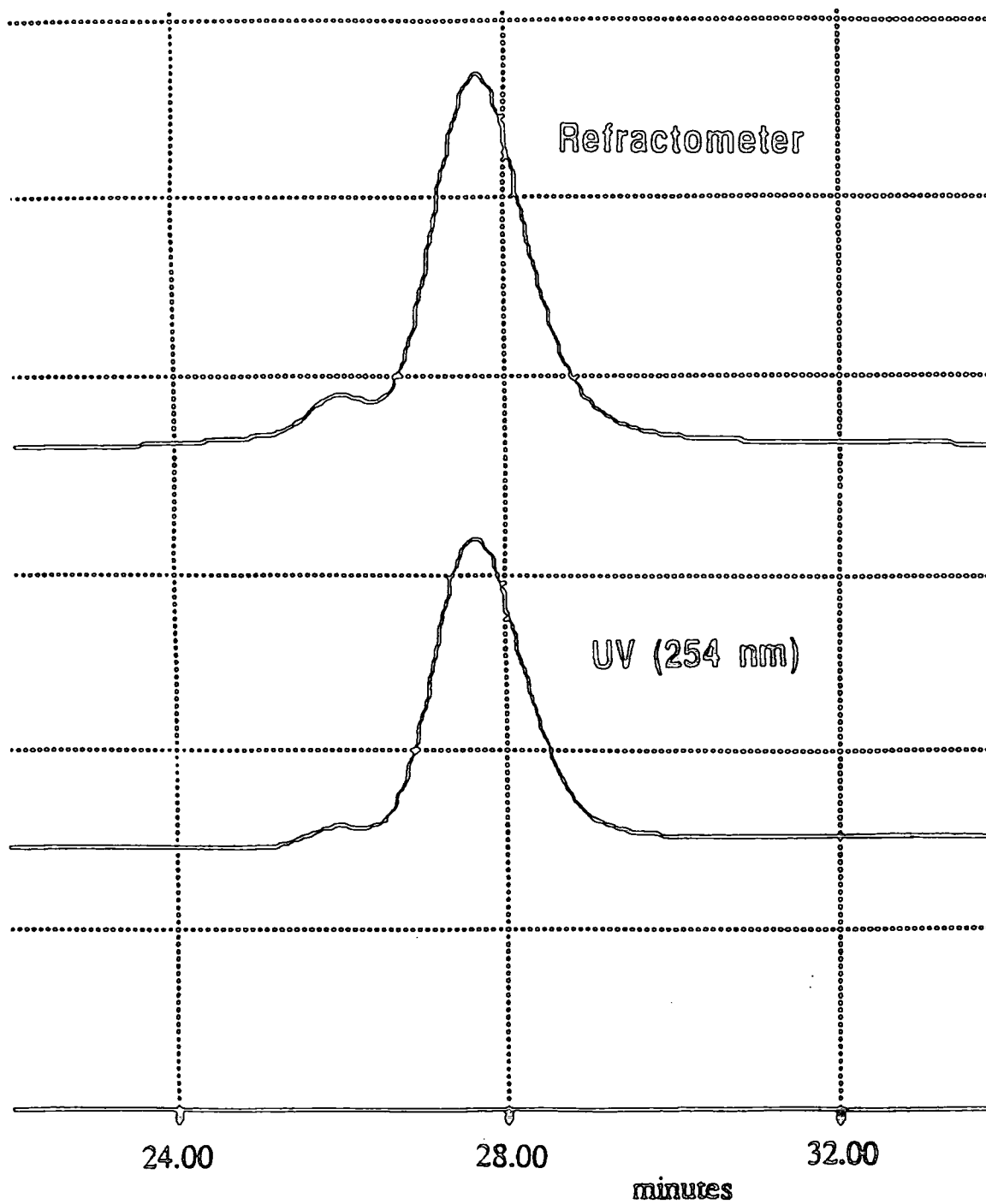
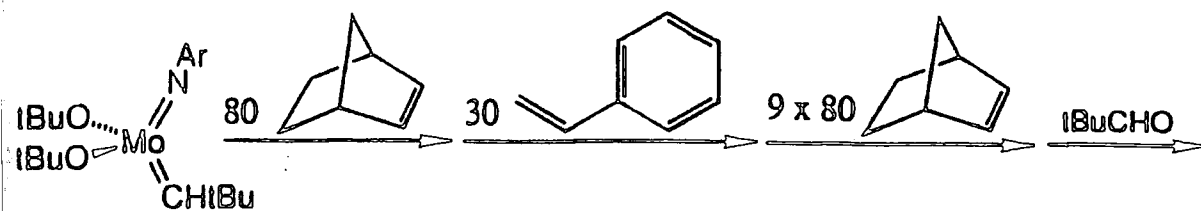
In fact, it has proven possible to increase the number of pulses and still achieve controlled chain transfer. Treatment of a mixture of $\text{Mo}(\text{NAr})(\text{CH-t-Bu})(\text{O-t-Bu})_2$ and styrene (30 equivalents, increased to keep the concentration of chain transfer agent high) at 40 minute intervals with 10 pulses of 80 equivalents of norbornene resulted in a polymer that had the weight average expected for an 80-mer ($M_n = 18760$) and a polydispersity of 1.07. This is shown in Figure 3.10. The main peak is approximately 95 % of the total area (small peak at twice the expected molecular weight peak observed at $M_n = 37540$, PDI for entire distribution = 1.13).

This pulsing technique can also be applied to other styrene derivatives. An analogous reaction involving 5 pulses of norbornene in the presence of 25 equivalents of *p*-methoxystyrene resulted in a low molecular weight distribution polymer (PDI = 1.10) whose molecular weight corresponds to a 100-mer (THF, $M_n = 17310$). Similar results are obtained using *p*-methylstyrene as the chain transfer agent (THF, $M_n = 17950$, PDI = 1.09), again showing chain transfer to be a controlled process.

Chain transfer with DCMND as the monomer in a "5 x 50 equivalent" pulse experiment, employing styrene as the chain transfer agent, gave a polymer whose molecular weight was correct for a 50-mer ($M_n = 13470$) and had a polydispersity of 1.27.

The success of many-stepped pulsed chain transfer depends critically (as has been shown for the monomer BTFMND) on the relative reactivities of the cyclic monomer and the chain transfer agent, and will be limited by impurities in the feed, by eventual decomposition of intermediates, and by incomplete chain transfer.

Figure 3.10



3.5 Kinetic Study of Benzylidene Formation.

The success of styrene as a chain transfer agent is dependant upon a relatively fast rate of polymerization compared with the rate of reaction of living alkylidenes with styrene. The observation that BTFMND affords a distribution of oligomers in the presence of styrene indicates that the rate of propagation for this relatively unreactive monomer is comparable to the rate of benzylidene formation.

It was envisaged that the rate of chain transfer may be strongly influenced by electron releasing or withdrawing groups attached to the phenyl ring, and if so, it might prove possible to match a particular styrene to a monomer of interest.

Therefore a kinetic study was undertaken, using ^1H NMR spectroscopy, to ascertain the relative rates of reaction of several substituted styrene derivatives with the initiator. This can then be compared to the rate of reaction of the initiator with a monomer (k_i). Ideally, to gain direct information about chain transfer, we would like to monitor the rate of reaction of living polymers with styrenes and compare this to the rate of reaction of living polymers with more monomer (k_p). However, this is not achievable, as the chain transfer reaction with living oligomers is too fast to be monitored by ^1H NMR spectroscopy.

$\text{Mo}(\text{NAr})(\text{CH-t-Bu})(\text{O-t-Bu})_2$ (1) and a large excess of styrene derivative (30 equivalents) were mixed in C_6D_6 and the resulting solution immediately frozen till the kinetic run commenced. After thawing the solution in the NMR spectrometer, the ensuing reaction was monitored at 30°C by observing the disappearance of the alkylidene proton resonance at 11.25 ppm for (1) and the simultaneous appearance of the new alkylidene proton resonance for the benzylidene complex. This is shown in Figure 3.11 for the formation of $\text{Mo}(\text{NAr})(\text{CHC}_6\text{H}_5)(\text{O-t-Bu})_2$.

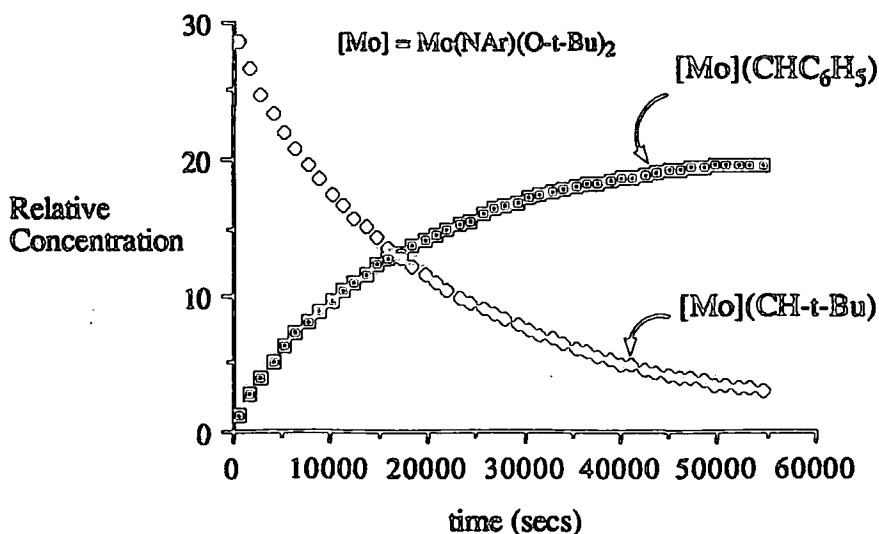


Figure 3.11 *Relative concentrations of $\text{Mo}(\text{NAr})(\text{CH-t-Bu})(\text{O-t-Bu})_2$ and $\text{Mo}(\text{NAr})(\text{CHC}_6\text{H}_5)(\text{O-t-Bu})_2$ as a function of time at 30°C*

In each case the data was found to obey first order kinetics and a plot of $\ln(N/N_0)$ vs time yielded a straight line whose slope = $-k_1$ (N = concentration of neopentylidene initiator, N_0 = concentration of neopentylidene initiator at zero time). A representative plot for the formation of $\text{Mo}(\text{NAr})(\text{CHC}_6\text{H}_5)(\text{O-t-Bu})_2$ is shown in figure 3.12.

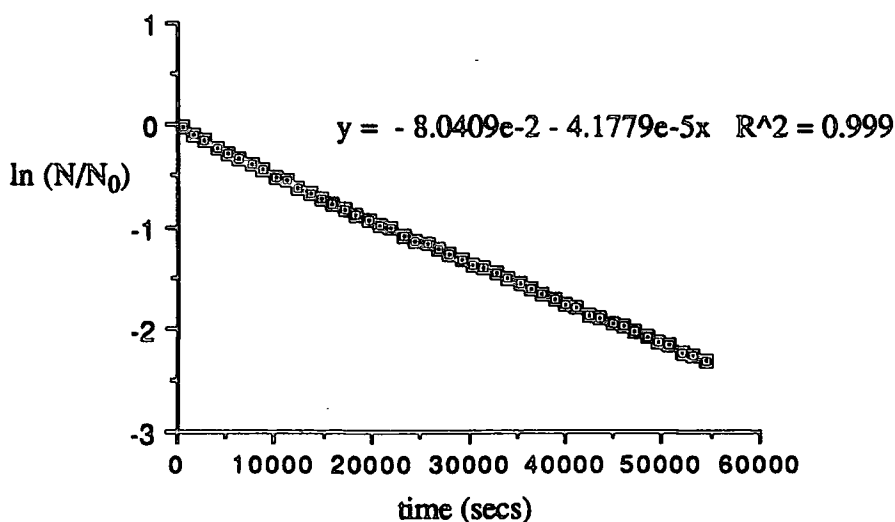


Figure 3.12 *First order plot for the formation of $\text{Mo}(\text{NAr})(\text{CHC}_6\text{H}_5)(\text{O-t-Bu})_2$.*

Table 3.2 lists the observed first order rate constants for reaction of (1) with several substituted styrene derivatives.

styrene derivative	$k_1(\text{obs}) \text{ s}^{-1}$
$\text{C}_6\text{H}_5\text{CH}=\text{CH}_2$	$4.2 (3) \times 10^{-5}$
$p\text{-ClC}_6\text{H}_4\text{CH}=\text{CH}_2$	$4.9 (3) \times 10^{-5}$
$p\text{-MeC}_6\text{H}_4\text{CH}=\text{CH}_2$	$5.9 (7) \times 10^{-5}$
$p\text{-MeOC}_6\text{H}_4\text{CH}=\text{CH}_2$	$5.5 (8) \times 10^{-5}$

Table 3.2 *Observed rate constants at 30°C for the reaction of $\text{Mo}(\text{NAr})(\text{CH-}i\text{-Bu})(\text{O-}i\text{-Bu})_2$ with substituted styrene derivatives.*

As can be seen, for the limited number of styrene derivatives evaluated in this way, the rate of reaction with the initiator appears to be rather insensitive to substituent effects in the para-position, with all the rates being approximately equal within experimental error. Thus the rate of chain transfer is not strongly influenced by the nature of the para-substituent.

Comparing these rates with k_i for BTFMND ($0.057 \text{ M}^{-1} \text{ s}^{-1}$), we can see that styrene reacts with the initiator approximately 1000 \times slower than does BTFMND. One might therefore expect this difference to be large enough for chain transfer with this monomer to be successful. However, the formation of oligomers using this monomer rather than controlled chain transfer indicates that the rates of reaction of living BTFMND with styrene and with more monomer must be much closer in value.

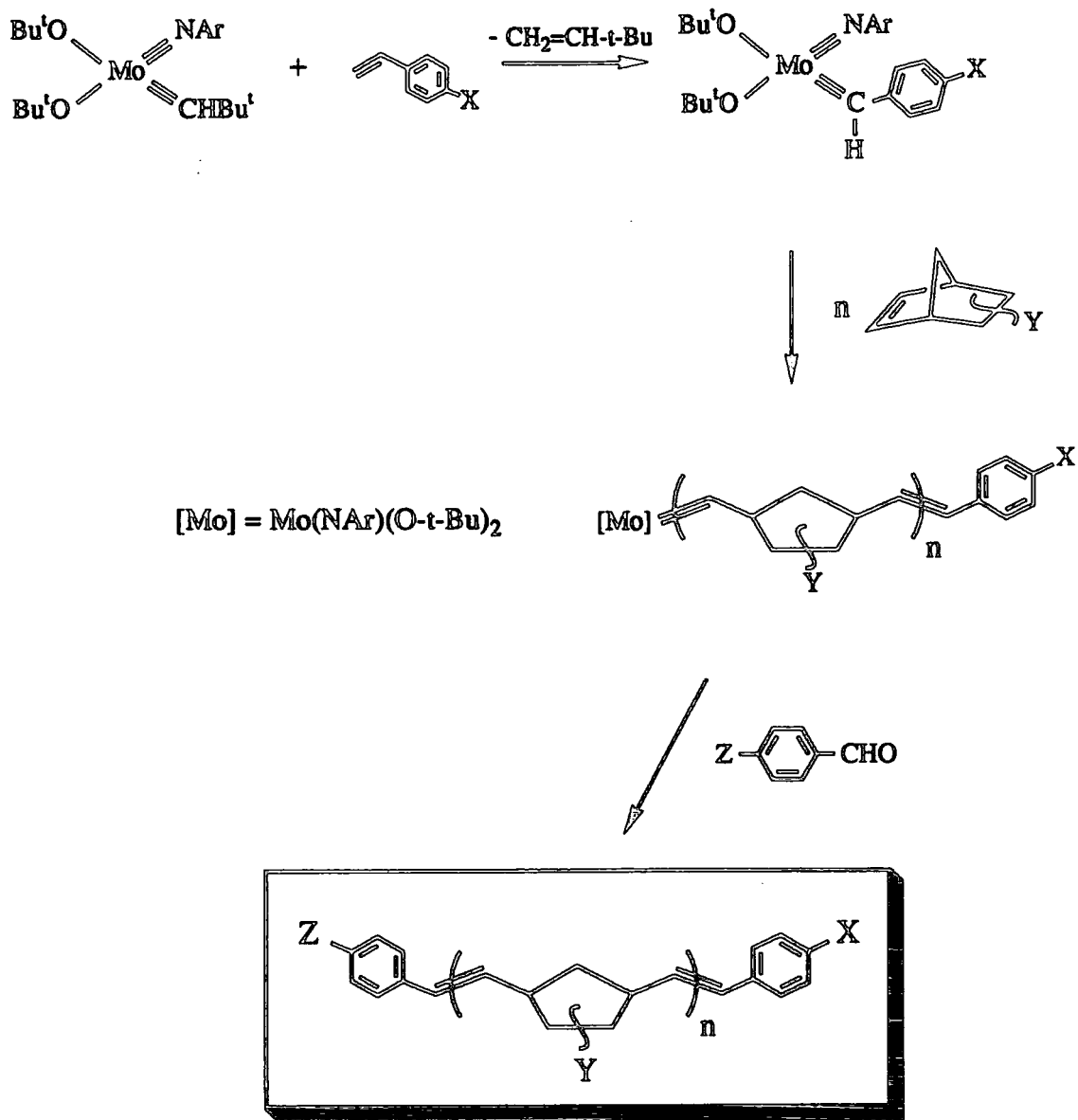


Figure 3.13 Total Functionalization of Polymers formed via ROMP.

3.6 Summary.

The work in this chapter has shown that a wide range of benzylidene complexes can be prepared either by the direct reaction of $\text{Mo}(\text{NAr})(\text{CH-t-Bu})(\text{O-t-Bu})_2$, or by the reaction of living polymers, with excess substituted styrenes. These benzylidene complexes act as efficient initiators for further polymerizations, thus allowing styrene derivatives to act as chain transfer agents in these living ROMP systems. The use of functionalized styrenes as CT agents, in conjunction with the use of functionalized benzaldehydes in the capping reaction (Chapter 2 of this thesis) and functionalized monomers, allows for total functionalization of the polymer chain, as outlined in figure 3.13.

3.7 References.

1. R.R. Schrock, J.S. Murdzek, G.C. Bazan, J. Robbins, M. DiMare, M.B. O'Regan, *J. Am. Chem. Soc.* 1990, 112, 3875.
2. R.R. Schrock, R.T. Depue, J. Feldman, K.B. Yap, D.C. Yang, W.M. Davis, L.Y. Park, M. DiMare, M.H. Schofield, J.A. Anhaus, E. Walborsky, E. Evitt, C. Kruger, P. Betz, *Organometallics*, 1990, 23, 158.
3. G.C. Bazan, R.R. Schrock, H.N. Cho, V.C. Gibson, *Macromolecules*, 1991, 24, 4495.
4. G.C. Bazan, E. Khosravi, R.R. Schrock, W.J. Feast, V.C. Gibson, M.B. O'Regan, J.K. Thomas, W.M. Davis, *J. Am. Chem. Soc.*, 1990, 112, 8378.
5. J.P. Mitchell, V.C. Gibson, R.R. Schrock, *Macromolecules*, 1991, 24, 1220.
6. K.J. Ivin, "*Olefin Metathesis*", Academic Press, London, 1983.
7. R.H. Grubbs, "*Alkene and Alkyne Metathesis Reactions*", in *Comprehensive Organometallic Chemistry*, G. Wilkinson, F.G.A. Stone, E.W. Abel Eds., Vol 8, Pergamon, 1982.

8. V. Draughton, A.T. Balaban, M. Dimonic, "*Olefin Metathesis and the Ring Opening Polymerization of Cyclo Olefins*", 2nd Ed, Wiley Interscience, 1985.
9. R.R. Schrock, K.B. Yap, D.C. Yang, H. Sitzman, L.R. Sita, G.C. Bazan, *Macromolecules*, 1989, 22, 3191.
10. W.E. Crowe, R.R. Schrock, Personal Communication.
11. R.R. Schrock, W.E. Crowe, G.C. Bazan, M. DiMare, M.B. O'Regan, M.H. Schofield, *Organometallics*, 1991, 10, 1832.
12. R. Schlund, R.R. Schrock, W.E. Crowe, *J. Am. Chem. Soc.* 1989, 111, 8004.
13. K. Knoll, R.R. Schrock, *J. Am. Chem. Soc.* 1989, 111, 7989.
14. W.E. Crowe, J.P. Mitchell, V.C. Gibson, R.R. Schrock, *Macromolecules*, 1990, 23, 3536.
15. G.C. Bazan, Ph.D Thesis, Massachusetts Institute of Technology, 1990.

CHAPTER FOUR

Heteroatom Exchange Reactions of
Four Coordinate Molybdenum Compounds

4.1 Introduction.

Four co-ordinate molybdenum species containing multiply bonded oxo, imido or alkylidene ligands are of considerable relevance to a large number of catalytic processes, including heterogeneous oxidation¹⁻⁵, and ammoxidation⁵⁻⁸, and homogeneous ring opening metathesis polymerization (ROMP)⁹⁻¹². As discussed in the preceding chapters of this thesis, important developments in the latter have centred around imido alkylidene complexes of the type $\text{Mo}(\text{NAr})(\text{CHCMe}_2\text{R})(\text{O-t-Bu})_2$ ¹³ (R = Me, Ph), which polymerize a range of functionalized cyclic monomers in a living manner⁹⁻¹². The success of such molybdenum based initiators is dependent upon preventing termination of the polymerization reaction via alkylidene coupling pathways. One way in which this could occur is by the exchange of imido and alkylidene groups between metal centres and subsequent coupling of the CHR units. For these initiator systems the use of the sterically demanding 2,6-di-isopropylphenylimido ligand in combination with bulky substituents on the other ancillary ligands effectively prevents such decomposition pathways. However, for less hindered multiply bonded units, exchange reactions may be more facile than previously recognized, and may offer a rationale for the instability of "unprotected" low co-ordinate alkylidene complexes.

To date, such "heteroatom exchange" reactions have not been subjected to detailed scrutiny, although closely related transformations have been exploited briefly in the past by Schrock and co-workers to prepare new tungsten alkylidene complexes of the type $\text{W}(\text{X})(\text{CH-t-Bu})(\text{PMe}_3)_2$ (X = O, NPh)^{14,15}. Here the alkylidene unit is transferred from $\text{Ta}(\text{CH-t-Bu})\text{Cl}_3(\text{PMe}_3)_2$ to the tungsten centres of $\text{W}(\text{X})(\text{O-t-Bu})_4$ and, at the same time, is accompanied by a re-distribution of the anionic one electron (Cl) and neutral two electron (PMe_3) ligands.

This chapter describes some heteroatom exchange reactions of multiply bonded oxo, imido and alkylidene units, and also anionic one electron ligands such as alkoxide and chloride.

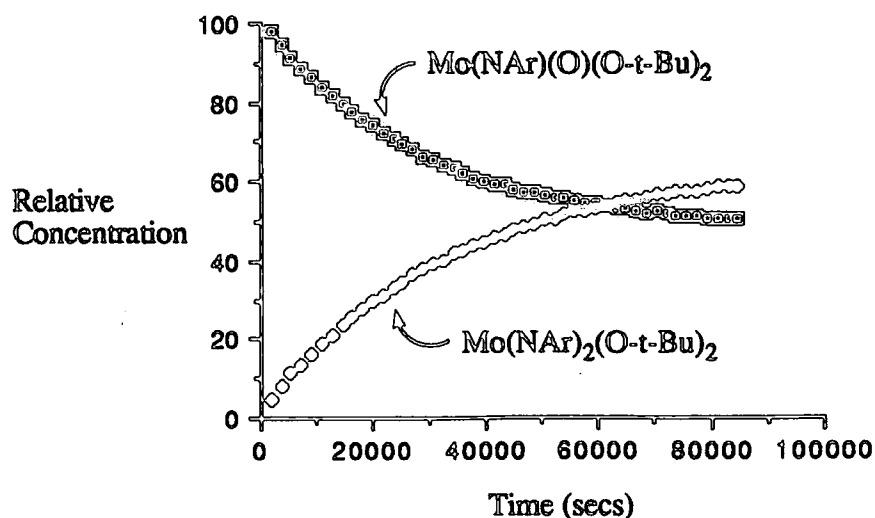
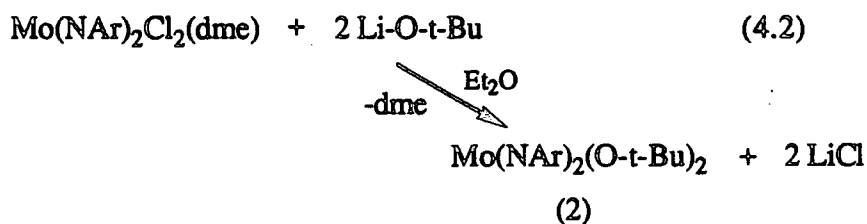


Figure 4.1 *Relative Concentrations of (1) and (2) as a function of time at 30°C.*

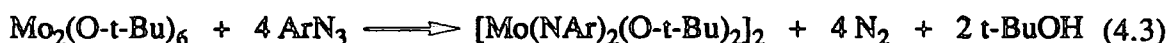
4.2.1 Reaction of $\text{Mo}(\text{NAr})_2\text{Cl}_2(\text{dme})$ with Li-O-t-Bu .
Preparation of $\text{Mo}(\text{NAr})_2(\text{O-t-Bu})_2$ (2).

Reaction of $\text{Mo}(\text{NAr})_2\text{Cl}_2(\text{dme})$ with two equivalents of Li-O-t-Bu in ether proceeds smoothly at room temperature over a period of 14 hours to afford $\text{Mo}(\text{NAr})_2(\text{O-t-Bu})_2$ (2) as an orange solid, according to equation 4.2. Dme is lost from the co-ordination sphere of the metal upon introduction of the two *t*-butoxide ligands presumably due to steric reasons. Recrystallization from ether at -78°C gave the product as orange crystals in 69% yield.



Compound (2) is moisture sensitive and highly soluble in hydrocarbon solvents. The 400 MHz ^1H NMR spectrum (C_6D_6) shows doublet and triplet resonances at δ 1.19 and 3.84 due to the isopropyl methyl and methine protons respectively of the arylimido ligands. A singlet due to the equivalent *t*-butoxide groups is observed at δ 1.42, and the expected triplet and doublet resonances of the three aromatic protons are observed at δ 6.93 and 7.01 respectively. Elemental analysis reveals a stoichiometry of $\text{MoC}_{32}\text{H}_{52}\text{N}_2\text{O}_2$ and the mass spectrum reveals an envelope for the parent ion (^{98}Mo) at $m/z = 594$. Compound (2) is stable indefinitely under an inert atmosphere at room temperature, but is thermally unstable in C_6D_6 solution at elevated temperatures, decomposing to give free arylamine, *t*-butanol and other, as yet, unidentified products.

Chisholm and co-workers have prepared the related phenyl and *p*-tolyl imido analogues of this compound via the reaction of $\text{Mo}_2(\text{O-}t\text{-Bu})_6$ with the appropriate aryl azide (equation 4.3)^{16,17}.



The *p*-tolyl derivative is found to be dimeric in the solid state with unsymmetric bridging imido ligands, as shown in figure 4.2. However, cryoscopic molecular weight determinations revealed that the dimeric structure found in the solid state was not maintained in solution.

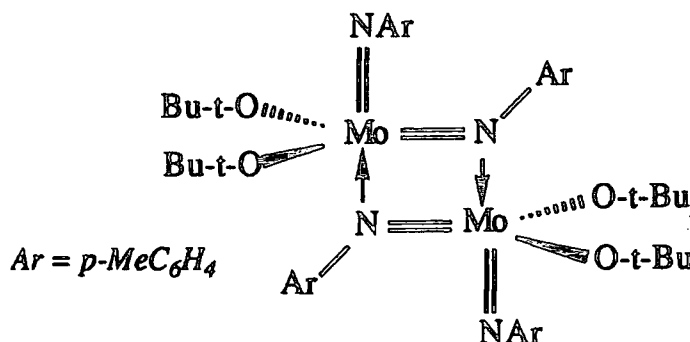


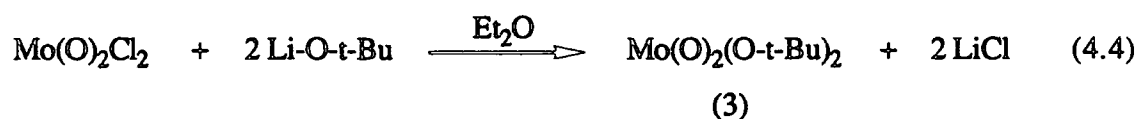
Figure 4.2 Molecular structure of $[\text{Mo}(\text{N-}p\text{-tol})_2(\text{O-}t\text{-Bu})_2]_2$.

A crystal structure of (2) would be of interest, as the sterically encumbered 2,6-di-isopropylphenylimido ligands may prevent dimerization in the solid state. Complexes of the type $M(\text{NAr})(\text{CH-t-Bu})(\text{O-t-Bu})_2$ ($M = \text{Mo}, \text{W}$), containing the less sterically hindered combination of arylimido and alkylidene ligands, are known to be monomeric in the solid state⁹.

4.2.2 Reaction of $\text{Mo}(\text{O})_2\text{Cl}_2$ with Li-O-t-Bu .

Preparation of $\text{Mo}(\text{O})_2(\text{O-t-Bu})_2$ (3).

Treatment of $\text{Mo}(\text{O})_2\text{Cl}_2$ with 2 equivalents of Li-O-t-Bu in ether gives $\text{Mo}(\text{O})_2(\text{O-t-Bu})_2$ (3) as a colourless oil upon filtration and removal of the volatile components *in vacuo* (equation 4.4).

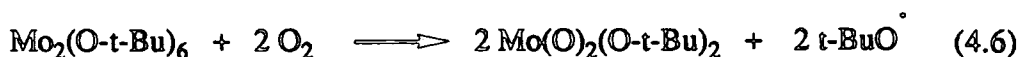


The product may be purified by distillation (55°C at 10^{-4} torr) or by recrystallization from Et_2O at -78°C to give a white solid presumed to be the bis etherate. This solid melts at room temperature and loses its co-ordinated ether upon exposure to dynamic vacuum. The ^1H NMR spectrum of (3) (C_6D_6) shows a singlet resonance at δ 1.15, consistent with equivalent t-butoxide environments. Elemental analysis supports the formulation $\text{MoC}_8\text{H}_{18}\text{O}_4$ and the mass spectrum shows a protonated molecular ion peak at $m/z = 277$ (^{98}Mo). In addition, a small number of higher molecular weight peaks can be observed, corresponding to dimeric fragments. These could arise by partial hydrolysis of (3), as shown in equation 4.5.



Compound (3) is stable under an atmosphere of dry nitrogen, but rapidly decomposes to give blue molybdenum oxides when exposed to moisture. Upon standing in C_6D_6 solution for several days (0.07M), decomposition to a complex mixture of olefinic and other unidentified species is observed.

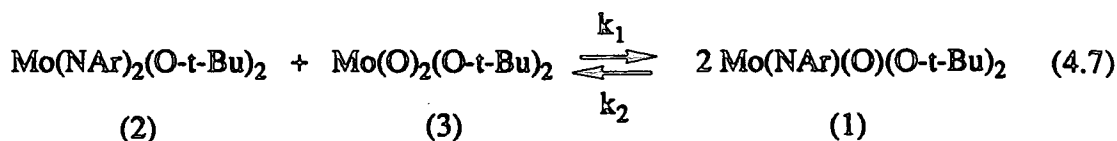
$\text{Mo}(\text{O})_2(\text{O}-t\text{-Bu})_2$ has also been prepared by Chisholm and co-workers¹⁸, via treatment of $\text{Mo}_2(\text{O}-t\text{-Bu})_2$ with O_2 , according to equation 4.6.



A cryoscopic molecular weight determination indicated a monomeric formulation in benzene solution¹⁸.

4.2.3 Kinetic Analysis of Oxo/Imido Exchange.

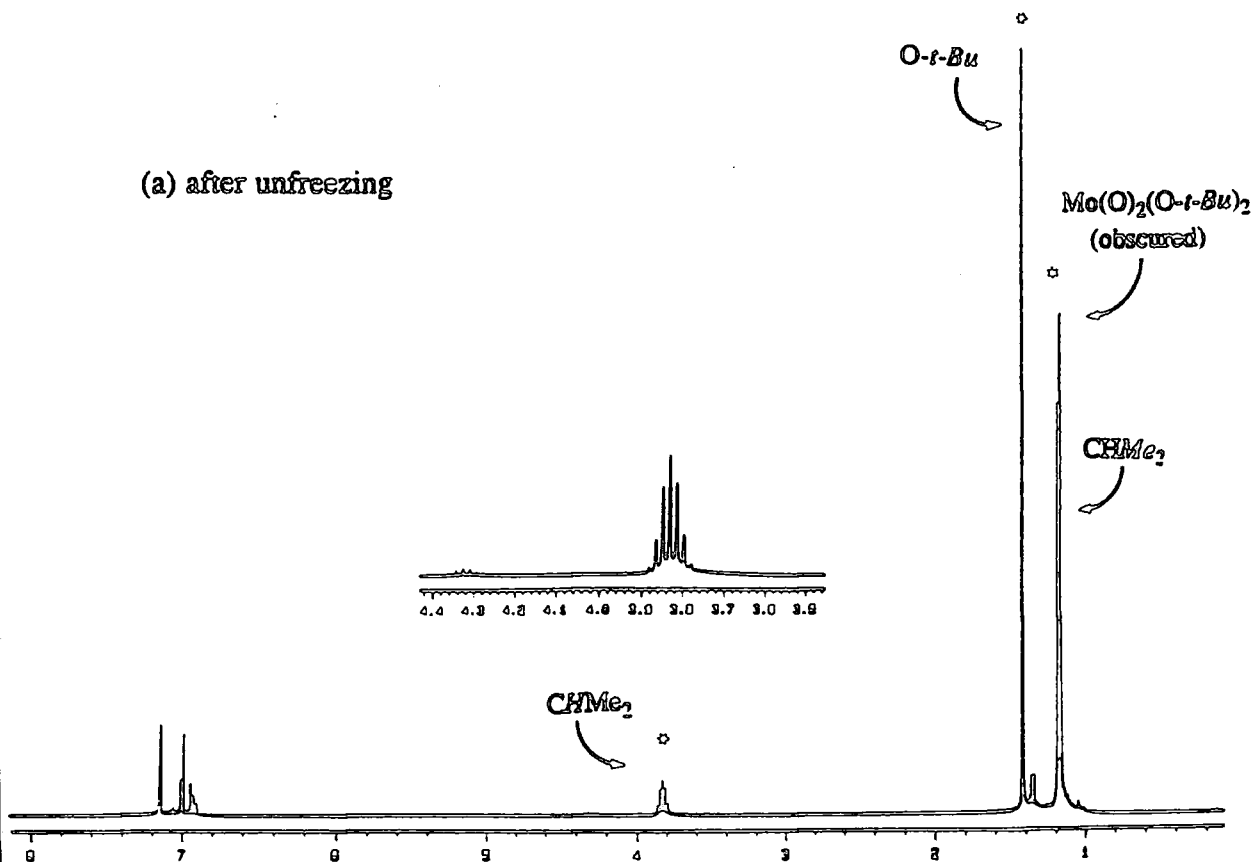
To demonstrate that the exchange of oxo and imido units, as shown in equation 4.1, is indeed a reversible equilibrium, (2) was treated with an equimolar amount of (3) in C_6D_6 and the resulting reaction (equation 4.7) monitored by ^1H NMR spectroscopy. Clean conversion to the same equilibrium mixture of (1), (2) and (3) as shown in figure 4.1 was observed ($K_{\text{eqm}} = k_1/k_2 = 0.08$).



Representative ^1H NMR spectra of the starting mixture of complexes (2) and (3) and the resulting equilibrium mixture are shown in Figure 4.3.

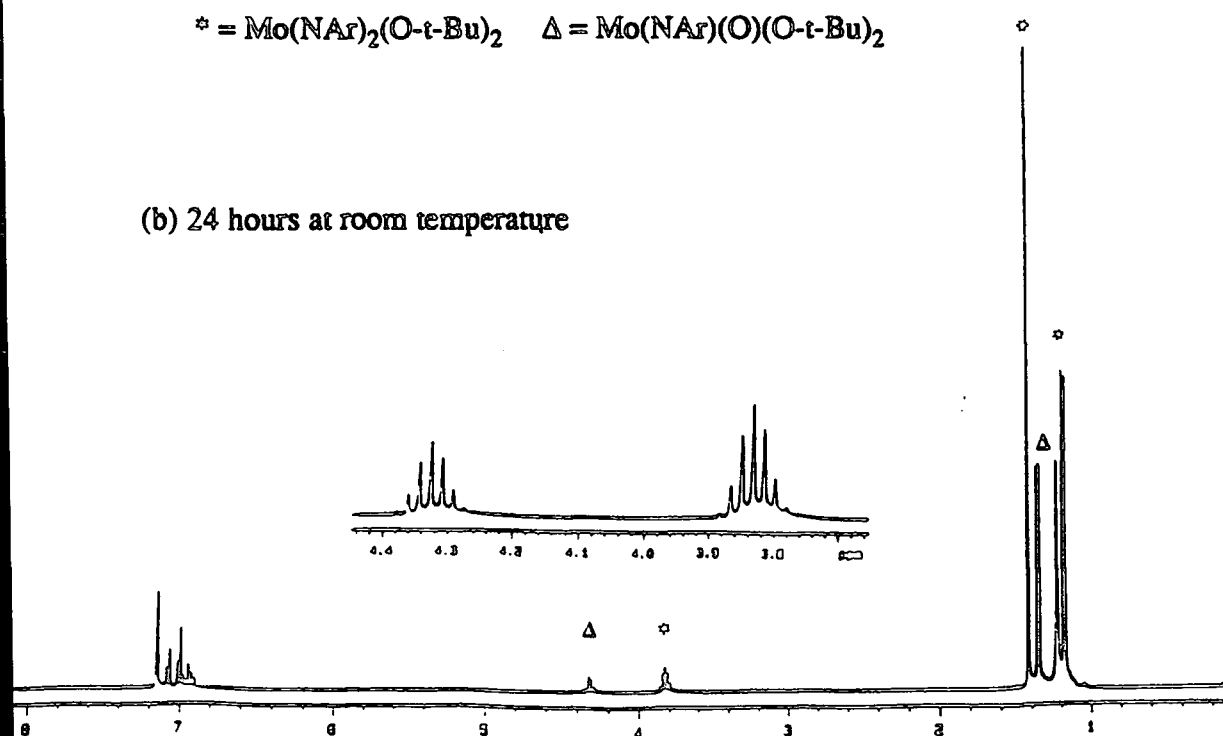
Figure 4.3 400 MHz ^1H NMR spectra (C_6D_6) of the reaction between $\text{Mo}(\text{NAr})_2(\text{O}-t\text{-Bu})_2$ (2) and $\text{Mo}(\text{O})_2(\text{O}-t\text{-Bu})_2$ (3)

(a) after unfreezing



* = $\text{Mo}(\text{NAr})_2(\text{O}-t\text{-Bu})_2$ Δ = $\text{Mo}(\text{NAr})(\text{O})(\text{O}-t\text{-Bu})_2$

(b) 24 hours at room temperature



Values for k_1 in equation 4.7 were determined by ^1H NMR spectroscopy over the temperature range 20-50°C. The progress of the reaction was quantified by integration of the methine resonances of the isopropyl arylimido substituents of (1) and (2) (δ 4.34 and 3.84 ppm respectively). A representative plot showing the relative concentrations of (1) and (2) at 40°C as a function of time is shown in figure 4.4.

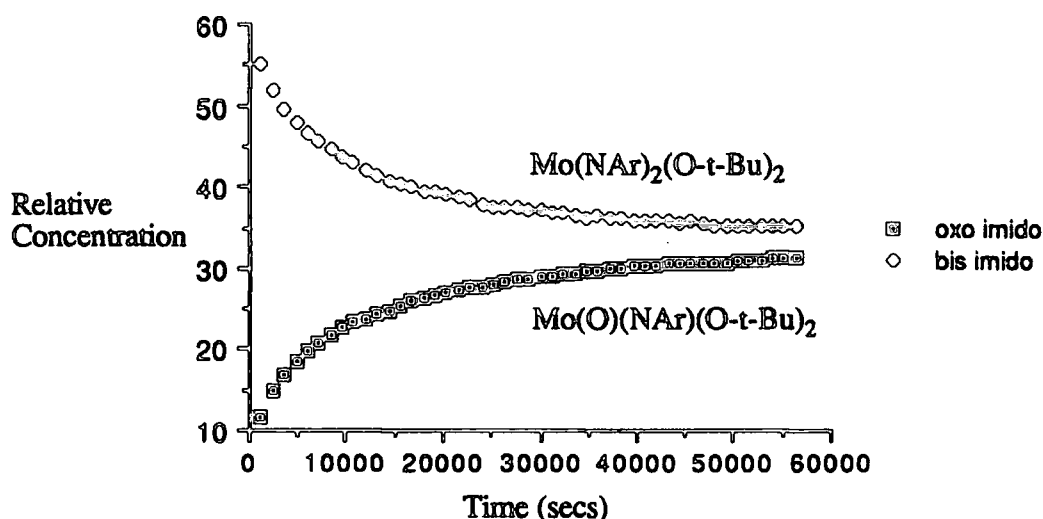


Figure 4.4 *Relative concentrations of (1) and (2) as a function of time at 40°C.*

The kinetic data was analysed according to the integrated rate law for a second order reversible reaction¹⁹, as shown in equation 4.8.

$$\ln \left[\frac{x(a - 2x_e) + ax_e}{a(x_e - x)} \right] = \left[\frac{2a(a - x_e)}{x_e} \right] k_1 t \quad (4.8)$$

where a = starting concentration of (2),

x = concentration of (1) at time t ,

x_e = equilibrium concentration of (1).

A plot of $\ln [x (a-2x_e) + ax_e / a (x_e-x)]$ versus time gives a straight line whose slope is $[2a (a-x_e) / x_e] k_1$ thus allowing k_1 to be determined. The rate constants at differing temperatures are listed in table 4.1.

Temperature (K)	k_1 (l mol ⁻¹ s ⁻¹)
293	$2.1 (3) \times 10^{-7}$
303	$7.3 (5) \times 10^{-7}$
313	$24 (5) \times 10^{-7}$
323	$59 (4) \times 10^{-7}$

Table 4.1 *Calculated rate constants for equation 4.7.*

The Arrhenius plot for these data is shown in figure 4.5, affording the parameters $\Delta H^\ddagger = 20.6 (4) \text{ kcal mol}^{-1}$, $\Delta S^\ddagger = -19 (2) \text{ e.u.}$, $\Delta G^\ddagger(298\text{K}) = 26.2 (5) \text{ kcal mol}^{-1}$, $A = 21.1$, and $E_a = 21.2 (1.0) \text{ kcal mol}^{-1}$.

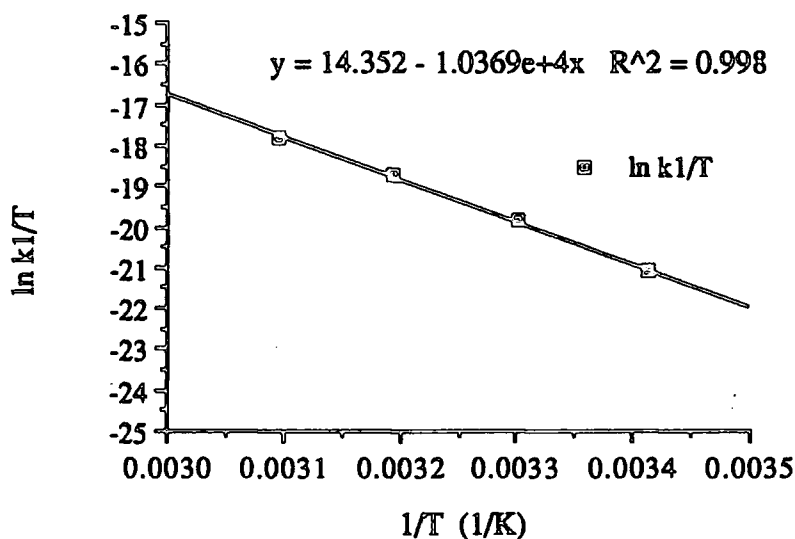


Figure 4.5 *Arrhenius Plot for Equation 4.7.*



The negative ΔS^\ddagger value is consistent with the exchange of oxo and imido units via an ordered four-centred transition state as shown in figure 4.6.

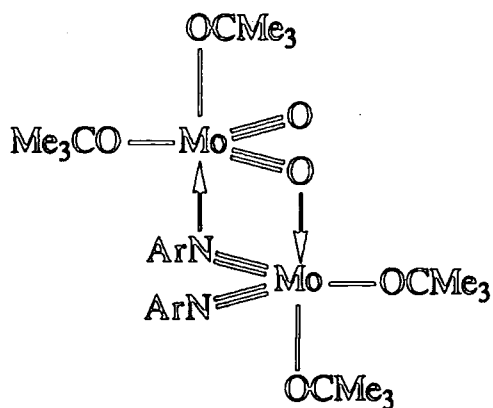


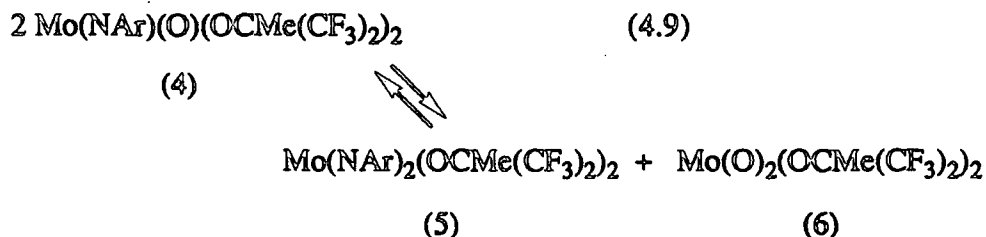
Figure 4.6 *Proposed Transition State for Oxo/Imido Exchange.*

Here, each molybdenum is assumed to adopt a trigonal bipyramidal coordination geometry similar to that seen for the bridged imido dimer $[\text{Mo}(\text{N-}i>p\text{-tol})_2(\text{O-}i>t\text{-Bu})_2]_2$ shown in figure 4.2¹⁶, and simple base adducts of $\text{Mo}(\text{NAr})(\text{CH-}i>t\text{-Bu})(\text{OR})_2$ ²⁰. It is also worth noting the close similarity of this transition state to the mechanistic pathway established for olefin metathesis²¹.

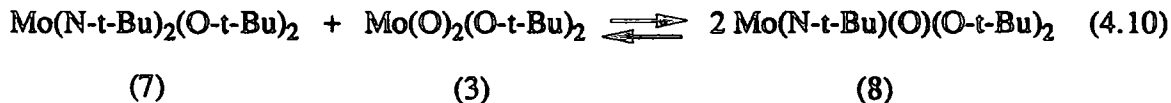
Oxo/imido exchange in this system is dramatically slowed in the presence of a coordinating base such as pyridine. This is presumably due to pyridine binding to the coordinatively unsaturated molybdenum centre, thus hindering formation of the oxo and imido bridges necessary for exchange to occur.

The reaction was also carried out on the hexafluoro-*t*-butoxide analogues of (1) and (2). These exchange oxo and imido groups much less readily than their non-fluorinated counterparts; several days at 60° are required before the equilibrium concentrations of $\text{Mo}(\text{NAr})(\text{O})(\text{OCMe}(\text{CF}_3)_2)_2$ (4), $\text{Mo}(\text{NAr})_2(\text{OCMe}(\text{CF}_3)_2)_2$ (5) and $\text{Mo}(\text{O})_2(\text{OCMe}(\text{CF}_3)_2)_2$ (6) are obtained (equation 4.9). This most likely results from a combination of the increased steric hindrance of the $\text{OCMe}(\text{CF}_3)_2$ groups and the

greater strength of the metal-oxo and metal-imido multiple bonds in the hexafluoro-*t*-butoxide analogues. However it is not possible, upon the available evidence, to assess which of these effects may be predominant.



For the bis *t*-butylimido derivative $\text{Mo(N-}t\text{-Bu)}_2\text{(O-}t\text{-Bu)}_2$ (7), oxo-imido ligand exchange with $\text{Mo(O)}_2\text{(O-}t\text{-Bu)}_2$ (3) occurs much more readily than for the corresponding reaction of (2) with (3), as shown in equation 4.10²².



Monitoring the reaction by ¹H NMR spectroscopy shows it to be complete within 50 minutes at room temperature, with no residual reactants remaining. The initial rate of reaction is very rapid, thus preventing a detailed kinetic analysis by ¹H NMR spectroscopy. This faster rate of reaction can be understood on steric grounds, with the smaller *t*-butylimido group favouring formation of the oxo-imido bridge in the transition state. The observation that this reaction favours the oxo-imido species ($K_{\text{eqm}} > 100$), whereas the corresponding reaction of (3) with (2) favours the starting materials at room temperature ($K_{\text{eqm}} = 0.08$), is presumably due to an electronic effect, and is discussed further in section 4.4.7.

4.3 Attempted Preparation of $\text{Mo}(\text{O})_2(\text{OAr})_2$ Complexes.

The relative instability of compound (3) may in part be attributed to the presence of the two *t*-butoxide groups. Therefore an attempt was made to prepare analogous aryloxide derivatives, where hopefully bulky substituted phenyl groups would help to prevent decomposition. In this laboratory Alan Shaw attempted to prepare compounds of the type $\text{M}(\text{O})_2(\text{OAr})_2$ ($\text{M} = \text{Mo}, \text{W}$) via the reaction of $\text{M}(\text{O})_2\text{Cl}_2$ with two equivalents of LiOAr in toluene solvent²³. However, it was found that for molybdenum there was a preference for oxo abstraction over metathetical exchange of chloride ligands, and no molybdenum di-oxo bis aryloxide compounds were isolated. The success of forming $\text{Mo}(\text{O})_2(\text{O-}t\text{-Bu})_2$ (3) in ether solvent led us to believe that such complexes may be formed in this co-ordinating solvent.

However, the reaction of $\text{Mo}(\text{O})_2\text{Cl}_2$ with two equivalents of lithium 2,6-diisopropylphenoxide in ether solvent proceeds quite differently. Stirring the mixture at room temperature under dry nitrogen affords a purple crystalline solid and a red-green dichroic supernatant solution, according to equation 4.11.



Analysis of the solid reveals that the chlorides are not exchanged for aryloxide groups. Instead lithium is incorporated into the $\text{Mo}(\text{O})_2\text{Cl}_2$ lattice, as has been observed previously for similar reactions involving $\text{W}(\text{O})_2\text{Cl}_2$ ^{23,24}. This unexpected observation is discussed further in appendix three.

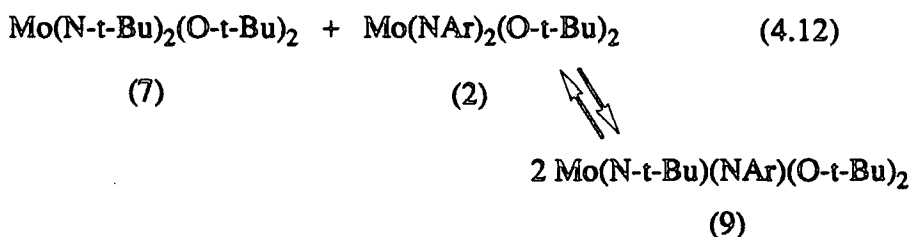
4.4 Further Heteroatom Exchange Reactivity of $\text{Mo}(\text{NAr})_2(\text{O-}t\text{-Bu})_2$ (2)

Having shown in the preceding section that the imido groups of $\text{Mo}(\text{NAr})_2(\text{O-}t\text{-Bu})_2$ (2) could be exchanged for oxo groups, further investigations were undertaken to determine how widespread this exchange reactivity might be. A

variety of both organic reagents and other multiply bonded metal complexes were used as "heteroatom exchange" reagents, and in most cases reactions were performed on an NMR scale and monitored by ^1H NMR spectroscopy.

4.4.1 Reaction of $\text{Mo}(\text{NAr})_2(\text{O}-t\text{-Bu})_2$ (2) with $\text{Mo}(\text{N}-t\text{-Bu})_2(\text{O}-t\text{-Bu})_2$ (7).

Treatment of $\text{Mo}(\text{NAr})_2(\text{O}-t\text{-Bu})_2$ (2) with an equimolar amount of $\text{Mo}(\text{N}-t\text{-Bu})_2(\text{O}-t\text{-Bu})_2$ (7) in C_6D_6 gives an equilibrium mix of (2), (7) and the mixed bis-imido species $\text{Mo}(\text{NAr})(\text{N}-t\text{-Bu})(\text{O}-t\text{-Bu})_2$ (9)²², as shown in equation 4.12.

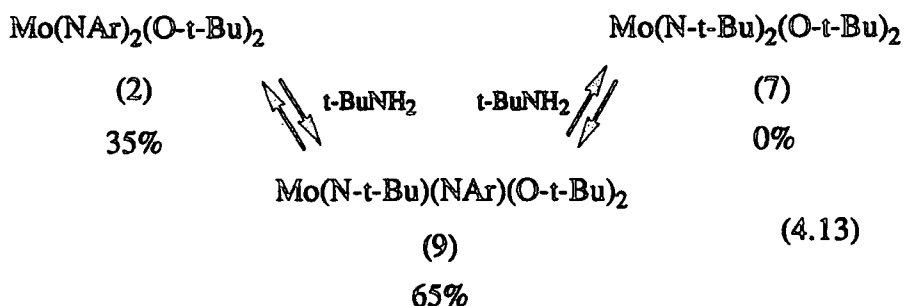


$\text{Mo}(\text{NAr})(\text{N}-t\text{-Bu})(\text{O}-t\text{-Bu})_2$ (9) is characterized in the ^1H NMR spectrum (250 MHz, C_6D_6) by septet and doublet resonances at δ 3.73 and 1.34 for the arylimido isopropyl methine and methyl protons respectively, a singlet at δ 1.20 for the *t*-butylimido methyl protons and a singlet at δ 1.39 for the equivalent *t*-butoxide groups.

In this system imido ligand exchange is much slower than imido for oxo exchange, requiring several days to reach equilibrium. This is consistent with the increased steric congestion provided by the bulky exchanging imido groups, disfavoring imido bridge formation. After monitoring the reaction at 60°C for five days, no further change in the concentrations of (2), (7) or (9) was observed, the equilibrium lying heavily in favour of the mixed imido species (9) ($K_{\text{eqbm}} \approx 25$).

4.4.2 Reaction of $\text{Mo}(\text{NAr})_2(\text{O-t-Bu})_2$ (2) with t-BuNH_2 .

$\text{Mo}(\text{NAr})_2(\text{O-t-Bu})_2$ was mixed with 2 equivalents of t-BuNH_2 in C_6D_6 at room temperature. No reaction was observed after several hours therefore the mixture was heated to 60°C . After 12 hours at this temperature, peaks corresponding to the mixed bis-imido species $\text{Mo}(\text{NAr})(\text{N-t-Bu})(\text{O-t-Bu})_2$ (9), $\text{Mo}(\text{N-t-Bu})_2(\text{O-t-Bu})_2$ (7) and free ArNH_2 could be observed. After 11 days equilibrium was attained, with the approximate equilibrium percentage concentrations given in equation 4.13.



Notably, the mixed imido complex (9) is again the most favoured species. It is also interesting to observe that whilst some bis arylimido complex remains, virtually no bis *t*-butylimido species is present at equilibrium. A similar equilibrium mixture of these three species is obtained upon treatment of $\text{Mo}(\text{N-t-Bu})_2(\text{O-t-Bu})_2$ with two equivalents of arylamine²².

The reaction of (2) with t-BuNH_2 is believed to proceed via a trigonal base-adduct (10), which must then undergo a proton transfer to give a bis-amide intermediate (11) (figure 4.7). This is then likely to adopt a distorted square based pyramidal structure by analogy with 5-coordinate phenoxide^{23,25} and amide²⁶ complexes of this general type .

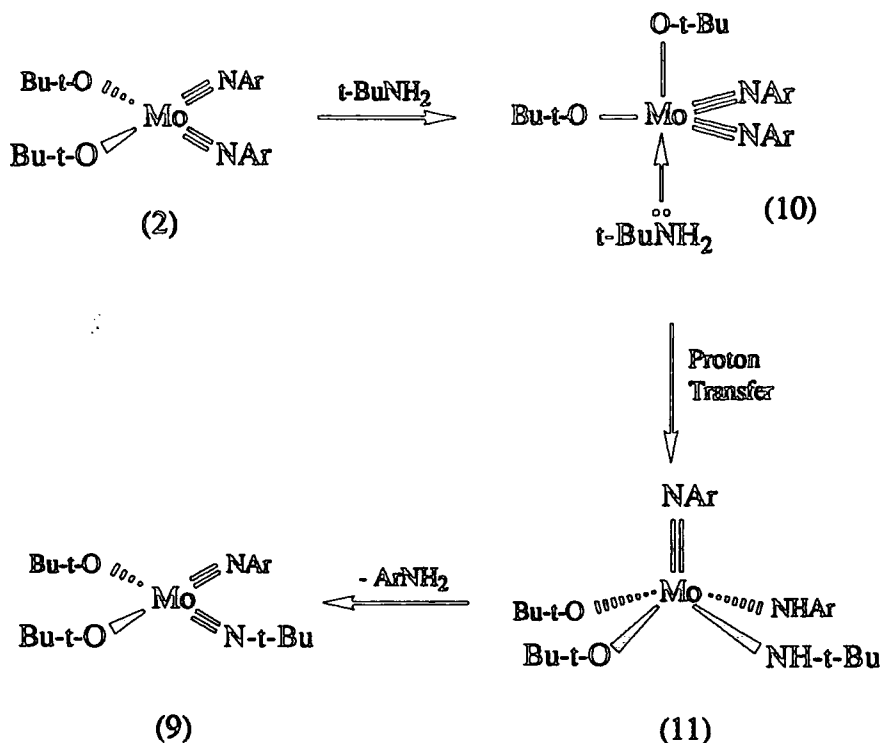


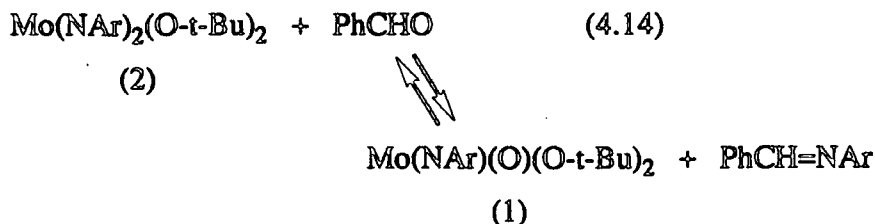
Figure 4.7 The reaction of (2) with $t\text{-BuNH}_2$.

The exchange of imido groups using amines is unusual and to our knowledge has only been observed at iridium and osmium metal centres, with conversion of $\text{Cp}^*\text{Ir}(\text{N-t-Bu})$ and $(\eta\text{-arene})\text{Os}(\text{N-t-Bu})$ to the corresponding arylimido complexes via exchange with $2,6\text{-Me}_2\text{C}_6\text{H}_3\text{NH}_2$ ^{27a,b}. The related species $\text{Cp}^*\text{Zr}(\text{N-t-Bu})$ reacts with $t\text{-BuNH}_2$ to give the stable bis amido $\text{Cp}^*\text{Zr}(\text{NH-t-Bu})_2$, also providing a model for the transformation of (10) to (11)^{27c}.

4.4.3 Reaction of $\text{Mo}(\text{NAr})_2(\text{O-t-Bu})_2$ (2) with Benzaldehyde.

The molybdenum bis-imido complex (2) reacts with excess benzaldehyde (typically 10 equivalents) very slowly at room temperature to afford the oxo-imido species $\text{Mo}(\text{NAr})(\text{O})(\text{O-t-Bu})_2$ (1) and the Schiff's base side product $\text{PhCH}=\text{NAr}$ (equation 4.14). After 2 weeks at room temperature there is only 12% conversion.

Upon heating to 60°C for a further seven days, the ratio of (2) : (1) is 1 : 1.6 but some decomposition to give t-butanol is observed.

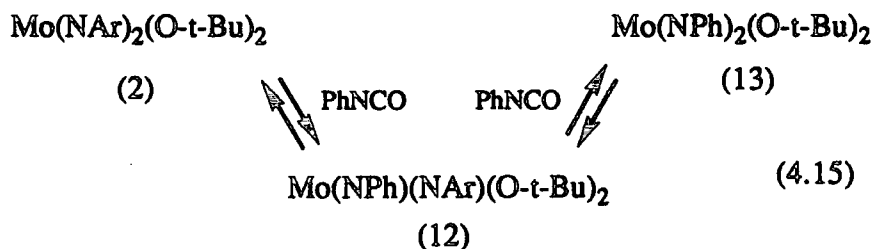


This observation may be compared to the reaction of $\text{Mo(N-t-Bu)}_2(\text{O-t-Bu})_2$ (7) with benzaldehyde which affords $\text{Mo(N-t-Bu)(O)(O-t-Bu)}_2$ (8) in greater than 95% yield after one week at room temperature. Prolonged heating at 60°C gave predominantly (3)²⁸.

4.4.4 Reaction of $\text{Mo(NAr)}_2(\text{O-t-Bu})_2$ (2) with Isocyanates.

(a) NMR Studies.

The exchange of terminal imido ligands by reaction with *p*-tolyl isocyanate has recently been shown for the binuclear complex $[\text{Mo(NPh)}(\mu\text{-NPh})(\text{MeC}_5\text{H}_4)]_2$ ²⁹. It was therefore envisaged that the reaction of $\text{Mo(NAr)}_2(\text{O-t-Bu})_2$ (2) with phenyl isocyanate may proceed according to equation 4.15, to yield the mixed imido complex (12) and the bis phenylimido complex (13).



However, the reaction of (2) with one equivalent of PhNCO in C₆D₆ is not clean, affording at least four, as yet, unidentified species. Upon heating to 60°C, a small amount of free ArNCO is observed in the ¹H NMR spectrum, showing that some heteroatom exchange of arylimido for phenylimido groups has occurred. This is accompanied by a darkening of the solution to a deep red colour. Upon prolonged heating to 100°C, resonances due to the oxo-imido species Mo(NAr)(O)(O-t-Bu)₂ (1) can also be observed, indicating that some metathesis of the C=O bond of the isocyanate occurs at elevated temperature.

The reaction with an excess of phenyl isocyanate appears more straightforward. After unfreezing, a C₆D₆ solution containing (2) and 10 equivalents of phenyl isocyanate shows a variety of new species by ¹H NMR spectroscopy. These are the same as those observed upon addition of one equivalent. After standing at room temperature for 24 hours, a single species predominates, characterized by an arylimido methine septet resonance at δ 3.76, two broad arylimido methyl doublets at δ 1.13 and 0.96 and a singlet t-butoxide resonance at δ 1.43. Aryl proton resonances could not be assigned unambiguously due to the presence of excess phenyl isocyanate. Again, at room temperature, only a small amount (≈ 5%) of free ArNCO is observed, indicating that little heteroatom exchange has occurred.

These observations suggested the formation of a relatively stable intermediate, possibly an adduct or metallacycle. Therefore the reaction was repeated on a preparative scale.

(b) Reaction of Mo(NAr)₂(O-t-Bu)₂ (2) with excess PhNCO

Preparation of Mo[N(Ar)C(O)N(Ph)]₂(O-t-Bu)₂ (14).

Treatment of Mo(NAr)₂(O-t-Bu)₂ (2) with 10 equivalents of phenyl isocyanate in pentane at room temperature gave a deep red solution from which red crystals could be isolated in 56% yield by recrystallization at -78°C. ¹H NMR analysis (400MHz, C₆D₆) showed the same species to that observed previously on the NMR scale reaction. The

aromatic proton resonances could be observed (due to the absence of excess PhNCO) as a doublet at δ 7.59, a multiplet at δ 6.97 and 2 triplets at δ 6.81 and 6.75. Internal integration is consistent with two equivalents of phenyl isocyanate coordinated to each molecule of (2). However, a simple bis phenyl isocyanate adduct seems unlikely, as PhNCO resonances are not observed in the infrared spectrum. In the ^{13}C NMR spectrum, a singlet is observed at δ 227.24. This can be assigned to the oxygen bearing ring carbon of the four membered metallacyclic unit $\text{Mo}[\text{N}(\text{Ar})\text{C}(\text{O})\text{N}(\text{Ph})]$. The product is therefore believed to be the bis-metallacycle $\text{Mo}[\text{N}(\text{Ar})\text{C}(\text{O})\text{N}(\text{Ph})]_2(\text{O}-t\text{-Bu})_2$ (14), formed via the formal [2+2] coupling of the phenyl isocyanate with the metal imido linkages (equation 4.16)



Elemental analysis confirms the stoichiometry $\text{MoN}_4\text{O}_4\text{C}_{16}\text{H}_{24}$, whilst in the mass spectrum (^{98}Mo) the ion of highest mass (at $m/z = 594$) corresponds to the base free complex (2), with an additional peak at $m/z = 119$ for free phenyl isocyanate.

Related metallacycles have been observed for the reaction of phenyl isocyanate with metal oxo linkages³⁰⁻³², and the complex $\text{Cp}_2\text{Mo}[\text{OC}(\text{O})\text{N}(\text{Ph})]$ has been structurally characterized^{30,31}. These metallacycles are remarkably stable, but prolonged heating leads to decomposition rather than to carbon dioxide loss giving the corresponding phenylimido complex.

The formation of (14) is believed to proceed as shown in figure 4.8.

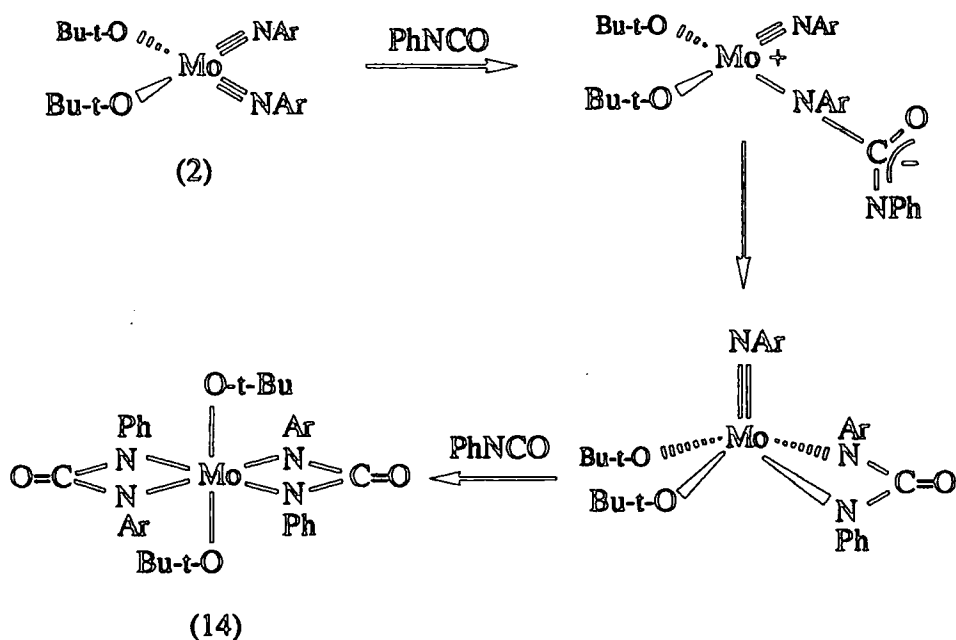
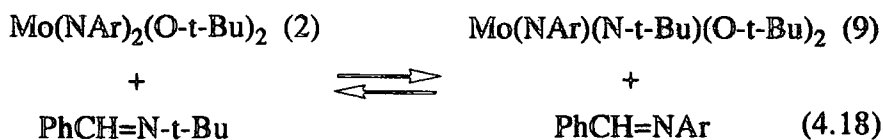


Figure 4.8 *Postulated Mechanism for the formation of (14).*

This also accounts for a variety of species being observed on an NMR scale when only one equivalent of phenyl isocyanate is added. The exact geometry of (14) is not known, but equivalent *t*-butoxide ligands (as shown by ^1H NMR) indicate a symmetrical species (one of which is shown in figure 4.8).

Compound (14) appears to be remarkably stable in C_6D_6 solution. It is only after heating to 100°C for several days that further free ArNCO is observed. However, no evidence for formation of the heteroatom exchange product of (2) (i.e. possessing terminal phenylimido groups) could be obtained.

No reaction was observed (by ^1H NMR spectroscopy) upon treatment of (2) with 10 equivalents of *t*-butyl isocyanate, even after prolonged heating at 60°C . This is consistent with the increased steric bulk of a three-dimensional *t*-butyl group relative to the planar phenyl group of PhNCO .



Significantly, no $\text{Mo(N-t-Bu)}_2(\text{O-t-Bu})_2$ (7) is observed upon prolonged heating at 60°C , showing that displacement of the second arylimido group to give the bis *t*-butylimido species is disfavoured, an observation that agrees with those discussed previously in section 4.4.2.

4.4.7 Factors Affecting Bonding in *Cis* Multiply-Bonded Species.

For several of the reactions discussed in the previous sections, an apparent electronic preference has been noted for mixed imido or imido-oxo species. The origin of this may lie in the ability of the metal centre in tetrahedral complexes to form only three π -type interactions with the two *cis* multiply-bonded ligands. Thus, for complexes of the type $\text{Mo(X)}_2(\text{O-t-Bu})_2$ ($\text{X} = \text{CH-t-Bu}, \text{N-t-Bu}, \text{NAr}, \text{O}$), one of the multiply bonded ligands can form at most a double bond. For alkylidene imido complexes, this is not a problem since the alkylidene unit is a single faced π donor and hence can only form one π bond, but for bis imido and oxo-imido complexes a competition will ensue for the available d_π orbitals. It might be expected, therefore, that *cis* multiply-bonded species will be favoured if they possess an electron donating unit (favouring formation of a relatively strong triple bond) and an electron withdrawing group (favouring a double bond). Similarly, the more electronegative oxygen atom will form weaker π -interactions with the metal than the nitrogen of the imido ligand. This also accounts for the much higher equilibrium constant observed for formation of $\text{Mo(N-t-Bu)(O)(O-t-Bu)}_2$ (8) over $\text{Mo(NAr)(O)(O-t-Bu)}_2$ (1).

In conclusion, stability may be enhanced for complexes containing electronically disparate multiply bonded groups in a tetrahedral environment.

4.4.8 Further Reactivity Studies on $\text{Mo}(\text{NAr})_2(\text{O}-t\text{-Bu})_2$ (2).

No detectable reaction was observed between $\text{Mo}(\text{NAr})_2(\text{O}-t\text{-Bu})_2$ (2) and

- (a) $\text{PhCH}=\text{PPh}_3$ (0.9 equivalents, 14 days at 100°C)
- (b) nitrobenzene (5.0 equivalents, 4 days at 60°C)
- (c) azobenzene (1.0 equivalent, 7 days at 60°C) and
- (d) $t\text{-BuOH}$ (4.4 equivalents, 14 days at 60°C)

With TMSN_3 (3.0 equivalents, 4 weeks at 140°C), several new trimethylsilyl resonances at δ 0.11, 0.16 and 0.29, and a new arylimido septet resonance at δ 3.78 were observed in the ^1H NMR spectrum. However, the reaction was not clean and substantial decomposition of the starting bis imido complex (2) was observed.

Degassed water (2.0 equivalents) reacted instantly in C_6D_6 accompanied by a darkening of the solution to give free arylamine and t -butanol, with no molybdenum containing species being identified.

With PMe_3 (3.0 equivalents in C_6D_6), no reaction was observed at room temperature. However, if the sealed NMR tube sample is frozen in liquid nitrogen, a darkening of the sample colour is observed; reverting back to its original orange colour upon warming to room temperature. This suggests that some adduct formation may occur at low temperature. However, variable temperature ^1H NMR studies in C_7D_8 revealed no change in the NMR spectrum at temperatures as low as -80°C , indicating that any adduct must form below this temperature.

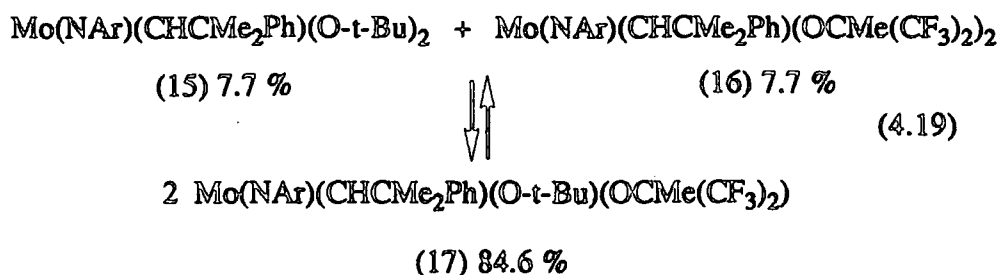
4.5 Alkoxide Exchange in Four Coordinate Molybdenum Alkylidene Complexes.

Thus far, this chapter has been concerned with the exchange of *multiply* bonded ligands between metal centres. However, it is well documented that the catalytic activity of four coordinate alkylidene complexes of the type $\text{Mo}(\text{NAr})(\text{CHCMe}_2\text{R})(\text{OR}')_2$ ($\text{R} = \text{Me, Ph}$; $\text{R}' = \text{CMe}_3, \text{CMe}_2\text{CF}_3, \text{CMe}(\text{CF}_3)_2$) is dependent upon the nature of the ancillary mono-anionic alkoxide ligands¹³. Catalysts possessing electron withdrawing hexafluoro-*t*-butoxide groups are active for the metathesis of acyclic olefins whereas those possessing electron donating *t*-butoxide groups are inactive for this purpose, although ideal for cyclic olefins and therefore living ROMP.

A range of modified catalysts have been investigated by Schrock and coworkers¹³, where the two *t*-butoxides are replaced by phenoxides. Linked alkoxide complexes have also recently been prepared³⁵.

For the purpose of comparing the exchange chemistry of one-electron anionic ligands with the dianionic ligands discussed previously, and its potential for providing a convenient route to modified ROMP initiators, we now consider the exchange of alkoxide ligands between metal centres.

It is found that the alkoxides readily exchange between the metal centres of the *t*-butoxide (15) and hexafluoro-*t*-butoxide (16) neophylidene complexes. When the neophylidene bis *t*-butoxide complex (15) is treated with an equimolar amount of the corresponding hexafluoro-*t*-butoxide complex (16) in C_6D_6 an equilibrium mix of (15), (16), and the mixed alkoxide species $\text{Mo}(\text{NAr})(\text{CHCMe}_2\text{Ph})(\text{O-}t\text{-Bu})(\text{OCMe}(\text{CF}_3)_2)$ (17) is obtained, according to equation 4.19.

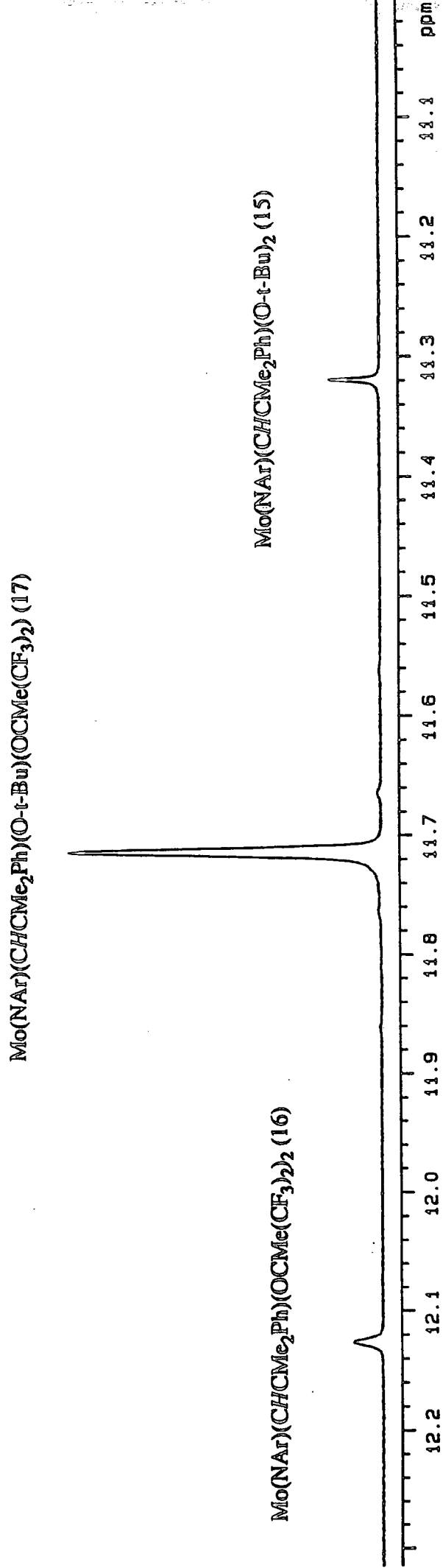


At room temperature, or even at -80°C , the reaction is virtually instantaneous, with the equilibrium lying heavily in favour of the mixed alkoxide species (17) ($K_{\text{eqm}} \approx 120$). This confirms that exchange of one electron ligands is much more facile than exchange of multiply bonded groups. The fact that the equilibrium favours the right hand side of equation 4.19 again reflects the preference for having electron donating and electron withdrawing ligands present on the same metal centre (see section 4.4.7).

The mixed alkoxide species (17) can be isolated as orange crystals in 61% yield by selective crystallization at -78°C from a saturated pentane solution containing the equilibrium mixture of all three species. Elemental analysis is consistent with the formulation $\text{MoNO}_2\text{C}_{30}\text{H}_{41}\text{F}_6$, and the mass spectrum shows a peak (^{98}Mo) at $m/z = 660$, corresponding to the molecular ion. At room temperature, the ^1H NMR spectrum (C_6D_6) of (17) shows the same equilibrium mixture of all three catalyst species observed previously for the NMR scale exchange reaction (figure 4.9). An increased pulse delay of 3 seconds is required in order to observe (15) and (16) in the expected 1:1 ratio. A "normal" pulse delay of 0.00 seconds reveals alkylidene proton resonances for (15), (16) and (17) in the ratio 5 : 10 : 85. This is attributed to differing spin lattice (T_1) relaxation times for the alkylidene proton in each of these complexes, possibly reflecting the relative strengths of the agostic interaction.

The 400 MHz ^1H NMR spectrum of (17) shows a singlet resonance at δ 11.71 for the alkylidene α proton, and septet and doublet resonances at δ 3.77 and 1.22 for the isopropyl methine and methyl resonances of the 2,6-di-isopropylphenylimido group. The diastereotopic methyl groups of the neophylidene ligand occur at δ 1.62 and 1.58, whilst a singlet resonance at δ 1.18 is observed for the t-butoxide ligand methyl

Figure 4.9 Room temperature equilibrium mix (C_6D_6) of (15), (16) and (17)



protons. The methyl protons of the hexafluoro-*t*-butoxide ligand could not be assigned unambiguously, presumably due to overlap with other signals. In the 100 MHz ^{13}C NMR spectrum, the alkylidene α carbon occurs at δ 274.02. It is interesting to note that the alkylidene proton resonance and the arylimido methine septet resonance of the mixed alkoxide species (17) occur almost exactly half way between those observed for the bis *t*-butoxide (15) and bis hexafluoro-*t*-butoxide (16) complexes. This is consistent with the intermediate electron density on the metal centre for (17), possessing both an electron withdrawing and an electron donating alkoxide ligand.

By altering the relative ratios of (15) to (16) on an NMR scale, the equilibrium position can be altered, so that only two of the initiator species are present in solution (i.e. by adding excess bis hexafluoro-*t*-butoxide initiator, all the bis *t*-butoxide initiator is removed, thus leaving only the mixed alkoxide and bis hexafluoro-*t*-butoxide species present). A vice-versa effect is seen upon adding excess bis *t*-butoxide initiator. This is shown in figure 4.10.

This observation has subsequently been exploited by Mr E.L. Marshall in this laboratory to alter the *cis/trans* content of poly 2,3 bis(trifluoromethyl)norborene, by varying the relative ratios of initiating species present in the reaction mixture³⁶.

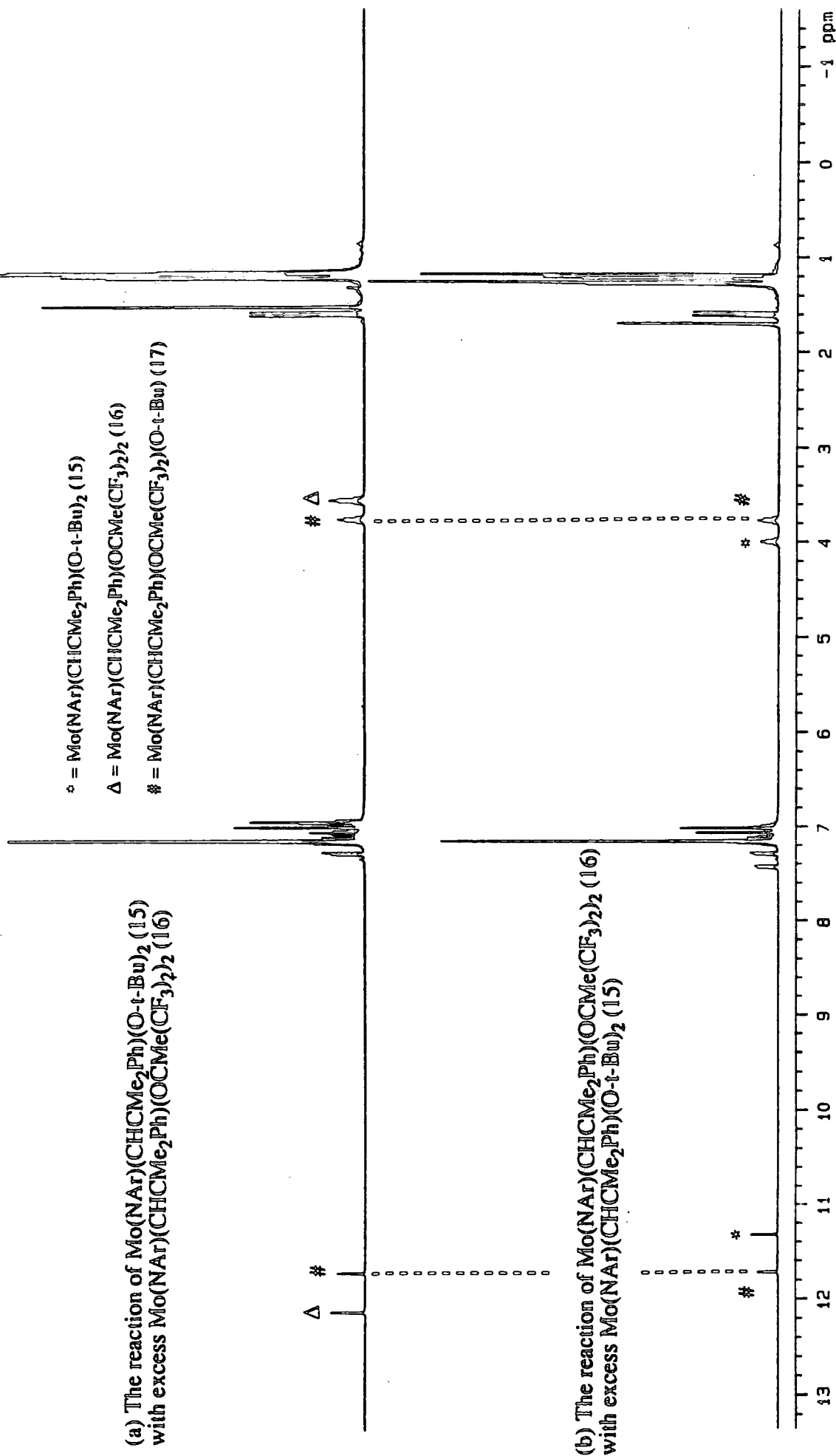
4.6 Relative Solution State Stabilities of Alkylidene Complexes.

To gain a further insight into the stability and decomposition modes of alkylidene complexes, the thermal stability and reactivity toward dioxygen of the three alkylidene complexes (15), (16) and (17) was investigated by ^1H NMR spectroscopy.

4.6.1 Thermal Stability.

$\text{Mo}(\text{NAr})(\text{CHCMe}_2\text{Ph})(\text{O-}t\text{-Bu})_2$ (15) was mixed with an excess of $\text{Mo}(\text{NAr})(\text{CHCMe}_2\text{Ph})(\text{OCMe}(\text{CF}_3)_2)_2$ (16) in C_6D_6 in a sealed NMR tube. Immediately after unfreezing, resonances due to the mixed alkoxide complex (17) and

Figure 4.10 ^1H NMR spectra (C_6D_6) for the reaction of (15) with (16).



Mo(NAr)(CH-t-Bu)(O-t-Bu) ₂ (11.25 ppm)	Mo(NAr)(CHCMe ₂ Ph)(O-t-Bu) ₂ (11.34 ppm)
Mo(NAr)(CH-t-Bu)(O-t-Bu)(OCMe(CF ₃) ₂) (11.64 ppm)	Mo(NAr)(CHCMe ₂ Ph)(O-t-Bu)(OCMe(CF ₃) ₂) (11.71 ppm)
Mo(NAr)(CH-t-Bu)(OCMe(CF ₃) ₂) ₂ (12.06 ppm)	Mo(NAr)(CHCMe ₂ Ph)(OCMe(CF ₃) ₂) ₂ (12.12 ppm)

Figure 4.11 *¹H NMR alkylidene proton resonances (C₆D₆) for the six possible alkoxide exchange species.*

Upon prolonged heating at 60°C decomposition occurred, with the more fluorinated derivatives again being the most stable. However, for each pair of alkoxide resonances, the neopentylidene resonance was observed to decompose faster than its corresponding neophylidene analogue, indicating that neophylidene complexes may be marginally more thermally stable than neopentylidene complexes.

4.6.2 Stability Towards Dioxygen.

To test the relative stabilities of the three alkylidene complexes (15), (16) and (17) towards dioxygen, experiments were performed on analogous reaction mixtures to those described in section 4.6.1, except that the NMR tube was sealed under one atmosphere of dry dioxygen and left at room temperature. The relative rates at which the alkylidene proton resonances disappeared, and formation of the corresponding oxo-imido complexes were then monitored by ¹H NMR spectroscopy. Again, it was found that the bis hexafluoro-t-butoxide analogue reacted less readily with dioxygen than did the mixed alkoxide complex, which in turn reacted less readily than the bis t-butoxide

analogue. It was also observed that the formation of *t*-BuCHO (from the neopentylidene complexes) was marginally faster than the formation of PhCMe₂CHO (from the neophylidene complexes). These observations agree with those in the previous section, showing the bis *t*-butoxide derivatives to be less stable than their fluorinated counterparts. A mechanism for the reaction of alkylidene complexes with dioxygen is discussed further in section 4.7.6.

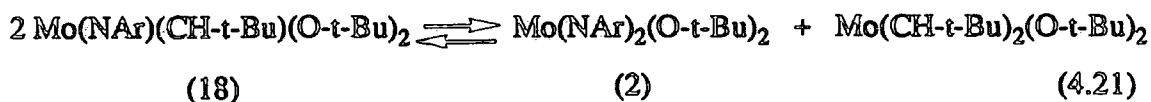
4.7 Heteroatom Exchange in Four Coordinate Alkylidene Complexes.

The previous work in this chapter has clearly shown that for relatively unhindered multiply bonded units, exchange between metal centres can be quite facile. For alkylidene complexes, this type of reactivity has important consequences, since the success of such initiators in living ROMP relies upon the absence of any such chain terminating steps.

Exchange of the one electron alkoxide ligands in Mo(NAr)(CHR)(OR')₂ compounds, and the relative stabilities of these alkylidene complexes have been addressed. It was of therefore of considerable interest to establish under what conditions exchange of the multiply bonded ligands might occur.

4.7.1 Thermal Stability of Mo(NAr)(CH-*t*-Bu)(O-*t*-Bu)₂ (18).

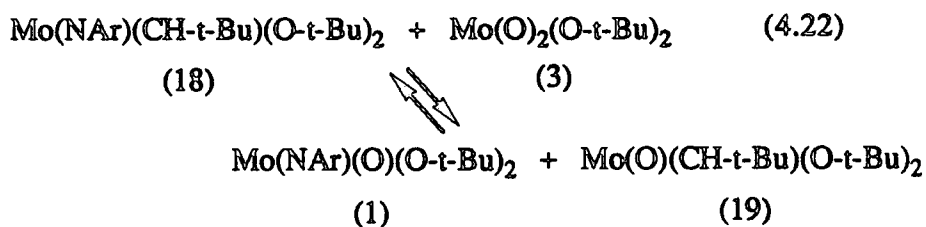
Upon heating a C₆D₆ solution (0.03M) of Mo(NAr)(CH-*t*-Bu)(O-*t*-Bu)₂ (18) to 60°C for 21 days, resonances in the ¹H NMR spectrum attributable to Mo(NAr)₂(O-*t*-Bu)₂ (2) and *t*-Bu-CH=CH-*t*-Bu can be observed. These products are thought to arise by imido/alkylidene exchange resulting in the bis imido complex (2) (observed) and initially the bis alkylidene complex (not observed) which subsequently undergoes reductive coupling of the alkylidene units (equation 4.21).



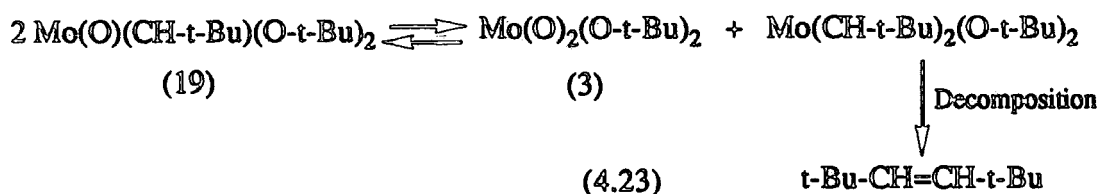
This observation demonstrates that it is indeed possible to induce alkylidene and imido group migration in these compounds, and gives an insight into the mode of decomposition of highly reactive transition metal alkylidene complexes.

4.7.2 Reaction of $\text{Mo}(\text{NAr})(\text{CH-t-Bu})(\text{O-t-Bu})_2$ (18) with $\text{Mo}(\text{O})_2(\text{O-t-Bu})_2$ (3).

Treatment of (18) with an equimolar amount of (3) in C_6D_6 would be expected to afford the oxo-imido species $\text{Mo}(\text{NAr})(\text{O})(\text{O-t-Bu})_2$ (1) and the oxo-alkylidene complex $\text{Mo}(\text{O})(\text{CH-t-Bu})(\text{O-t-Bu})_2$ (19), according to equation 4.22.



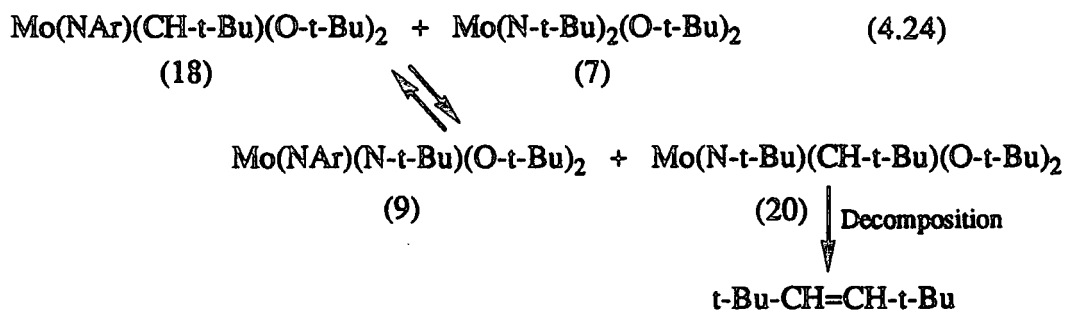
After 12 hours at room temperature, resonances in the ^1H NMR spectrum corresponding to the oxo-imido species (1) are observed. However, no oxo-alkylidene species is evident. Rather, *trans*-2,2,5,5-tetramethylhex-3-ene (t-Bu-CH=CH-t-Bu) is again observed as a sharp singlet at δ 5.46. This product must arise by coupling of the alkylidene groups facilitated by ready exchange of oxo and alkylidene units in the relatively unhindered oxo-alkylidene complex (19) (equation 4.23).



Again, the bis alkylidene species is not observed, further suggesting that decomposition of this product to the olefin, with contaminant reduction of the metal, is facile at room temperature.

4.7.3 Reaction of $\text{Mo(NAr)(CH-t-Bu)(O-t-Bu)}_2$ (18) with $\text{Mo(N-t-Bu)}_2\text{(O-t-Bu)}_2$ (7).

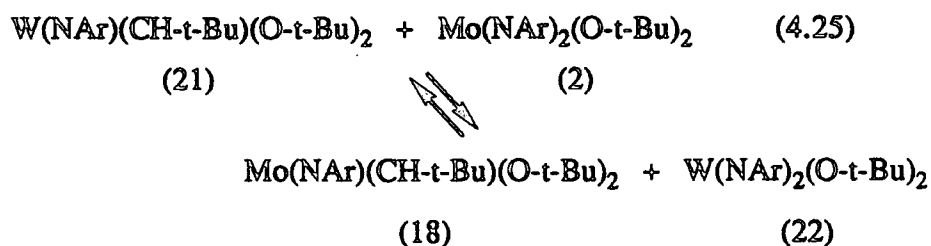
After seven hours at room temperature, ^1H NMR spectroscopic analysis of an equimolar mixture of (18) and (7) revealed resonances due to the mixed imido species $\text{Mo(NAr)(N-t-Bu)(O-t-Bu)}_2$ (9), but no new alkylidene resonance attributable to the *t*-butylimido alkylidene complex (20) was observed. Rather, prolonged heating at 60°C led only to *trans*-2,2,5,5-tetramethylhex-3-ene and residual (9). The formation of the olefin is again rationalized by alkylidene coupling in the *in-situ* formed complex $\text{Mo(N-t-Bu)(CH-t-Bu)(O-t-Bu)}_2$ (20), as shown in equation 4.24.



This result is also consistent with Osborn's observation that *t*-butylimido alkylidene complexes are isolable only when they possess highly electron withdrawing alkoxides e.g. hexafluoro-isopropoxide $\text{Mo(N-t-Bu)(CH-t-Bu)(OCH(CF}_3)_2)_2$ ³⁷.

4.7.4 Reaction of $W(NAr)(CH-t-Bu)(O-t-Bu)_2$ (21)
with $Mo(NAr)_2(O-t-Bu)_2$ (2).

The exchange of imido and alkylidene units between tungsten and molybdenum, to give a stable alkylidene product, can be achieved according to equation 4.25. The reaction is reasonably slow, taking approximately one week at 60°C for a significant amount of the molybdenum alkylidene complex (18) to be observed in the 1H NMR spectrum.



No olefinic resonance is observed, as the newly formed molybdenum alkylidene complex (17) is sufficiently sterically protected to be stable. This gives an indication that this is the *minimum* steric protection required around the metal centre in order to prevent decomposition of the *in situ* formed alkylidene complex via reductive coupling of the alkylidene units.

4.7.5 Reaction of $Mo(NAr)(CHCMe_2Ph)(OCMe(CF_3)_2)_2$ (16)
with $t-BuNH_2$.

The reaction depicted in equation 4.13 demonstrated that amines could be used to exchange imido groups at metal centres. It was therefore envisaged that the reaction of $Mo(NAr)(CHCMe_2Ph)(OCMe(CF_3)_2)_2$ (16) with *t*-butylamine may proceed according to equation 4.26. It was hoped that the electron withdrawing alkoxides would stabilize

The alkylidene J_{CH} coupling constant could not be obtained for the *syn* rotamer of this complex, due to its relatively rapid conversion to the corresponding *anti* isomer.

Studies by Schrock and coworkers on related five coordinate complexes of this type²⁰ indicate that a substantially lower coupling constant of approximately 110 Hz would be expected for the *syn* rotamer (c.f. PMe_3 adduct of (16); *syn* $J_{CH} = 110$ Hz, *anti* $J_{CH} = 138$ Hz). The difference in values for J_{CH} in five coordinate complexes can be viewed as resulting from interaction of the alkylidene C-H_α bond with the metal centre. The orbital on the molybdenum available for C-H_α activation is oriented away from the imido ligand, a circumstance that leads to a stronger M-C-H_α interaction in the *syn* rotamer and hence a lower J_{CH} coupling constant.

The interconversion of the two rotamers can be followed by ^1H NMR spectroscopy, monitoring the relative percentages of the two alkylidene proton resonances. Figure 4.12 shows the interconversion of (24) to (25) as a function of time at 30°C .

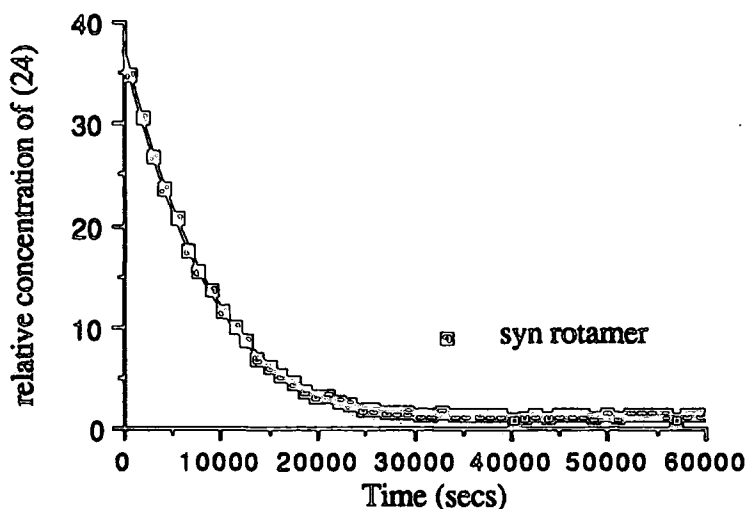
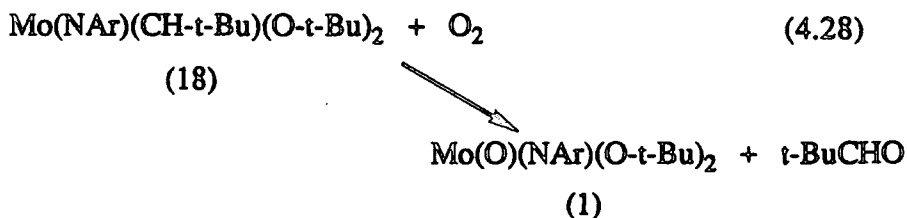


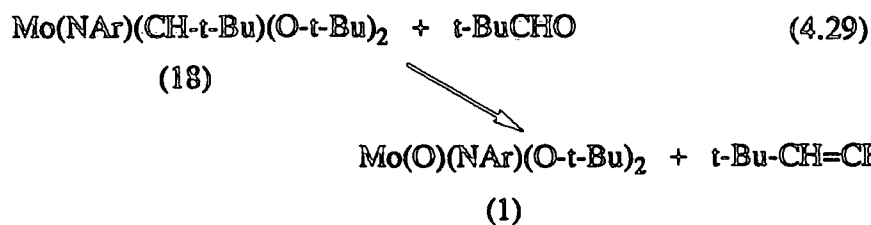
Figure 4.12 *Relative Concentration of syn rotamer (24) as a function of time at 30°C .*

As can be seen, equilibrium is attained after approximately 8 hours at 30°C. This is substantially faster than the rate observed for *syn* / *anti* conversion of the PMe_3 adduct $\text{Mo}(\text{NAr})(\text{CHCMe}_3)(\text{OCMe}(\text{CF}_3)_2)_2(\text{PMe}_3)^{38}$. It has also been shown that the rate of conversion is increased in the presence of added base free initiator, indicating that an intramolecular process is unlikely and the base must presumably dissociate before rotation of the metal-carbon double bond occurs³⁸. The slower rate of conversion for the trimethylphosphine adduct must be a consequence of the fact that this is a stronger base than *t*-butylamine and is therefore more strongly bound to the metal centre. Indeed, the ^1H NMR resonances for the *t*-butyl adducts are slightly broadened at room temperature, indicating that exchange of bound amine for free amine occurs at a rate comparable to the NMR time scale.

4.7.6 Reaction of $\text{Mo}(\text{NAr})(\text{CHR})(\text{OR}')_2$ with Dioxygen.

$\text{Mo}(\text{NAr})(\text{CH-}t\text{-Bu})(\text{O-}t\text{-Bu})_2$ (18) was treated with dry dioxygen (1 atmosphere) in C_6D_6 in a sealed NMR tube, and the reaction monitored by ^1H NMR spectroscopy. After 40 minutes at room temperature, resonances could be observed due to the oxoimido species (1) and pivaldehyde (equation 4.28), which was subsequently observed to react with remaining initiator to generate *trans*-2,2,5,5-tetramethylhex-3-ene. (equation 4.29).





The reaction of dioxygen with transition metal alkylidene complexes is likely to proceed via a radical mechanism, as depicted in figure 4.13.

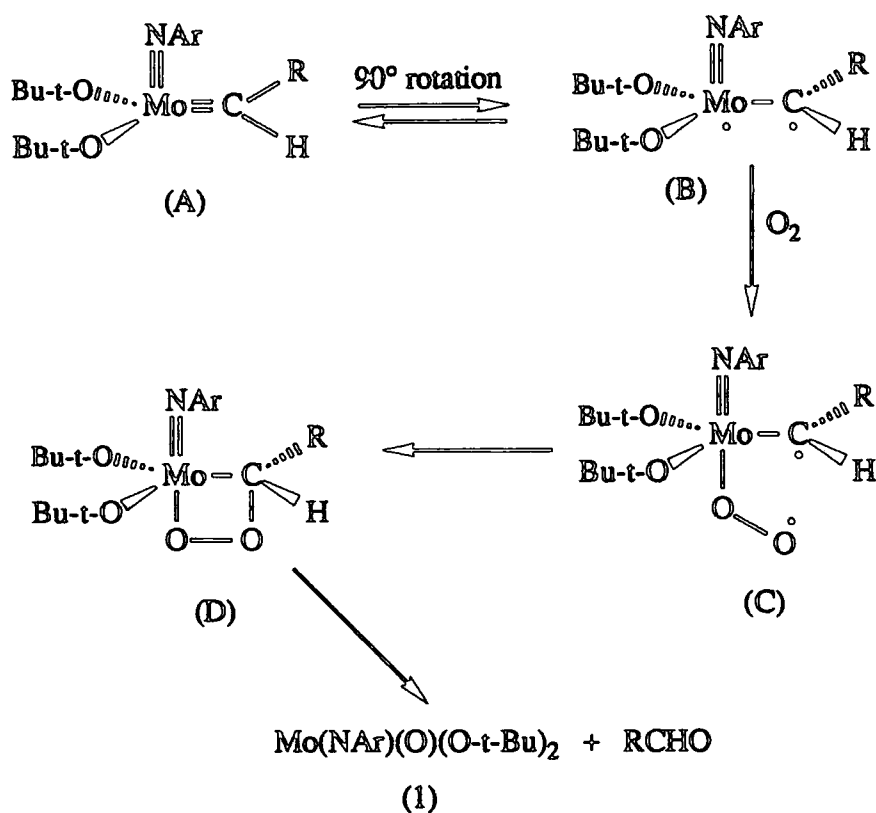


Figure 4.13 *A Postulated Mechanism for the reaction of $\text{Mo(NAr)(CHR)(O-t-Bu)}_2$ with dioxygen.*

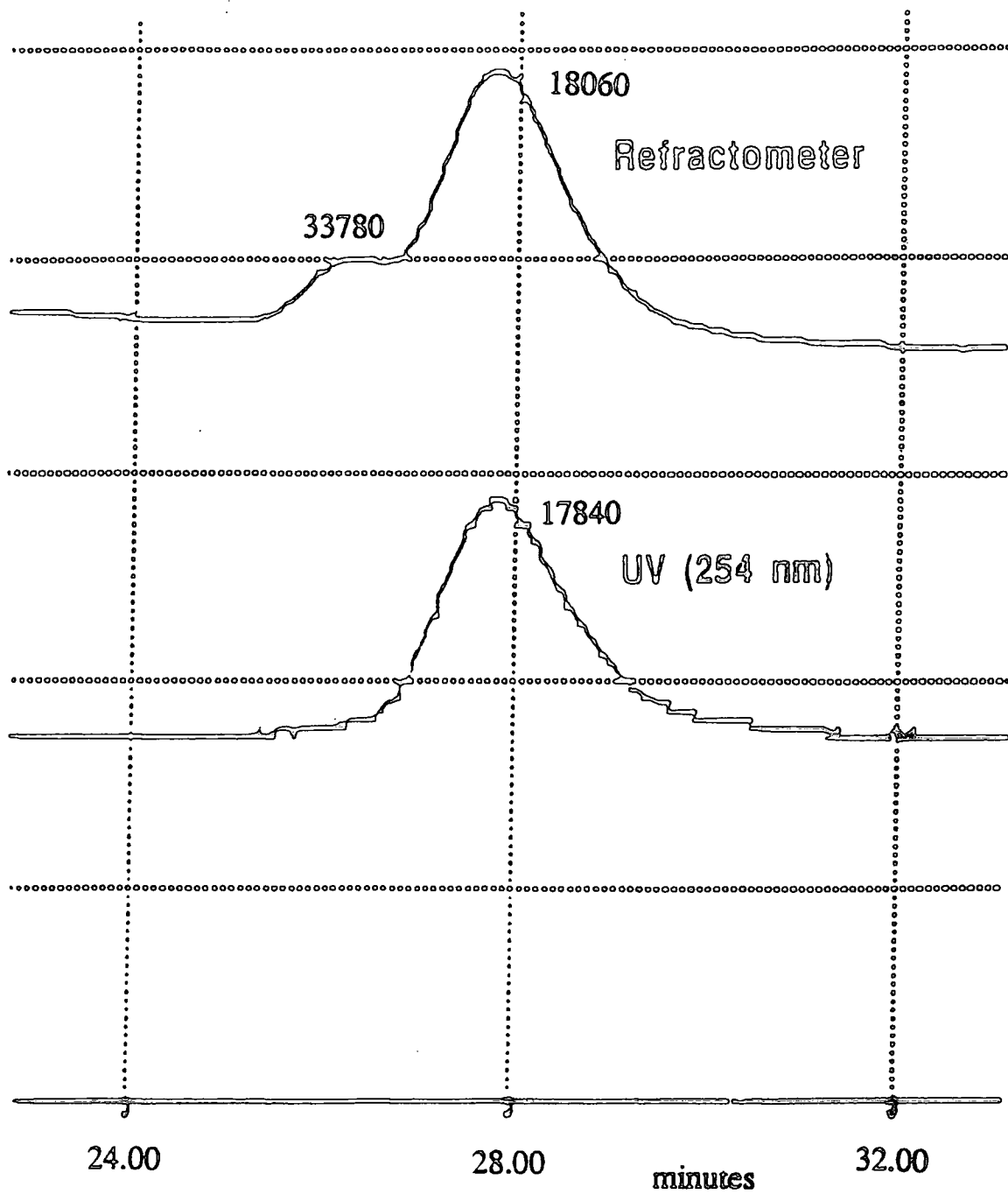
In the initiator (A), the molybdenum, imido nitrogen and α and β carbon atoms of the alkylidene ligand lie in the same plane. The principal metal d-orbital that interacts with the α carbon atom is perpendicular to this plane (δ in relation to the imido nitrogen atom). However, if the alkylidene ligand rotates by 90° (mid-way between the *syn* and

anti forms) the formal metal-carbon double bond is broken, and the alkylidene ligand is likely to possess a significant degree of triplet character, with one electron of the electron pair more localized on each of the metal and α carbon atoms (B). This formally Mo (V) complex would be expected to react very rapidly with the dioxygen, which also has triplet character. Interaction with the metal will most probably occur first (C), followed by interaction of the second oxygen atom with the α carbon atom to form the Mo-O-O-C metallacycle (D). This can then ring open to give the expected oxo-imido and aldehydic products.

In a related experiment, $\text{Mo}(\text{NAr})(\text{CHCMe}_2\text{Ph})(\text{OCMe}(\text{CF}_3)_2)_2$ (16) was sealed in an NMR tube (C_6D_6) under one atmosphere of dry dioxygen. The reaction to form the oxo-imido species $\text{Mo}(\text{NAr})(\text{O})(\text{OCMe}(\text{CF}_3)_2)_2$ (4) is much slower, with traces of initiator still observable in the ^1H NMR spectrum after 24 hours at room temperature. This is consistent with the above postulated mechanism, as the increased electron withdrawing ability of the hexafluoro-*t*-butoxide ligands enhances the electrophilicity of the metal centre and strengthens the metal ligand multiple bonds. This increases the barrier to rotation of the alkylidene ligand and therefore is also likely to decrease accessibility to the more reactive triplet state.

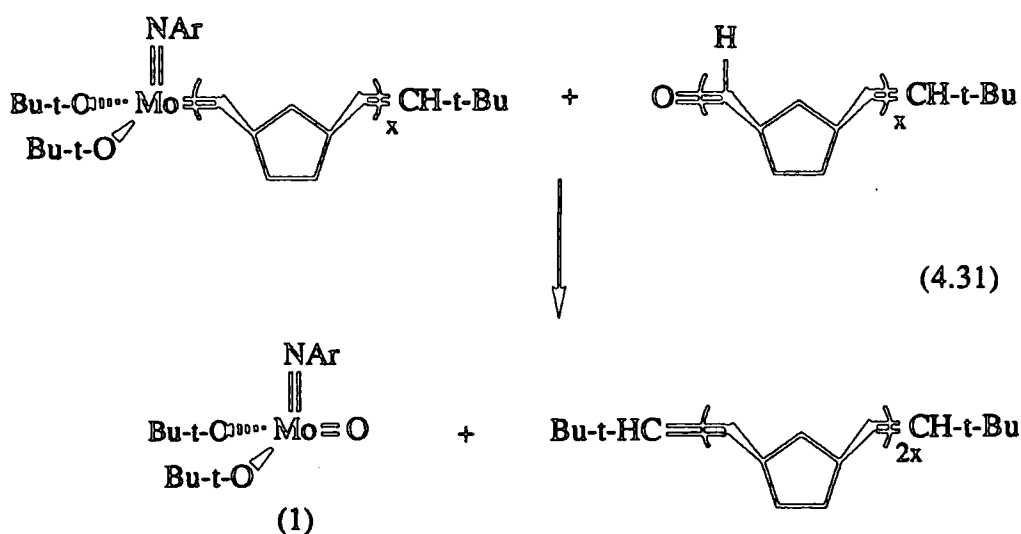
The reaction between dioxygen and a living oligomer of norbornene (formed by the reaction of (18) with 10 equivalents of norbornene in C_6D_6) occurs much more readily. The oxo-imido species (1) is formed within minutes after unfreezing the NMR sample (equation 4.30), with a singlet resonance at δ 9.28 being attributable to the aldehydic proton on the polymer chain end.

Figure 4.14 Gel Permeation Chromatograph of poly(5-trifluoromethyl)norbornene



minor peak is only observed in the refractometer trace, indicating that the UV-active phenyl end-group, arising from the capping reaction with benzaldehyde, is not present in the high molecular weight impurity. This observation, and the fact that both peaks still have narrow molecular weight distributions, suggests that the double molecular weight impurity is formed after the polymerization is complete, by dimerization of living polymer chains possessing a non UV-active t-butyl end-group.

An explanation can be provided for this phenomenon based on a bimolecular termination induced by trace amounts of dioxygen present⁴⁴. Previous work in this chapter has shown that dioxygen reacts with the initiator and with living oligomers to generate the metal oxo-imido species (1) and pivaldehyde or an aldehydic end-capped polymer respectively. However, this end-capped polymer can subsequently react with a living oligomer to regenerate the metal oxo-imido species (1) and a bimolecular terminated polymer of twice the expected molecular weight (equation 4.31).



The rate of reaction of oxygen with living oligomers is slower than the rate of propagation of the monomer, although much faster than the rate of reaction with the initiator. This difference in rates allows all the monomer to be polymerized before termination via reaction with oxygen occurs, thus giving impurity of twice the expected molecular weight and not a general molecular weight distribution broadening.

The reaction of living oligomers with the metal oxo-imido species can be ruled out as an explanation for the high molecular weight material produced, as it is found that the amount of this impurity can be reduced or eliminated by careful exclusion of oxygen from the reaction mixture.

4.9 Summary.

This chapter has shown that exchange of multiply bonded dianionic ligands between metal centres can occur and such processes may be more facile than previously considered. Mono-anionic ligands exchange much more rapidly, and advantage can be taken of this to prepare modified ROMP catalysts.

The bis imido complex $\text{Mo}(\text{NAr})_2(\text{O-t-Bu})_2$ (2) similarly undergoes exchange of imido ligands with a range of external substrates including benzaldehyde, t-butylamine and dioxygen. A relatively stable novel bis-metallacycle is formed with phenyl isocyanate.

The thermal stability, and exchange reactivity of alkylidene complexes (particularly with dioxygen) is very important for assessing the stability of such initiators under polymerization conditions, and such studies have helped to identify bimolecular decomposition pathways responsible for the high molecular weight impurities sometimes observed in polymer samples prepared by living ROMP.

4.10 References.

1. W.A. Nugent, J.M. Mayer, "*Metal Ligand Multiple Bonds*", Wiley Interscience, New York 1988.
2. G.W. Keulks, L.D. Grenze, T.M. Notermann, *Adv. Catal.* 1978, 27, 183.
3. P.C.H. Mitchell, F.J. Trifiro, *J. Chem. Soc. A.* 1970, 3183.
4. F.J. Trifiro, I. Pasquon, *J. Catal.* 1968, 12, 412.
5. R.K. Grasselli, *J. Chem. Educ.* 1986, 63, 216.
6. J.D. Burrington, R.K. Grasselli, *J. Catal.* 1979, 59, 79.
7. A. Anderson, *J. Catal.* 1986, 100, 414.
8. T. Otsuba, H. Miura, Y. Morikawa, T. Shirasaki, *J. Catal.* 1975, 36, 240.
9. R.R. Schrock, *Acc. Chem. Res.* 1990, 23, 158.
10. G.C. Bazan, R.R. Schrock, H.N. Cho, V.C. Gibson, *Macromolecules*, 1991, 24, 4495.
11. G.C. Bazan, R.R. Schrock, E. Khosravi, W.J. Feast, V.C. Gibson, M.B. O'Regan, J.K. Thomas, W.M. Davis, *J. Am. Chem. Soc.* 1990, 112, 8378.
12. This Thesis, Chapters 1-3.
13. R.R. Schrock, J.S. Murdzek, G.C. Bazan, J. Robbins, M. DiMare, M.B. O'Regan, *J. Am. Chem. Soc.* 1990, 112, 3875.
14. J.H. Wengrovius, R.R. Schrock, *Organometallics*, 1982, 1, 148.
15. S.F. Pederson, R.R. Schrock, *J. Am. Chem. Soc.* 1982, 104, 7438.
16. M.H. Chisholm, K. Folting, J.C. Huffman, A.L. Ratermann, *Inorg. Chem.* 1982, 21, 978.
17. Experimentally, less than four equivalents of arylazide is used, followed by fractional crystallization to remove any unreacted $\text{Mo}_2(\text{O-t-Bu})_6$.
18. M.H. Chisholm, K. Folting, J.C. Huffman, C.C. Kirkpatrick, *Inorg. Chem.* 1984, 23, 1021.

19. A.A. Frost, R.G. Pearson, "*Kinetics and Mechanism*", 2nd Ed. John Wiley and Sons, Ch. 8, 1961.
20. R.R. Schrock, W.E. Crowe, G.C. Bazan, M. DiMare, M.B. O'Regan, M.H. Schofield, *Organometallics*, 1991, 10, 1832.
21. J.L. Herrison, Y. Chauvin, *Makromol. Chem.* 1970, 141, 161.
22. M.Jolly, J.P. Mitchell, V.C. Gibson, Unpublished Results.
23. A. Shaw, Ph.D Thesis, University of Durham, 1989.
24. J.F. Ackerman, *Mater. Res. Bull.*, 1988, 23, 165.
25. M.L. Listemann, R.R. Schrock, J.C. Dewan, R.M. Kolodziej, *Inorg. Chem.* 1988, 27, 264
26. D.M. Berg, P.R. Sharp, *Inorg. Chem.* 1987, 26, 2959
27. (a) D.S. Glueck, J. Wu, F.J. Hollander, R.G. Bergman, *J. Am. Chem. Soc.* 1991, 113, 2041.
(b) R.I. Michelman, R.A. Anderson, R.G. Bergman, *J. Am. Chem. Soc.* 1991, 113, 5100.
(c) P.J. Walsh, F.J. Hollander, R.G. Bergman, *J. Am. Chem. Soc.* 1988, 110, 8729.
28. M. Jolly, V.C. Gibson, Unpublished Results.
29. G. Hogarth, P.C. Konidaris, *J. Organomet. Chem.* 1990, 399, 149.
30. P. Jernakoff, G.L. Geoffrey, A.L. Rheingold, S.J. Geib, *J. Chem. Soc. Chem. Comm.*, 1987, 1610.
31. R.S. Pilato, C.E. Housmekerides, P.Jernakoff, D. Rubin, G.L. Geoffroy, *Organometallics*, 1990, 9, 2333.
32. U. Kusthardt, W.A. Herrmann, M.L. Ziegler, T. Zahn, B. Nuber, *J. Organomet. Chem.* 1986, 311, 163.
33. G. Lamonica, S. Cenini, *Inorg. Chim. Acta.* 1978, 29, 183.
34. G. Lamonica, S. Cenini, *J. Chem. Soc. Dalton. Trans.* 1980, 1145.
35. M. DiMare, Research Report, Massachusetts Institute of Technoogy, 1989.
36. E.L. Marshall, V.C. Gibson, Unpublished Results.

37. G. Schoettel, J. Kress, J.A. Osborn, *J. Chem. Soc. Chem. Comm.* 1989, 1062.
38. G.C. Bazan, Ph.D Thesis, Massachusetts Institute of Technoogy, 1990.
39. J.S. Murdzek, R.R. Schrock, *Macromolecules*, 1987, 20, 2642.
40. R.R. Schrock, J. Feldman, L.F. Cannizzo, R.H. Grubbs, *Macromolecules*, 1987, 20, 1169.
41. W. Risse, R.H. Grubbs, *Macromolecules*, 1989, 22, 1558.
42. L.F. Cannizzo, R.H. Grubbs, *Macromolecules*, 1988, 21, 1961.
43. Polymerization Performed by Dr. E. Khosravi.
44. W.J. Feast, V.C. Gibson, E. Khosravi, E.L. Marshall, J.P. Mitchell, *Polymer Comm.* 1992, 33, 872.

CHAPTER FIVE

Synthesis and Heteroatom Exchange Reactivity
of Half-Sandwich Imido and Alkylidene Complexes
of Niobium and Tantalum.

5.1 Introduction.

The preceding chapter of this thesis has shown that the exchange of multiply bonded oxo, imido and alkylidene ligands between coordinatively unsaturated four coordinate molybdenum centres is a relatively facile process, and can offer a way of preparing compounds not generally accessible by other routes.

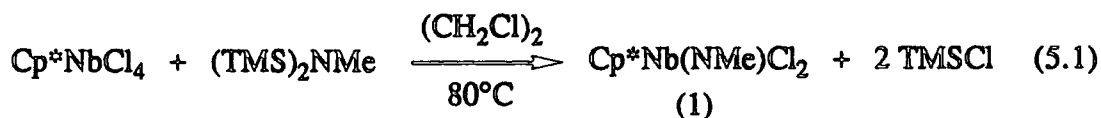
In an effort to further delineate this important type of reactivity, a complementary study of the exchange of imido and alkylidene ligands in half-sandwich group five complexes was undertaken.

A series of half-sandwich imido complexes of the type $\text{Cp}^*\text{Nb}(\text{NR})\text{Cl}_2$ ($\text{R} = \text{Me}$, $t\text{-Bu}$, $2,6\text{-iPr}_2\text{C}_6\text{H}_3$) have previously been prepared in this laboratory by Dr. D.N. Williams¹, via the treatment of Cp^*NbCl_4 with the appropriate silylated amine. However, to study heteroatom exchange reactivity in this type of system, a number of analogues possessing the pentamethylcyclopentadienyl ligand had first to be synthesized.

5.2 Reaction of Cp^*NbCl_4 with $(\text{TMS})_2\text{NMe}$.

Preparation of $\text{Cp}^\text{Nb}(\text{NMe})\text{Cl}_2$ (1).*

The reaction of Cp^*NbCl_4 with one molar equivalent of $(\text{TMS})_2\text{NMe}$ in 1,2-dichloroethane at 80°C for 20 hours affords a brown mixture from which $\text{Cp}^*\text{Nb}(\text{NMe})\text{Cl}_2$ (1) may be isolated as a dark orange solid in 49% yield upon removal of volatile components *in vacuo*. An analytically pure sample may be obtained as light orange crystals by recrystallization from pentane at -78°C . The reaction is envisaged to occur according to equation 5.1.

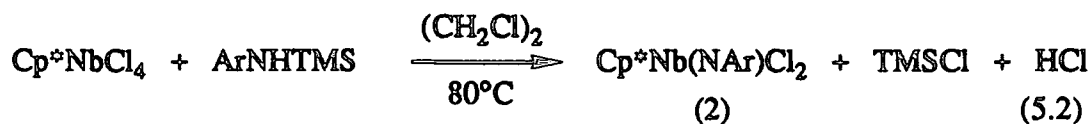


Compound (1) was first prepared by Dr. U. Siemeling and is moisture sensitive and soluble in aromatic and chlorocarbon solvents. The 250 MHz ^1H NMR spectrum (C_6D_6) reveals a singlet at δ 3.25, typical for group five methylimido protons^{2,3}, and a singlet at δ 1.77, attributable to the equivalent methyl protons of the pentamethylcyclopentadienyl ligand. In the ^{13}C NMR spectrum, the methylimido carbon resonance is located at δ 49.11, lying in the expected region for such species⁴. The infrared spectrum shows a band at 1258 cm^{-1} attributable to the terminal alkylimido ligand, while strong bands in the $300\text{--}450\text{ cm}^{-1}$ range are indicative of Nb-Cl stretches⁵. The mass spectrum gives an envelope due to the parent ion at $m/z = 327$ (^{35}Cl), whilst elemental analysis is consistent with the stoichiometry $\text{C}_{11}\text{H}_{18}\text{Cl}_2\text{NNb}$. The structure of (1) is assumed to be similar to that of the tantalum imido complex $\text{Cp}^*\text{Ta}(\text{NAr})\text{Cl}_2$ (3) discussed in section 5.4.2.

5.3 Reaction of Cp^*NbCl_4 with ArNHTMS .

Preparation of $\text{Cp}^\text{Nb}(\text{NAr})\text{Cl}_2$ (2).*

The reaction of Cp^*NbCl_4 with two equivalents of ArNHTMS in 1,2-dichloroethane at elevated temperature (equation 5.2) affords the red compound $\text{Cp}^*\text{Nb}(\text{NAr})\text{Cl}_2$ (2) which may be recrystallized from toluene at -78°C in 73% yield.



The second equivalent of silylated amine is necessary for neutralizing the HCl formed during the reaction (equation 5.3).

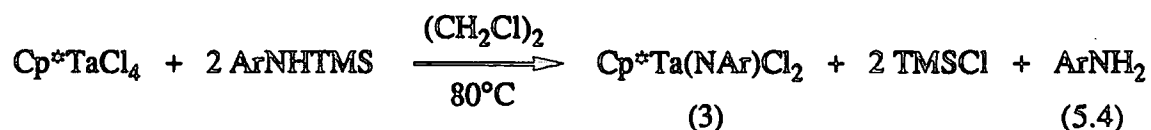


$\text{Cp}^*\text{Nb}(\text{NAr})\text{Cl}_2$ (2) was first prepared by Dr. U. Siemeling in this laboratory. The infrared spectrum reveals characteristic imido bands at 1285 cm^{-1} and 805 cm^{-1} . The 400 MHz ^1H NMR spectrum (C_6D_6) shows doublet and septet resonances at δ 1.29 and 3.52 due to the isopropyl methyl and methine protons respectively of the arylimido unit. A singlet resonance at δ 1.78 is observed for the methyl protons of the C_5Me_5 ligand, and the expected triplet and doublet resonances for the three aromatic protons are seen at δ 6.92 and δ 7.03. In the mass spectrum, an envelope at $m/z = 473$ (^{35}Cl) corresponds to the parent ion.

5.4.1 Reaction of Cp^*TaCl_4 with ArNHTMS .

Preparation of $\text{Cp}^\text{Ta}(\text{NAr})\text{Cl}_2$ (3).*

Cp^*TaCl_4 reacts with two equivalents of ArNHTMS over a period of 10 days at 80°C in 1,2-dichloroethane to give an orange solution from which $\text{Cp}^*\text{Ta}(\text{NAr})\text{Cl}_2$ (3) may be isolated as an orange solid (equation 5.4). Further purification can be achieved by recrystallization from toluene at -78°C , to give light orange crystals of (3) in 72% yield.

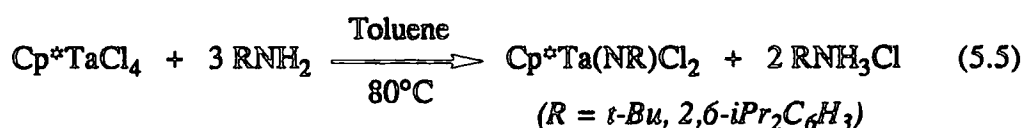


It should be noted that a much longer reaction time is required to obtain similar yields for this tantalum imido complex compared to the niobium analogue (2) described in the previous section.

Compound (3) is soluble in aromatic and chlorocarbon solvents, but has limited solubility in low polarity hydrocarbon solvents such as pentane. Elemental analysis confirms a stoichiometry of $\text{C}_{22}\text{H}_{32}\text{Cl}_2\text{NTa}$ whilst the infrared spectrum shows characteristic terminal imido absorptions at 1300 cm^{-1} and 805 cm^{-1} , close in frequency to the vibrations observed in the niobium analogue (2). The 400 MHz ^1H NMR

spectrum reveals doublet and septet resonances at δ 1.33 and 3.53 due to the isopropyl methyl and methine protons respectively of the arylimido ligand. The three aromatic protons occur as a doublet and triplet at δ 7.16 and 6.87, whilst the methyl protons of the pentamethylcyclopentadienyl ligand occur as a singlet at δ 1.86. A parent ion is observed in the mass spectrum at $m/z = 561$.

Compound (3) can also be prepared in much lower yield (10%) via the reaction of Cp^*TaCl_4 with three equivalents of arylamine in toluene at elevated temperature (equation 5.5). The corresponding *t*-butylimido analogue $\text{Cp}^*\text{Ta}(\text{N-}t\text{-Bu})\text{Cl}_2$ (4) (characterized by elemental analysis and ^1H NMR spectroscopy) can also be prepared by this route (^1H NMR (C_6D_6 , 250 MHz) δ 1.23 (NCMe_3), δ 1.94 (C_5Me_5)). This method has recently been used successfully by Herrmann in the synthesis of rhenium imido complexes of the type $\text{Cp}^*\text{Re}(\text{NR})\text{Cl}_2$ ($\text{R} = \text{Me}, t\text{-Bu}$)³.



Some derivative chemistry of (3) and (4) is discussed briefly in appendix three.

5.4.2 The Molecular Structure of $\text{Cp}^*\text{Ta}(\text{NAr})\text{Cl}_2$ (3).

Having successfully synthesized the half-sandwich tantalum imido complex (3), we were interested to establish whether the general structural features of this species were similar to those observed for related cyclopentadienyl niobium analogues, whose structures had been previously determined^{2,6}.

Orange crystals of (3) were obtained by cooling a saturated pentane solution to -20°C overnight. A crystal of dimensions 0.20 x 0.38 x 0.56 mm was chosen for a crystallographic study and mounted in a Lindemann capillary tube under an inert atmosphere. The data were collected and the structure solved by Dr. W. Clegg and D.C.R. Hockless at the University of Newcastle-upon-Tyne (appendix 1). The

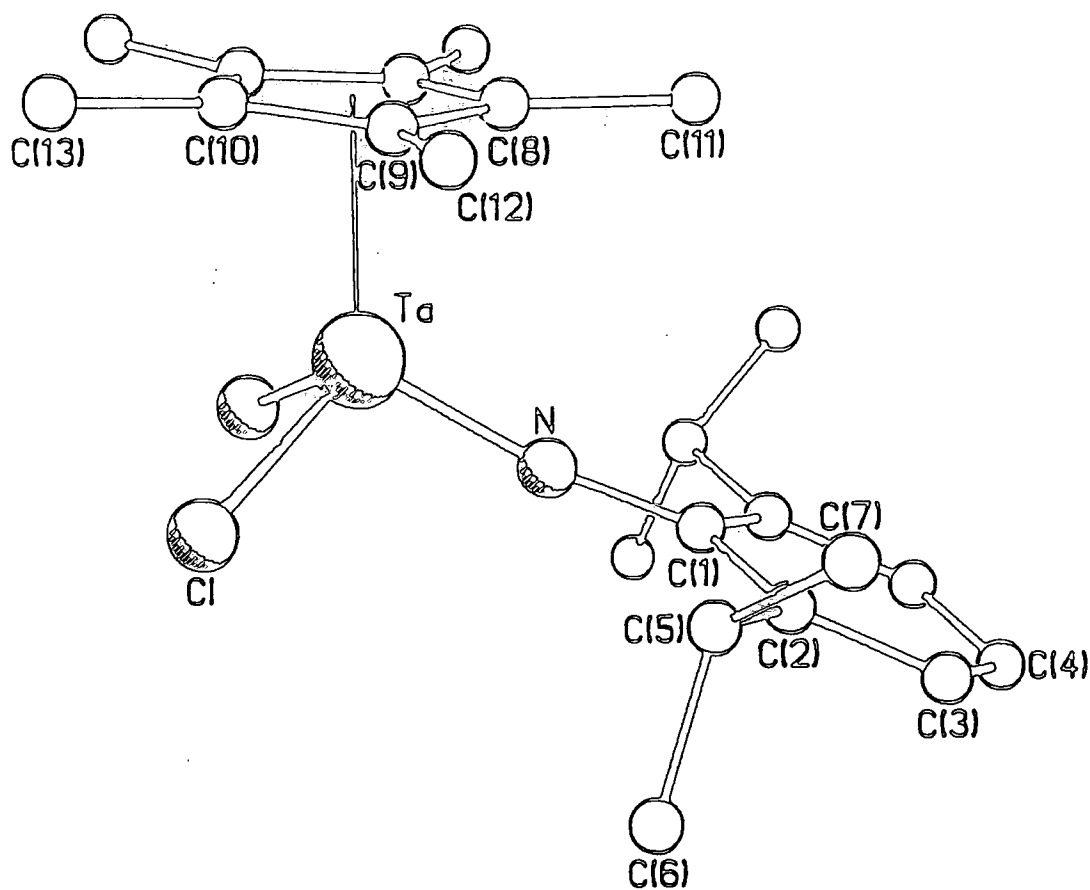
molecular structure of (3) is illustrated in figures 5.1(a) and 5.1(b) and selected bond angles and distances given in table 5.1.

The molecule is best described as possessing a three-legged piano stool geometry. The metal-nitrogen bond length (1.780 (5) Å) is within the expected range for niobium and tantalum nitrogen triple bonds⁷⁻⁹, arising from donation of the nitrogen lone pair of electrons to the tantalum metal centre. The imido unit is quasi-linear, the Ta-N-C_{ipso} angle being 171.4 (5)°, again typical of a terminal imido ligand possessing sp-hybridized nitrogen⁴. The deviation from linearity (8.6°) arises from a bending of the 2,6-di-isopropylphenylimido substituent towards the pentamethylcyclopentadienyl ring. Similar deviations are observed in the structures of CpNb(NMe)Cl₂ ((5), 16.6°)^{1,6,10}, CpNb(N-t-Bu)Cl₂ ((6), 10.0° and 7.5° for the two independent molecules)^{1,6} and CpNb(NAr)Cl₂ ((7), 14.4°)^{1,6}. This suggests that the interaction of the nitrogen lone pair containing p-orbital is with a lobe of a vacant metal orbital projecting *trans* to the pentamethylcyclopentadienyl ring. Comparing the above deviations, we see that the increased steric congestion around the metal centre provided by the C₅Me₅ ligand in (3) and the t-butyl substituent in CpNb(N-t-Bu)Cl₂ (6) appears to favour a more linear M-N-C arrangement.

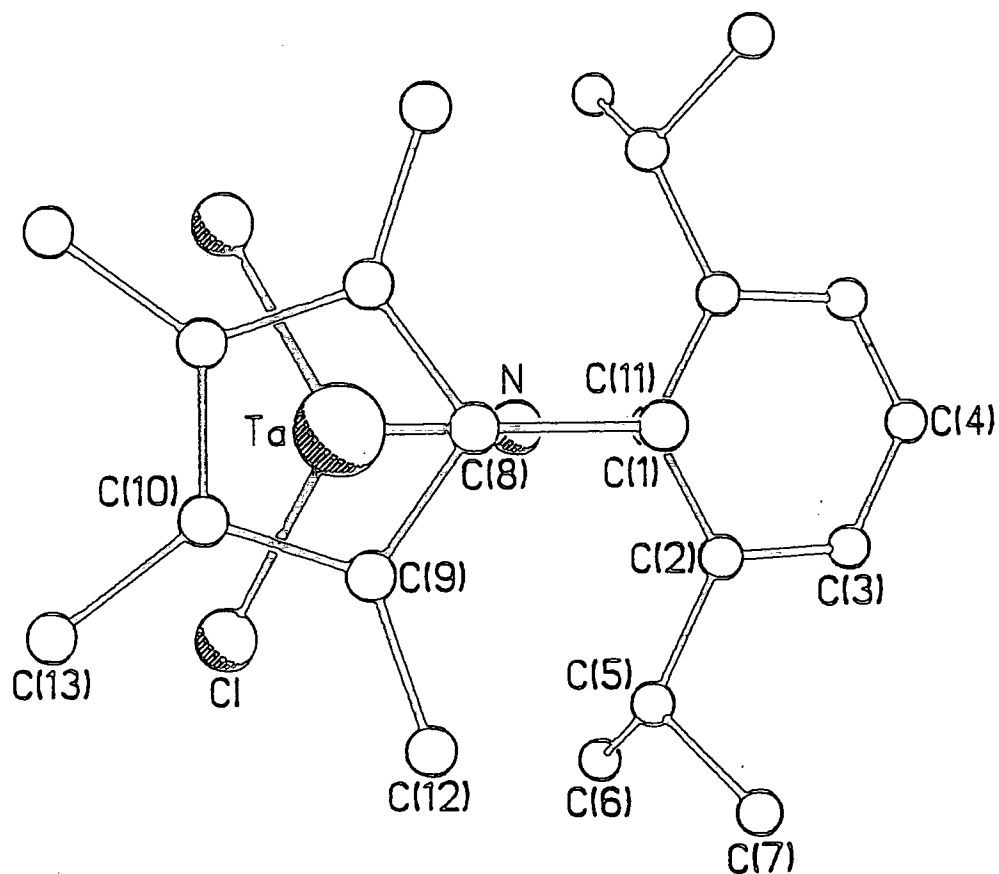
Compound (3) is therefore analogous to the previously studied niobium imido analogues, and can be considered as a sixteen electron complex containing a "linear" terminal imido ligand which may be regarded as a four electron (neutral) or six electron (dianionic) donor ligand.

The pentamethylcyclopentadienyl moiety is not coordinated in an ideal η^5 fashion; instead, a trend towards η^3 / η^2 coordination (allyl-ene) is observed, leading to three short and two long Ta-Cp* ring carbon distances. The maximum deviation of the Ta-Cp* ring distance is 0.134 Å, whilst the maximum deviation of inter-ring carbon distances is 0.023 Å. The distance between the Cp* ring centroid and the point where the Ta-Cp* ring normal meets the best plane for the Cp* ring (giving an indication of the ring slippage) is 0.165 Å; the largest value for the structurally characterized complexes of this type. This allyl-alkene type structure is similar to that found in

Figure 5.1 The molecular structure of $Cp^*Ta(NAr)Cl_2$ (3)



(a) View showing the atom labelling (H atoms omitted for clarity)



(b) View along the ring centroid-Ta vector

Ta - Cl	2.345 (2)	Ta - N	1.780 (5)
Ta - C(8)	2.366 (8)	Ta - C(9)	2.396 (5)
Ta - C(10)	2.500 (6)	N - C(1)	1.380 (8)
C(1) - C(2)	1.412 (6)	C(2) - C(3)	1.392 (8)
C(2) - C(5)	1.516 (8)	C(3) - C(4)	1.363 (8)
C(5) - C(6)	1.529 (14)	C(5) - C(7)	1.520 (13)
C(8) - C(9)	1.424 (8)	C(8) - C(11)	1.529 (14)
C(9) - C(10)	1.425 (9)	C(9) - C(12)	1.488 (9)
C(10) - C(13)	1.506 (11)	C(10) - C(10')	1.402 (14)
Cl - Ta - N	102.2 (1)	Cl - Ta - C(8)	124.2 (1)
N - Ta - C(8)	90.8 (3)	Cl - Ta - C(9)	90.5 (1)
N - Ta - C(9)	108.2 (2)	C(8) - Ta - C(9)	34.8 (2)
Cl - Ta - C(10)	85.5 (2)	N - Ta - C(10)	141.9 (2)
C(8) - Ta - C(10)	55.8 (2)	C(9) - Ta - C(10)	33.8 (2)
Cl - Ta - Cl'	105.8 (1)	C(9) - Ta - Cl'	141.5 (1)
C(10) - Ta - Cl'	111.6 (2)	C(9) - Ta - C(9')	58.0 (3)
C(10) - Ta - C(9')	56.0 (2)	C(10) - Ta - C(10')	32.6 (3)
Ta - N - C(1)	171.4 (5)	N - C(1) - C(2)	120.0 (3)
C(2) - C(1) - C(2')	120.0 (6)	C(1) - C(2) - C(3)	118.2 (5)
C(1) - C(2) - C(5)	121.1 (5)	C(3) - C(2) - C(5)	120.7 (5)
C(2) - C(3) - C(4)	121.8 (6)	C(3) - C(4) - C(3')	119.9 (8)
C(2) - C(5) - C(6)	110.0 (6)	C(2) - C(5) - C(7)	112.1 (6)
C(6) - C(5) - C(7)	111.1 (7)	Ta - C(8) - C(9)	73.8 (4)
Ta - C(8) - C(11)	121.1 (5)	C(9) - C(8) - C(11)	125.3 (4)
C(9) - C(8) - C(9')	109.3 (8)	Ta - C(9) - C(8)	71.5 (4)
Ta - C(9) - C(10)	77.1 (3)	C(8) - C(9) - C(10)	106.4 (5)
Ta - C(9) - C(12)	121.5 (4)	C(8) - C(9) - C(12)	126.4 (7)
C(10) - C(9) - C(12)	127.0 (6)	Ta - C(10) - C(9)	69.1 (3)
Ta - C(10) - C(13)	125.0 (5)	C(9) - C(10) - C(13)	124.6 (6)
Ta - C(10) - C(10')	73.7 (2)	C(9) - C(10) - C(10')	108.8 (4)
C(13) - C(10) - C(10')	126.6 (4)		

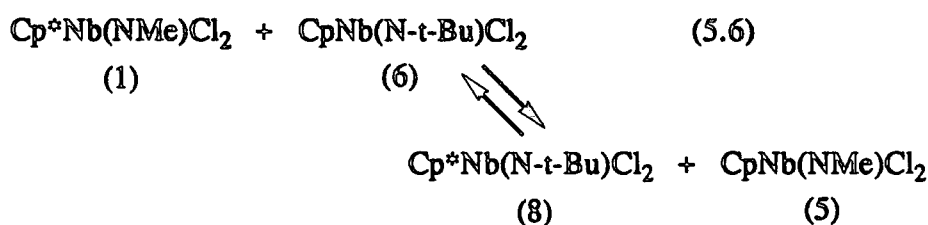
Table 5.1 Bond distances (Å) and angles (°) for $Cp^*Ta(NAr)Cl_2$ (3).

$\text{Cp}^*\text{Re}(\text{N-t-Bu})\text{Cl}_2$ described recently by Herrmann³. The Cp^* ring is arranged in an eclipsed fashion with respect to the imido ligand (as seen for $\text{CpNb}(\text{NMe})\text{Cl}_2$ (5) and $\text{CpNb}(\text{NAr})\text{Cl}_2$ (7)). This leads to a bending of the eclipsed ring methyl substituent away from the Cp^* ring plane by 5.8° (for comparison, the corresponding angles of the other ring methyl substituents are 2.3° and 2.8° respectively).

5.5 Imido Exchange Reactivity

5.5.1 Reaction of $\text{Cp}^*\text{Nb}(\text{NMe})\text{Cl}_2$ (1) with $\text{CpNb}(\text{N-t-Bu})\text{Cl}_2$ (6).

When an equimolar mixture of $\text{Cp}^*\text{Nb}(\text{NMe})\text{Cl}_2$ (1) and $\text{CpNb}(\text{N-t-Bu})\text{Cl}_2$ (6) is heated to 100°C in a sealed NMR tube (C_6D_6) and monitored by ^1H NMR spectroscopy, a mixture of four imido species is obtained according to the equilibrium shown in equation 5.6.

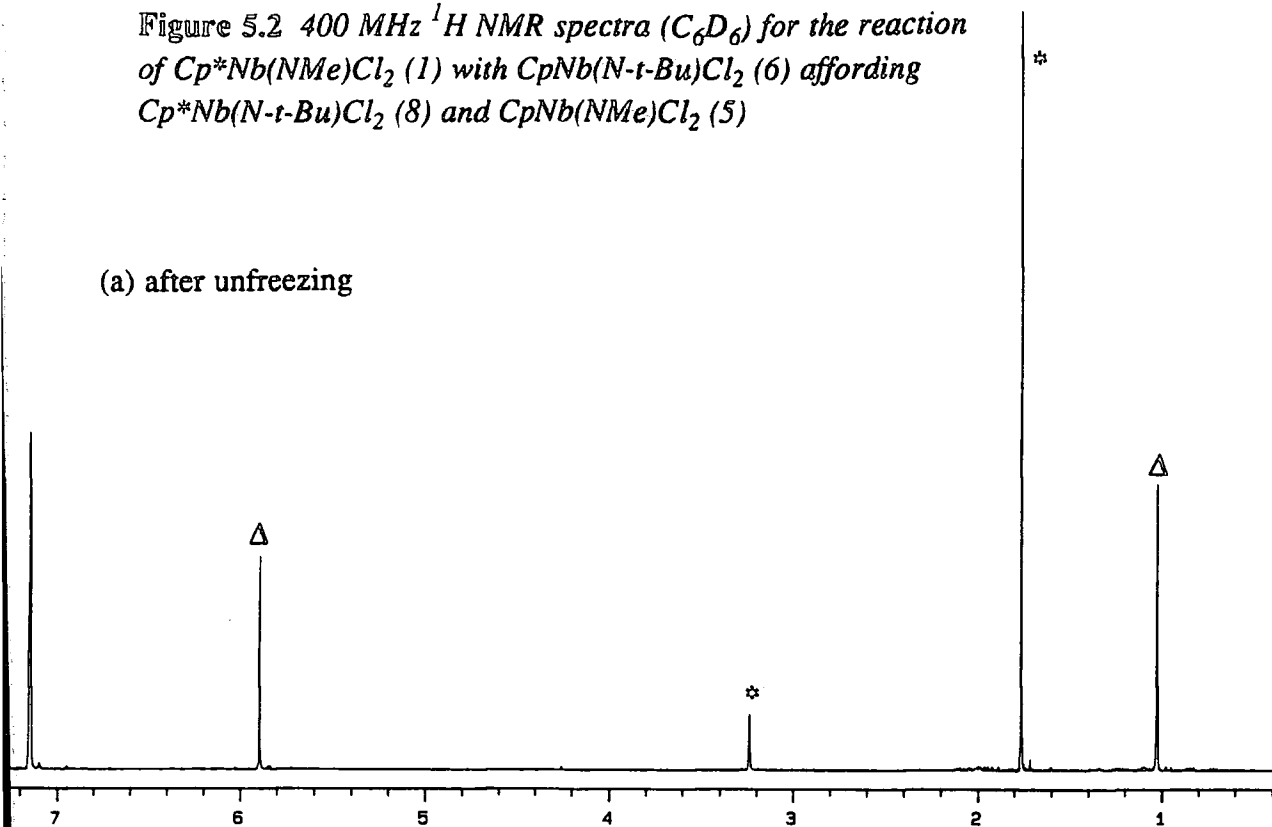


The starting spectrum for the $\text{Cp}^*\text{Nb}(\text{NMe})\text{Cl}_2 / \text{CpNb}(\text{N-t-Bu})\text{Cl}_2$ mixture is shown in figure 5.2(a) and shows that no reaction occurs at room temperature. The resultant spectrum after warming to 100°C for several days is shown in figure 5.2(b).

$\text{Cp}^*\text{Nb}(\text{N-t-Bu})\text{Cl}_2$ (8) has not previously been synthesized on a preparative scale, but can be characterized in this case by ^1H NMR spectroscopy with two singlet resonances at δ 1.87 and 1.18 for the methyl protons of the C_5Me_5 and N-t-Bu ligands respectively. Prolonged warming at this temperature does not lead to any further change in the ratio of the products, confirming that equilibrium has been reached ($K_{\text{eqm}} = 0.18$ (2), $\Delta G^\circ = -RT \ln K_{\text{eqm}} = 1.3$ (1) kcal mol^{-1}). The position of the equilibrium

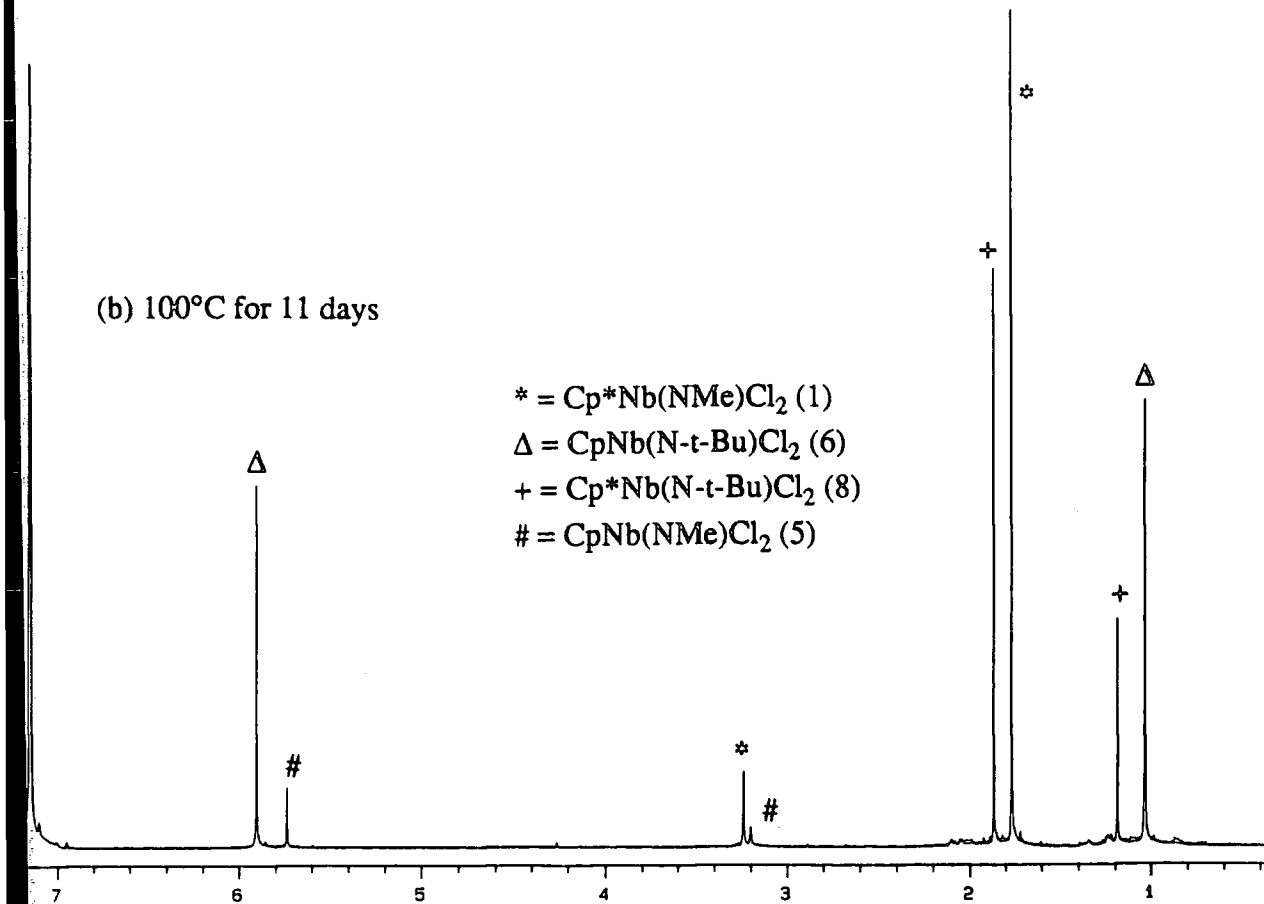
Figure 5.2 400 MHz ^1H NMR spectra (C_6D_6) for the reaction of $\text{Cp}^*\text{Nb}(\text{NMe})\text{Cl}_2$ (1) with $\text{CpNb}(\text{N-}t\text{-Bu})\text{Cl}_2$ (6) affording $\text{Cp}^*\text{Nb}(\text{N-}t\text{-Bu})\text{Cl}_2$ (8) and $\text{CpNb}(\text{NMe})\text{Cl}_2$ (5)

(a) after unfreezing



(b) 100°C for 11 days

* = $\text{Cp}^*\text{Nb}(\text{NMe})\text{Cl}_2$ (1)
 Δ = $\text{CpNb}(\text{N-}t\text{-Bu})\text{Cl}_2$ (6)
 + = $\text{Cp}^*\text{Nb}(\text{N-}t\text{-Bu})\text{Cl}_2$ (8)
 # = $\text{CpNb}(\text{NMe})\text{Cl}_2$ (5)

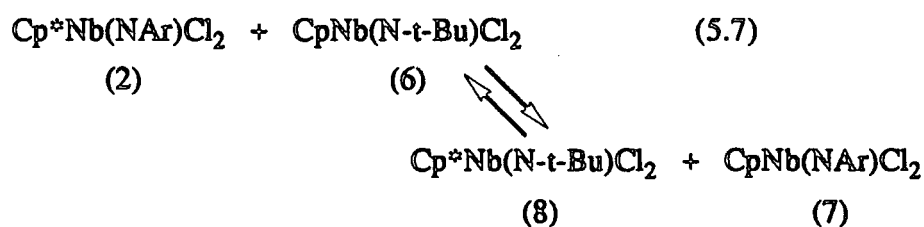


favouring the reactants is believed to reflect the less favoured steric environment around the niobium centre afforded by the combination of the bulky *t*-butylimido and pentamethylcyclopentadienyl substituents of the product species $\text{Cp}^*\text{Nb}(\text{N-}t\text{-Bu})\text{Cl}_2$ (8). The higher temperatures required for imido exchange to occur in this half-sandwich system relative to the four coordinate molybdenum species described in chapter four is likely to be a consequence of their higher formal metal electron count (hence decreased acidity) and also possibly the enhanced reactivity of species with two *cis* multiply bonded ligands¹¹.

Not surprisingly, the rate of approach to equilibrium is slowed dramatically as the size of the imido substituent is increased to the more sterically demanding 2,6-*i*-Pr₂C₆H₃ unit.

5.5.2 Reaction of $\text{Cp}^*\text{Nb}(\text{NAr})\text{Cl}_2$ (2) with $\text{CpNb}(\text{N-}t\text{-Bu})\text{Cl}_2$ (6).

$\text{Cp}^*\text{Nb}(\text{NAr})\text{Cl}_2$ (2) and $\text{CpNb}(\text{N-}t\text{-Bu})\text{Cl}_2$ (6) react in an equimolar ratio in C_6D_6 to give an equilibrium distribution of the four imido species shown in equation 5.7.

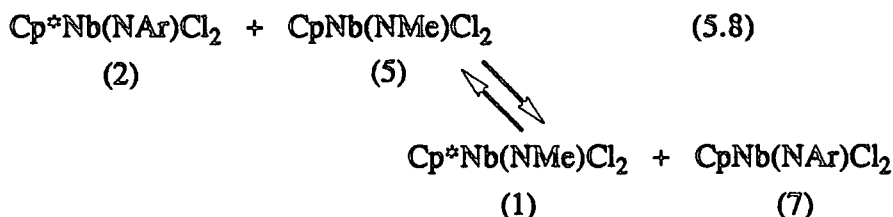


Several weeks at 140°C are required before equilibrium is reached. The position of equilibrium appears to favour the reactants, suggesting that the niobium metal centre possessing a *t*-butylimido substituent (8) is more sterically hindered than that possessing an arylimido substituent (2). However, slight decomposition at this temperature precluded an accurate measurement of the equilibrium constant. The lower rate of imido exchange can be attributed to a combination of bulky C₅Me₅ and

arylimido substituents on (2) disfavours formation of the transition state for imido exchange, as discussed further in section 5.5.5.

5.5.3 Reaction of $\text{Cp}^{\circ}\text{Nb}(\text{NAr})\text{Cl}_2$ (2) with $\text{CpNb}(\text{NMe})\text{Cl}_2$ (5).

The reaction of $\text{Cp}^{\circ}\text{Nb}(\text{NAr})\text{Cl}_2$ (2) with an equimolar amount of $\text{CpNb}(\text{NMe})\text{Cl}_2$ (5) in C_6D_6 at 140°C proceeds in an analogous manner as described above to give an equilibrium mixture of (2), (5), and the imido exchange species $\text{Cp}^{\circ}\text{Nb}(\text{NMe})\text{Cl}_2$ (1) and $\text{CpNb}(\text{NAr})\text{Cl}_2$ (7), as shown in equation 5.8.

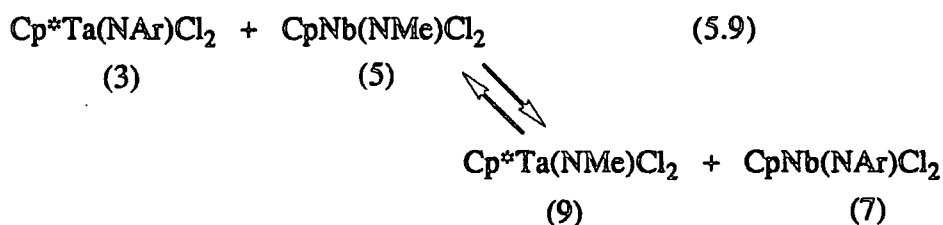


Equilibrium is reached faster at 140°C than for the reaction depicted in equation 5.7, again consistent with the lessened steric hindrance provided by the methylimido unit of (5) relative to the *t*-butylimido group of (6). The equilibrium constant at this temperature is 1.13 (3) ($\Delta G^\circ = -0.10$ (2) kcal mol⁻¹), reflecting a preference for the products, where the bulky Cp° ligand is in combination with the least sterically demanding methylimido unit in $\text{Cp}^{\circ}\text{Nb}(\text{NMe})\text{Cl}_2$ (1).

To confirm that the exchange of imido groups between metal centres is indeed an equilibrium situation, the reverse reaction to that shown in equation 5.8 (i.e. treatment of $\text{Cp}^{\circ}\text{Nb}(\text{NMe})\text{Cl}_2$ (1) with one equivalent of $\text{CpNb}(\text{NAr})\text{Cl}_2$ (7) in C_6D_6) was undertaken. After heating to 140°C approximately the same ratio of all four imido species was obtained ($K_{140^\circ\text{C}} = 0.92$ (4) R \rightarrow L in equation 5.8).

5.5.4 Reaction of $\text{Cp}^*\text{Ta}(\text{NAr})\text{Cl}_2$ (3) with $\text{CpNb}(\text{NMe})\text{Cl}_2$ (5).

In order to establish that the apparent exchange of imido ligands is not a consequence of simple exchange between niobium centres of the Cp and Cp^* ligands, a triple labelling experiment was performed, whereby $\text{CpNb}(\text{NMe})\text{Cl}_2$ (5) was treated with an equimolar amount of the tantalum imido species $\text{Cp}^*\text{Ta}(\text{NAr})\text{Cl}_2$ (3) in C_6D_6 . The reaction resulted in an equilibrium mixture of (3), (5), $\text{CpNb}(\text{NAr})\text{Cl}_2$ (7) (and presumably $\text{Cp}^*\text{Ta}(\text{NMe})\text{Cl}_2$ (9)) exclusively (equation 5.9). The ^1H NMR resonances for (9) were not detected, presumably due to overlap.



The absence of $\text{CpTa}(\text{NAr})\text{Cl}_2$ (10) or $\text{Cp}^*\text{Nb}(\text{NMe})\text{Cl}_2$ (1) amongst the exchange products therefore rules out the possibility of ring transfer giving rise to the observed products in exchange between two niobium metal centres. Because the ^1H NMR resonances for (9) could not be detected, this unfortunately precludes measurement of an equilibrium constant for this reaction, and therefore no comparison to the reaction using $\text{Cp}^*\text{Nb}(\text{NAr})\text{Cl}_2$ (2) (equation 5.8) can be made.

5.5.5 The mechanism of Imido Ligand Exchange.

The mechanism of this exchange reaction is believed to proceed via an ordered four centred transition state (figure 5.3) similar to that proposed for the exchange of imido and oxo groups between four coordinate molybdenum metal centres (see previous chapter).

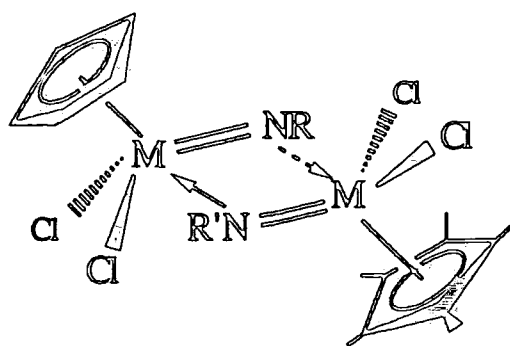


Figure 5.3 *Proposed Transition State for Imido Exchange between $CpM(NR)Cl_2$ and $Cp^*M(NR')Cl_2$.*

It is likely that the initial orientation of the $M_2(NR)(NR')$ unit is as shown in figure 5.3, in which the nitrogen lone pair donates into the LUMO of the $Cp^*M(NR)Cl_2$ fragment, adopting a similar structure to that observed for $CpNb(NMe)Cl_2(PMe_3)$ (11). Fenske-Hall calculations performed on the trimethylphosphine adduct (figure 5.4)^{1,6} show that the LUMO lies essentially in the $NbCl_2$ plane and may be compared with the LUMO for the bent metallocene moiety^{12,13}.

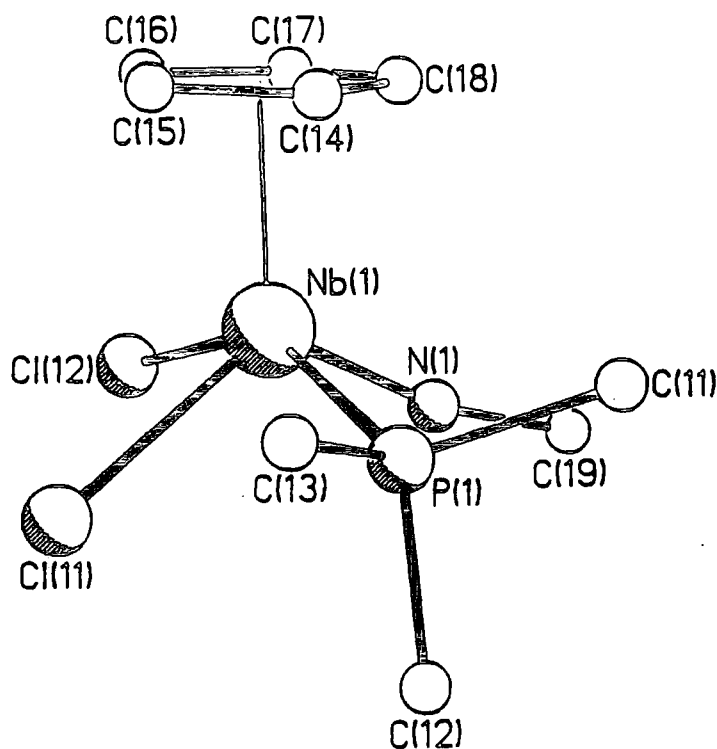
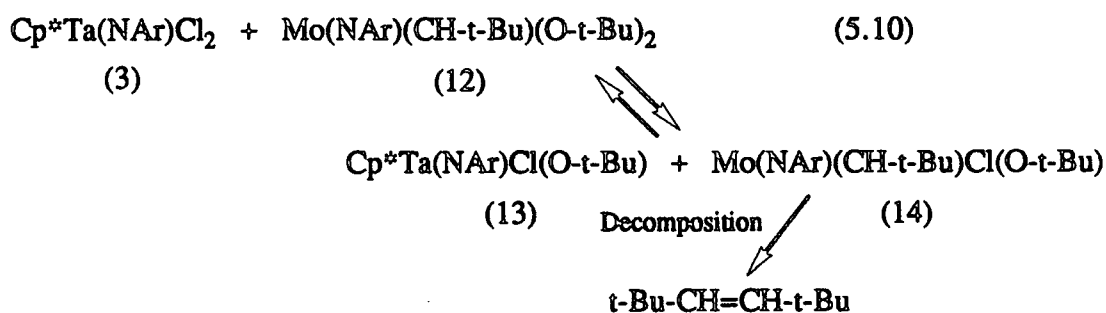


Figure 5.4 *The Molecular Structure of $CpNb(NMe)Cl_2(PMe_3)$ (11).*

5.5.6 Reaction of $\text{Cp}^*\text{Ta}(\text{NAr})\text{Cl}_2$ (3) with
 $\text{Mo}(\text{NAr})(\text{CH-t-Bu})(\text{O-t-Bu})_2$ (12).

In order to ascertain whether exchange of imido ligands could occur between the half-sandwich tantalum centre and a four coordinate molybdenum centre, $\text{Cp}^*\text{Ta}(\text{NAr})\text{Cl}_2$ (3) was treated with an equimolar amount of $\text{Mo}(\text{NAr})(\text{CH-t-Bu})(\text{O-t-Bu})_2$ (12) in C_6D_6 . No reaction was observed at room temperature indicating that the exchange of ancillary one electron chloride and t-butoxide ligands is much slower in the half-sandwich system than for exchange between the four coordinate molybdenum centres discussed in chapter four. Upon heating to 70°C for four days, the major product (as identified by ^1H NMR spectroscopy) was the mixed chloride/t-butoxide species $\text{Cp}^*\text{Ta}(\text{NAr})\text{Cl}(\text{O-t-Bu})$ (13), identified by comparison with a previously prepared sample (see appendix three). A sharp singlet at δ 5.46 is also observed, due to the olefinic protons of the decomposition product t-Bu-CH=CH-t-Bu. This observation is consistent with the expected instability of the *in-situ* formed alkylidene product $\text{Mo}(\text{NAr})(\text{CH-t-Bu})\text{Cl}(\text{O-t-Bu})$ (14), which decomposes via coupling of alkylidene units as shown in equation 5.10.



A significant quantity of neohexene is also observed in the ^1H NMR spectrum. The presence of this species is not as readily explained, although it must be due to some as yet not understood rearrangement of either the alkylidene ligand or the coupled alkylidene product. Although two further arylimido septets are observed in low

concentrations at δ 3.48 and 3.14, no conclusive evidence is apparent for formation of a half-sandwich tantalum alkylidene species or a molybdenum bis-imido species.

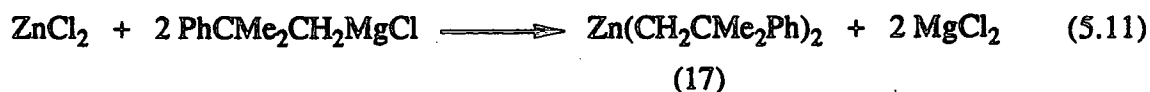
5.6 Preparation of $\text{CpTa}(\text{CHCMe}_2\text{Ph})\text{Cl}_2$ (15).

Having established that imido ligands can be exchanged between niobium and tantalum metal centres in a relatively facile manner, an analogous investigation into alkylidene transfer between these half sandwich complexes was undertaken. These studies involved the synthesis of the half sandwich alkylidene complex $\text{CpTa}(\text{CHCMe}_2\text{Ph})\text{Cl}_2$ (15). The procedure described below is a modified preparation of the corresponding analogue $\text{CpTa}(\text{CH-t-Bu})\text{Cl}_2$ (16)^{14,15}.

5.6.1 Reaction of ZnCl_2 with $\text{PhCMe}_2\text{CH}_2\text{MgCl}$.

Preparation of $\text{Zn}(\text{CH}_2\text{CMe}_2\text{Ph})_2$ (17).

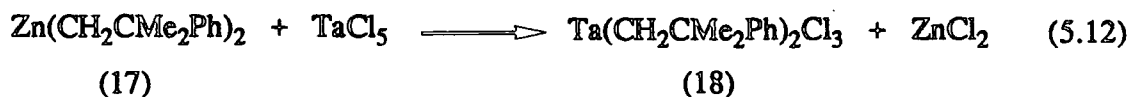
The reaction of ZnCl_2 and two molar equivalents of $\text{PhCMe}_2\text{CH}_2\text{MgCl}$ in diethyl ether affords $\text{Zn}(\text{CH}_2\text{CMe}_2\text{Ph})_2$ (17) as a pale yellow liquid in 67% yield (equation 5.11). The 250 MHz ^1H NMR spectrum (C_6D_6) reveals two broad singlets (in a three to one ratio) at δ 1.21 and 0.64 for the methyl and methylene protons respectively. A series of overlapping resonances between δ 7.00 and 7.26 correspond to the aromatic protons.



5.6.2 Reaction of $\text{Zn}(\text{CH}_2\text{CMe}_2\text{Ph})_2$ (17) with TaCl_5 .

Preparation of $\text{Ta}(\text{CH}_2\text{CMe}_2\text{Ph})_2\text{Cl}_3$ (18).

Treatment of TaCl_5 with one molar equivalent of $\text{Zn}(\text{CH}_2\text{CMe}_2\text{Ph})_2$ (17) in toluene gives a yellow orange solution from which $\text{Ta}(\text{CH}_2\text{CMe}_2\text{Ph})_2\text{Cl}_3$ (18) can be isolated as a dark brown oil upon removal of the volatile components *in vacuo* (equation 5.12).



The product may be purified by stirring a pentane solution of the oil over decolourizing charcoal for thirty minutes. Filtration, and subsequent removal of volatile components affords $\text{Ta}(\text{CH}_2\text{CMe}_2\text{Ph})_2\text{Cl}_3$ (18) as a canary yellow oil in 59% yield. Compound (18) has been characterized by ^1H and ^{13}C NMR spectroscopy. The 400 MHz ^1H NMR spectrum (C_6D_6) reveals two singlet resonances at δ 2.97 and 1.39 for the methylene and methyl protons respectively of the neophyl ligands, with the aromatic protons appearing as an overlapping series of multiplets between δ 6.97 and 7.28. Careful analysis of the ^1H NMR spectrum reveals the presence of two further singlets at δ 2.72 and 1.36. These may be attributed to the presence of approximately 5% $\text{Ta}(\text{CH}_2\text{CMe}_2\text{Ph})_3\text{Cl}_2$. This "3 : 2" impurity has also been observed by Schrock and coworkers in the preparation of $\text{Ta}(\text{CH}_2\text{CMe}_3)_2\text{Cl}_3$ ¹⁴. Upon standing in the light at room temperature for several days, the product is observed to darken, and several new resonances can be seen in the ^1H NMR spectrum.

and the tantalum centre. This value is reasonable, as the coupling constant for a terminal C-H bond is typically 120-130 Hz¹⁸ and that for a bridging agostic interaction typically 70-100 Hz^{19,20}. The infrared spectrum (nujol mull) also supports the presence of an agostic interaction, with a low ν (C-H _{α}) stretch being observed at 2520 cm⁻¹ (shoulder at 2495 cm⁻¹). Similar low frequency C-H stretches are found in related alkylidene complexes^{15,16}.

A single crystal X-Ray structure determination of CpTa(CH-t-Bu)Cl₂ (16) reveals a Ta-C _{α} -C _{β} angle of 165.0 (3)°, and a Ta-C _{α} -H _{α} angle of 81°, with the t-butyl group pointing towards the cyclopentadienyl ring, thus allowing the α hydrogen atom to approach the metal centre from below¹⁵ (figure 5.5).

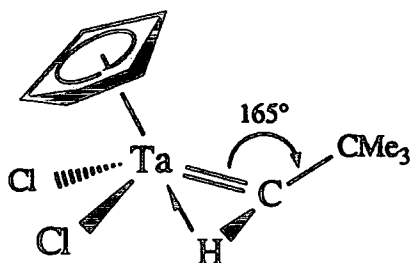


Figure 5.5 *The Molecular Structure of CpTa(CH-t-Bu)Cl₂ (16).*

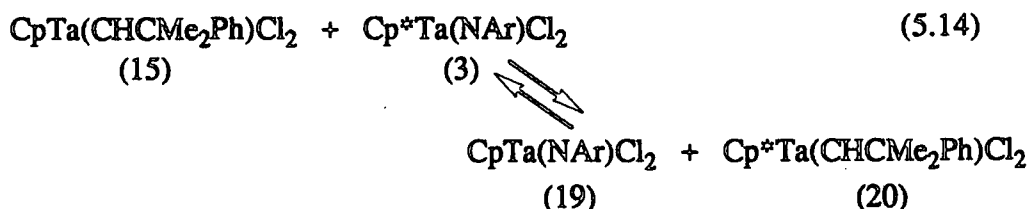
It therefore seems probable that the neophylidene analogue CpTa(CHCMe₂Ph)Cl₂ (15) will adopt a closely related structure.

5.7 Investigation of the Alkylidene Exchange Reactivity of
 $\text{CpTa}(\text{CHCMe}_2\text{Ph})\text{Cl}_2$ (15).

5.7.1 Reaction of $\text{CpTa}(\text{CHCMe}_2\text{Ph})\text{Cl}_2$ (15) with
 $\text{Cp}^*\text{Ta}(\text{NAr})\text{Cl}_2$ (3).

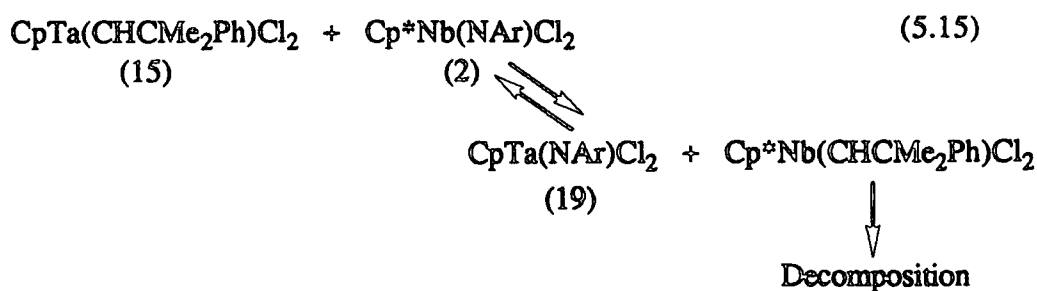
$\text{CpTa}(\text{CHCMe}_2\text{Ph})\text{Cl}_2$ (15) was mixed with an equimolar amount of $\text{Cp}^*\text{Ta}(\text{NAr})\text{Cl}_2$ (3) in C_6D_6 in a sealed NMR tube. No reaction was observed (by ^1H NMR spectroscopy) at room temperature. However, after several days at 120°C , a variety of new proton resonances could be observed. A new arylimido septet and doublet at δ 3.71 and 1.27 can be attributed to the methine and methyl protons respectively of the aryl imido group for the exchange product $\text{CpTa}(\text{NAr})\text{Cl}_2$ (19)¹. A new C_5H_5 resonance is also observed at δ 5.75. A singlet at δ 2.14 can be tentatively assigned to the methyl protons of the C_5Me_5 moiety of the other exchange product $\text{Cp}^*\text{Ta}(\text{CHCMe}_2\text{Ph})\text{Cl}_2$ (20) (c.f. δ 1.99 for the pentamethylcyclopentadienyl protons of $\text{Cp}^*\text{Ta}(\text{CH-t-Bu})\text{Cl}_2$)¹⁵. In the ^{13}C NMR spectrum, a small resonance is observed at δ 234.38, which can be attributed to the α carbon atom of the neophylidene group in (20).

The above spectroscopic observations suggest that exchange of alkylidene and imido groups has occurred, according to equation 5.14.



5.7.2 Reaction of $\text{CpTa}(\text{CHCMe}_2\text{Ph})\text{Cl}_2$ (15) with $\text{Cp}^*\text{Nb}(\text{NAr})\text{Cl}_2$ (2).

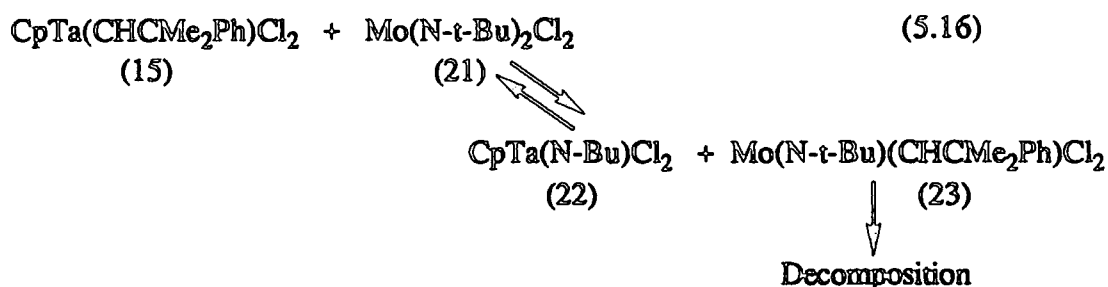
An attempt to transfer the alkylidene unit from tantalum to niobium was less successful. ^1H NMR spectroscopic analysis (C_6D_6 , 400 MHz) of an equimolar mixture of $\text{CpTa}(\text{CHCMe}_2\text{Ph})\text{Cl}_2$ (15) and $\text{Cp}^*\text{Nb}(\text{NAr})\text{Cl}_2$ (2) at 120°C in a sealed NMR tube revealed identical resonances to those seen in section 5.7.1 for the exchange product $\text{CpTa}(\text{NAr})\text{Cl}_2$ (19) (equation 5.15) but no new identifiable resonances for the other exchange product $\text{Cp}^*\text{Nb}(\text{CHCMe}_2\text{Ph})\text{Cl}_2$. No resonance was seen at low field in the ^{13}C NMR spectrum that could be attributed to a new niobium alkylidene α carbon atom. This is presumably due to decomposition of the exchange product $\text{Cp}^*\text{Nb}(\text{CHCMe}_2\text{Ph})\text{Cl}_2$ at the temperatures required for alkylidene transfer to take place. This is consistent with earlier observations by Schrock regarding the relative instability of niobium alkylidenes^{15,16,20}.



5.7.3 Reaction of $\text{CpTa}(\text{CHCMe}_2\text{Ph})\text{Cl}_2$ (15) with $\text{Mo}(\text{N-t-Bu})_2\text{Cl}_2$ (21).

In order to ascertain whether the alkylidene moiety could be transferred from (15) to the four coordinate molybdenum complex $\text{Mo}(\text{N-t-Bu})_2\text{Cl}_2$ (21), the two were mixed in an equimolar amount in C_6D_6 in a sealed NMR tube. After twenty minutes at room temperature two new singlet resonances could be observed at δ 5.81 and 1.11. These

can be attributed to the heteroatom exchange product $\text{CpTa}(\text{N-t-Bu})\text{Cl}_2$ (22), by comparison with data from an authentic sample^{1,21}. Upon prolonged heating at 55°C, the concentration of (22) increases; however, no new alkylidene resonance is observed for the other exchange product $\text{Mo}(\text{N-t-Bu})(\text{CHCMe}_2\text{Ph})\text{Cl}_2$ (23) (equation 5.16).

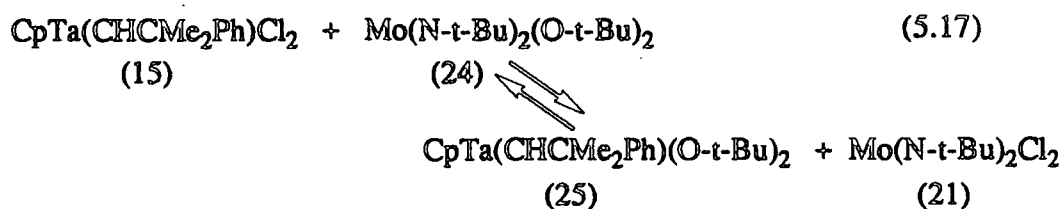


This is consistent with earlier observations²² that such alkylidene species are not stable if insufficiently sterically hindered around the metal centre. Broad resonances in the ¹H NMR spectrum at δ 1.91 and 0.88 can be attributed to the decomposition product, with no resonance being observed for the coupled product $\text{PhCMe}_2\text{CH}=\text{CHCMe}_2\text{Ph}$. It therefore appears that (23) decomposes via a different mechanism other than bimolecular coupling of the alkylidene units. However, these decomposition products, and the mechanism of their formation, are still unclear.

5.7.4 Reaction of $\text{CpTa}(\text{CHCMe}_2\text{Ph})\text{Cl}_2$ (15) with $\text{Mo}(\text{N-t-Bu})_2(\text{O-t-Bu})_2$ (24).

The corresponding reaction of (15) with $\text{Mo}(\text{N-t-Bu})_2(\text{O-t-Bu})_2$ (24) in C_6D_6 occurs rapidly at room temperature, leading to exchange of the one electron chloride and t-butoxide ligands. Over a period of four hours at room temperature, a singlet resonance at δ 1.28 can be seen to increase, characteristic of the species $\text{Mo}(\text{N-t-Bu})_2\text{Cl}_2$ (21). The corresponding exchange product, $\text{CpTa}(\text{CHCMe}_2\text{Ph})(\text{O-t-Bu})_2$ (25) may be characterized by a new alkylidene proton resonance at δ 6.94, a singlet at

δ 5.59 for the cyclopentadienyl protons, and two further singlets at δ 1.50 and 1.43 for the diastereotopic methyl protons of the neophylidene ligand. The reaction can be envisaged according to equation 5.17.



Identical ^1H NMR resonances are observed for species (25) upon reaction of $\text{CpTa}(\text{CHCMe}_2\text{Ph})\text{Cl}_2$ (15) with two equivalents of Li-O-t-Bu in C_6D_6 , the reaction proceeding to completion within twelve hours at room temperature. This reaction favours the molybdenum dichloride species and tantalum bis t-butoxide species (rather than the mixed chloride/t-butoxide species as seen previously) presumably due to the increased oxophilicity of the tantalum.

Upon heating the NMR tube to 60°C , a small amount of the exchange product $\text{CpTa}(\text{N-t-Bu})\text{Cl}_2$ (22) is observed, but the reaction is not clean.

An identical reaction of (15) with $\text{Mo}(\text{NAr})_2(\text{O-t-Bu})_2$ (26) also leads to chloride for t-butoxide exchange products.

5.8 Summary.

A series of imido complexes of niobium and tantalum possessing the pentamethylcyclopentadienyl ligand have been synthesized, and a single crystal structure determination on $\text{Cp}^*\text{Ta}(\text{NAr})\text{Cl}_2$ (3) has revealed a three legged piano stool geometry similar to those observed for related $\text{CpNb}(\text{NR})\text{Cl}_2$ complexes ($\text{R} = \text{Me}$, t-Bu, Ar)^{1,6}. These complexes have been shown to undergo exchange of their imido groups at elevated temperature.

The half-sandwich alkylidene complex $\text{CpTa}(\text{CHCMe}_2\text{Ph})\text{Cl}_2$ (15) has also been synthesized, and preliminary studies indicate that related exchange reactivity may be obtained for the alkylidene ligand, offering the possibility of preparing new alkylidene complexes of technological importance.

5.9 References.

1. D.N. Williams, Ph.D Thesis, University of Durham, 1990.
2. J.M. Mayer, C.J. Curtis, J.E. Bercaw, *J. Am. Chem. Soc.* 1983, 105, 2651.
3. W.A. Herrmann, G. Weichselbaumer, R.A. Paciello, R.A. Fischer, E. Herdtweck, J. Okudo, D.W. Marz, *Organometallics*, 1990, 9, 489.
4. W.A. Nugent, J.M. Mayer, "*Metal Ligand Multiple Bonds*", J. Wiley New York, 1988.
5. D.M. Adams, "*Metal Ligand and Related Vibrations*", Edward Arnold, 1967.
6. D.N. Williams, J.P. Mitchell, A.D. Poole, U. Siemeling, W. Clegg, D.C.R. Hockless, P.A. O'Neil, V.C. Gibson, *J. Chem. Soc. Dalton. Trans.* in press.
7. W.A. Nugent, R.L. Harlow, *J. Chem. Soc. Chem. Comm.* 1978, 579.
8. F.A. Cotton, W.T. Hall, *Inorg. Chem.* 1978, 17, 3525.
9. L.R. Chamberlain, I.P. Rothwell, J.C. Huffman, *J. Chem. Soc. Chem. Comm.* 1986, 1203.
10. V.C. Gibson, D.N. Williams, W. Clegg, D.C.R. Hockless, *Polyhedron*, 1989, 8, 1819.
11. A.K. Rappe, W.A. Goddard III, *J. Am. Chem. Soc.* 1982, 104, 448.
12. J.W. Lauher, R. Hoffmann, *J. Am. Chem. Soc.* 1976, 98, 1729.
13. L. Zhu, N.M. Kostic, *J. Organomet. Chem.* 1987, 335, 395.
14. R.R. Schrock, J.D. Fellmann, *J. Am. Chem. Soc.* 1978, 100, 3359.
15. C.D. Wood, S.J. McLain, R.R. Schrock, *J. Am. Chem. Soc.* 1979, 101, 3210.

16. R.R. Schrock, "*Alkylidene Complexes of the Earlier Transition Metals*", in *Reactions of Coordinated Ligands*, Vol 1, P.S. Braterman Ed. Plenum Press, New York, 1986.
17. R.R. Schrock, L.W. Messerle, C.D. Wood, L.J. Guggenberger, *J. Am. Chem. Soc.* 1978, 100, 3793.
18. M. Brookhart, M.L.H. Green, *J. Organomet. Chem.* 1983, 250, 395.
19. M. Brookhart, T.H. Whitesides, J.M. Crockett, *Inorg. Chem.* 1976, 15, 1550.
20. G.A. Rupprecht, L.W. Messerle, J.D. Fellmann, R.R. Schrock, *J. Am. Chem. Soc.* 1980, 102, 6236.
21. I. Manners, P. Paetzold, *J. Chem. Soc. Chem. Comm.* 1988, 183.
22. This Thesis, Chapter 4.

CHAPTER SIX

Experimental Details.

6.1 General.

6.1.1 Experimental Techniques.

All manipulations of air and/or moisture sensitive materials were performed on a conventional vacuum/inert atmosphere (nitrogen or argon) line using standard Schlenk and cannular techniques, or in an inert atmosphere (nitrogen or argon) filled glove box.

Elemental analyses were performed by the microanalytical services of this department.

Infrared spectra were recorded on Perkin-Elmer 577 and 457 grating spectrophotometers using either KBr or CsI windows. Absorptions abbreviated as follows: vs (very strong), s (strong), m (medium), w (weak), br (broad), sp (sharp), sh (shoulder).

Mass spectra were recorded on a VG 7070E Mass Spectrometer.

NMR spectra were recorded on the following instruments, at the frequencies listed, unless stated otherwise: Varian VXR400, ^1H (399.95 MHz), ^{13}C (100.58 MHz), ^{19}F (376.29 MHz); Bruker AC250, ^1H (250.13 MHz), ^{13}C (62.90 MHz), ^{19}F (235.36 MHz); Varian Gemini 200, ^1H (199.98 MHz), ^{13}C (50.29 MHz). The following abbreviations have been used for band multiplicities: s (singlet), d (doublet), t (triplet), q (quartet), sept (septet), m (multiplet). Chemical shifts are quoted as δ in ppm with respect to the following references, unless stated otherwise: ^{13}C (C_6D_6 , 128.0 ppm); ^1H (C_6D_6 , 7.15 ppm, CDCl_3 , 7.24 ppm, C_7D_8 , 6.98 ppm); ^{19}F (CFCl_3 , 0.00 ppm).

GPC traces were recorded on the following instruments : (1) Knauer differential refractometer with a Spectroflow 757 absorbance detector and Shodex KF 802.5, 803, 804 and 800P columns (dichloromethane, flow rate of 1 ml / min). (2) Viscotek differential refractometer fitted with a Knauer HPLC pump 64 and two PLgel 10 μ mixed columns (THF, flow rate 1 ml / min). Samples (0.1 - 0.3 % w/v) were filtered through a Millex SR 0.5 μm filter before injection in order to remove particulates. The

columns were calibrated using commercially available polystyrene standards (Polymer Laboratories Ltd.) ranging from 1206 to 1.03×10^6 MW.

6.1.2 Solvents and Reagents.

The following NMR solvents were dried by vacuum distillation from a suitable drying agent (in parentheses) and passed through a column of activated alumina before use:

d^6 -benzene (phosphorus (V) oxide), d^8 -toluene (phosphorus (V) oxide) and d -chloroform (phosphorus (V) oxide).

The following solvents were dried by prolonged reflux over a suitable drying agent, and were freshly distilled and deoxygenated before use (drying agent in parentheses): toluene (sodium metal), pentane (lithium aluminium hydride), tetrahydrofuran (sodium benzophenone ketyl), acetonitrile (calcium hydride), dichloromethane (calcium hydride), 1,2-dichloroethane (calcium hydride) and diethylether (lithium aluminium hydride).

The following chemicals were prepared by previously published procedures: LiOAr^1 (Ar = 2,6- $i\text{Pr}_2\text{C}_6\text{H}_3$), Li-O-t-Bu^1 , PMe_3^2 , CpNbCl_4^3 , CpTaCl_4^3 , $\text{Cp}^*\text{TaCl}_4^4$, $\text{Cp}^*\text{NbCl}_4^5$, CpNb(NMe)Cl_2^6 , $\text{CpNb(N-t-Bu)Cl}_2^6$, CpNb(NAr)Cl_2^6 , $\text{Mo(N-t-Bu)}_2\text{Cl}_2^7$, $\text{Mo(N-t-Bu)}_2(\text{O-t-Bu})_2^8$, $(\text{Me}_3\text{Si})\text{NHR}^9$ (R = t-Bu, 2,6- $i\text{Pr}_2\text{C}_6\text{H}_3$), $\text{Mo(O)}_2\text{Cl}_2^9$, $\text{Mo(NAr)(CHCMe}_2\text{Ph)(O-t-Bu)}_2^9$, $\text{Mo(NAr)}_2\text{Cl}_2(\text{dme})^9$, $\text{Mo(NAr)(CHCMe}_2\text{Ph)(OCMe(CF}_3)_2)_2^9$, $\text{Me}_3\text{CCH}_2\text{MgCl}^{10}$, $\text{W(NAr)(CHCMe}_3)(\text{O-t-Bu})_2^{11}$, DCMND^{12} ,

Due to the relevance of four-coordinate imido alkylidene complexes to the general theme of this thesis and their extensive use as metathesis initiators, the modified Schlenk line synthesis of $\text{Mo(NAr)(CH-t-Bu)(O-t-Bu)}_2^9$ is described in section 6.6.1.

The following chemicals were obtained commercially and used as received unless stated otherwise: molybdenum dioxide (Strem), tungsten hexachloride (Aldrich), tantalum pentachloride (Aldrich), niobium pentachloride (Aldrich), chlorotrimethylsilane (Aldrich), heptamethyldisilazane (Aldrich, dried and stored over 4Å molecular sieves), phenol (Aldrich), 2,6-di-isopropylphenol (Aldrich), trimethylsilylazide (Fluka, dried and stored over 4Å molecular sieves), n-butyl lithium (Aldrich, 1.6M in hexane), 2,6-lutidine (Aldrich, distilled before use), 2,6-di-isopropylaniline (Aldrich, distilled before use), nitrobenzene (Aldrich, dried and stored over 4 Å molecular sieves), norbornene (Aldrich, distilled before use), *p*-XC₆H₄CHO (Aldrich, distilled before use where appropriate, X = H, CN, CF₃, Cl, MeO, OH, NMe₂, CO₂Me, NO₂, CHO, NH₂), 3,5-di-*t*-butyl-4-hydroxybenzaldehyde (Aldrich), *trans*-cinnamaldehyde (Aldrich), pyridine (Aldrich, distilled before use), 4-pyridinecarboxaldehyde (Aldrich), 5-norbornene-2-carboxaldehyde (Aldrich), urea (Aldrich), tetramethylurea (Aldrich), methyl formate (Aldrich, distilled before use), *p*-XC₆H₄CH=CH₂ (Aldrich, distilled before use, X = H, Me, OMe, Cl), 3,5-bis(trifluoromethyl)styrene (Aldrich, distilled before use), vinylanthracene (Aldrich), pentafluorostyrene (BDH, distilled before use), 3-vinylpyridine (Aldrich, distilled before use), *cis*-stilbene (Aldrich), allylbenzene (Aldrich), azobenzene (Aldrich), RNCO (Aldrich, distilled before use, R = Ph, *t*-Bu, 2,6-*i*Pr₂C₆H₃), *t*-butanol (Aldrich), *t*-butylamine (Aldrich), cyclopentadienylthallium (Strem), neophyl chloride (Aldrich, washed with 2 x 500 cm³ H₂SO₄ and distilled (bpt. 66°C, 2 x 10⁻¹ torr) before use), neopentyl chloride (Aldrich, distilled through a Fischer column before use), ZnCl₂ (Aldrich, dried by reflux over SOCl₂ before use).

6.2 Experimental Details to Chapter 2.

6.2.1 Typical Capping Reaction of $\text{Mo}(\text{NAr})(\text{CH-t-Bu})(\text{OR})_2$ with a Substituted Aldehyde.

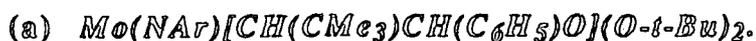
Typically, 10 mg of $\text{Mo}(\text{NAr})(\text{CH-t-Bu})(\text{OR})_2$ was dissolved in 350 μl C_6D_6 and a solution of 1-2 equivalents of substituted aldehyde in 350 μl C_6D_6 added. The resulting solution was transferred to an NMR tube and sealed under nitrogen. (CDCl_3 solutions were used in the cases of *p*- $\text{ClC}_6\text{H}_4\text{CHO}$ and *p*- $\text{NH}_2\text{C}_6\text{H}_4\text{CHO}$ due to their low solubility in C_6D_6). Formation of $\text{Mo}(\text{NAr})(\text{O})(\text{OR})_2$ (2) $\text{R} = \text{t-Bu}$ and (3) $\text{R} = \text{CMe}(\text{CF}_3)_2$ was then monitored by ^1H NMR spectroscopy.

(2) ^1H NMR data (250 MHz, d^6 -benzene, 298K): 7.07 (d, 2, H_m), 6.97 (t, 1, H_p), 4.33 (sept, 2, $^3J_{\text{HH}} = 6.8$ Hz, CHMe_2), 1.35 (d, 12, $^3J_{\text{HH}} = 6.8$ Hz, CHMe_2), 1.26 (s, 18, O-*t-Bu*).

(3) ^1H NMR data (250 MHz, d^6 -benzene, 298K): 4.25 (sept, 2, $^3J_{\text{HH}} = 6.80$ Hz, CHMe_2), 1.46 (s, 6, $\text{OCMe}(\text{CF}_3)_2$), 1.27 (d, 12, $^3J_{\text{HH}} = 6.80$ Hz, CHMe_2). Aromatic proton resonances were obscured by those for excess benzaldehyde and therefore cannot be assigned.

6.2.2 ^1H NMR Observation of 2-Oxametallacycles.

Typically, $\text{Mo}(\text{NAr})(\text{CH-t-Bu})(\text{O-t-Bu})_2$ (20 mg, 0.042 mmol) was dissolved in 420 μl C_6D_6 and a solution of 1-2 equivalents of *p*-substituted benzaldehyde in 420 μl C_6D_6 added. The resulting solution was transferred to an NMR tube, frozen immediately and sealed under nitrogen; the tube remaining frozen till the first spectrum was taken. Ring opening of the metallacycle was then monitored by ^1H NMR spectroscopy at room temperature.



1H NMR data (250 MHz, d^6 -benzene, 298K): 6.22 (d, 1, $J_{H\alpha H\beta} = 7.6$ Hz, $H\beta$), 4.21 (sept, $^3J_{HH} = 6.8$ Hz, $CHMe_2$), 2.23 (d, 1, $J_{H\alpha H\beta} = 7.6$ Hz, $H\alpha$), 1.54 (s, 9, *O-t-Bu*), 1.45 (s, 9, *O-t-Bu*), 1.32 (d, 12, $^3J_{HH} = 6.9$ Hz, $CHMe_2$), 1.14 (s, 9, $CHCMe_3$). Aryl protons could not be unambiguously assigned due to overlap.



1H NMR data (250 MHz, d^6 -benzene, 298K): 6.07 (d, 1, $J_{H\alpha H\beta} = 6.8$ Hz, $H\beta$), 4.20 (sept, 2, $^3J_{HH} = 6.8$ Hz, $CHMe_2$), 2.72 (d, 1, $J_{H\alpha H\beta} = 6.8$ Hz, $H\alpha$), 1.66 (s, 3, CMe_2Ph), 1.58 (s, 3, CMe_2Ph), 1.48 (s, 9, *O-t-Bu*), 1.43 (s, 9, *O-t-Bu*). Aryl proton resonances and resonances due to $CHMe_2$ not located due to signal overlap.



1H NMR data (250 MHz, d^6 -benzene, 298K): 6.02 (d, 1, $J_{H\alpha H\beta} = 7.1$ Hz, $H\beta$), 4.11 (sept, 2, $^3J_{HH} = 6.9$ Hz, $CHMe_2$), 1.95 (d, 1, $J_{H\alpha H\beta} = 7.1$ Hz, $H\alpha$), 1.48 (s, 9, *O-t-Bu*), 1.42 (s, 9, *O-t-Bu*), 1.31 (d, 6, $^3J_{HH} = 6.8$ Hz, $CHMe_2$), 1.29 (d, 6, $^3J_{HH} = 6.8$ Hz, $CHMe_2$), 1.04 (s, 9, $CHCMe_3$). Aryl proton resonances could not be detected due to signal overlap.



1H NMR data (250 MHz, d^6 -benzene, 298K): 6.07 (d, 1, $J_{H\alpha H\beta} = 7.4$ Hz, $H\beta$), 4.11 (sept, 2, $^3J_{HH} = 6.8$ Hz, $CHMe_2$), 1.96 (d, 1, $J_{H\alpha H\beta} = 7.4$ Hz, $H\alpha$), 1.49 (s, 9, *O-t-Bu*), 1.44 (s, 9, *O-t-Bu*), 1.31 (d, 6, $^3J_{HH} = 6.6$ Hz, $CHMe_2$), 1.29 (d, 6, $^3J_{HH} = 6.7$ Hz, $CHMe_2$), 1.06 (s, 9, $CHCMe_3$). Aryl resonances could not be readily assigned.

(e) $Mo(NAr)[CH(CMe_3)CH(p-CHO C_6H_4)O](O-t-Bu)_2$.

1H NMR data (250 MHz, d^6 -benzene, 298K): 9.68 (s, 1, CHC_6H_4CHO), 6.16 (d, 1, $J_{H\alpha H\beta} = 7.1$ Hz, $H\beta$) 4.15 (sept, 2, $^3J_{HH} = 6.8$ Hz, $CHMe_2$), 2.08 (d, 1, $J_{H\alpha H\beta} = 7.1$ Hz, $H\alpha$), 1.51 (s, 9, $O-t-Bu$), 1.44 (s, 9, $O-t-Bu$), 1.33 (d, 6, $^3J_{HH} = 6.9$ Hz, $CHMe_2$), 1.30 (d, 6, $^3J_{HH} = 7.0$ Hz, $CHMe_2$), 1.10 (s, 9, $CHCMe_3$). Aryl resonances could not be assigned due to overlap.

(f) $Mo(NAr)[CH(CMe_3)CH(p-MeO_2CC_6H_4)O](O-t-Bu)_2$.

1H NMR data (250 MHz, d^6 -benzene, 298K): 6.18 (d, 1, $J_{H\alpha H\beta} = 7.6$ Hz, $H\beta$), 4.20 (sept, 2, $^3J_{HH} = 6.8$ Hz, $CHMe_2$), 2.16 (d, 1, $J_{H\alpha H\beta} = 7.6$ Hz, $H\alpha$), 1.73 (s, 3, $CHC_6H_4CO_2Me$), 1.52 (s, 9, $O-t-Bu$), 1.45 (s, 9, $O-t-Bu$), 1.12 (s, 9, $CHCMe_3$). Aryl proton resonances and those due to $CHMe_2$ could not be located accurately due to overlap.

6.2.3 Typical formation of Polynorbornene Capped with a *p*-Substituted Benzaldehyde.

Polymerizations were performed using stock solutions of $Mo(NAr)(CH-t-Bu)(O-t-Bu)_2$ (0.1M), norbornene (5.0M) and capping benzaldehyde (0.1M) in toluene. (THF solutions of the benzaldehydes $p-ClC_6H_4CHO$ and $p-NH_2C_6H_4CHO$ were used due to their low solubility in toluene).

45 μ l (4.5 μ mol) of $Mo(NAr)(CH-t-Bu)(O-t-Bu)_2$ solution was diluted to 721 μ l with toluene and 90 μ l (450 μ mol, 100 equivalents) of norbornene solution added. The resulting mixture was stirred vigorously for 10 minutes, quenched by the addition of 90 μ l (45 μ mol, 10 equivalents) of *p*-substituted benzaldehyde solution and allowed to stir for a further 30 minutes. The polymer was then purified by dropwise addition of the resulting solution into a large excess of methanol, filtration, a subsequent precipitation

from chloroform into methanol and dried *in vacuo* for a minimum of 12 hours. In each case the polynorbornene was isolated in > 95% yield.

Gel Permeation Chromatographic data and characteristic infrared end-group absorptions for the isolated polymers are given in chapter 2 (tables 2.3 and 2.4)

6.3 Experimental Details to Chapter 3.

6.3.1 Typical Reaction of $\text{Mo}(\text{NAr})(\text{CH-}t\text{-Bu})(\text{O-}t\text{-Bu})_2$ with a Substituted Styrene.

Typically, 10 mg (0.021 mmol) of $\text{Mo}(\text{NAr})(\text{CH-}t\text{-Bu})(\text{O-}t\text{-Bu})_2$ was dissolved in 350 μl C_6D_6 and a solution of 5 - 10 equivalents of substituted styrene in 350 μl C_6D_6 added. The resulting mixture was transferred to an NMR tube and sealed under nitrogen. Formation of $\text{Mo}(\text{NAr})(\text{CHAr})(\text{O-}t\text{-Bu})_2$ was then monitored by ^1H NMR spectroscopy (typically taking 4 - 5 days at room temperature or 24 hours at 40° C).

NMR Characterizing Data (Major Isomers) for:

(a) $\text{Mo}(\text{NAr})(\text{CHC}_6\text{H}_5)(\text{O-}t\text{-Bu})_2$.

^1H NMR data (250 MHz, d^6 -benzene, 298K): 12.09 (s, 1, CHC_6H_5), 7.00 - 7.02 (overlapping multiplets, NAr and CHPh), 4.03 (sept, 2, $^3\text{J}_{\text{HH}} = 7.0$ Hz, CHMe_2), 1.33 (s, 18, $\text{O-}t\text{-Bu}$), 1.23 (d, 12, $^3\text{J}_{\text{HH}} = 7.3$ Hz, CHMe_2).

^{13}C NMR Data (100 MHz, d^6 -benzene, 298K): 247.84 (d, $\text{J}_{\text{CH}} = 125.1$ Hz, CHC_6H_5), 153.23 (Ar), 149.71 (Ar), 146.19 (Ar), 145.54 (Ar), 123.25 (Ar), 109.24, 78.35 (OCMe_3), 31.97, 29.25, 28.45, 23.82.

(b) $Mo(NAr)(CH-p-CH_3C_6H_4)(O-t-Bu)_2$.

1H NMR Data (400 MHz, d^6 -benzene, 298K): 12.10 (s, 1, $CH-p-CH_3C_6H_4$), 4.05 (sept, 2, $^3J_{HH} = 6.8$ Hz, $CHMe_2$), 2.06 (s, 3, $CH-p-CH_3C_6H_4$), 1.34 (s, 18, $O-t-Bu$), 1.25 (d, 12, $^3J_{HH} = 6.8$ Hz, $CHMe_2$). Aryl protons could not be accurately assigned.

^{13}C NMR Data (100 MHz, d^6 -benzene, 298K): 247.94 (d of t, $CH-p-CH_3C_6H_4$, $J_{CH} = 123.3$ Hz, $J_{HH} = 4.83$ Hz), 153.28 (Ar), 149.65 (Ar), 146.22 (Ar), 143.10 (Ar), 136.65 (Ar), 128.97 (Ar), 127.38 (Ar), 123.23 (Ar), 109.25, 78.17 (s, $OCMe_3$), 31.97 (q, CH_3 , $J_{CH} = 125.72$ Hz), 29.21 (q, CH_3 , $J_{CH} = 125.12$ Hz), 28.45 (d, $CHMe_2$, $J_{CH} = 129.34$ Hz), 23.83 (q, CH_3 , $J_{CH} = 126.32$ Hz).

(c) $Mo(NAr)(CH-p-ClC_6H_4)(O-t-Bu)_2$.

1H NMR Data (400 MHz, d^6 -benzene, 298K): 11.88 (s, 1, $CH-p-ClC_6H_4$), 3.95 (sept, 2, $CHMe_2$, $^3J_{HH} = 6.80$ Hz), 1.30 (s, 18, $OCMe_3$), 1.19 (d, 12, $^3J_{HH} = 6.80$ Hz). Aryl protons could not be accurately assigned due to overlap.

^{13}C NMR Data (100 MHz, d^6 -benzene, 298K): 245.39 (d of t, $CH-p-ClC_6H_4$, $J_{CH} = 125.12$ Hz, $J_{HH} = 4.83$ Hz), 153.53 (Ar), 149.67 (Ar), 146.22 (Ar), 143.78 (Ar), 132.41 (Ar), 128.42 (Ar), 128.38 (Ar), 122.98 (Ar), 109.25, 78.55 (s, $OCMe_3$), 31.88 (q, CH_3 , $J_{CH} = 125.72$ Hz), 29.21 (q, CH_3 , $J_{CH} = 125.12$ Hz), 28.43 (d, $CHMe_2$, $J_{CH} = 129.34$ Hz), 23.77 (q, CH_3 , $J_{CH} = 125.72$ Hz).

(d) $Mo(NAr)(CH-p-CH_3OC_6H_4)(O-t-Bu)_2$.

1H NMR Data (400 MHz, d^6 -benzene, 298K): 12.06 (s, 1, $CH-p-CH_3OC_6H_4$), 4.07 (sept, 2, $^3J_{HH} = 7.1$ Hz, $CHMe_2$), 3.19 (s, 3, OMe), 1.37 (s, 18, $O-t-Bu$), 1.27 (d, 12, $^3J_{HH} = 7.1$ Hz, $CHMe_2$). Aryl protons could not be assigned due to overlap.

(e) $Mo(NAr)(CH-3,5-(CF_3)_2C_6H_3)(O-t-Bu)_2$.

1H NMR Data (400 MHz, d^6 -benzene, 298K): 11.81 (s, 1, $CH-3,5-(CF_3)_2C_6H_3$), 3.82 (sept, 2, $CHMe_2$, $^3J_{HH} = 6.90$ Hz), 1.29 (s, 18, $OCMe_3$), 1.18 (d, 12, $CHMe_2$, $^3J_{HH} = 6.90$ Hz). Aryl protons could not be unambiguously assigned due to overlap.

6.3.2 Typical NMR Scale Chain Transfer Experiment employing Norbornene.

NMR scale chain transfer reactions were performed using stock solutions of $Mo(NAr)(CH-t-Bu)(O-t-Bu)_2$ (0.1M), norbornene (1.0M) and styrene derivative (1.0M) in C_6D_6 .

Typically, 90 μ l (9.0 μ mol) of $Mo(NAr)(CH-t-Bu)(O-t-Bu)_2$ was diluted to 360 μ l with C_6D_6 and 225 μ l (225 μ mol, 25 equivalents) of norbornene solution added. The resulting mixture was stirred vigorously for 5 minutes then 90 μ l (90 μ mol, 10 equivalents) of styrene solution added. The sample was then transferred to an NMR tube, frozen immediately and sealed under nitrogen.

6.3.3 Typical Preparative Scale Chain Transfer Experiment.

Polymerizations were carried out using stock solutions of catalyst (0.1M), monomer (5.0M) and chain transfer agent (0.5M) in toluene.

45 μ l (4.5 μ mol) of $Mo(NAr)(CH-t-Bu)(O-t-Bu)_2$ solution was diluted to 721 μ l with toluene and 90 μ l (450 μ mol, 100 equivalents) norbornene solution added. This yellow solution was vigorously stirred for 8 minutes before 45 μ l (22.5 μ mol, 5 equivalents) of styrene solution added. This was stirred for a further 30 minutes to give an orange/red solution indicative of the benzylidene complex. Upon the addition of a further 180 μ l (900 μ mol, 200 equivalents) of norbornene solution the colour immediately bleached back to yellow due to the formation of living polynorbornene.

This resulting solution was stirred for a further 8 minutes, quenched via the addition of 30 μl of pivaldehyde and stirred for a further 45 minutes. The polymer was precipitated via dropwise addition into an excess of rapidly stirred methanol and dried *in vacuo* for 12 hours.

GPC data are given in table 6.1.

6.3.4 Typical Chain Transfer "Pulse" Experiment.

NMR scale chain transfer reactions were performed using stock solutions of $\text{Mo}(\text{NAr})(\text{CH-t-Bu})(\text{O-t-Bu})_2$ (0.1M), norbornene (5.0M) and styrene derivative (0.5M) in toluene.

Typically, 45 μl of $\text{Mo}(\text{NAr})(\text{CH-t-Bu})(\text{O-t-Bu})_2$ solution (4.5 μmol) was diluted to 721 μl with toluene and 90 μl (450 μmol , 100 equivalents) norbornene solution added. This yellow solution was vigorously stirred for 8 minutes before 225 μl (112.5 μmol , 25 equivalents) styrene solution added. Stirring for a further 32 minutes gave an orange solution indicative of the benzylidene complex. Upon the addition of a second pulse of norbornene solution (90 μl , 450 μmol , 100 equivalents) the colour immediately bleached back to yellow again (formation of living polynorbornene). This resulting solution was diluted with a further 720 μl toluene and stirred for 40 minutes to allow polymerization and subsequent chain transfer to occur.

Subsequent pulses of norbornene solution (90 μl , 450 μmol , 100 equivalents each pulse) were added at 40 minute intervals then the reaction quenched by the addition of 30 μl of pivaldehyde. After 45 minutes continued stirring the polymer was precipitated from excess methanol and dried *in vacuo* for 9 hours.

GPC data are given in table 6.2.

Initiator	Monomer	Monomer Equivalents	CT Agent (Equivalents)	M _m (found) (Refractometer)	PDI (Refractometer) (entire distribution)	M _m (found) (UV/VIS)	PDI (UV/VIS) (entire distribution)
Mic ^a	norbornene	100 / 200	styrene (5)	19000 41860 60300 99680	1.32 (entire distribution)	41200 92140	1.16 (entire distribution)
Mic ^a	norbornene	100 / 200	styrene (20)	19240 41200	1.05 1.07	41860 22200	1.11 1.05
Mic ^a	norbornene	200 / 100	styrene (20)	21910 38720	1.15 (entire distribution)		
Wa	norbornene	100 / 200	styrene (20)	19240 50010 442800	1.34 (entire distribution)	50850	5.49
Mob	norbornene	100 / 200	<i>p</i> -methylstyrene (20)	15760 29783	1.20 (entire distribution)		
Mic ^a	norbornene	100 / 200	<i>p</i> -methoxystyrene (20)	20840 40360	1.17 (entire distribution)	36420	1.07
Mob ^b	DCMND	100 / 200	styrene (20)	20900 47490	1.28 (entire distribution)		
Mob ^b	BTFMND	100 / 200	styrene (10)	6630, 1160 740, 371, 228	1.25 (entire distribution)		

Table 6.1 Mo = Mo(NAr)(CH-*t*-Bu)(O-*t*-Bu)₂, W = W(NAr)(CH-*t*-Bu)(O-*t*-Bu)₂

^a GPC run in CH₂Cl₂, ^b GPC run in THF.

Initiator	Monomer	Number of pulses and Equivalents	CT Agent (Equivalents)	M _n (found) (Refractometer)	PDI (Refractometer)	M _n (found) (UV/VIS)	PDI (UV/VIS)
Mo ^a	norbornene	5 x 100	styrene (25)	21910	1.10	22200	1.05
Mo ^a	norbornene	10 x 80	styrene (30)	18760 37540	1.07 1.13 (entire distribution)	19000	1.08
Mo ^b	norbornene	5 x 100	<i>p</i> -methoxystyrene (25)	17310	1.10		
Mo ^b	norbornene	5 x 100	<i>p</i> -methylstyrene (25)	17950	1.09		
Mo ^b	DCMIND	5 x 50	styrene (25)	13470	1.27		

Table 6.2 Mo = Mo(NAr)(CH-*t*-Bu)(O-*t*-Bu)₂, ^a GPC run in CH₂Cl₂, ^b GPC run in THF.

6.3.5 Reaction of $\text{Mo}(\text{NAr})(\text{CH-t-Bu})(\text{O-t-Bu})_2$ with Substituted Styrenes.

^1H NMR Determination of the Rate of Benzylidene Formation.

Typically, $\text{Mo}(\text{NAr})(\text{CH-t-Bu})(\text{O-t-Bu})_2$ (19 mg, 0.039 mmol) was dissolved in 700 μl C_6D_6 and 30 equivalents of substituted styrene added. The resulting solution was transferred to an NMR tube, immediately frozen and sealed under nitrogen. The sample was then thawed and placed in a preset and calibrated NMR probe at 303 K and allowed to equilibrate for 5 minutes. ^1H NMR spectra were collected every 20 minutes for a minimum of 15 hours. The reaction was followed by integration of the alkylidene proton resonances for the neopentylidene and benzylidene complexes, and the data treated assuming first order kinetics¹³. Errors in the rate constants were calculated by an average of three determinations.

Observed rate constants are given in chapter 3 (table 3.2).

6.4 Experimental Details to Chapter Four.

6.4.1 Reaction of $\text{Mo}(\text{NAr})_2\text{Cl}_2(\text{dme})$ with Li-O-t-Bu

Preparation of $\text{Mo}(\text{NAr})_2(\text{O-t-Bu})_2$ (2).

To a mixture of $\text{Mo}(\text{NAr})_2\text{Cl}_2(\text{dme})$ (4.25 g, 7.0 mmol) and Li-O-t-Bu (1.12 g, 14.0 mmol) was added dropwise 80 ml cold (-78°C) Et_2O . The resulting mixture was allowed to warm to room temperature and stirred for 14 hours. Filtration followed by removal of volatiles *in vacuo* yielded an orange solid. This was purified by recrystallization from Et_2O at -78°C to give orange crystals of $\text{Mo}(\text{NAr})_2(\text{O-t-Bu})_2$ (2) (3.27 g, 69%). This compound has also been prepared independently by Schrock and co-workers¹⁴.

$^1\text{H NMR Data}$ (400 MHz, d^6 -benzene, 298K): 7.01 (d, 2, $^3J_{\text{HH}} = 7.80$ Hz, H_m), 6.93 (t, 1, $^3J_{\text{HH}} = 7.80$ Hz, H_p), 3.84 (sept, 4, $^3J_{\text{HH}} = 6.80$ Hz, CHMe_2), 1.42 (s, 18, O-*t*-Bu), 1.19 (d, 24, $^3J_{\text{HH}} = 6.80$ Hz, CHMe_2).

$^{13}\text{C NMR Data}$ (100 MHz, d^6 -benzene, 298K): 153.9 (C_{ipso}), 142.8 (C_{ortho}), 127.0 (C_{meta}), 80.2 (OCMe_3), 32.1 (OCMe_3), 28.6 (CHMe_2), 23.7 (CHMe_2).

Infrared Data (Nujol, CsI, cm^{-1}): 3050 (w), 1430 (s), 1365 (vs), 1340 (s, sh), 1330 (s), 1280 (s), 1165 (br, s), 1115 (w, sh), 1110 (m), 1060 (w), 1045 (w), 985 (s), 930 (vs, br), 905 (vs), 798 (s), 785 (vs), 755 (vs), 600 (m), 580 (m, br), 380 (w), 368 (m).

Elemental Analysis for $\text{MoN}_2\text{O}_2\text{C}_{32}\text{H}_{52}$ (592.75): Found (Required): %C 65.00 (64.85); %H 8.81 (8.84); %N 4.59 (4.73).

Mass Spectral Data (EI^+ , isobutane carrier gas, m/z , ^{98}Mo): 594 $[\text{M}]^+$, 482 $[\text{M} - \text{C}_4\text{H}_{16}]^+$.

6.4.2 Reaction of $\text{Mo}(\text{O})_2\text{Cl}_2$ with Li-O-*t*-Bu

Preparation of $\text{Mo}(\text{O})_2(\text{O}-t\text{-Bu})_2$ (3).

To a mixture of $\text{Mo}(\text{O})_2\text{Cl}_2$ (1.59 g, 8.0 mmol) and Li-O-*t*-Bu (1.28 g, 16.0 mmol) was added dropwise 100 ml cold (-78°C) Et_2O . The resulting mixture was allowed to warm to room temperature and stirred for 2 hours. Filtration, followed by removal of volatiles *in vacuo* gave $\text{Mo}(\text{O})_2(\text{O}-t\text{-Bu})_2$ (3) as a colourless oil. Yield 0.79 g (36%). The product may be purified by recrystallization from Et_2O at -78°C to give a white solid that melts upon warming to room temperature or by vacuum distillation (55°C at 10^{-4} torr).

^1H NMR Data (400 MHz, d^6 -benzene, 298K): 1.15 (O-*t*-Bu)

^{13}C NMR Data (100 MHz, d^6 -benzene, 298K): 85.63 (OCMe₃), 30.44 (OCMe₃)

Infrared Data (Neat, CsI, cm^{-1}): 2960 (vs), 2923 (s), 2865 (m), 1470 (m, sh), 1460 (m), 1395 (m), 1369 (vs), 1245 (s), 1150 (vs, br), 792 (vs, sp), 595 (m, br), 465 (m, br), 383 (m), 359 (w), 329 (w).

Elemental Analysis: for MoO₄C₈H₁₈ (274.17) Found (Required) : %C 35.32 (35.05); %H 6.73 (6.62).

Mass Spectral Data (EI⁺, isobutane carrier gas, m/z , ^{98}Mo): 475 [2M - *t*-BuOH]⁺, 419 [2M - *t*-Bu-O-*t*-Bu]⁺, 360 [2M - *t*-Bu-O-*t*-Bu - C₄H₁₀]⁺, 277 [M + H]⁺, 261 [M - O]⁺, 205 [M - C₄H₉]⁺, 131 [*t*-Bu-O-*t*-Bu]⁺, 75 [*t*-BuOH]⁺, 59 [C₄H₁₀]⁺.

6.4.3 Reaction of Mo(NAr)₂(O-*t*-Bu)₂ (2) with Mo(O)₂(O-*t*-Bu)₂ (3).

*Determination of the Rate of Equilibration with Mo(NAr)(O)(O-*t*-Bu)₂ (1)*

Typically, a C₆D₆ solution of Mo(NAr)₂(O-*t*-Bu)₂ (2) (25.0 mg, 0.042 mmol in 420 μl) was added to a C₆D₆ solution of Mo(O)₂(O-*t*-Bu)₂ (3) (12.0 mg, 0.044 mmol in 420 μl). The resulting mixture was transferred to an NMR tube, frozen immediately and sealed under nitrogen. The tube remained frozen until the kinetic run commenced. The reaction was monitored at 293, 303, 313 and 323 K by integration of the arylimido methine protons at 4.33 ppm (oxo imido) and 3.84 ppm (*bis* imido). Data were collected every 20 minutes and treated as a second order reversible process¹⁵. Errors are calculated from an average of three determinations.

Rate constants ($l\ mol^{-1}\ s^{-1}$) 293 K, $k_1 = 2.1\ (3) \times 10^{-7}$, 303 K, $k_1 = 7.3\ (5) \times 10^{-7}$, 313 K, $k_1 = 24\ (5) \times 10^{-7}$, 323 K, $k_1 = 59\ (4) \times 10^{-7}$.

From an Arrhenius Plot of $\ln k_1/T$ vs $1/T$ ($\rho = 0.998$) $\Delta H^\ddagger = 20.6\ (4)\ kcal\ mol^{-1}$, $\Delta S^\ddagger = -19\ (2)\ e.u.$, $\Delta G^\ddagger\ (298\ K) = 26.2\ (5)\ kcal\ mol^{-1}$, $A = 21.1$, $E_a = 21.2\ (1.0)\ kcal\ mol^{-1}$

6.4.4 1H NMR Investigation of $Mo(NAr)_2(O-t-Bu)_2$ (2) Reactivity.

Typically, $Mo(NAr)_2(O-t-Bu)_2$ (2) (15 mg, 0.025 mmol) was dissolved in 420 μl C_6D_6 and a solution of reagent (number of equivalents for each reagent shown below) in 420 μl C_6D_6 added. The resulting mixture was transferred to an NMR tube, frozen immediately and sealed under nitrogen. The reaction was monitored by 1H NMR spectroscopy, first at room temperature and then at elevated temperature as detailed in chapter 4.

The reaction with oxygen involved sealing a solution of $Mo(NAr)_2(O-t-Bu)_2$ (15 mg, 0.025 mmol in 840 μl C_6D_6) in an NMR tube under one atmosphere of dry oxygen.

The reaction with deoxygenated water was undertaken by stoppering the NMR tube with a septum suba-seal and injecting the water from a microlitre syringe through this seal outside the dry-box.

Reagents Used

$Mo(N-t-Bu)_2(O-t-Bu)_2$ (1.0 equivalent), $t-BuNH_2$ (9.9 equivalents), $PhCHO$ (10.1 equivalents), $PhNCO$ (1.0 equivalent, 10.0 equivalents), $t-BuNCO$ (9.9 equivalents), O_2 (1 atmosphere), $PhCH=N-t-Bu$ (10.2 equivalents), $Ph_3P=CHPh$ (0.9 equivalents), $PhNO_2$ (5.0 equivalents), $PhN=NPh$ (1.0 equivalent),

t-BuOH (4.4 equivalents), TMSN₃ (3.0 equivalents), H₂O (2.0 equivalents), PMe₃ (3.0 equivalents).

6.4.5 Reaction of Mo(NAr)₂(O-*t*-Bu)₂ (2) with PhNCO

*Preparation of Mo[N(Ar)C(O)N(Ph)]₂(O-*t*-Bu)₂ (14).*

To a stirring solution of Mo(NAr)₂(O-*t*-Bu)₂ (2) (450 mg, 0.759 mmol) in 40 cm³ pentane was added, via syringe, PhNCO (1104 mg, 10.17 mmol, 13.4 equivalents). The solution went dark brown immediately, but lightened to a deep red colour upon stirring at room temperature for 19 hours. The solution was filtered, reduced in volume to 10 cm³ and chilled to -78°C to afford a crop of red crystals that were collected and dried *in vacuo*. Yield 353 mg (56%).

¹H NMR Data (400 MHz, d⁶-benzene, 298K): 7.59 (d, 4, ³J_{HH} = 7.5 Hz, *ArH*), 6.7 - 7.0 (overlapping multiplets, *ArH*), 3.76 (sept, 4, ³J_{HH} = 6.4 Hz, CHMe₂), 1.43 (s, 18, O-*t*-Bu), 1.13 (d, br, 12, ³J_{HH} = 5.6 Hz, CHMe₂), 0.96 (d, br, 12, ³J_{HH} = 6.4 Hz, CHMe₂).

¹³C NMR Data (100 MHz, d⁶-benzene, 298K): 227.24 (s, CO), 163.71, 153.88, 145.22, 142.61, 125.81, 125.30, 124.29, 122.49, 82.44 (OCMe₃), 28.22, 28.15, 23.68.

Infrared Data (Nujol, CsI, cm⁻¹): 3050 (m), 2275 (w), 2260 (w), 1600 (m), 1585 (w) 1540 (s, sh), 1530 (vs), 1500 (s), 1435 (vs), 1420 (vs), 1328 (m), 1275 (vs), 1250 (m), 1160 (s), 1055 (s), 1023 (m), 979 (m), 945 (w), 930 (w), 830 (m), 795 (m), 855 (vs), 848 (vs), 695 (s), 662 (s), 515 (m), 375 (m), 350 (m).

Elemental Analysis for MoN₄O₄C₄₆H₆₂ (830.96): Found (required): %C 66.20 (66.49); %H 7.54 (7.52); %N 6.60 (6.74).

Mass Spectral Data (CI, isobutane carrier gas, m/z, ^{98}Mo): 594 [M - 2PhNCO] $^-$, 537 [M - 2 PhNCO - C₄H₉] $^-$, 178 [ArNH₂] $^-$, 119 [PhNCO] $^-$.

6.4.6 Alkoxide Exchange in Four Coordinate Molybdenum Alkylidene Complexes

6.4.6a Reaction of Mo(NAr)(CHCMe₂Ph)(O-*t*-Bu)₂ (15) with
Mo(NAr)(CHCMe₂Ph)(OCMe(CF₃)₂)₂ (16).

*Preparation of Mo(NAr)(CHCMe₂Ph)(OCMe(CF₃)₂)(O-*t*-Bu) (17).*

Pentane (5 cm³) was added to a mixture of Mo(NAr)(CHCMe₂Ph)(O-*t*-Bu)₂ (15) (72.5 mg, 0.132 mmol) and Mo(NAr)(CHCMe₂Ph)(OCMe(CF₃)₂)₂ (16) (101.5 mg, 0.133 mmol). The resultant solution was stirred at room temperature for 5 minutes then chilled to -78°C to yield orange crystals of Mo(NAr)(CHCMe₂Ph)(OCMe(CF₃)₂)(O-*t*-Bu) (17), which were collected and dried *in vacuo*. Yield 106 mg (61%).

¹H NMR Data (400 MHz, d⁶-benzene, 298K): 11.71 (s, 1, CHCMe₂Ph), 7.29 (d, 2, aromatic), 6.90 - 7.11 (overlapping multiplets, aromatic), 3.77 (sept, 2, ³J_{HH} = 6.8 Hz, CHMe₂), 1.62 (s, 3, CHCMe₂Ph), 1.58 (s, 3, CHCMe₂Ph), 1.22 (d, 12, ³J_{HH} = 6.8 Hz, CHMe₂), 1.18 (s, 9, O-*t*-Bu).

¹³C NMR Data: (100 MHz, d⁶-benzene, 298K): 274.02 (m, CHCMe₂Ph), 153.42, 148.91, 147.91, 146.80, 126.30, 126.05, 125.90, 123.30, 79.99, 53.76, 31.95, 31.56, 31.18, 30.73, 28.46, 24.09, 23.77, 23.57, 19.08.

Elemental Analysis for MoNO₂F₆C₃₀H₄₁ (657.59) Found (Required): %C 55.40 (54.80); %H 6.51 (6.28); %N 2.08 (2.13).

Mass Spectral Data (CI^+ , isobutane carrier gas, m/z , ^{98}Mo): 660 $[\text{M}]^+$, 586 $[\text{M} - t\text{-BuOH}]^+$, 527 $[\text{M} - \text{CMe}_2\text{Ph}]^+$, 478 $[\text{M} - \text{CMe}(\text{CF}_3)_2\text{OH}]^+$, 342 $[\text{M} - \text{CMe}(\text{CF}_3)_2\text{OH} - \text{PhCMe}_3]^+$, 264 $[(\text{PhCMe}_2\text{CH})_2]^+$.

6.4.6b ^1H NMR Investigations of Alkoxide Exchange in Four-Coordinate Alkylidene Complexes.

Typically $\text{Mo}(\text{NAr})(\text{CHCMe}_2\text{Ph})(\text{O}-t\text{-Bu})_2$ (20 mg, 0.041 mmol) was dissolved in 840 μl C_6D_6 and this solution added to an equimolar amount of $\text{Mo}(\text{NAr})(\text{CHCMe}_2\text{Ph})(\text{OCMe}(\text{CF}_3)_2)_2$ (31 mg, 0.040 mmol). The resulting mixture was transferred to an NMR tube, frozen immediately and sealed under nitrogen. The reaction was then followed by ^1H NMR spectroscopy.

To test *relative* thermal stabilities of these alkylidene complexes, a 1.5 fold equivalents excess of either complex was used.

To test *relative* stabilities to oxygen, the above procedure was performed but the NMR tube was sealed under one atmosphere of dry oxygen instead of nitrogen.

6.4.7 ^1H NMR Investigation of Alkylidene Exchange in Four-Coordinate Alkylidene Complexes

The reactivity of the alkylidene moiety in various four coordinate alkylidene complexes was undertaken as described generally below.

Typically, approximately 15 mg of alkylidene complex was dissolved in 840 μl C_6D_6 and this added to an equimolar amount of reagent listed below. The resulting mixture was transferred to an NMR tube, frozen immediately and sealed under nitrogen. The subsequent reaction was monitored by ^1H NMR spectroscopy at the temperatures detailed in Chapter 4.

Reagents used

Mo(NAr)(CH-*t*-Bu)(O-*t*-Bu)₂, Mo(NAr)(CHCMe₂Ph)(OCMe(CF₃)₂)₂, W(NAr)(CH-*t*-Bu)(O-*t*-Bu)₂, Mo(O)₂(O-*t*-Bu)₂, Mo(N-*t*-Bu)₂(O-*t*-Bu)₂, Mo(NAr)₂(O-*t*-Bu)₂, *t*-BuNH₂.

NMR Characterizing Data for:

syn-Mo(NAr)(CHCMe₂Ph)(OCMe(CF₃)₂)₂(*t*-BuNH₂).

¹H NMR Data (400 MHz, d⁶-benzene, 298K): 12.50 (s, 1, CHCMe₂Ph), 7.23 (d, ³J_{HH} = 7.23 Hz, ArH), 7.07 (t, ³J_{HH} = 7.07 Hz, ArH), 6.95 (s, ArH), 3.75 (sept, 2 ³J_{HH} = 6.80 Hz, CHMe₂), 1.61 (s, 6, CHMe₂Ph), 1.24 (d, 12, ³J_{HH} = 6.80 Hz, CHMe₂), 0.85 (s, 9, *t*-BuNH₂). Resonances for OCMe(CF₃)₂, and *t*-BuNH₂ could not be identified.

¹³C NMR Data (100 MHz, d⁶-benzene, 298K): 294.07 (s, CHCMe₂Ph), 152.67, 148.13, 147.61, 129.36, 128.69, 126.67, 123.57, 124.06, 81.00 (OCMe(CF₃)₂), 55.54, 31.64, 31.05, 30.89, 28.51, 24.11, 18.08.

anti-Mo(NAr)(CHCMe₂Ph)(OCMe(CF₃)₂)₂(*t*-BuNH₂).

¹H NMR Data (400 MHz, d⁶-benzene, 298 K): 13.37 (s, CHCMe₂Ph), 7.32 (d, ³J_{HH} = 7.60 Hz, ArH), 7.07 (t, ³J_{HH} = 7.20 Hz, ArH), 6.91 (s, ArH), 4.45 (sept, 1, CHMe₂), 3.57 (sept, 1, ³J_{HH} = 6.40 Hz, CHMe₂), 2.51 (m, 2, *t*-BuNH₂), 2.12 (s, 3, OCMe(CF₃)₂), 2.00 (s, 3, OCMe(CF₃)₂), 1.46 (s, 3, CHCMe₂Ph), 1.41 (s, 3, CHCMe₂Ph), 1.30 (d, 6, ³J_{HH} = 6.40 Hz, CHMe₂), 1.18 (d, 6, ³J_{HH} = 6.60 Hz, CHMe₂), 0.36 (s, 9, *t*-BuNH₂).

¹³C NMR Data (100 MHz, d⁶-benzene, 298K): 306.52 (d, J_{CH} = 144.6 Hz, CHCMe₂Ph), 153.29, 148.22, 147.72, 145.15, 129.17, 126.63, 126.16, 124.06, 123.57, 80.25 (sept, ²J_{CF} = 27.76 Hz, OCMe(CF₃)₂), 81.71 (sept, ²J_{CF} = 27.76 Hz, OCMe(CF₃)₂), 51.67, 50.71, 31.16, 30.03, 29.05, 27.58, 24.63, 24.43.

The reactivity toward dry dioxygen was undertaken by sealing the NMR tube under one atmosphere of cylinder dioxygen.

The reactivity of a living oligomer of norbornene toward oxygen was undertaken as follows.

To a stirring solution of Mo(NAr)(CH-t-Bu)(O-t-Bu)₂ (10 mg, 0.021 mmol) in 400 μl C₆D₆ was added a C₆D₆ solution of norbornene (22 mg, 0.234 mmol in 400 μl, 11.1 equivalents) and the resulting mixture stirred for 5 minutes. This was then sealed under nitrogen in an NMR tube and the ¹H NMR spectrum determined. The tube was then cracked open in the glove box and the solution resealed in a fresh NMR tube under one atmosphere of dry oxygen; remaining frozen till the ¹H NMR spectrum could again be acquired.

6.5 Experimental Details to Chapter Five

6.5.1 Reaction of Cp^oNbCl₄ with (TMS)₂NMe

Preparation of Cp^oNb(NMe)Cl₂

A solution of (TMS)₂NMe (280 mg, 1.90 mmol) in 10 cm³ 1,2-dichloroethane was added to a stirring suspension of Cp^oNbCl₄ (700 mg, 1.89 mmol) in 30 cm³ 1,2-dichloroethane and the resulting mixture stirred at 80 °C for 20 hours. Volatiles were then removed *in vacuo* to give a dark orange solid. Recrystallization from a minimum amount of pentane gave the product as light orange crystals which were collected and dried *in vacuo*. Yield 304 mg (49%).

$^1\text{H NMR Data}$ (250 MHz, d^6 -benzene, 298K): 3.25 (s, 3, NMe), 1.77 (s, 15, C_5Me_5)

$^{13}\text{C NMR Data}$ (100 MHz, d^6 -benzene, 298K): 122.2 (C_5Me_5), 49.1 (NMe), 11.3 (C_5Me_5).

Elemental Analysis for $\text{NbNCl}_2\text{C}_{11}\text{H}_{18}$ (328.08) Found (Required): %C 40.18 (40.27); %H 5.62 (5.53); %N 3.79 (4.27).

Infrared Data (Nujol, CsI , cm^{-1}): 1258 (m), 1029 (w, br), 745 (w, sh), 728 (w), 592 (w), 449 (m), 410 (m), 389 (s), 340 (w)

Mass Spectral Data (CI^+ , isobutane carrier gas, m/z , ^{35}Cl): 327 $[\text{M}]^+$, 298 $[\text{M} - \text{NMe}]^+$, 135 $[\text{C}_5\text{Me}_5]^+$.

6.5.2 Reaction of Cp^*NbCl_4 with ArNHTMS

Preparation of $\text{Cp}^\text{Nb}(\text{NAr})\text{Cl}_2$*

To a 1,2-dichloroethane suspension of Cp^*NbCl_4 (7.10 g, 19.2 mmol in 100 cm^3) was added a solution of ArNHTMS (9.57 g, 38.4 mmol) in 50 cm^3 1,2-dichloroethane and the resulting mixture stirred at 80°C for 48 hours. After cooling to room temperature the volatile components were removed under reduced pressure and the resultant oily red solid washed with 30 cm^3 pentane. Recrystallization of this crude product from toluene afforded a crop of shiny dark red crystals which were collected and dried *in vacuo*. Yield 6.63 g (73%).

$^1\text{H NMR Data}$ (400 MHz, d^6 -benzene, 298K): 7.03 (d, 2, $^3J_{\text{HH}} = 7.6$ Hz, H_m), 6.92 (t, 1, $^3J_{\text{HH}} = 7.6$ Hz, H_p), 3.52 (sept, 2, $^3J_{\text{HH}} = 6.8$ Hz, CHMe_2), 1.78 (s, 15, C_5Me_5), 1.29 (d, 12, $^3J_{\text{HH}} = 6.8$ Hz, CHMe_2).

^{13}C NMR Data (100 MHz, d^6 -benzene, 298K): 148.9 (Ar), 145.6 (Ar), 125.8 (Ar), 123.3 (C_5Me_5), 122.7 (Ar), 28.5 (CHMe_2), 24.3 (CHMe_2), 11.6 (C_5Me_5)

Infrared Data (Nujol, CsI , cm^{-1}): 1570 (w), 1330 (s), 1285 (s), 1110 (m), 1030 (m), 985 (m), 805 (s), 760 (vs), 460 (m), 445 (m), 390 (s), 375 (vs), 360 (s), 320 (m)

Elemental Analysis for $\text{NbNCl}_2\text{C}_{22}\text{H}_{32}$ (474.32) Found (Required): %C 56.08 (55.71); %H 7.26 (6.80); %N 2.55 (2.95)

Mass Spectral Data (Cl^+ , isobutane carrier gas, m/z , ^{35}Cl): 473 [M] $^+$, 298 [$\text{M} - \text{NAr}$] $^+$, 177 [ArNH_2] $^+$, 166 [ArH] $^+$.

6.5.3 Reaction of Cp^*TaCl_4 with ArNHTMS

Preparation of $\text{Cp}^\text{Ta}(\text{NAr})\text{Cl}_2$*

To a stirring suspension of Cp^*TaCl_4 (0.556 g, 1.22 mmol) in 20 cm^3 1,2-dichloroethane was added a solution of ArNHTMS (0.606 g, 2.43 mmol) in 10 cm^3 1,2-dichloroethane. The resulting mixture was stirred at 80°C for 10 days, to give an orange solution. Filtration, followed by removal of volatiles *in vacuo* yielded an orange solid. This was washed with 20 cm^3 pentane and extracted with 20 cm^3 toluene. Chilling this toluene solution to -78°C overnight gave orange crystals which were collected and dried *in vacuo*. Yield 491 mg (72%).

^1H NMR Data (400 MHz, d^6 -benzene, 298K): 7.16 (d, 2, $^3J_{\text{HH}} = 7.6$ Hz, H_m), 6.87 (t, 1, $^3J_{\text{HH}} = 7.6$ Hz, H_p), 3.53 (sept, 2, $^3J_{\text{HH}} = 6.8$ Hz, CHMe_2), 1.86 (s, 15, C_5Me_5), 1.33 (d, 12, $^3J_{\text{HH}} = 6.8$ Hz, CHMe_2).

^{13}C NMR Data (100 MHz, d^6 -benzene, 298K): 148.28 (s, C_{ipso}), 145.46 (s, C_{ortho}), 124.97 (d, $J_{\text{CH}} = 157.9$ Hz, C_{para}), 122.25 (d, $J_{\text{CH}} = 144.2$ Hz, C_{meta}), 121.39 (s, C_5Me_5), 28.16 (d, $J_{\text{CH}} = 127.0$ Hz, CHMe_2), 24.44 (q, $J_{\text{CH}} = 129.6$ Hz, CHMe_2), 11.22 (q, $J_{\text{CH}} = 128.1$ Hz, C_5Me_5)

Infrared Data (Nujol, CsI, cm^{-1}): 3040 (w), 2845 (vs), 1439 (s), 1350 (vs), 1300 (m), 1260 (w), 1253 (w), 1161 (w), 1110 (m), 990 (m, sp), 937 (w), 805 (s, sp), 762 (vs, sp), 725 (w, br), 460 (w), 441 (w), 373 (m, sp), 357 (s, sp)

Elemental Analysis for $\text{TaNCl}_2\text{C}_{22}\text{H}_{32}$ (562.36) Found (Required): %C 47.43 (46.99); %H 5.77 (5.74); %N 2.21 (2.49).

Mass Spectral Data (Cl^+ , isobutane carrier gas, m/z, ^{35}Cl , ^{181}Ta) 561 $[\text{M}]^+$, 546 $[\text{M} - \text{Me}]^+$, 386 $[\text{M} - \text{NAr}]^+$, 177 $[\text{ArNH}_2]^+$, 162 $[\text{ArH}]^+$.

6.5.4 ^1H NMR Investigation of Imido Exchange

The following procedure described below is for the reaction of $\text{CpNb}(\text{NMe})\text{Cl}_2$ with $\text{Cp}^*\text{Nb}(\text{NAr})\text{Cl}_2$, but is applicable for all analogous reactions described in chapter five.

Typically, 10 mg (0.039 mmol) of $\text{CpNb}(\text{NMe})\text{Cl}_2$ was dissolved in 840 μl C_6D_6 and this solution added to 18 mg (0.038 mmol) of $\text{Cp}^*\text{Nb}(\text{NAr})\text{Cl}_2$. The resulting mixture was transferred to an NMR tube and sealed under nitrogen. The reaction was monitored by ^1H NMR spectroscopy at the temperatures described in Chapter 5, equilibrium constants being calculated by careful integration of the ^1H NMR resonances of each species present at equilibrium.

6.5.5 Preparation of $\text{CpTa}(\text{CHCMe}_2\text{Ph})\text{Cl}_2$ (15).

6.5.5a Reaction of ZnCl_2 with $\text{PhCMe}_2\text{CH}_2\text{MgCl}$

Preparation of $\text{Zn}(\text{CH}_2\text{CMe}_2\text{Ph})_2$ (17).

The Grignard reagent was prepared by refluxing for 2 hours a stirred solution of $\text{PhCMe}_2\text{CH}_2\text{Cl}$ (100 cm^3 , 0.621 mol) in 800 cm^3 diethylether containing magnesium turnings (16g, 0.658 mol, slight excess) and then stirring at room temperature for a further 24 hours. The solution was cooled to 0°C and ZnCl_2 (42.8 g, 0.314 mol) added slowly as a solid so that the temperature did not exceed 30°C . The solution was stirred at room temperature for 18 hours and clouded as MgCl_2 precipitated out of solution. Filtration, followed by removal of volatiles *in vacuo* afforded the product as a pale yellow liquid. Yield 68.9 g (67%).

$^1\text{H NMR Data}$ (400 MHz, d^6 -benzene, 298K): 7.00 - 7.26 (overlapping multiplets, 10, *ArH*), 1.21 (s, 12, $\text{CH}_2\text{CMe}_2\text{Ph}$), 0.64 (s, 4, $\text{CH}_2\text{CMe}_2\text{Ph}$)

$^{13}\text{C NMR Data}$ (100 MHz, d^6 -benzene, 298K): 154.19, 128.58, 126.15 ($\text{CH}_2\text{CMe}_2\text{Ph}$), 125.55 (C_{ring}), 125.06 (C_{ring}), 38.04 ($\text{CH}_2\text{CMe}_2\text{Ph}$), 34.7 ($\text{CH}_2\text{CMe}_2\text{Ph}$)

6.5.5b Reaction of TaCl_5 with $\text{Zn}(\text{CH}_2\text{CMe}_2\text{Ph})_2$ (17).

Preparation of $\text{Ta}(\text{CH}_2\text{CMe}_2\text{Ph})_2\text{Cl}_3$ (18).

A toluene solution of $\text{Zn}(\text{CH}_2\text{CMe}_2\text{Ph})_2$ (16.67 g, 0.050 mol in 30 cm^3) was added dropwise over 30 minutes to a rapidly stirring suspension of TaCl_5 (18.03 g, 0.050 mol) in 500 cm^3 toluene. The resulting mixture was stirred at room temperature for 18 hours and changed from orange to brown as ZnCl_2 precipitated out of solution. The toluene was filtered off and the residue washed with further toluene ($2 \times 100\text{ cm}^3$).

The extracts were combined and volatiles removed *in vacuo* to give a dark brown oil. The oil was taken up into 50 cm³ pentane to which some activated decolourising charcoal was added. Filtration gave a canary yellow solution, which afforded a pale yellow oil upon removal of the pentane *in vacuo*. Yield 16.5 g (59%). ¹H NMR spectroscopic analysis of the product revealed approximately 5% contamination by what is believed to be Ta(CH₂CMe₂Ph)₃Cl₂. Upon standing in the light for several days, the product is observed to darken in colour and several new resonances can be seen in the ¹H NMR spectrum.

¹H NMR Data (400 MHz, d⁶-benzene, 298K): 6.97 - 7.28 (overlapping multiplets, 10, CH₂CMe₂Ph), 2.97 (s, 4, CH₂CMe₂Ph), 1.39 (s, 12, CH₂CMe₂Ph)

¹³C NMR Data (100 MHz, d⁶-benzene, 298K): 150.91, 128.74, 126.66, 125.89, 123.06 (CHCMe₂Ph), 43.19 (CHCMe₂Ph), 33.57 (CHCMe₂Ph)

6.5.5c Reaction of Ta(CH₂CMe₂Ph)₂Cl₃ (18) with TiCp

Preparation of CpTa(CHCMe₂Ph)Cl₂ (15).

To a stirring solution of Ta(CH₂CMe₂Ph)₂Cl₃ (14.36 g, 0.026 mol) in 300 cm³ toluene was added solid TiCp (7.37 g, 0.027 mol) over a period of 30 minutes and the resulting mixture stirred for 18 hours. The solution changed from yellow to brick red as TiCl precipitated out of solution. This solid was isolated by filtration, washed with toluene (2 x 20 cm³) and the extracts combined. Removal of volatiles *in vacuo* afforded a deep red oil which was taken back up into diethyl ether (40 cm³). Filtration, followed by removal of volatiles *in vacuo* again afforded a red oil which upon washing with chilled (-78°C) pentane (2 x 10 cm³) gave the product as a brick red crystalline solid. Yield 7.95 g (68%).

^1H NMR Data (400 MHz, d^6 -benzene, 298K): 7.06 - 7.33 (overlapping multiplets, 5, CHCMe_2Ph), 6.88 (s, 1, CHCMe_2Ph), 5.41 (s, 5, C_5H_5), 1.25 (s, 6, CHCMe_2Ph)

^{13}C NMR Data (100 MHz, d^6 -benzene, 298K): 244.36 (d, $J_{\text{CH}} = 81.97$ Hz, CHCMe_2Ph), 150.87 (s, C_{ipso}), 129.15 (d, C_{ortho}), 126.64 (d, C_{meta}), 126.39 (d, C_{para}), 107.14 (d, $J_{\text{CH}} = 180.0$ Hz, C_5H_5), 53.53 (s, CHCMe_2Ph), 32.63 (q, $J_{\text{CH}} = 127.3$ Hz, CHCMe_2Ph)

Infrared Data (Nujol, CsI , cm^{-1}): 3100 (m, br), 3059 (w), 3010 (w), 2860 (w), 2615 (m), 2520 (m), 2495 (m, sh), 1775 (m, br), 1680 (m, br), 1602 (s, sp), 1585 (m), 1495 (s), 1465 (s, sh), 1385 (m), 1315 (m), 1255 (m), 1185 (s, br), 1108 (m), 1075 (m), 1030 (s), 1015 (s), 830 (s, br), 770 (m, br), 700 (m, br), 620 (w), 575 (s, br), 500 (m, br), 340 (vs, br).

Elemental Analysis for $\text{TaCl}_2\text{C}_{15}\text{H}_{17}$ Found (Required): %C 40.82 (40.11); %H 4.12 (3.81)

Mass Spectral Data (Cl^+ , isobutane carrier gas, m/z , ^{35}Cl , ^{181}Ta) 449 [$\text{M} + \text{H}$] $^+$, 413 [$\text{M} - \text{Cl}$] $^+$, 350 [$\text{M} - 2\text{Me}$] $^+$, 316 [$\text{M} - \text{CHCMe}_2\text{Ph}$] $^+$, 134 [PhCMe_3] $^+$, 119 [PhCMe_2] $^+$.

6.5.6 ^1H NMR Investigation of the Alkylidene Exchange Reactivity of $\text{CpTa}(\text{CHCMe}_2\text{Ph})\text{Cl}_2$ (15).

The reaction of $\text{CpTa}(\text{CHCMe}_2\text{Ph})\text{Cl}_2$ (15) toward a variety of reagents was undertaken as described generally below.

Typically, a C_6D_6 solution of $\text{CpTa}(\text{CHCMe}_2\text{Ph})\text{Cl}_2$ (10 mg, 0.022 mmol in 420 μl) was added to a solution of the reagent listed below in 420 μl C_6D_6 . The resulting mixture was transferred to an NMR tube, frozen immediately and sealed under

nitrogen. The reaction was then monitored by ^1H NMR spectroscopy at the temperatures detailed in Chapter 5.

Reagents Used

$\text{Cp}^*\text{Ta}(\text{NAr})\text{Cl}_2$ (1.00 equivalent), $\text{Cp}^*\text{Nb}(\text{NAr})\text{Cl}_2$ (1.04 equivalents), $\text{Mo}(\text{N-t-Bu})_2\text{Cl}_2$ (1.03 equivalents), $\text{Mo}(\text{N-t-Bu})_2(\text{O-t-Bu})_2$ (1.04 equivalents), $\text{Mo}(\text{NAr})_2(\text{O-t-Bu})_2$ (0.93 equivalents), Li-O-t-Bu (2.01 equivalents).

6.6 Further Experimental Details.

6.6.1 Preparation of $\text{Mo}(\text{NAr})(\text{CH-t-Bu})(\text{O-t-Bu})_2$

6.6.1a Preparation of $\text{Mo}(\text{NAr})_2\text{Cl}_2(\text{dme})$.

$\text{Mo}(\text{O})_2\text{Cl}_2$ (10.00 g, 0.05 mol) was added to rapidly stirring dimethoxyethane at -30°C over a period of 30 minutes. To the resulting mixture were added the following in succession :- a solution of 2,6-lutidine (11.7 cm^3 , 0.10 mol) in dme (20 cm^3 , -30°C) over a period of ten minutes, a solution of chlorotrimethylsilane (25.5 cm^3 , 0.20 mol) in dme (30 cm^3 , -30°C) over a period of 5 minutes and a solution of N-(trimethylsilyl)-2,6-di-isopropylaniline (25.09 g, 0.10 mol) in dme (50 cm^3 , -30°C). The colour changed from grey / blue to deep red as a precipitate formed. The resulting mixture was allowed to warm to room temperature and stirred for six hours. The solution was then removed by filtration and the resulting precipitate washed with diethylether ($2 \times 100\text{ cm}^3$). The extracts were combined and volatile components removed *in vacuo* to give the product as a brick red solid that need not be purified further. Yield 28.49 g (93%).

6.6.1b Reaction of $\text{Mo}(\text{NAr})_2\text{Cl}_2(\text{dme})$ with $\text{Me}_3\text{CCH}_2\text{MgCl}$.

Preparation of $\text{Mo}(\text{NAr})_2(\text{CH}_2\text{CMe}_3)_2$.

An ethereal solution of neopentylmagnesium chloride (53.2 cm^3 , 1.80M, 0.10 mol) in 20 cm^3 diethylether was added dropwise over a period of twenty minutes to a stirred solution of $\text{Mo}(\text{NAr})_2\text{Cl}_2(\text{dme})$ (28.49 g, 0.05 mol) in 300 cm^3 Et_2O at -30°C . The resulting mixture was stirred at room temperature for 12 hours, before the solution was filtered and the remaining precipitate (MgCl_2) washed with pentane ($3 \times 30 \text{ cm}^3$). The extracts were combined and volatile components removed *in vacuo* to give the product as an orange solid. Recrystallization from pentane at -78°C gave 19.48 g (71%) of analytically pure orange crystals.

6.6.1c Reaction of $\text{Mo}(\text{NAr})_2(\text{CH}_2\text{CMe}_3)_2$ with $\text{CF}_3\text{SO}_3\text{H}$.

Preparation of $\text{Mo}(\text{NAr})(\text{CH-}i\text{-Bu})(\text{OSO}_2\text{CF}_3)_2(\text{dme})$.

Chilled trifluoromethanesulphonic acid (3.2 cm^3 , 0.04 mmol, -30°C) was added to pre-chilled dimethoxyethane (20 cm^3 , -30°C) and the resulting solution added dropwise over a period of 15 minutes to a stirred solution of $\text{Mo}(\text{NAr})_2(\text{CH}_2\text{CMe}_3)_2$ (7.02 g, 0.01 mmol) in 200 cm^3 dme at -30°C . A purple colouration may sometimes be adopted upon addition of the acid to dme, but this does not seem to affect the ensuing reaction. The resulting mixture was allowed to room temperature and stirred for four hours. Removal of the solvent *in vacuo* overnight gave a green solid, that was subsequently extracted with cold toluene ($2 \times 100 \text{ cm}^3$, 0°C). Removal of volatile components overnight afforded the product as a green yellow solid. Yield 6.21 g (69%). It is important that all remaining solvent be removed under dynamic vacuum overnight before the toluene extraction is attempted, as residual dme may help to solublize the anilinium triflate byproduct and this is detrimental to the final synthetic step if present. The product should therefore be checked for contamination with anilinium triflate (by ^1H NMR spectroscopy) before proceeding.

6.6.1d Reaction of $\text{Mo}(\text{NAr})(\text{CH-t-Bu})(\text{OSO}_2\text{CF}_3)_2(\text{dme})$
with Li-O-t-Bu .

Preparation of $\text{Mo}(\text{NAr})(\text{CH-t-Bu})(\text{O-t-Bu})_2$.

A solution of Li-O-t-Bu (1.44 g, 0.02 mol) in 50 cm³ diethylether was added dropwise over a period of 10 minutes to a rapidly stirring solution of $\text{Mo}(\text{NAr})(\text{CH-t-Bu})(\text{OSO}_2\text{CF}_3)_2(\text{dme})$ (6.06 g, 0.01 mol) in 300 cm³ diethylether at -30°C. The resulting mixture was allowed to warm to room temperature and stirred for a maximum of three hours. Prolonged stirring leads to a darkening of the solution and gives a reduced product yield. Removal of volatile components *in vacuo* gave a dark orange solid, which was then extracted with pentane (3 x 30 cm³). Removal of the solvent under reduced pressure gave the product as a light orange solid. Recrystallization from a minimum amount of pentane at -78°C afforded 2.87 g (71%) of $\text{Mo}(\text{NAr})(\text{CH-t-Bu})(\text{O-t-Bu})_2$ as light orange crystals. The product may also be purified by slow sublimation at high vacuum over a period of several days (water cooled probe, 60°C, 10⁻⁶ torr).

6.6.2 Reaction of $\text{Mo}(\text{O})_2\text{Cl}_2$ with $\text{Li-O-2,6-iPr}_2\text{C}_6\text{H}_3$

Preparation of $\text{Mo}(\text{O})_2\text{Cl}_2\text{Li}$

Chilled diethylether (-78°C, 50 cm³) was added dropwise to a weighed mixture of $\text{Mo}(\text{O})_2\text{Cl}_2$ (1.08 g, 5.42 mmol) and lithium 2,6-di-isopropylphenoxide (2.00 g, 10.84 mmol). The resulting mixture was stirred at room temperature for five hours, to give a dark purple solid and a red-green dichroic solution. The solid was isolated by filtration, washed with diethylether (2 x 20 cm³) and dried *in vacuo*. Yield 0.94 g (84%).

Elemental analysis for $\text{LiO}_2\text{Cl}_2\text{Mo}$ Found (Required): %Mo, 45.36 (46.62); %Cl, 33.02 (34.45); %Li, 3.54 (3.37).

6.6.3 Reaction of $\text{Cp}^*\text{Ta}(\text{NAr})\text{Cl}_2$ with Li-O-*t*-Bu.

Preparation of $\text{Cp}^\text{Ta}(\text{NAr})\text{Cl}(\text{O-}i\text{-Bu})$.*

Diethylether (40 cm³) at -78°C was added, via cannula, to a weighed mixture of $\text{Cp}^*\text{Ta}(\text{NAr})\text{Cl}_2$ (0.49 g, 0.87 mmol) and Li-O-*t*-Bu (0.14 g, 1.75 mmol). The solution was allowed to warm to room temperature and stirred for 12 hours during which time a light green solution and pale precipitate formed. The suspension was filtered from the supernatant solution, and the solvent removed under reduced pressure to yield a yellow solid. This was washed with chilled (-78°C) pentane and dried *in vacuo*. Yield 384 mg (74%).

¹H NMR data (400 MHz, d⁶-benzene, 298K): 7.16 (d, 2, ³J_{HH} = 7.60 Hz, H_m), 6.91 (t, 1, ³J_{HH} = 7.20 Hz, H_p), 3.75 (sept, ³J_{HH} = 6.80 Hz, CHMe₂), 1.92 (s, 15, C₅Me₅), 1.39 (d, 6, ³J_{HH} = 6.80 Hz, CHMe₂), 1.32 (d, 6, ³J_{HH} = 6.80 Hz, CHMe₂), 1.29 (s, 9, O-*t*-Bu).

¹³C NMR data (100 MHz, d⁶-benzene, 298K): 149.57 (s, C_{ipso}), 144.12 (s, C_{ortho}), 122.97 (d, J_{CH} = 156.80 Hz, C_{meta}), 122.58 (d, J_{CH} = 153.78 Hz, C_{para}), 119.29 (s, C₅Me₅), 81.13 (s, OCMe₃), 31.90 (q, J_{CH} = 125.52 Hz, OCMe₃), 27.37 (d, J_{HH} = 130.05 Hz, CHMe₂), 25.59 (q, J_{HH} = 125.52 Hz, CHMe₂), 11.07 (s, C₅Me₅).

Infrared data (Nujol, cm⁻¹): 3045 (w), 1440 (m, sh), 1365 (m), 1349 (m), 1297 (w), 1260 (w), 1241 (w), 1172 (m, br), 1105 (w, br), 1026 (w), 989 (m), 973 (m), 931 (w), 807 (w), 792 (m), 753 (m, sp), 720 (w), 558 (w), 365 (m), 340 (m).

Elemental analysis for TaNClOC₂₆H₄₁ Found (Required): %C, 51.90 (52.05); %H, 6.76 (6.89); %N, 2.08 (2.33).

Mass spectral data (EI⁺, isobutane carrier gas, m/z, ³⁵Cl): 598 [M]⁺, 542 [M - C₄H₉]⁺.

6.6.4 Reaction of $\text{Cp}^*\text{Ta}(\text{N-t-Bu})\text{Cl}_2$ with $\text{Me}_3\text{CCH}_2\text{MgCl}$

Preparation of $\text{Cp}^*\text{Ta}(\text{N-t-Bu})\text{Cl}(\text{CH}_2\text{CMe}_3)$.

To a chilled (-78°C) solution of $\text{Cp}^*\text{Ta}(\text{N-t-Bu})\text{Cl}_2$ (0.16 g, 0.34 mmol) in 20 cm^3 diethylether was added an ethereal solution of neopentyl chloride (0.4 cm^3 , 1.8M, 0.69 mmol). The reaction mixture was allowed to warm to room temperature and stirred for six hours to give a light green solution and pale precipitate. The supernatant solution was isolated by filtration and volatile components removed under reduced pressure to afford an oily light brown solid. This was dissolved in pentane (10 cm^3) and cooled to -78°C to yield pale yellow crystals, which were isolated and dried *in vacuo*. Yield 108 mg (63%).

^1H NMR data (400 MHz, d^6 -benzene, 298K): 1.84 (s, 15 C_5Me_5), 1.39 (s, 9, NCMe_3), 1.38 (s, 9, CH_2CMe_3), 1.26 (d, 2, $^3J_{\text{HH}} = 14.40$ Hz, CH_2CMe_3), 0.80 (d, 2, $^3J_{\text{HH}} = 14.40$ Hz, CH_2CMe_3).

^{13}C NMR data (100 MHz, d^6 -benzene, 298K): 118.02 (s, C_5Me_5), 83.26 (t, $J_{\text{CH}} = 114.40$ Hz CH_2CMe_3), 65.20 (s, NCMe_3), 34.87, 33.69, 33.60, 11.54 (q, $J_{\text{CH}} = 126.63$ Hz, C_5Me_5). The J_{CH} coupling constant for the resonances at δ 34.87, 33.69 and 33.60 could not be obtained due to overlap of the signals.

Elemental analysis for $\text{TaNCIC}_{19}\text{H}_{35}$ Found (Required): %C, 44.62 (46.21); %H, 7.52 (7.14); %N, 2.76 (2.84).

6.7 References.

1. T.V. Lubben, P.T. Wolkzanski, G.D. Van Duyne, *Organometallics*, 1984, 3, 982.
2. W. Wolfsberger, H. Schmidbaur, *Synth. React. Inorg. Metal. Org. Chem.* 1974, 4, 149.
3. M. J. Bunker, A. De Cian, M.L.H. Green, J.J.E. Moreau, N. Siganporia, *J. Chem. Soc. Dalton. Trans.* 1980, 2155.
4. V.C. Gibson, J.E. Bercaw, W.J. Burton Jr. R.D. Sanner, *Organometallics*, 1986, 5, 976.
5. T.P. Kee, Ph.D. Thesis, University of Durham, 1989.
6. D.N. Williams, J.P. Mitchell, A.D. Poole, U. Siemeling, W. Clegg, D.C.R. Hockless, P.A. O'Neil, V.C. Gibson, *J. Chem. Soc. Dalton. Trans.* in press.
7. G. Schoettel, J. Kress, J.A. Osborn, *J. Chem. Soc. Chem. Comm.* 1989, 1062.
8. Sample of $\text{Mo}(\text{N-t-Bu})_2(\text{O-t-Bu})_2$ kindly donated by Mr. M. Jolly.
9. R.R. Schrock, J.S. Murdzek, G.C. Bazan, J. Robbins, M. DiMare, M.B. O'Regan, *J. Am. Chem. Soc.* 1990, 112, 3875
10. R.R. Schrock, *J. Am. Chem. Soc.* 1985, 107, 5957.
11. R.R. Schrock, R.T. Depue, J. Feldman, K.B. Yap, D.C. Yang, W.M. Davis, L. Park, M. DiMare, M. Schofield, J. Anhaus, E. Walborsky, E. Evitt, C. Kruger, P. Betz, *Organometallics*, 1990, 9, 2262.
12. D.C. Tabor, F.H. White, L.W. Collier IV, S.A. Evans Jr. *J. Org. Chem.* 1983, 48, 1638.
13. P.W. Atkins, "*Physical Chemistry*", 2nd Edition, Oxford University Press, 1982, Chapter 27.
14. G.C. Bazan, Ph.D. Thesis, Massachusetts Institute of Technology, 1990.
15. A.A. Frost, R.G. Pearson, "*Kinetics and Mechanism*", 2nd Edition, J. Wiley and Sons, 1961, Chapter 8.

Appendices.

Appendix 1

Crystal Data for Cp^oTa(N-2,6-iPr₂C₆H₃)Cl₂.

C ₂₂ H ₃₂ NCl ₂ Ta	562.36
Crystal System	Monoclinic
Space Group	P2 ₁ /m
Cell Dimensions	a = 6.975 (1) Å
	b = 17.433 (3) Å
	c = 9.842 (2) Å
	β = 99.18 (2)°
	V = 1181.4 Å ³
	Z = 2
	D _x = 1.581 g cm ⁻³
λ (Mo K _α)	0.71073 Å
μ	4.83 mm ⁻¹
F(000)	556
T	295 K
R _{int}	0.014
R _{sigma}	0.013

Appendix 2

First Year Induction Courses: October 1988

The course consists of a series of one hour lectures on the services available in the department.

1. Departmental Organisation
2. Safety Matters
3. Electrical appliances and infrared spectroscopy
4. Chromatography and Microanalysis
5. Atomic absorption and inorganic analysis
6. Library facilities
7. Mass spectroscopy
8. Nuclear Magnetic Resonance
9. Glass blowing techniques

Research Colloquia, Seminars and Lectures Organised
by the Department of Chemistry.

* - Indicates Colloquia attended by the author

During the Period: 1988-1989

- | | |
|---|--------------------|
| <u>ASHMAN</u> , Mr. A. (Durham Chemistry Teacher's Centre)
<i>The Chemical Aspects of the National Curriculum</i> | 3rd May 1989 |
| <u>AVEYARD</u> , Dr. R. (University of Hull)
<i>Surfactants at your Surface</i> | 15th March 1989 |
| <u>AYLETT</u> , Prof. B.J. (Queen Mary College, London)
<i>Silicon-Based Chips: - The Chemist's Contribution</i> | 16th February 1989 |
| * <u>BALDWIN</u> , Prof. J.E. (University of Oxford)
<i>Recent Advances in the Bioorganic Chemistry of Penicillin Biosynthesis</i> | 9th February 1989 |

- * BALDWIN & WALKER, Drs. R.R. & R.W. (Hull Univ.) 24th November 1988
Combustion: Some Burning Problems
- BOLLEN, Mr. F. (Durham Chemistry Teacher's Centre) 18th October 1988
Lecture about the use of SATIS in the classroom
- BUTLER, Dr. A.R. (St. Andrews University) 15th February 1989
Cancer in Linxiam: The Chemical Dimension
- * CADOGAN, Prof. J.I.G. (British Petroleum) 10th November 1988
From Pure Science to Profit
- CASEY, Dr. M. (University of Salford) 20th April 1989
Sulphoxides in Stereoselective Synthesis
- WATERS & CRESSEY, Mr. D. & T. (Durham Chemistry Teacher's Centre) 1st February 1989
GCSE Chemistry 1988: "A Coroners Report"
- CRICH, Dr. D. (University College London) 27th April 1989
Some Novel Uses of Free Radicals in Organic Synthesis
- DINGWALL, Dr. J. (Ciba Geigy) 18th October 1988
Phosphorus-containing Amino Acids: Biologically Active Natural and Unnatural Products
- * ERRINGTON, Dr. R.J. (University of Newcastle) 1st March 1989
Polymetalate Assembly in Organic Solvents
- FREY, Dr. J. (Southampton University) 11th May 1989
Spectroscopy of the Reaction Path: Photodissociation Raman Spectra of NOCl
- * GRADUATE CHEMISTS, (Polytechs and Universities in North East England) 12th April 1989
Symposium for presentation of papers by postgraduate students

- * HALL, Prof. L.D. (Addenbrooke's Hospital Cambridge) 2nd February 1989
NMR - A Window to the Human Body
- * HARDGROVE, Dr. G. (St. Olaf College U.S.A.) December 1988
Polymers in the Physical Chemistry Laboratory
- HARWOOD, Dr. L.(Oxford University) 25th January 1988
Synthetic Approaches to Phorbols Via Intramolecular Furan Diels-Alder Reactions: Chemistry under Pressure
- JAGER, Dr. C. (Friedrich-Schiller University GDR) 9th December 1988
NMR Investigations of Fast Ion Conductors of the NASICON Type
- * JENNINGS, Prof. R.R. (Warwick University) 26th January 1989
Chemistry of the Masses
- JOHNSON, Dr. B.F.G. (Cambridge University) 23rd February 1989
The Binary Carbonyls
- JONES, Dr. M.E. (Durham Chemistry Teacher's Centre) 14th June 1989
Discussion Session on the National Curriculum
- JONES, Dr. M.E. (Durham Chemistry Teacher's Centre) 28th June 1989
GCSE and A Level Chemistry 1989
- * LUDMAN, Dr. C.J. (Durham University) 18th October 1988
The Energetics of Explosives
- MACDOUGALL, Dr. G. (Edinburgh University) 22nd February 1989
Vibrational Spectroscopy of Model Catalytic Systems
- MARKO, Dr. I. (Sheffield University) 9th March 1989
Catalytic Asymmetric Osmylation of Olefins
- McLAUCHLAN, Dr. K.A. (University of Oxford) 16th November 1988
The Effect of Magnetic Fields on Chemical Reactions

- MOODY, Dr. C.J. (Imperial College) 17th May 1989
Reactive Intermediates in Heterocyclic Synthesis
- MORTIMER, Dr. C. (Durham Chemistry Teacher's Centre) 14th December 1988
The Hindenberg Disaster - an Excuse for Some Experiments
- * NICHOLLS, Dr. D. (Durham Chemistry Teacher's Centre) 11th July 1989
Demo. "Liquid Air"
- * PAETZOLD, Prof. P. (Aachen) 23rd May 1989
Iminoboranes XB=NR: Inorganic Acetylenes
- PAGE, Dr. P.C.B. (University of Liverpool) 3rd May 1989
Stereocontrol of Organic Reactions Using 1,3-dithiane-1-oxides
- POLA, Prof. J. (Czechoslovak Academy of Science) 15th June 1989
*Carbon Dioxide Laser Induced Chemical Reactions
New Pathways in Gas-Phase Chemistry*
- REES, Prof. C.W. (Imperial College London) 27th October 1988
Some Very Heterocyclic Compounds
- REVELL, Mr. P. (Durham Chemistry Teacher's Centre) 14th March 1989
Implementing Broad and Balanced Science 11-16
- SCHMUTZLER, Prof. R. (Techn. Univ. Braunschweig) 6th October 1988
*Fluorophosphines Revisited - New Contributions to an
Old Theme*
- * SCHROCK, Prof. R.R. (M.I.T.) 13th February 1989
Recent Advances in Living Metathesis
- SINGH, Dr. G. (Teesside Polytechnic) 9th November 1988
Towards Third Generation Anti-Leukaemics

* SNAITH, Dr. R. (Cambridge University) 1st December 1988
Egyptian Mummies: What, Where, Why and How

STIBR, Dr. R. (Czechoslovak Academy of Sciences) 16th May 1989
Recent Developments in the Chemistry of Intermediate-Sited Carboranes

VON RAGUE SCHLEYER, Prof. P. (Univ. Erlangen) 21st October 1988
The Fruitful Interplay Between Computational and Experimental Chemistry

* WELLS, Prof. P.B. (Hull University) 10th May 1989
Catalyst Characterisation and Reactivity

During the Period 1989-1990

ASHMAN, Mr.A. (Durham Chemistry Teachers' Centre) 11th October, 1989
The National Curriculum - an update

* BADYAL, Dr J.P.S. (Durham University) 1st November 1989
Breakthroughs in Heterogeneous Catalysis

BECHER, Dr.J. (Odense University) 13th November 1989
Synthesis of New Macrocyclic Systems using Heterocyclic Building Blocks

* BERCAW, Prof. J.E. (California Institute of Technology) 10th November 1989
Synthetic and Mechanistic Approaches to Ziegler-Natta Polymerisation of Olefins

BLEASDALE, Dr. C. (Newcastle University) 21st February 1990
The Mode of Action of some anti-tumour Agents

BOLLEN, Mr.F. (Former Science Advisor, Newcastle LEA) 27th March 1990
Whats New in Satis, 16-19

- BOWMAN, Prof. J.M. (Emory University) 23rd March 1990
Fitting Experiment with Theory in Ar-OH
- * BUTLER, Dr. A. (St. Andrews University) 7th December 1989
The Discovery of Penicillin: Facts and Fancies
- CAMPBELL, Mr. W.A. (Durham Chemistry Teachers Centre) 12th September 1989
Industrial Catalysis- some ideas for the National Curriculum
- CHADWICK, Dr. P. (Dept. Physics, Durham University) 24th January 1990.
Recent Theories of the Universe (with reference to National Curriculum Attainment Target 16)
- CHEETHAM, Dr.A.K. (Oxford University) 8th March 1990
Chemistry of Zeolite Cages
- CLARK, Prof. D.T. (ICI Wilton) 22nd February 1990
Spatially Resolved Chemistry (using Nature's Paradigm in the Advanced Materials Arena)
- * COLE-HAMILTON, Prof. D.J. (St. Andrews University) 29th November 1989
New Polymers from Homogeneous Catalysis
- CROMBIE, Prof. L. (Nottingham University) 15th February 1990
The Chemistry of Cannabis and Khat
- DYER, Dr. U. (Glaxo) 31st January 1990
Synthesis and Conformation of C-Glycosides
- FLORIANI, Prof. C. (Lausanne Univ., Switzerland) 25th October 1989
Molecular Aggregates- A Bridge Between Homogeneous and Heterogeneous Systems
- GERMAN, Prof. L.S. (USSR Academy of Sciences) 9th July 1990
New Syntheses in Fluoroaliphatic Chemistry: Recent Advances in the Chemistry of Fluorinated Oxiranes

- GRAHAM, Dr.D. (B.P. Research Centre) 4th December 1989
How Proteins Absorb to Interfaces
- * GREENWOOD, Prof. N.N. (University of Leeds) 9th November 1989
Novel Cluster Geometries in Metalloborane Chemistry
- * HOLLOWAY, Prof. J.H. (University of Leicester) 1st February 1990
Noble Gas Chemistry
- HUGHES, Dr.M.N. (King's College, London) 30th November 1989
A Bug's Eye View of the Periodic Table
- HUISGEN, Prof. R. (Universität München) 15th December 1989
Recent Mechanistic Studies of [2+2] Additions
- IDDON, Dr.B. (University of Salford) 15th December 1989
*Schools' Christmas Lecture-
The Magic of Chemistry*
- JONES, Dr.M.E. (Durham University Teachers Centre) 3rd July 1990
The Chemistry A Level 1990
- JONES, Dr. M.E. (Durham University Teachers Centre) 21st November 1989
*GCSE and Dual Award Science as a Starting Point
for A level Chemistry- How Suitable are They?*
- JOHNSON, Dr. G.A.L. (Durham University Teachers Centre) 8th February 1990
Some Aspects of Local Geology in the National Science Curriculum (Attainment Target 9)
- KLINOWSKI, Dr.J. (Cambridge University) 13th December 1989
Solid State NMR Studies of Zeolite Catalysts
- * LANCASTER, Rev. R. (Kimbolton Fireworks) 8th February 1990
Fireworks - Principles and Practice

- LUNAZZI, Prof. L. (University of Bologna) 12th February 1990
Application of Dynamic NMR to the Study of Conformational Enantiomerism
- * PALMER, Dr. F. (Nottingham University) 17th October 1989
Thunder and Lightning
- PARKER, Dr. D. (Durham University) 16th November 1989
Macrocycles, Drugs and Rock'N'Roll
- * PERUTZ, Dr. R.N. (York University) 24th January 1990
Plotting the Course of C-H Activations with Organometallics
- PLATONOV, Prof. V.E. (USSR Academy of Sciences) 9th July 1990
Polyfluoroindanes: Synthesis and Transformation
- POWELL, Dr.R.L. (I.C.I.) 6th December 1989
The Development of CFC Replacements
- POWIS, Dr. I. (Nottingham University) 21st March 1990
Spinning off in a Huff: Photodissociation of Methyl Iodide
- RICHARDS, Mr. C. (Health and Safety Exec., Newcastle) 28th February 1990
Safety in School Science Laboratories and COSHH
- ROZHKOV, Prof. I.N. (USSR Academy of Sciences, Moscow) 9th July 1990
Reactivity of Perfluoroalkyl Bromides
- STODDART, Dr.J.F. (Sheffield University) 1st March 1990
Molecular Lego
- * SUTTON, Prof. D. (Simon Fraser Univ., Vancouver) 14th February 1990
Synthesis and Applications of Dinitrogen and Diazo Compounds of Rhenium and Iridium

THOMAS, Dr.R.K. (Oxford University) 28th February 1990
Neutron Reflectometry from Surfaces

THOMPSON, Dr. D.P. (Newcastle University) 7th February 1990
*The Role of Nitrogen in Extending Silicate
Crystal Chemistry*

During the Period 1990-1991

ALDER, Dr. B.J. (Lawrence Livermore Labs., California) 15th January 1991
Hydrogen in all its Glory

* BELL, Prof. T. (SUNY, Stony Brook, U.S.A.) 14th November 1990
*Functional Molecular Architecture and
Molecular Recognition*

* BOCHMANN, Dr. M. (University of East Anglia) 24th October 1990
*Synthesis, Reactions and Catalytic Activity of
Cationic Titanium Alkyls*

BRIMBLE, Dr. M.A. (Massey University, New Zealand) 29th July 1991
*Synthetic Studies Towards the Antibiotic
Griseusin-A*

* BROOKHART, Prof. M.S. (University of N. Carolina) 20th June 1991
*Olefin Polymerizations, Oligomerizations and Dimerizations
using Electrophilic Late Transition Metal Catalysts*

BROWN, Dr. J. (Oxford University) 28th February 1991
*Can Chemistry provide Catalysts Superior
to Enzymes*

BUSHBY, Dr. R. (Leeds University) 6th February 1991
Biradicals and Organic Magnets

* COWLEY, Prof. A.H. (University of Texas) 13th December 1990
New Organometallic Routes to Electronic Materials

- CROUT, Prof D. (Warwick University) 29th November 1990
Enzymes in Organic Synthesis
- DOBSON, Dr. C.M. (Oxford University) 6th March 1991
NMR Studies of Dynamics in Molecular Crystals
- GERRARD, Dr. D. (British Petroleum) 7th November 1990
Raman Spectroscopy for Industrial Analysis
- HUDLICY, Prof. T. (Virginia Polytechnic Institute) 25th April 1991
Biocatalysis and Symmetry Based Approaches to the Efficient Synthesis of Complex Natural Products
- JACKSON, Dr. R. (Newcastle University) 31st October 1990
New Synthetic Methods: α -Amino Acids and Small Rings
- * KOCOVSKY, Dr. P. (Uppsala University) 6th November 1990
Stereo-Controlled Reactions Mediated by Transition and Non-Transition Metals
- LACEY, Dr. D. (Hull University) 31st January 1991
Liquid Crystals
- LOGAN, Dr. N. (Nottingham University) 1st November 1990
Rocket Propellants
- MACDONALD, Dr. W. A. (I.C.I. Wilton) 11th October 1990
Materials for the Space Age
- * MARKHAM, Dr. R. (ICI Pharmaceuticals) 7th March 1991
DNA Fingerprinting
- PETTY, Dr. M. C. (Durham University) 14th February 1991
Molecular Electronics

- * PRINGLE, Dr. P. G. (Bristol University) 5th December 1990
Metal Complexes with Functionalised Phosphines
- PRITCHARD, Prof. J. (Queen Mary College, London) 21st November 1990
Copper Surfaces and Catalysts
- SADLER, Dr. P. J. (Birbeck College, London) 24th January 1991
Design of Inorganic Drugs : Precious Metals, Hypertension + HIV
- * SARRE, Dr. P. (Nottingham University) 17th January 1991
Comet Chemistry
- * SCHROCK, Prof. R. R. (M.I.T.) 24th April 1991
Metal Ligand Multiple Bonds and Metathesis Initiators
- SCOTT, Dr. S. K. (Leeds University) 8th November 1990
Clocks, Oscillators and Chaos
- * SHAW, Prof. B. L. (Leeds University) 20th February 1991
Syntheses with Coordinated, Unsaturated Phosphine Ligands
- * SINN, Prof. E. (Hull University) 30th January 1991
Coupling of Little Electrons in Big Molecules. Implications for the Active Sites of (Metalloproteins and other) Macromolecules
- * SOULEN, Prof. R. (South Western University, Texas) 26th October 1990
Preparation and Reactions of Bicycloalkenes
- WHITTAKER, Dr. B. J. (Leeds University) 28th November 1990
Two-Dimensional Velocity Imaging of State-Selected Reaction Products

Conferences and Symposia Attended.

(* denotes paper presentation)

(# denotes poster presentation)

1. *"International Conference on the Chemistry of the Early Transition Metals"*,
The University of Sussex, Brighton, 10-14th July 1989.
2. *"North East Graduate Symposium"*,
The University of Newcastle-upon-Tyne, 2nd April 1990.
3. *"Symposium in Honour of Professor Peter L. Pauson - Organometallic Chemistry of the Transition Metals"*,
University of Strathclyde, Glasgow, 19th October 1990.
- 4.* *"Waddington Graduate Symposium on Inorganic Chemistry"*,
The University of Durham, 17th December 1990.
- 5.# *"Macro Group UK Meeting - Aspects of Contemporary Polymer Chemistry"*,
The University of Lancaster, 26-28th March 1991.
- 6.* *"North East Graduate Symposium"*,
The University of Newcastle upon Tyne, 15th May 1991.
- 6.* *"Society of Chemical Industry, Annual General Meeting"*,
14/15 Belgrave Square, London, 15th July 1991.
- 7.# *"Ninth International Symposium on Olefin Metathesis and Polymerization"*,
Ursinus College, Pennsylvania, U.S.A., 21-26th July 1991.
- 8.* *"IRC in Polymer Science and Technology, Industrial Club Seminar"*
The University of Durham, 17-18th September 1991.

Publications.

Chain Transfer Agents for Living Ring Opening Metathesis Polymerization Reactions of Norbornene.

W.E. Crowe, J.P. Mitchell, V.C. Gibson, R.R. Schrock, *Macromolecules*, 1990, 23, 3534.

Chain-End Functionalization of Living Polymers Formed by the Ring Opening Metathesis Polymerization of Norbornene.

J.P. Mitchell, V.C. Gibson, R.R. Schrock, *Macromolecules*, 1991, 24, 1220.

Bimolecular Termination in Living Ring Opening Metathesis Polymerization.

W.J. Feast, V.C. Gibson, E. Khosravi, E.L. Marshall, J.P. Mitchell, *Polymer Comm.* 1992, 33, 872.

Imido Ligand Reactivity in Four Coordinate Bis(Imido) Complexes of Molybdenum (VI).

M. Jolly, J.P. Mitchell, V.C. Gibson, *J. Chem. Soc. Dalton. Comm.* in press.

Inter-Metal Exchange of Oxo, Imido and Alkylidene Ligands.

M. Jolly, J.P. Mitchell, V.C. Gibson, *J. Chem. Soc. Dalton. Comm.* in press.

Half-sandwich Imido Complexes of Niobium and Tantalum, Synthesis, Structure and Bonding.

D.N. Williams, J.P. Mitchell, A.D. Poole, U. Siemeling, W. Clegg,

D.C.R. Hockless, P.A. O'Neil, V.C. Gibson, *J. Chem. Soc. Dalton Trans.* in press.

Ring Opening Metathesis Polymerization of syn- and anti- 7-methylbicyclo[2.2.1]hept-2-ene initiated by $\text{Mo}(\text{CHCMe}_3)(\text{NC}_6\text{H}_3\text{-2,6-i-Pr}_2)(\text{OCMe}_3)_2$.

W.J. Feast, V.C. Gibson, K.J. Ivin, E. Khosravi, A.M. Kenwright, J.P. Mitchell, *Makromol. Chem.* submitted.

Appendix 3

Synthesis and Characterization of $\text{Mo}(\text{O})_2\text{Cl}_2\cdot\text{Li}$

Compounds of the type $\text{W}(\text{O})_2\text{Cl}_2\cdot\text{Li}_x$ ($0 < x \leq 1$) have previously been prepared in this laboratory by Alan Shaw via the reaction of $\text{W}(\text{O})_2\text{Cl}_2$ with alkali metal aryloxides in toluene solvent¹. The corresponding reaction with $\text{Mo}(\text{O})_2\text{Cl}_2$ led to the formation of molecular molybdenum aryloxide complexes. It was found that lithium may also be incorporated into the layered $\text{Mo}(\text{O})_2\text{Cl}_2$ lattice via reaction of $\text{Mo}(\text{O})_2\text{Cl}_2$ with Li-O-2,6-iPr₂C₆H₃ in ether solvent. The reaction proceeds smoothly over a period of five hours to afford a purple crystalline solid and a red-green dichroic solution. The reaction can be envisaged to occur as shown below.



The solid has a metallic lustre and is insoluble in all common solvents. Characterization is provided by elemental analysis (chapter 6, section 6.6.2) which confirms the stoichiometry $\text{LiO}_2\text{Cl}_2\text{Mo}$, with only one lithium atom being incorporated into the lattice. The organic products have been shown¹ to consist of a mixture of 2,6-di-isopropylphenol and the coupled biphenol $[\text{HO}-2,6\text{-iPr}_2\text{C}_6\text{H}_2]_2$.

It is presumed that the reaction proceeds via an electron transfer from LiOAr to $\text{Mo}(\text{O})_2\text{Cl}_2$ to give phenoxy radicals, followed by migration of lithium metal ions into the $\text{Mo}(\text{O})_2\text{Cl}_2$ lattice. Once atomic lithium is generated, C-C coupling of the phenoxy radicals takes place, followed by enolization of the resultant dimer, to generate the observed biphenol.

Synthesis and Characterization of $\text{Cp}^*\text{Ta}(\text{NAr})(\text{O}-t\text{-Bu})\text{Cl}$.

It has been shown in chapter five that imido groups can be exchanged between the metal centres of half sandwich imido complexes of the type $\text{Cp}'\text{M}(\text{NR})\text{Cl}_2$ ($\text{Cp}' = \text{C}_5\text{H}_5, \text{C}_5\text{Me}_5$; $\text{M} = \text{Nb}, \text{Ta}$; $\text{R} = \text{Me}, t\text{-Bu}, \text{Ar}$). However, if ancillary ligands other than chlorides are present, exchange of these one electron ligands occurs much more readily, and can lead to a mixture of products. It was therefore desirable to synthesize a bis *t*-butoxide derivative of the half-sandwich imido system, so that exchange reactivity with alkylidene complexes of the type $\text{M}(\text{NAr})(\text{CHCMe}_2\text{R})(\text{O}-t\text{-Bu})_2$ ($\text{M} = \text{Mo}, \text{W}$; $\text{R} = \text{Me}, \text{Ph}$) could be investigated. However, it proved possible only to prepare a mixed chloride / *t*-butoxide derivative as described below.

Treatment of $\text{Cp}^*\text{Ta}(\text{NAr})\text{Cl}_2$ with two equivalents of $\text{Li}-\text{O}-t\text{-Bu}$ in diethyl ether affords a light green solution from which $\text{Cp}^*\text{Ta}(\text{NAr})(\text{O}-t\text{-Bu})\text{Cl}$ can be isolated in 74% yield.



Characterization is provided by infrared spectroscopy, elemental analysis, ^1H and ^{13}C NMR spectroscopies and mass spectrometry (see chapter 6, section 6.6.3). In particular, elemental analysis confirms the stoichiometry $\text{C}_{26}\text{H}_{41}\text{NOClTa}$ and the mass spectrum shows a parent ion peak at $m/z = 598$. Prolonged reaction times or heating of a sample to 60°C in C_6D_6 does not lead to the formation of any bis *t*-butoxide complex $\text{Cp}^*\text{Ta}(\text{NAr})(\text{O}-t\text{-Bu})_2$.

Synthesis and characterization of $\text{Cp}^{\ominus}\text{Ta}(\text{N-t-Bu})(\text{CH}_2\text{CMe}_3)\text{Cl}$.

Recently, a series of half sandwich niobium imido complexes with ancillary neopentyl ligands have been synthesized, and have been shown to possess agostic interactions between the α C-H bond of the neopentyl group and the electron deficient niobium metal centre². For comparison, an attempt was undertaken to prepare the tantalum bis neopentyl derivative $\text{Cp}^{\ominus}\text{Ta}(\text{N-t-Bu})(\text{CH}_2\text{CMe}_3)_2$, as this may provide a synthetic route to tantalum neopentylidene complexes which may be of interest as initiators in living ROMP.

The reaction between $\text{Cp}^{\ominus}\text{Ta}(\text{N-t-Bu})\text{Cl}_2$ and two equivalents of neopentyl magnesium chloride in diethylether proceeds smoothly over six hours to give a pale green solution from which the mono neopentyl derivative $\text{Cp}^{\ominus}\text{Ta}(\text{N-t-Bu})(\text{CH}_2\text{CMe}_3)\text{Cl}$ may be isolated as pale yellow crystals in 63% yield.



Characterization is provided by elemental analysis and ^1H and ^{13}C NMR spectroscopies (chapter 6, section 6.6.4). Elemental analysis confirms the stoichiometry $\text{C}_{19}\text{H}_{35}\text{NCITa}$ whilst the ^1H NMR spectrum reveals a singlet at δ 1.38 for the methyl protons and two doublets at δ 1.26 and 0.80 (ratio 1:1, $^3J_{\text{HH}} = 14.40$ Hz) for the diastereotopic methylene protons of the neopentyl ligand. The different chemical shifts for the methylene protons are believed to arise due to averaged H_{up} (toward the Cp^{\ominus} ring) and H_{down} (away from the Cp^{\ominus} ring) α proton environments. NOE experiments² indicate that the high field doublet resonance corresponds to H_{up} . The ^{13}C NMR spectrum shows a resonance at δ 83.26 due to the methylene carbon of the neopentyl group. The J_{CH} coupling constant of 114.40 Hz is reasonable for an averaging of a terminal C-H bond (typically $J_{\text{CH}} = 120 - 130$ Hz)³ and a bridging agostic interaction (typically $J_{\text{CH}} = 70 - 100$ Hz)^{3,4}. However, to fully confirm this

α C-H agostic interaction, variable temperature ^1H NMR studies and partial deuteration of the neopentyl group methylene protons are required.

References.

1. A. Shaw, Ph.D Thesis, University of Durham, 1989.
2. A.D. Poole, V.C. Gibson, unpublished observations.
3. M. Brookhart, M.L.H. Green, *J. Organomet. Chem.* 1983, 250, 395.
4. M. Brookhart, T.H. Whitesides, J.M. Crockett, *Inorg. Chem.* 1976, 15, 1550.

